

Investigating Eco-Physiological Mechanisms of Stress Response and Temperate Trees

Zur Erlangung des akademischen Grades eines
DOKTORS DER NATURWISSENSCHAFTEN (Dr. rer. nat.)

von der KIT-Fakultät für
Bauingenieur-, Geo-, und Umweltwissenschaften
des Karlsruher Instituts für Technologie (KIT)

genehmigte
DISSERTATION

von

M.Sc. Franklin Alongi
aus Paris

Tag der mündlichen Prüfung: 06.02.2026

Referentin: Prof. Dr. Nadine K. Rühr

Korreferentin: Dr. Christine Scoffoni

Garmisch-Partenkirchen
(2026)

Table of Contents

<i>Summary</i>	V
<i>Zusammenfassung</i>	VII
<i>List of Publications</i>	X
<i>Abbreviations</i>	XIII
<i>List of Figures</i>	XV
<i>List of Tables</i>	XVII
1 <i>Introduction</i>	1
1.1 Forests under a changing climate.....	1
1.2 Impacts of abiotic stress on tree gas exchange	2
1.3 Limitations of plant function during post-drought recovery	3
1.3.1 Restoration of gas exchange	3
1.3.2 Restoration of growth.....	4
1.4 Long-term legacy effects of drought on tree function	5
1.5 Objectives of the thesis	7
1.6 Experimental approach.....	8
1.7 Structure of thesis	9
2 <i>Drought and heat stress interactions modify photorespiration and hydrogen peroxide content in Silver fir</i>	11
2.1 Introduction	12
2.2 Materials and Methods	14
2.2.1 Plant material and growth conditions.....	14
2.2.2 Experimental Conditions.....	15
2.2.3 Gas exchange and fluorescence measurements	15
2.2.4 Chemical analysis: Hydrogen peroxide and Peroxidase activity.....	16
2.2.5 Statistical analysis.....	17
2.3 Results	18
2.3.1 Treatment progression.....	18
2.3.2 Photorespiration and chlorophyll fluorescence	19
2.3.3 Foliar hydrogen peroxide and peroxidase	22
2.4 Discussion.....	23
2.4.1 PR depends on timing and interactions between drought and heat.....	24
2.4.2 H ₂ O ₂ accumulation is tightly regulated despite variable PR during stress	25
2.5 Conclusion.....	27
2.6 Supplementary Materials.....	28
3 <i>Drought-induced delays in stem hydraulic development shape gas exchange and growth recovery in Douglas fir</i>	31
3.1 Introduction	32
3.2 Results	36
3.2.1 Dynamics of water potential, abscisic acid, and stomatal conductance	37
3.2.2 Carbon assimilation and accumulation	40

3.2.3	<i>Nonstructural carbohydrates (NSC)</i>	42
3.2.4	<i>Growth and Biomass accumulation</i>	43
3.3	Discussion	45
3.3.1	<i>Drought severity-induced hydraulic and ABA control of stomatal conductance</i>	45
3.3.2	<i>Drought severity increasingly limits recovery of C accumulation</i>	47
3.3.3	<i>Reduced recovery of growth not limited by NSC</i>	48
3.3.4	<i>Modified diurnal patterns restrict growth recovery</i>	50
3.4	Conclusion	51
3.5	Materials & Methods	52
3.5.1	<i>Plant material and environmental conditions</i>	52
3.5.2	<i>Experimental conditions</i>	52
3.5.3	<i>Tree gas flux chamber system</i>	55
3.5.4	<i>Nonstructural carbohydrate quantification</i>	57
3.5.5	<i>Abscisic acid quantification</i>	57
3.5.6	<i>Statistical methods</i>	58
3.6	Supplementary Materials	59
4	<i>Carbon-mediated drought legacy effects differ between two forest species with contrasting leaf habit</i>	67
4.1	Introduction	68
4.2	Materials and Methods	72
4.2.1	<i>Plant material and environmental conditions</i>	72
4.2.2	<i>Experimental design</i>	72
4.2.3	<i>Leaf phenology determination</i>	74
4.2.4	<i>Tissue sampling</i>	75
4.2.5	<i>Nonstructural carbohydrate quantification</i>	75
4.2.6	<i>Assessment of new leaf photosynthetic function</i>	76
4.2.7	<i>Growth and new tissue morphology</i>	76
4.2.8	<i>Statistical methods</i>	77
4.3	Results	79
4.3.1	<i>Drought Treatment Effects</i>	79
4.3.2	<i>Bud Morphological Development</i>	80
4.3.3	<i>Autumn Leaf Phenology</i>	80
4.3.4	<i>Spring Budburst Phenology</i>	81
4.3.5	<i>Bud nonstructural carbohydrates (NSC)</i>	82
4.3.6	<i>Branch nonstructural carbohydrates (NSC)</i>	84
4.3.7	<i>New Leaf Function in the Following Growing Season</i>	84
4.3.8	<i>New Tissue Morphology in the Following Growing Season</i>	85
4.3.9	<i>Relationships between legacy NSC, phenology, and morphology</i>	86
4.4	Discussion	87
4.4.1	<i>Drought affects NSC composition into the following growing season</i>	88
4.4.2	<i>Altered autumn and spring leaf phenology as drought legacy effects</i>	89
4.4.3	<i>NSC legacy effects are largely correlated with reduced tissue production in the following year</i>	90
4.4.4	<i>Evidence for leaf-habit influencing the expression of drought legacy effects</i>	92
4.5	Conclusion	92
4.6	Supplementary Materials	94
5	<i>Somatic Drought Stress Memory Affects Leaf Morpho-Physiological Traits of Plants via Epigenetic Mechanisms and Phytohormonal Signalling</i>	109
5.1	Introduction	110
5.2	Epigenetic mechanisms in drought stress memory	114
5.2.1	<i>DNA methylation and histone modification</i>	115

5.2.2	<i>Role of non-coding RNAs</i>	116
5.3	<i>Crosstalk between epigenetic mechanisms and phytohormones</i>	117
5.3.1	<i>Abscisic acid</i>	119
5.3.2	<i>Jasmonic acid</i>	119
5.3.3	<i>Ethylene</i>	120
5.3.4	<i>Salicylic acid</i>	121
5.3.5	<i>Auxins</i>	122
5.3.6	<i>Cytokinins</i>	122
5.4	<i>Leaf morpho-physiological changes after drought stress release</i>	123
5.4.1	<i>Leaf morphology: size and thickness</i>	124
5.4.2	<i>Stomatal morphology: size and density</i>	125
5.4.3	<i>Stomatal responsiveness and transpiration</i>	126
5.4.4	<i>Cuticular structure and residual water loss</i>	127
5.4.5	<i>Antioxidant defenses and osmolyte accumulation</i>	129
5.4.6	<i>Leaf senescence: water loss avoidance, nutrient reallocation or assimilation recovery</i>	129
5.5	<i>Conclusion and future prospects</i>	130
6	<i>Synthesis</i>	132
6.1	<i>Physiological Responses to Abiotic stress</i>	133
6.1.1	<i>Responses to mild stress</i>	133
6.1.2	<i>Response to severe stress</i>	134
6.2	<i>Drought recovery and legacy effects</i>	136
6.2.1	<i>Early recovery from drought</i>	136
6.2.2	<i>Extended recovery and drought legacy</i>	138
6.3	<i>Research Advances, Limitations, and Future Directions</i>	140
6.3.1	<i>Key advances</i>	140
6.3.2	<i>Limitations</i>	141
6.3.3	<i>Future directions</i>	142
6.4	<i>Conclusions</i>	144
7	<i>References</i>	146
8	<i>Acknowledgements</i>	168

Summary

Forests play a critical role in the global carbon cycle, sequestering approximately 2.4 petagrams of atmospheric CO₂ annually. However, forest functioning is increasingly threatened by climate extremes, particularly drought events that are projected to increase in frequency, intensity, and duration throughout the 21st century. Despite the importance of extreme events on forest biogeochemical cycles, we lack a mechanistic understanding of the physiological processes which govern stress responses, recovery dynamics, and subsequent multi-year alterations in forest function. Stress-induced functional impairment can operate through multiple physiological pathways such as through hydraulic damage, metabolic downregulation, and carbon depletion. Nonetheless, how drought characteristics like severity and duration modulate which physiological mechanisms determine stress and recovery responses remains poorly understood.

The present thesis aims to improve our understanding of how drought impacts tree physiological processes across multiple temporal scales, investigating immediate stress responses, short-term recovery, and long-term legacy. The following research questions are addressed: (1) How do progressive drought and heat stress interact to affect photorespiration and subsequent regulation of oxidative stress? (2) How does drought severity mechanistically impact the short-term recovery of plant gas exchange and growth? (3) How do summer drought events alter internal plant carbon reserve dynamics to mediate the expression of legacy effects in the subsequent growing season?

To answer these questions, three greenhouse experiments were conducted using temperate conifer species. In the first experiment, silver fir (*Abies alba*) juveniles were exposed to progressive drought combined with heat treatment (40°C for 6 hours). Gas exchange measurements under ambient and reduced oxygen conditions assessed the variable contribution of photorespiration to photosynthetic efficiency, while foliar hydrogen peroxide and peroxidase content evaluated oxidative stress regulation. In the second experiment, Douglas fir (*Pseudotsuga menziesii*) juveniles were subjected to either mild or severe drought followed by 35 days of recovery. A custom-built gas exchange chamber system continuously measured above- and belowground CO₂ and H₂O fluxes, while stem dendrometers tracked growth dynamics. Periodic destructive sampling assessed water potential, foliar abscisic acid, and nonstructural carbohydrates to identify physiological constraints on recovery. In the third experiment, European larch (*Larix decidua*) and Scots pine (*Pinus sylvestris*) juveniles, which possess differing seasonal leaf habits (deciduous vs. evergreen), were exposed to extended summer drought, then monitored outdoors through the following growing season. Bud and branch nonstructural carbohydrates were sampled at four timepoints spanning autumn, winter, and spring to track seasonal carbon dynamics, while phenology was monitored and new tissue function and morphology assessed to quantify legacy effects.

Results from the first experiment demonstrated that photorespiration's contribution to plant carbon assimilation varied along the gradient of drought severity. Mild drought modestly increased photorespiration (+5%) as stomatal closure reduced intercellular CO₂, while severe drought decreased photorespiration (-14%) as non-stomatal metabolic limitations became dominant. Despite variable photorespiration rates, hydrogen peroxide accumulation was tightly regulated through rapid increases in peroxidase enzyme activity, limiting oxidative stress signaling potential under all combinations drought and heat stress.

The second experiment revealed that recovery from drought is governed primarily by structural hydraulic constraints rather than carbon availability or phytohormonal signaling. Following severe drought that induced an estimated 70-85% loss of hydraulic conductivity, water potential and abscisic acid recovered to control levels within two days of rewatering, yet stomatal conductance and growth remained depressed for weeks. The ratio of sapwood area to leaf area (Huber value) emerged as the primary determinant of recovery, with drought-suppressed stem development leading to insufficient hydraulic supply. Nonstructural carbohydrates remained at or above control levels throughout recovery, challenging assumptions that carbon availability constrains post-drought function.

In the third experiment, moderate extended drought altered nonstructural carbohydrate composition and mobilization into the following growing season. Autumn branch carbohydrate accumulation was reduced by >70% in larch despite normal autumn senescence patterns, while pine maintained normal autumn accumulation. Winter mobilization patterns indicated compensatory redistribution from distal storage pools in drought-stressed trees of both species. By mid-budburst, the deciduous larch displayed a significant carbohydrate deficit, while pine accumulated substantial carbohydrates prior to budburst, presumably due to persisting mature foliage due to its evergreen nature, and displayed a carbohydrate surplus. These altered carbohydrate dynamics correlated with earlier and slower budburst in larch, as well as large reductions in new tissue production (~50% in deciduous larch, ~25% in evergreen pine), establishing a carbon-mediated pathway in drought legacy expression, while suggesting leaf habit as a determinant of legacy vulnerability.

The findings of this thesis demonstrate that drought characteristics such as severity and duration largely determine which physiological mechanisms dominate stress responses and shape recovery trajectories. Mild drought induces primarily passive stomatal regulation without triggering severe hydraulic damage or hormonal responses, enabling quicker functional restoration. Nonetheless, mild drought, when extended over significant periods, disrupts seasonal carbohydrate dynamics, resulting in altered spring phenology and reduced tissue production in the following growing season. Severe drought initiates qualitatively different pathways involving abscisic acid signaling, non-stomatal metabolic limitations, and xylem cavitation that create additional bottlenecks to recovery. The identification of Huber value as a measurable predictor of recovery capacity and leaf habit as a determinant of legacy vulnerability provides trait-based frameworks for assessing species-specific resilience. As drought frequency intensifies, understanding these severity-dependent responses is essential to develop mechanistic predictions of forest composition and productivity under novel climate regimes.

Zusammenfassung

Wälder spielen eine entscheidende Rolle im globalen Kohlenstoffkreislauf und binden jährlich etwa 2,4 Petagramm atmosphärisches CO₂. Die Funktion der Wälder wird jedoch zunehmend durch Klimaextreme bedroht, insbesondere durch Dürreereignisse, deren Häufigkeit, Intensität und Dauer im Laufe des 21. Jahrhunderts voraussichtlich zunehmen werden. Trotz der Bedeutung extremer Ereignisse für die biogeochemischen Kreisläufe der Wälder fehlt uns ein mechanistisches Verständnis der physiologischen Prozesse, die Stressreaktionen, Erholungsdynamiken und Langzeitauswirkungen steuern, die zu mehrjährigen Veränderungen der Waldfunktionen führen. Stressbedingte Funktionsbeeinträchtigungen können über verschiedene physiologische Wege wie hydraulische Schäden, metabolische Herunterregulierung und Kohlenstoffverarmung ablaufen. Dennoch ist nach wie vor wenig darüber bekannt, wie Dürremerkmale wie Schweregrad und Dauer bestimmen, welche Mechanismen Stress- und Erholungsreaktionen dominieren.

Die vorliegende Arbeit zielt darauf ab, das Verständnis dafür zu verbessern, wie sich Dürre auf die physiologischen Prozesse von Bäumen über mehrere zeitlichen Skalen hinweg auswirkt, von unmittelbaren Stressreaktionen über kurzfristige Erholung bis hin zu langfristigen Spätfolgen. Die folgenden Forschungsfragen wurden untersucht: (1) Wie wirken sich fortschreitende Dürre und Hitzestress auf die Photorespiration und die anschließende Regulierung von oxidativem Stress aus? (2) Wie begrenzt die Schwere der Dürre mechanistisch das kurzfristige Erholungspotenzial des Gasaustauschs und des Wachstums von Pflanzen? (3) Wie verändern sommerliche Dürreereignisse die Dynamik der internen Kohlenstoffreserven der Pflanzen und beeinflussen so die Ausprägung der Langzeitauswirkungen in der folgenden Vegetationsperiode?

Um diese Fragen zu beantworten, wurden drei Gewächshausversuche mit gemäßigten Nadelbaumarten durchgeführt. Im ersten Versuch wurden Weißtannenkeimlinge (*Abies alba*) einer fortschreitenden Dürre in Kombination mit einer Wärmebehandlung (40 °C für 6 Stunden) ausgesetzt. Gasaustauschmessungen unter Umgebungsbedingungen und reduzierten Sauerstoffbedingungen bewerteten den Beitrag der Photorespiration zur Kohlenstoffaufnahme, während der Gehalt an Wasserstoffperoxid und Peroxidase in den Blättern die Regulierung des oxidativen Stresses bewertete. Im zweiten Experiment wurden Douglasienkeimlinge (*Pseudotsuga menziesii*) entweder einer leichten oder einer schweren Dürre ausgesetzt, gefolgt von einer 35-tägigen Erholungsphase. Ein speziell angefertigtes Gasaustauschkammersystem maß kontinuierlich die CO₂- und H₂O-Flüsse über und unter der Erde, während Stammdendrometer die Wachstumsdynamik verfolgten. Durch regelmäßige destruktive Probenahmen wurden das Wasserpotenzial, das Abscisinsäuregehalt der Blätter und die nichtstrukturellen Kohlenhydrate bewertet, um physiologische Einschränkungen der Erholung zu identifizieren.

Im dritten Experiment wurden junge Europäische Lärchen (*Larix decidua*) und Waldkiefern (*Pinus sylvestris*), die unterschiedliche saisonale Blattgewohnheiten aufweisen (laubabwerfend vs. immergrün), einer längeren Sommerdürre ausgesetzt und anschließend während der folgenden Vegetationsperiode im Freien überwacht. An vier Zeitpunkten im Herbst, Winter und Frühjahr wurden Proben von nichtstrukturellen Kohlenhydraten aus Knospen und Zweigen genommen, um die saisonale Kohlenstoffdynamik zu verfolgen, während die Phänologie überwacht und die Produktion von neuem Gewebe bewertet wurde, um die Auswirkungen zu quantifizieren. Die Ergebnisse des ersten Experiments zeigten, dass

der Beitrag der Photorespiration zur Kohlenstoffassimilation der Pflanzen entlang des Gradienten der Dürreintensität variierte. Eine leichte Dürre führte zu einem leichten Anstieg der Photorespiration (+5 %), da die Schließung der Spaltöffnungen das interzelluläre CO₂ reduzierte, während eine schwere Dürre die Photorespiration verringerte (-14 %), da nicht-stomatal bedingte Stoffwechselbeschränkungen dominierten. Trotz variabler Photorespirationsraten wurde die Anreicherung von Wasserstoffperoxid durch einen raschen Anstieg der Peroxidase-Enzymaktivität streng reguliert, wodurch das Potenzial für oxidative Stresssignale selbst unter kombiniertem Dürre- und Hitzestress begrenzt wurde. Das zweite Experiment zeigte, dass die Erholung von Trockenheit in erster Linie durch strukturelle hydraulische Einschränkungen und weniger durch die Kohlenstoffverfügbarkeit oder hormonelle Signale bestimmt wird. Nach einer schweren Trockenheit, die zu einem geschätzten Verlust der hydraulischen Leitfähigkeit von 70–85 % führte, erholten sich das Wasserpotenzial und die Abscisinsäure innerhalb von zwei Tagen nach der Wiederbewässerung auf das Kontrollniveau, während die Stomatalleitfähigkeit und das Wachstum noch wochenlang beeinträchtigt blieben. Das Verhältnis von Splintholzfläche zu Blattfläche (Huber-Wert) erwies sich als der wichtigste Faktor für die Erholung, da die durch die Trockenheit gehemmte Stammentwicklung zu einer unzureichenden hydraulischen Versorgung führte. Nichtstrukturelle Kohlenhydrate blieben während der gesamten Erholungsphase auf oder über dem Kontrollniveau, was die Annahme in Frage stellte, dass die Kohlenstoffverfügbarkeit die Funktion nach einer Trockenheit einschränkt.

Das zweite Experiment ergab, dass die Erholung nach einer Dürre in erster Linie durch strukturelle hydraulische Einschränkungen und weniger durch die Verfügbarkeit von Kohlenstoff oder hormonelle Signale bestimmt wird. Nach einer schweren Dürre, die zu einem geschätzten Verlust der hydraulischen Leitfähigkeit von 70 bis 85 % führte, erholten sich das Wasserpotenzial und die Abscisinsäure innerhalb von zwei Tagen nach der Wiederbewässerung auf das Kontrollniveau, während die Stomatalleitfähigkeit und das Wachstum noch wochenlang beeinträchtigt blieben. Das Verhältnis von Splintholzfläche zu Blattfläche (Huber-Wert) erwies sich als der wichtigste Faktor für die Erholung, da die durch die Dürre gehemmte Stammentwicklung zu einer unzureichenden hydraulischen Versorgung führte. Nichtstrukturelle Kohlenhydrate blieben während der gesamten Erholungsphase auf oder über dem Kontrollniveau, was die Annahme in Frage stellte, dass die Kohlenstoffverfügbarkeit die Funktion nach einer Dürre einschränkt.

Im dritten Experiment veränderte eine moderate, längere Dürre die Zusammensetzung und Mobilisierung nichtstruktureller Kohlenhydrate in der folgenden Vegetationsperiode. Die Kohlenhydratakkumulation in den Zweigen im Herbst war bei Lärchen trotz normaler Herbstalterungsmuster um >70 % reduziert, während Kiefern eine normale Akkumulation aufwiesen. Die Mobilisierungsmuster im Winter deuteten auf eine kompensatorische Umverteilung aus distalen Speicherpools bei dürrestressbefallenen Bäumen beider Arten hin. Bis zur Mitte des Knospenaufbruchs wiesen Lärchen ein signifikantes Kohlenhydratdefizit auf, während Kiefern vor dem Knospenaufbruch vermutlich aufgrund des anhaltenden Laubbestands erhebliche Kohlenhydrate akkumulierten und einen Kohlenhydratüberschuss aufwiesen. Diese veränderte Kohlenhydratdynamik korrelierte mit einem früheren und langsameren Knospenaufbruch bei Lärchen sowie einer starken Verringerung der Produktion von neuem Gewebe (~50 % bei laubabwerfenden Lärchen, ~25 % bei immergrünen Kiefern), wodurch ein kohlenstoffvermittelter Weg in der Ausprägung von Trockenheitsfolgen etabliert wurde, während gleichzeitig die Blattform als Determinante für die Anfälligkeit gegenüber Folgen identifiziert wurde.

Die Ergebnisse dieser Arbeit zeigen, dass Trockenheitsmerkmale wie Schweregrad und Dauer weitgehend bestimmen, welche physiologischen Mechanismen die Stressreaktionen dominieren und die Erholungsprozesse prägen. Eine milde Dürre induziert in erster Linie eine passive Stomatalregulation, ohne schwere hydraulische Schäden oder hormonelle Reaktionen auszulösen, was eine schnellere funktionelle Wiederherstellung ermöglicht. Dennoch stört eine milde Dürre, wenn sie sich über einen längeren Zeitraum erstreckt, die saisonale Kohlenhydratdynamik, was zu einer veränderten Frühjahrsphänologie und einer verringerten Gewebeproduktion in der folgenden Vegetationsperiode führt. Eine schwere Dürre löst qualitativ unterschiedliche Wege aus, die Abscisinsäuresignale, nicht-stomatal Die Identifizierung des Huber-Wertes als messbarer Prädiktor für die Erholungsfähigkeit und der Blatttrieb als Determinante für die Vererbungsanfälligkeit bieten merkmalsbasierte Rahmenbedingungen für die Bewertung der artspezifischen Resilienz. Angesichts der zunehmenden Häufigkeit von Dürren ist das Verständnis dieser von der Schwere abhängigen Reaktionen unerlässlich, um mechanistische Vorhersagen über die Zusammensetzung und Produktivität von Wäldern unter neuen Klimabedingungen zu entwickeln.

List of Publications

The content and structure of the included publications is retained in the form of the original publication or submission. Chapters 2, 3, and 5 are included in the state following acceptance from peer-review but before journal typesetting. Chapter 4 is presented in the state of submission to the journal.

Chapter 2

Reference:

Alongi, F., Petrík, P., Ruehr, N.K., 2024. Drought and heat stress interactions modify photorespiration and hydrogen peroxide content in Silver fir. *Tree Physiology*.

[https://doi.org/10.1093/treephys/tpae126 tpae126](https://doi.org/10.1093/treephys/tpae126).

F.A., N.K.R., and P.P. conceived and designed the experiment. F.A. analyzed the data and drafted the initial manuscript, with input from N.K.R. and P.P.

Chapter 3

Reference:

Alongi, F.; Knüver, T.; McAdam, S.A.M.; Ziegler, Y.; Gast, A.; Ruehr, N.K., 2025. Drought-induced delays in stem hydraulic development shape gas exchange and growth recovery in Douglas fir. *Plant Physiology*. *Plant Physiology - Accepted*.

Credit statement:

F.A. and N.K.R. conceived and designed the experiment. F.A. and S.A.M. analyzed the data. F.A. drafted the initial manuscript with input from T.K., S.A.M., Y.Z., A.G., and N.K.R.

Chapter 4

Reference:

Alongi F.; Knüver T.; Blumstein M.; Sontheim A.; Zeppan J.; Reddy S.; Brandfonbrener J.; and Ruehr N.K. Carbon-mediated drought legacy effects differ between two forest species with contrasting leaf habit. *In review*

Credit Statement:

FA and NKR contributed to the conceptualization. FA and NKR contributed to the methodology. FA and NKR contributed to the funding acquisition. FA, TK, MB, AS, JZ, and SR contributed to the data collection and analysis. FA contributed to the writing – original draft. FA, TK, MB, SR, JZ, AS, and NKR contributed to the writing – review and editing.

Chapter 5

Reference:

Alongi, F.; Petek-Petrik, A.; Mukarram, M.; Torun H.; Schuldert B.; and Petrík P. 2025. “Somatic Drought Stress Memory Affects Leaf Morpho-Physiological Traits of Plants via Epigenetic Mechanisms and Phytohormonal Signalling.” *Plant Gene* 42 (June):100509.

Credit statement:

F.A., B.S., and PP wrote the original draft. P.P.A., M.M., and T.H. assisted with revisions and manuscript editing

During my PhD project, I have also contributed to the following publications. These papers are not included as chapters in this thesis, but were used in the interpretation of results.

- Ulrich D.; Wasteneys C.; Hoy-Skubik S.; **Alongi F.** Functional traits underlie specialist-generalist strategies in whitebark pine and limber pine. *Forest Ecology and Management* 2023, 542, 121113
- Ziegler Y.; **Alongi F.**; Knüver T., Grote, R.; Ruehr N.K. Capturing drought stress signals: The potential of micro-dendrometers for monitoring tree water status. *Tree Physiology* 2024, tpaе140
- Sparks K.; Hoy-Skubik S.; **Alongi F.**; Runyon J.; Banner K.; Smithers B.; Ulrich D. Comparing juvenile physiology and morphology of two high-elevation pines, *Pinus albicaulis* and *P. balfouriana*. *Forest Science* 2025, 1-29
- **Alongi F.**; Malone S.; Ulrich, D.E.M.; Hoy-Skubik S.; Trowbridge A. Drought and methyl jasmonate deplete non-structural carbohydrates to similar levels but induce divergent terpene responses in *Pinus edulis* seedlings. *Accepted - Tree Physiology*
- Knüver T.; **Alongi F.**; Mayr S.; Beikircher B.; Ruehr N.K. Metabolic inhibition of photosynthesis and carbon sink limitations suppress post-drought growth recovery in Norway spruce. *In Review*
- **Alongi F.**; Blumstein M.; Sontheim A.; Hoy-Skubik S.; Ulrich D.E.M.; Ruehr N.K. Nonstructural carbohydrate refilling following carbon starvation suggests an active to passive sink gradient. *In Prep*

Abbreviations

ABA	Abscisic acid
A_{net}	Net photosynthetic rate (also written as A)
ANOVA	Analysis of variance
APX	Ascorbate peroxidase
ATP	Adenosine triphosphate
C	Carbon
CBF	C-repeat binding factor
CEF	Cyclic electron flow
CO_2	Carbon dioxide
COR	Cold-regulated genes
DREB	Dehydration-responsive element-binding protein
DW	Dry weight
E	Transpiration rate
ETR	Electron transport rate
Fv/Fm	Maximum quantum efficiency of photosystem II
GPP	Gross primary productivity
gs	Stomatal conductance to water (also written as gsw)
H_2O_2	Hydrogen peroxide
JA	Jasmonic acid
LMA	Leaf mass per area
MPa	Megapascal
MS	Mass spectrometry
N	Nitrogen
NADPH	Nicotinamide adenine dinucleotide phosphate (reduced form)
NPQ	Non-photochemical quenching
NSC	Nonstructural carbohydrate
O_2	Oxygen gas

P	Phosphorus
PAR	Photosynthetically active radiation
PCA	Principal component analysis
PERMANOVA	Permutational multivariate analysis of variance
POD	Peroxidase
PR	Photorespiration
PSII	Photosystem II
PYL	Pyrabactin resistance 1-like protein
PYR	Pyrabactin resistance protein
RH	Relative humidity
ROS	Reactive oxygen species
RuBP	Ribulose-1,5-bisphosphate
Rubisco	Ribulose-1,5-bisphosphate carboxylase/oxygenase
SA	Salicylic acid
SE	Standard error
SLA	Specific leaf area
SWC	Soil water content
VPD	Vapor pressure deficit
WUE	Water use efficiency
WUEi	Intrinsic water use efficiency
Ψ	Water potential

List of Figures

Figure 2.1: Drought treatment impact on soil water content (SWC), branch water potential (Ψ_{md}), and changes in stem diameter during the experimental period.

Figure 2.2: Photorespiration and Rubisco carboxylation efficiency derived from measurements of photosynthetic carbon at the mid-drought and end-drought timepoint, with additional heat stress applied at end-drought.

Figure 2.3: Rubisco carboxylation efficiency in response to soil water content (SWC) in silver fir.

Figure 2.4: Treatment effects on electron transport rate (ETR) in silver fir.

Figure 2.5: Treatment effects on foliar hydrogen peroxide (H_2O_2) and peroxidase levels in silver fir.

Figure 3.1: Water potential, abscisic acid, and stomatal conductance during drought and recovery.

Figure 3.2: Relationship of stomatal conductance to Huber value development and water use efficiency.

Figure 3.3: 3D visualization of relationship between Huber value, VPD, and stomatal conductance.

Figure 3.4: Photosynthesis and net carbon accumulation during drought and recovery.

Figure 3.5: Nonstructural carbohydrate dynamics during drought and recovery.

Figure 3.6: Basal area and diurnal growth patterns during drought and recovery.

Figure 3.7: Schematic overview of the mechanistic recovery pathways.

Figure 3.8: Experimental overview and sampling timeframe.

Figure 4.1: Experimental overview.

Figure 4.2: Seasonal progression of autumn leaf phenology following the experimental summer drought.

Figure 4.3: Seasonal progression of spring leaf phenology (budburst) the year following an experimental drought.

Figure 4.4: Seasonal dynamics of non-structural carbohydrates (NSC) components in bud and branch tissues.

Figure 4.5: Interseasonal changes of total available NSC.

Figure 4.6: Leaf function and tissue morphology in newly developed growth during the growing season following an experimental summer drought

Figure 4.7: Correlation heatmap showing the relationship between legacy non-structural

carbohydrate (NSC) effects in branch tissue and phenological or morphological legacy effects.

Figure 5.1: Overview of drought memory pathways from epigenetic priming to adaptive outcomes at leaf level via hormonal signalling and leaf morpho-physiological changes.

Figure 5.2: Drought stress exposure and altered gene expression mechanisms.

Figure 5.3: Graphical overview of epigenetic pathways of phytohormone control as drought memory components after drought stress.

Figure 5.4: Genes and phytohormonal signals regulating drought priming responses.

Figure 5.5: Recovery trajectories as dependent upon drought priming.

Figure 6.1: Thesis synthesis figure.

List of Tables

Table 2.1: Summary of mixed-effect models comparing the individual and interactive effects of drought (mild-drought, severe-drought) and heat treatment.

Table 4.1: Summary of photosynthetic, hydraulic, and growth parameters during the two-month drought treatment.

Table 5.1: Overview of micro-RNAs and their regulation targets that affect leaf morphophysiological traits in relation to drought tolerance.

1 Introduction

1.1 Forests under a changing climate

Forests compose approximately one-third of the Earth's terrestrial surface and are among the most ecologically significant ecosystems on the planet. Forests provide valuable ecosystem services by supporting rich biodiversity, stabilizing soils and hydrological processes which reducing the risks of natural disasters, while serving as net carbon sinks to partially mitigate the effects of climate change. Forests store an estimated 600 gigatons (Gt) of carbon globally and absorb approximately 2.4 ± 0.4 petagrams of carbon dioxide annually (Pan et al. 2011), limiting the rise in atmospheric CO₂ from anthropogenic emissions. Additionally, healthy forests support economic development through sustainable timber production while providing for cultural and recreational livelihoods.

Forests regulate their biogeochemical cycles to dynamically interact with their local climate. Evapotranspiration from forest canopies largely influence local precipitation patterns and enhances moisture recycling. Evapotranspiration is crucial in moderating local temperatures, as energy used to evaporate liquid water can be removed from that system (Butt et al. 2023). This cooling function is particularly critical in the context of climate change, as abiotic stresses like drought reduce evapotranspiration, initiating feedback-loops which can drastically increase local temperatures.

Anthropogenic climate change has led to an increase of atmospheric CO₂ from pre-industrial levels from around 280 ppm to 425 ppm in 2025. While increasing atmospheric CO₂ can enhance C uptake in forests due to increased photosynthetic efficiency (Walker et al. 2021), this increase is also accompanied by a greater frequency, intensity, and duration of extreme climate events such as heatwaves and drought, negatively impacting the terrestrial C sink (Fan et al. 2023). Furthermore, the capacity of forests to remain as terrestrial C sinks remains unclear, with pressures such as ageing forests, land use change, and greater future disturbance all projected to reduce ecosystem productivity (Pan et al. 2024).

Across biomes, there is mounting evidence that forests are already responding to greater abiotic stress. Drought and heatwaves are known to lower forest productivity while increasing mortality risk and reducing forest regeneration. These impacts have been acutely

observed in recent years, where extreme stress events have led to widespread forest dieback (Hartmann et al. 2022). Compounding these challenges, the long generational times of most forest tree species constrain their capacity to respond to rapid climate-driven selection pressures through adaptive evolution. However, many species display considerable phenotypic plasticity, which allows them to modify key physiological traits to increase their resilience to extreme climate events. While plastic responses may convey measurable resistance to stress, these effects may only be beneficial at limited timescales. An increasing frequency of abiotic stress events can outpace the typical recovery window of critical plant functions, meaning stress events reoccur before full physiological function has been restored. As such, the temporal scale of tree recovery may become increasingly mismatched as extreme events become more frequent, leading to continuous reductions in forest resilience over time (Marchand et al. 2025). Despite a growing awareness of these threats to forest resilience, significant uncertainties remain regarding how such stress-induced physiological responses are reversed upon the restoration of optimal growth conditions.

1.2 Impacts of abiotic stress on tree gas exchange

One of the earliest physiological responses to drought stress in trees is the reduction in stomatal conductance, a mechanism which limits water losses through transpiration. However, reductions in stomatal conductance also restricts CO₂ entry into the leaf, lowering the concentration of intercellular CO₂, thereby reducing photosynthetic C assimilation. As substrate availability for carboxylation declines, Rubisco, which facilitates the fixation of C from CO₂ during photosynthesis, increases its relative rate of oxygenation (Ku and Edwards 1978). This shift enhances the occurrence of photorespiration (PR), where O₂ replaces CO₂ in the Rubisco active site, leading to the release of atmospheric CO₂ while consuming ATP and NADPH (Sharkey 1988; Bauwe et al. 2010). Nearly all forest tree species utilize C₃ photosynthesis, making them susceptible to C losses through PR, which are estimated to lower carbon assimilation losses by approximately 25% under normal conditions (Raghavendra 2003). Heat stress can further exacerbate PR, as rising temperatures increase the solubility of O₂ relative to CO₂, while also modifying Rubisco kinetics, decreasing its affinity for CO₂ while increasing misfire rates (Salvucci and Crafts-Brandner 2004; Bracher et al. 2017)

One of the major byproducts of PR is hydrogen peroxide (H₂O₂), which is primarily generated in the peroxisome via glycolate oxidation (Noctor et al. 2002). PR is responsible

for the production of approximately 70% of cellular H₂O₂. While H₂O₂ is traditionally viewed as a damaging oxidative agent (ROS), recent studies have emphasized its critical role as a stress-signaling molecule during abiotic stress (Voss et al. 2013; Strand et al. 2015). H₂O₂ is involved in transcription regulation of numerous stress-response genes and mediates hormonal signaling pathways, notably abscisic acid (ABA)-induced stomatal closure (Bright et al. 2006; Marinho et al. 2014). Furthermore, H₂O₂ signaling has been implicated in regulating the alternative oxidase pathway, which suppresses ROS accumulation by supporting antioxidant enzyme production (Sunil et al. 2019).

The role of H₂O₂ in regulating plant stress physiology is double-sided. While it may serve as a critical signaling molecule to regulate stress-sensitive gene expression and hormonal signaling pathways, H₂O₂ can become cytotoxic at high concentrations, leading to cellular membrane, protein, and DNA damage. To balance this, plants rely on antioxidant systems, including scavenging enzymes such as peroxidases to maintain H₂O₂ within functional limits (Abogadallah 2011). However, the efficacy of these regulatory mechanisms varies across species, tissue type, as well during periods of elevated PR like during drought and heat events. Despite this, the coordination between elevated H₂O₂ production, ROS signaling, and antioxidant regulation under concurrent drought and heat stress remains poorly understood, particularly in forest tree species. Experimental investigations into the regulation of H₂O₂ accumulation under compound climate stresses are rare (Zhou et al. 2013; Dewar et al. 2022), representing a significant knowledge gap in understanding the mechanisms that regulate physiological function during abiotic stress.

1.3 Limitations of plant function during post-drought recovery

1.3.1 Restoration of gas exchange

Recovery from stress events such as drought is often defined as a partial or full reopening of stomata to regain photosynthetic function. However, this process is not always immediate upon rehydration. One of the leading limitations to a rapid restoration of gas exchange is due to physical damage sustained by hydraulic failure during drought. Specifically, embolism - pockets of air which disrupt water flow – form during drought events as tension in the conductive xylem tissue exceeds species-specific thresholds for cavitation. These embolisms disrupt water flow, leading to permanent xylem dysfunction, and ultimately lower hydraulic

conductance necessary to maximize stomatal aperture (Rehschuh et al. 2020). This results in a sustained reduction in hydraulic conductivity, which delays or even prevents the full recovery of transpiration and gas exchange, likely until new xylem tissues are formed via sapwood growth to replace dysfunctional conduits (Brodribb and Cochard 2009).

In addition to hydraulic constraints, hormonal regulation plays a crucial role in regulating stomatal function during stress events. Under severe drought stress, abscisic acid (ABA) accumulates to maintain stomatal closure and limit transpiration to minimal levels (Daszkowska-Golec 2016). While ABA concentrations typically decline upon tissue rehydration, stress-induced disruptions in hormonal signaling may lead to hormone levels remaining elevated, leading to ABA-induced stomatal closure limiting the recovery of gas exchange (Brodribb and McAdam 2013).

Plants rely on osmotic regulation to maintain water movement through conductive tissues (Long and Adams 2023). Water moves along gradients of osmotic potential, with the accumulation of osmotically active substances such as free sugars, organic acids, and amino acids lowering cell osmotic potential and helping to maintain hydraulic supply. Among these solutes, soluble sugars derived from non-structural carbohydrates (NSC) play a key role. However, as stomatal conductance remains limited, photosynthetic carbon assimilation is constrained, limiting the new input of solutes. This can lead to a negative feedback loop, where insufficient NSC availability impairs osmotic regulation, which in turn impairs the restoration of hydraulic conductance, and ultimately gas exchange. Thus, carbohydrate availability, whether through stored reserves or new input, are likely to govern the physiological recovery from stress events.

1.3.2 Restoration of growth

Observational studies have documented that growth recovery following drought often lags behind the recovery of gas exchange (Kannenberg et al., 2022), suggesting that photosynthetic function alone does not ensure resumed structural development. Drought stress can disrupt carbon transport to sink tissues by reducing phloem transport of recent assimilates. Phloem tissues are osmotically balanced to the connected xylem tissues to maintain function (Thompson and Holbrook 2003). As xylem water potential declines during drought, phloem tissues osmotically adjust by increasing free sugar content. However, this

rise in phloem carbohydrate content exponentially increases phloem sap viscosity, which increases transport resistance and can lead to phloem collapse (Hölttä et al. 2009).

Furthermore, drought-induced decreases in cambial turgor pressure limit the turgor-sensitive processes of cell division and expansion (Körner 2015), leading to reduced C demand in sink tissues. Together, these hydraulic and transport limitations decouple growth from the availability of photoassimilates, and underscore the need for coordinated recovery of xylem and phloem function to regain growth processes following drought events.

The restoration of growth following drought may additionally be constrained by competition from additional carbon sinks, particularly storage and repair. Reductions in gas exchange during drought events can induce a negative carbon balance, where C losses through the maintenance respiration of living tissues exceeds carbon assimilation, leading to the depletion of NSC reserves in a process referred to as C starvation (Hartmann 2015). However, it remains debated whether NSC refilling is actively prioritized over growth, or whether NSC are only passively replenished after active sink demand (i.e., growth) is met (Landhäuser and Adams 2024; Stefaniak et al. 2024). Additionally, drought-induced tissue damage may necessitate substantial C be allocated for repair, including cellular membrane restoration, organelle regeneration, as well as replacing dysfunctional vascular tissues (Brodrribb and Cochard 2009; Ruehr et al. 2019). These overlapping demands may constrain carbon availability for growth, meaning that even when gas exchange resumes and turgor thresholds are met, growth may still remain restricted until carbohydrate reserves are refilled and cellular repair functions are complete. This complexity highlights the uncertainty regarding how trees allocate carbon following stress recovery and poses a challenge for accurately predicting recovery trajectories.

1.4 Long-term legacy effects of drought on tree function

One of the most consequential yet understudied effects of drought is its potential to induce legacy effects, which continue to alter tree function through subsequent growing seasons (Kannenberg and Phillips 2020; Kannenberg et al. 2020; Sterck et al. 2024). Such legacy effects have been documented to affect multiple plant physiological processes, including disruptions in seasonal phenology, modifications to new tissue function, altered allocation to NSC, and reductions in growing season productivity.

Phenological shifts are among the most commonly observed legacy effects from drought events. Summer drought events have been found to advance or delay autumn leaf senescence (Vander Mijnsbrugge et al. 2016; Sun et al. 2024; Vander Mijnsbrugge et al. 2025) and alter the timing of spring budburst in the following year (Sanz-Pérez and Castro-Díez 2010; Čehulić et al. 2019). These shifts directly influence the length of the growing season with implications for the recovery timeframe in temperate forests.

Another notable legacy effect is the ability for trees to modify foliar function in tissues produced following the drought event. Specifically, studies have reported reductions in specific leaf area and limited stomatal conductance in subsequent-year tissues, which effectively reduce water loss (albeit at the cost of C assimilation) and may enhance resilience to recurrent drought events (Petrik et al. 2022; Wang et al. 2024). However, such functional modifications are not universally observed (Bačurin et al. 2025), suggesting that their expression may depend on specific drought characteristics or even species-specific responses. Furthermore, while these adjustments may serve as a fitness advantage in the case of recurrent drought stress, they may conversely be a fitness disadvantage if such functional modifications restrict the plant's ability to take advantage of optimal growing conditions.

Reduced productivity during the growing season following drought is globally documented in forests, yet the mechanisms which govern this remain poorly understood (Kannenberg et al. 2022). One proposed mechanism resulting in reduced productivity is limited substrate availability. Specifically, drought-induced reductions to carbon assimilation may limit the seasonal accumulation of NSC, which support winter respiration and provide substrate for new tissue development in spring (Tixier et al. 2018). Thus, whether NSC deficits arising from drought persist into the subsequent growing season depends on the post-drought recovery of NSC reserves. However, this process is temporally limited, with the growing season ultimately constrained by the onset of autumn leaf senescence and winter dormancy. Understanding how drought-induced NSC deficits persist to affect subsequent growing season productivity remains poorly understood and requires tracking carbon reserve dynamics throughout the post-drought window while considering how phenological shifts influence NSC recovery.

The molecular basis for drought legacy effects involves epigenetic mechanisms that enable plants to “remember” previous stress exposure. Recent research has identified several

pathways through which drought can induce heritable changes in gene expression without altering DNA sequences, including DNA methylation, histone modifications, and regulation by non-coding RNAs (Luo et al. 2018; Gelaw and Sanan-Mishra 2021). These epigenetic modifications can persist following stress relief and mediate interactions with phytohormonal signaling pathways, particularly involving abscisic acid, jasmonic acid, and cytokinins, to coordinate downstream physiological responses (Liu et al. 2016; Martin et al. 2017; Jiang et al. 2023). Through such mechanisms, drought stress memory may influence the morphological and functional modifications observed in new leaf tissues, regulate the timing of phenological events, and alter stress response capacity during subsequent drought exposure. While most epigenetic research has focused on model species and annual crops, emerging evidence suggests that similar mechanisms operate in perennial woody species, though their specific roles in mediating multi-season legacy effects remain poorly understood.

The mechanistic pathways underlying drought legacy effects likely depend on the severity, duration, and timing of stress events. Severe drought that induces substantial hydraulic damage or triggers strong hormonal and metabolic stress responses may generate different legacy mechanisms than moderate, extended drought that primarily affects seasonal C acquisition. Additionally, species traits such as leaf habit may influence legacy vulnerability, as deciduous species rely entirely on stored NSC for spring leaf-out while evergreen species, which maintain mature foliage interannually, can supplement spring growth demand with recent assimilates. The high variability of legacy responses across studies underscores the need for controlled experiments that can isolate specific physiological mechanisms that determine which legacy pathways dominate.

1.5 Objectives of the thesis

This thesis aims to improve the understanding of the immediate, short-term, and long-term legacy effects of abiotic stress on tree physiological function and stress recovery. In detail, the research objectives of this theses are:

1. Identify how progressive drought and heat stress interact to affect the contribution of photorespiration to photosynthetic efficiency, as well as the resulting regulation of oxidative stress via hydrogen peroxide accumulation.
2. Determine how variable drought severity mechanistically affects the physiological short-term recovery of tree function.
3. Quantify how summer drought events alter nonstructural carbohydrate dynamics across seasons to mediate legacy expression in the following growing season.

1.6 Experimental approach

The objectives of this thesis were addressed in three separate experiments in a greenhouse facility at the Institute of Meteorology and Climate Research in Garmisch-Partenkirchen (KIT-IMKIFU), Germany (708 m a.s.l., 47°28'32.9"N, 11°3'44.2"E). These experiments were carried out on a variety of native and non-native juvenile trees which are commonly used in European forestry. Specifically, we utilized four-year-old silver fir (*Abies alba* Mill.) juveniles (Chapter 2), three-year-old Douglas fir (*Pseudotsuga menziesii*) (Chapter 3), and four-year-old European larch (*Larix decidua*) and Scots pine (*Pinus sylvestris*) in Chapter 4.

Experiment 1 (2023):

To address objective 1, we withheld irrigation from silver fir juveniles while monitoring soil water content and midday water potential. Gas exchange and fluorescence measurements, including net photosynthesis, stomatal conductance, and electron transport rate were collected at mid-drought (11 days) and end-drought (25 days) timepoints. Following end-drought, we imposed a six-hour heat treatment of 40°C, with gas exchange measurements repeated. Measurements on each individual were conducted under both ambient (~21% O₂) and low-oxygen (~2% O₂) conditions to assess Rubisco carboxylation efficiency and photorespiration. Additionally, leaf samples were collected at both the end-drought and heat treatment timepoints to assess foliar hydrogen peroxide and peroxidase content. This study design allowed us to assess the additive and interactive effects of drought and heat stress on

photorespiration as well as the resulting regulation of hydrogen peroxide. This study is reported as Chapter 2.

Experiment 2 (2023):

To address objective 2, Douglas fir juveniles were exposed to 28 days of either mild or severe drought, followed by a 35-day recovery period. “Pilot” individuals were measured periodically for midday water potential, branch NSC content, and foliar ABA content, while additional “chamber” individuals were continuously monitored for above- and below-ground gas exchange as well as changes to stem basal area using custom-built gas exchange chambers. This study design allowed us to identify the physiological impacts of drought severity and how these influenced to immediate functional recovery. This study is reported as Chapter 3.

Experiment 3 (2024-2025)

To address objective 3, juveniles of two species with contrasting leaf habit (deciduous European larch and evergreen Scots pine) were subjected to an extended summer drought period, then placed outside and monitored into the following growing season. We sampled bud and branch tissues for NSC content at four timepoints (end-drought, end-autumn, end-winter, and during active budburst) to track seasonal carbohydrate dynamics. We monitored autumn leaf senescence phenology using spectral indices and spring budburst phenology using a visual scale. Additionally, we quantified legacy responses by measuring the morphology and photosynthetic function of new tissues produced during the following growing season. This study design allowed us to identify how summer drought events mechanistically impact carbon reserve dynamics across dormancy and relate to legacy changes in phenology, morphology, and tissue function. This study is reported as Chapter 4.

1.7 Structure of thesis

The structure of the thesis is organized as follows. Chapter 2 explores the interactive effects of drought and heat stress on photorespiration and hydrogen peroxide accumulation in silver fir. Chapter 3 examines the physiological limitations to tree recovery following drought events of varied intensity in Douglas fir. Chapter 4 investigates legacy effects induced by

summer drought events in European larch and Scots pine, focusing on how altered nonstructural carbohydrate dynamics affect phenology and tissue production in the subsequent growing season. Chapter 5 provides a comprehensive review of epigenetic mechanisms underlying somatic drought stress memory which were not experimentally assessed. Specifically, Chapter 5 examines how DNA methylation, histone modifications, and phytohormonal signaling interact to mediate persistent changes in leaf morphology, physiology, and stress responsiveness. Chapter 6 synthesizes the main findings of this thesis and their implications for abiotic stress response at immediate, short-term, and long-term (legacy) timescales in forest species.

2 Drought and heat stress interactions modify photorespiration and hydrogen peroxide content in Silver fir

This chapter was published as:

Alongi, F., Petrík, P., Ruehr, N.K., 2024. Drought and heat stress interactions modify photorespiration and hydrogen peroxide content in Silver fir. *Tree Physiol.* <https://doi.org/10.1093/treephys/tpae126> tpae126.

Abstract

Photorespiration (PR) greatly reduces net carbon assimilation in trees (by c. 25%), but has received recent attention particular for its potential role in stress-signaling through the accumulation of hydrogen peroxide (H_2O_2), a stress signaling agent. Despite an increasing frequency of drought and heat events affecting forests worldwide, little is known about how concurrent abiotic stressors may interact to affect PR and subsequent H_2O_2 accumulation in trees. Here, we sought to identify how drought and a compounded one-day heat treatment individually and interactively affect PR (determined under variable O_2) in *Abies alba* Mill. seedlings. Additionally, we quantified foliar H_2O_2 accumulation and enzymatic scavenging via peroxidase in relation to PR rates. We found drought stress to slightly increase PR (+5.2%) during mild-drought (12 days, $\Psi_{md} = -0.85$ MPa), but ultimately to decrease PR (-13.6%) during severe-drought (26 days, $\Psi_{md} = -1.70$ MPa) compared to the control, corresponding to increasing non-stomatal limitations of photosynthesis (i.e., decreased electron transport rate). The response of PR to heat stress was dependent on soil water availability as heat stress increased PR in control seedlings (+37.8%), but not in drought-stressed seedlings. Decreased PR during severe-drought corresponded to ~2x lower foliar H_2O_2 compared to the control. Despite increased PR under heat stress in control seedlings, foliar H_2O_2 decreased to near-zero likely due to enhanced scavenging as observed in ~2x greater peroxidase activity. Our results demonstrate that carbon loss to PR during drought stress can be highly dynamic, depending on the severity of soil dehydration. Additionally, increased PR under abiotic stress does not necessarily lead to accumulated H_2O_2 , as tight regulation by scavenging enzymes instead minimize oxidative stress, reducing stress-signaling potential.

2.1 Introduction

The world's forests serve as a global carbon sink, currently accounting for a net removal of $-7.6 \pm 49 \text{ GtCO}_2\text{eyr}^{-1}$ from the atmosphere due to photosynthetic carbon assimilation minus respiratory processes. Photorespiration (PR) has a large impact on the global carbon cycle by reducing carbon assimilation from photosynthesis by c. 25% in nearly all tree species, which predominately utilize C₃ carbon fixation (Sharkey 1988; Raghavendra 2003; Young et al. 2020). Specifically, PR occurs when O₂ rather than CO₂ fills the active site of ribulose-1,5-bisphosphate carboxylase/oxygenase (Rubisco), ultimately consuming ATP and NADPH and releasing CO₂ (Bauwe et al. 2010). Abiotic stress events such as drought and heat have long been known to increase rates of PR (Hochberg et al. 2013; Wolf and Paul-Limoges 2023). Despite these associated losses in carbon assimilation, PR has recently received attention primarily for its potential role in stress tolerance affecting the cellular signaling of metabolic-intermediates such as hydrogen peroxide (H₂O₂; (Voss et al. 2013; Sunil et al. 2019; Ünlüsoy et al. 2023). With drought and heat risk expected to increase in forests worldwide, understanding the responses of PR to abiotic stress is important to better model both future forest carbon fluxes and tree stress responses (Allen et al. 2010; Lloyd et al. 2023; Wolf and Paul-Limoges 2023).

Both drought and heat stress can increase PR, as physiological responses to stress in trees modify the interaction of Rubisco and CO₂ (Ku and Edwards 1978). To minimize water loss during periods of drought stress, plants close stomata, increasing stomatal resistance and reducing the amount of intercellular CO₂ available for carboxylation by Rubisco (Ku and Edwards 1978; Martin-StPaul et al. 2017; Petek-Petrik et al. 2023). As Rubisco preferentially draws down CO₂, the resulting higher O₂:CO₂ ratio can increase PR rates during initial drought (Wingler et al. 1999; Fang et al. 2023). As drought progresses, non-stomatal limitations to photosynthesize may increase as processes in the photosynthetic light reactions like electron transport rate (ETR) become limiting, including a reduction in the regeneration of NADPH and ATP, which are essential for the Calvin cycle and overall carbon assimilation (Flexas and Medrano 2002; Lawlor and Tezara 2009). With increased non-stomatal limitations, intracellular CO₂ no longer is the greatest limitation to photosynthesis, which may relieve photorespiration rates. Heat stress can similarly increase PR rates in trees, as the increased

solubility of O₂ relative to CO₂ at warmer temperatures leads to higher O₂:CO₂ (Ku and Edwards 1977; Doehlert and Walker 1981). In addition, heat stress can enhance PR by altering Rubisco kinetics, such as by decreasing affinity to CO₂ and/or increasing rates of Rubisco misfire (Jordan and Ogren 1984; Salvucci and Crafts-Brandner 2004; Bracher et al. 2017). However, despite their mechanistic similarities and often simultaneous occurrence, the interacting effects of drought and heat stress on PR in trees remains to be directly experimentally investigated, and may represent a limitation in GPP modeling (Zhou et al. 2013; Dewar et al. 2022).

PR is suggested to facilitate abiotic stress tolerance through the regulation of excess photochemical products and/or by stress-signaling through the PR intermediate H₂O₂ (Voss et al. 2013; Sunil et al. 2019; Ünlüsoy et al. 2023). H₂O₂ activates transcription factors of stress-response genes (Marinho et al. 2014), and is used as a secondary messenger in plant-hormone pathways, such as abscisic acid induced stomatal regulation (Bright et al. 2006). During abiotic stress, reduced RuBP-regeneration can lead to an overaccumulation of ATP and NADPH from the light-reactions of photosynthesis, resulting in the inactivation of PSII and increased ROS production (Kato et al. 2003; Bambach et al. 2020). PR can help relieve photoinhibition by consuming excess NADPH and ATP to maintain cyclic electron flow (CEF) and dissipate excess energy, which may be particularly important for trees during heat stress (Flexas and Medrano 2002b; Peñuelas and Llusià 2002; Takagi et al. 2016). While H₂O₂ can originate from multiple cellular compartments such as chloroplasts during high light, in the mitochondrion during respiration, and the metabolism of ROS, 70% is produced via glycolate oxidation in the peroxisome during PR (Noctor et al. 2002; Voss et al. 2013; Strand et al. 2015). H₂O₂ can also upregulate the alternative oxidase pathway, which limits ROS accumulation and maintains redox balance by increasing scavenging enzyme activity (Sunil et al. 2019). As H₂O₂ itself is a ROS that can cause cellular damage, concentrations are continuously regulated by a series of scavenging enzymes like peroxidases and catalases, as well as chemical pathways like the glutathione-ascorbate cycle to minimize oxidative stress. Thus, it remains unclear how potential increases in PR during abiotic stress like drought and heat may affect H₂O₂ accumulation and enzymatic scavenging (Abogadallah 2011).

In this study, we aimed to identify how drought and heat stress individually and interactively affected the contribution of PR to carbon assimilation, as well as to H₂O₂ accumulation and scavenging in silver fir (*Abies alba* Mill.) seedlings. Silver fir is a native conifer widespread

throughout Europe. While silver fir is considered as a potential alternative to Norway spruce because it is able to draw water from deeper depths, it may still be particularly sensitive to drought and heat stress (Stangler et al. 2022). To further explore this sensitivity, we exposed silver fir seedlings to a 25-day drought, followed by a six-hour heat wave at 40°C. Gas exchange and electron transport rates were determined to estimate PR during mild and severe drought, as well as during a subsequent heat event. Additionally, we analyzed foliar concentrations of H₂O₂ and peroxidase (POD), a major enzymatic H₂O₂ scavenging class. We hypothesize that the relative contribution of PR to net carbon assimilation increases with drought progression, and would be greatest during combined drought and heat stress. Additionally, we hypothesize that foliar H₂O₂ concentration increase with PR during drought and heat stress, outpacing increased POD activity.

2.2 Materials and Methods

2.2.1 *Plant material and growth conditions*

We obtained bare-rooted four-year-old *Abies alba* seedlings from a tree nursery in Gunzenhausen, Germany in March 2023. Seedlings had an average aboveground height of 32.29 cm ± 0.78, and an average diameter of 9.53 mm ± 0.30 two cm above the soil level. Seedlings were planted in 5.7L pots containing a mixture of peat substrate and perlite (5:1). Osmocote® 5 8-9 month slow-release fertilizer (16-8-12 + 2.2MgO + TE; ICL Specialty Fertilizers) was added to all pots at a rate of 1g/L. During the pre-experimental period (March 2023 – August 2023) seedlings were kept outdoors at an experimental greenhouse facility in Garmisch-Partenkirchen, Germany (708 m a.s.l., 47°28'32.9" N, 11°3'44.2" E). In August 2023, seedlings were moved inside the greenhouse facility to acclimate to greenhouse conditions for three weeks. Seedlings were automatically drip irrigated with 60 mL water twice daily (08:00, 21:00; Rain Bird, Azusa, USA), with LED grow lamps maintaining a 15-h photoperiod (LED-KE 400 VSP, DHLicht, Wuelfrath, Germany). Continuously measured photosynthetic active radiation (PAR) reached daytime averages of 550-650 µmol m⁻², while temperature and relative humidity were maintained at 23 °C and 55% respectively (Figure S2.1, PQS 1, Kipp & Zonen, Delft, The Netherlands).

2.2.2 *Experimental Conditions*

Twenty seedlings were randomly assigned to either a well-watered control (n=10) or drought treatment (n=10). On August 26th 2023, irrigation was withheld completely from the drought treatment while the control treatment continued to receive drip irrigation. Soil volumetric water content (SWC) was measured throughout the experimental period in all pots (10HS, Meter Group, USA), with control seedlings maintaining ~37% SWC throughout the experimental period. Midday branch water potential (Ψ_{md}) was periodically measured on randomly selected individuals to track drought progression by removing axial branches and immediately measuring with a Scholander-type pressure chamber (Model 600D, PMS Instruments, Oregon, USA).

Gas exchange and fluorescence measurements were collected on August 26th (experimental start) September 6th (mild-drought), and September 20th 2023 (severe-drought), beginning at midday and lasting c. 3 hours. Additionally, leaf temperature (T_{leaf} ; PI 450, Optis, Germany), and samples for chemical analysis were collected on all individuals during severe-drought. On September 21st 2023 at 6:00, greenhouse daytime air temperature was increased to 40 °C, beyond the thermal optimal in silver fir (Robakowski et al. 2002; Húdoková et al. 2022). Heat stress was maintained for six hours before repeated collection of gas exchange and fluorescence measurements, leaf temperature, and samples for chemical analysis on both control + heat treatment (formerly control) and drought + heat treatment (formerly drought) individuals. All gas exchange and chemical analyses were performed on current-year growth.

2.2.3 *Gas exchange and fluorescence measurements*

Branches with c. 6 leaves (aligned flat for consistent coverage) were measured for net photosynthetic carbon assimilation rate (A_{net}), stomatal conductance (g_{sw}) and electron transport rate (ETR) using a LI-6800 portable photosynthesis system equipped with the 6800-01A multiphase flash fluorometer (LI-COR Biosciences, Lincoln, Nebraska, USA). The 2-cm² cuvette conditions were set to: 600 $\mu\text{mol m}^{-2} \text{s}^{-1}$ photosynthetic photon flux density (estimated saturation point from light-response curves, Figure S2.2), 400 ppm [CO₂] and a 750 $\mu\text{mol s}^{-1}$ flow rate using ambient humidity levels (~25-55%, Figure S2.1). Air temperature inside the

cuvette was set to 25°C at measurement timepoints before heat stress, and to 40°C during heat stress to reflect greenhouse air temperature. Directly following the measurement under ambient air (~21%-O₂), while the cuvette was still attached to the leaves, reduced oxygen air (~2% -O₂) at the same flow rate and same CO₂ concentration was supplied to the cuvette. The measurements were taken after instrumental stability of A_{net} (slope < 0.5 $\mu\text{mol CO}_2 \text{ m}^{-2} \text{ s}^{-1} \text{ min}^{-1}$) and g_{sw} (slope < 0.01 mol m⁻² s⁻¹ min⁻¹) was reached, with a minimum stabilization time of one minute. The ~2%-O₂ A_{net} was compared to that measured under ~21%-O₂, with their ratio being an estimation of Rubisco carboxylation efficiency, and their difference being the estimation of PR (Sharkey 1988; Yin et al. 2020). The air source provided to the LI-6800 was modified using a three-way valve connected to an air tank containing 2%-O₂ in N₂, with another valve open to ambient air. All parameters were recalculated using individually measured leaf area within the 2-cm² cuvette.

2.2.4 *Chemical analysis: Hydrogen peroxide and Peroxidase activity*

Axial branches of c. 10 cm were harvested from all individuals at both severe-drought and during subsequent heat stress, with leaves being removed and immediately flash frozen in liquid nitrogen. Frozen leaf material was ground to a fine powder in liquid nitrogen using mortar and pestle. Hydrogen peroxide (H₂O₂) concentration was quantified using the AmplexTM Red Hydrogen Peroxide/Peroxidase Assay Kit (ThermoFisher Scientific, Waltham, Massachusetts, USA), as described in Chakraborty et al. (2016). In short, the oxidation of AmplexTM Red reacts in 1:1 stoichiometry with H₂O₂ in the presence of peroxidase resulting in the fluorescent product resorufin, which we measured using a spectrophotometer for absorbance at 560nm following excitation between 530-560 nm (Epoch 2, BioTek, Vermont, USA). Sample H₂O₂ concentrations were determined by comparing absorbances to a standard curve of known H₂O₂ concentrations, with all samples saturated with horseradish peroxidase. Peroxidase enzymatic activity (POD) was quantified using the same reagents following a similar procedure, where concentrations were determined by comparing absorbances to a POD standard curve, with all samples instead saturated with H₂O₂. POD activity is reported in units (U), defined by the manufacturer as the amount of enzyme that forms 1.0 mg purpurogallin from pyrogallol in 20 seconds at pH 6.0 and 20°C. Additional fresh leaf samples were taken at each sampling day to standardize chemical concentrations from fresh material analyses to dry weight (DW) by weighing the fresh and dried (at 60°C for 48 hours) samples.

2.2.5 Statistical analysis

All statistical analyses and data visualizations were conducted in the R statistical programming environment v4.3.2 (R Core Team 2022). The contribution of PR to net carbon assimilation was assessed using linear mixed-effect regression to model the relationship between A_{net} at both 21%-O₂ (ambient) and 2%-O₂ (PR suppressed) using the package *nlme* (Pinheiro et al. 2023). This relationship indicates the relative efficiency of Rubisco carboxylation, where slopes closer to one represent less PR. Differences in slope (interactions) were assessed across levels of drought and heat treatments as main effects, with plant ID as a random effect to account for repeated measures during the heat treatment. Similar mixed effect models were used to evaluate the additive and interactive effects of drought and heat treatment on T_{leaf}, H₂O₂, and POD. Family-wise comparisons across treatment combinations were performed using Tukey's Honest Significant Difference (*emmeans* package; Lenth et al. 2024) and informed compact letter displays in figures with a 0.05 significance level. Parametric modeling assumptions of normality, equal variance, and influential points (Cook's distance > 0.5) were verified using diagnostic plots. Due to heteroscedasticity when modeling H₂O₂, weights were assigned to each observation based on variance of the residuals. All parameter means are reported with standard error.

2.3 Results

2.3.1 Treatment progression

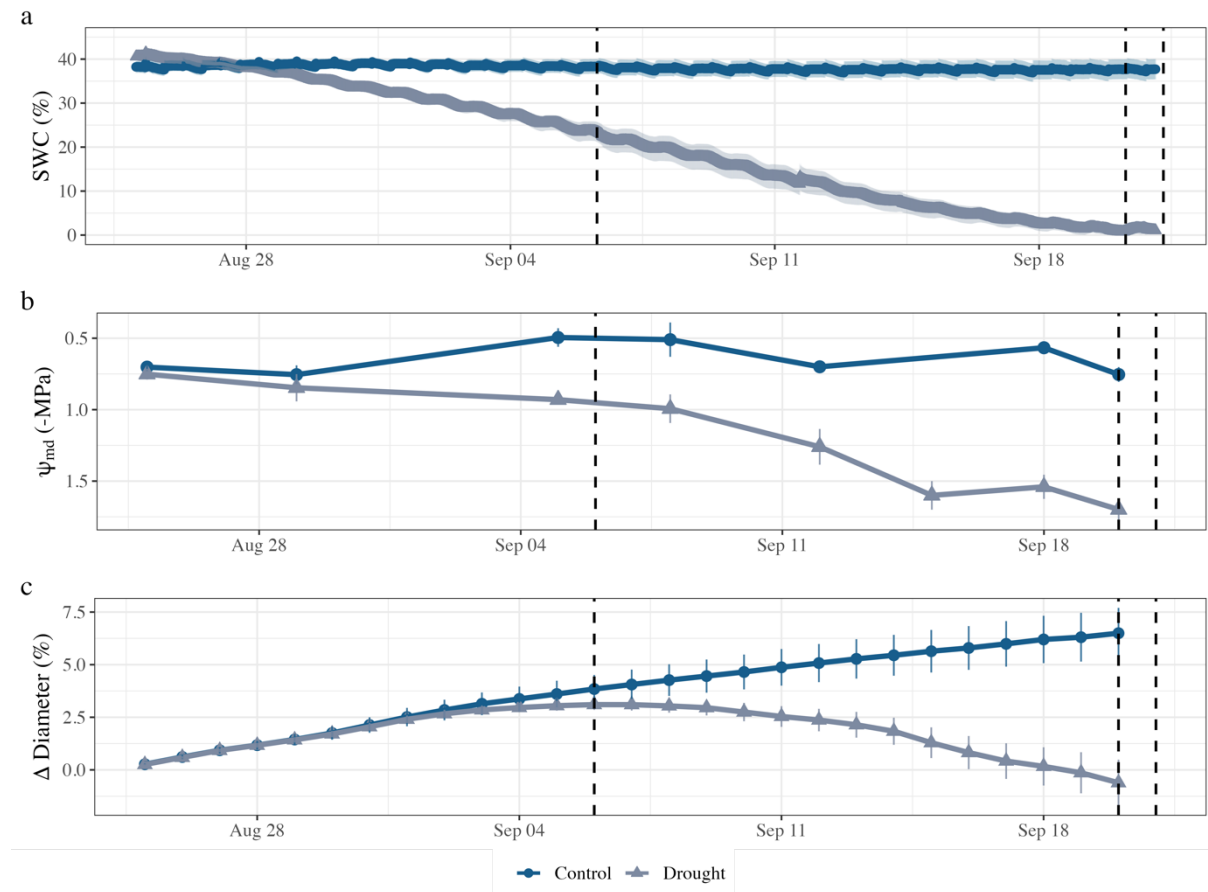


Figure 2.1: Time series visualization of volumetric soil water content (SWC, a), midday branch water potential (Ψ_{md} , b), and percent change in stem diameter (c) during the experimental period. Data points are displayed with standard error, while vertical black lines represent mild-drought, severe-drought, and heat treatment timepoints, respectively.

During the experiment drought, soil volumetric water content (SWC), midday plant water potential (Ψ_{md}), and stem radial diameter progressively declined (Figure 2.1), and were significantly different from control trees during both mild- and severe-drought (both $p < 0.001$). By severe-drought, volumetric SWC had declined to $2.28\% \pm 3.26$ compared to $37.01\% \pm 2.46$ in the control, while Ψ_{md} had declined to $-1.70 \text{ MPa} \pm 0.08$ compared to $-0.75 \text{ MPa} \pm 0.05$ in the control. Stem radial diameter in the drought treatment decreased by $0.61\% \pm 1.10$ during the experimental period, while control tree diameter increased by $6.50\% \pm 1.20$ over the same period.

During the one-day heat event, midday T_{air} increased by 16 °C to 39 °C, while RH decreased from 58% to 31.5% (Figure S2.1), corresponding to an increase of ambient vapor pressure deficit (VPD) from 1.18 kPa to 4.75 kPa. Both drought and heat stress individually increased T_{leaf} (both $p < 0.001$): in the drought + heat treatment it was highest with $42.4 \text{ }^{\circ}\text{C} \pm 0.36$, followed by the control + heat treatment with $40.5 \text{ }^{\circ}\text{C} \pm 0.41$, the drought treatment with $28.5 \text{ }^{\circ}\text{C} \pm 0.11$, and the control with $25.4 \text{ }^{\circ}\text{C} \pm 0.27$, (Figure S2.3).

2.3.2 Photorespiration and chlorophyll fluorescence

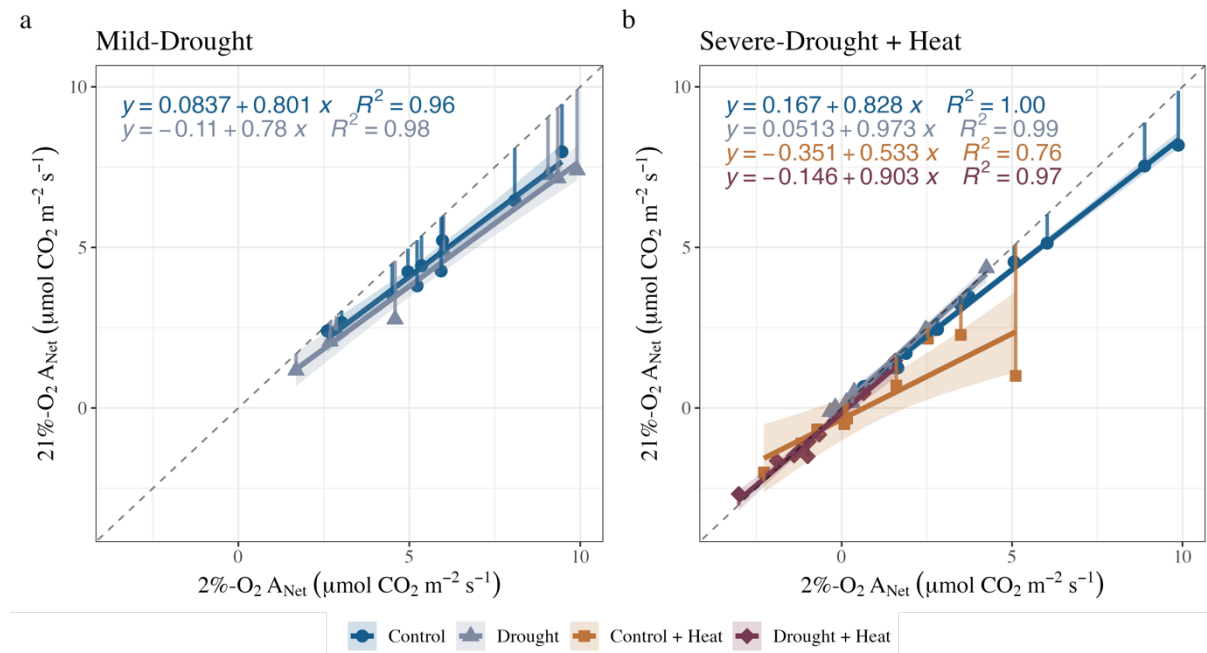


Figure 2.2: Photorespiration and Rubisco carboxylation efficiency derived from measurements of photosynthetic carbon assimilation (A_{net}) under 21% and 2%-O₂ in silver fir. Shown are the data points from the measurements of all individuals ($n=8$ per treatment) during both mild-drought (a), as well as during severe-drought and a one-day heat event (b). The ratio (slope) of these measures estimates Rubisco carboxylation efficiency. The 1:1 dotted line represents 100% carboxylation efficiency, while the regression line represents within treatment variation in photosynthetic assimilation. The length of the vertical line above each point estimates net photorespiration flux for each individual. Shaded area around regression lines represents 95% confidence intervals.

During mild-drought we found relative PR to increase ($p < 0.001$, Figure 2.2a, Table 1) as Rubisco carboxylation efficiency in the drought treatment slightly decreased to $76.3\% \pm 1.50$ compared to $81.46\% \pm 1.74$ in the control. Contrastingly, by severe-drought, we found relative PR to decrease to near zero ($p < 0.001$, Figure 2.2b, Table 1), as Rubisco carboxylation efficiency increased to $99.02\% \pm 7.23$ compared to $85.43\% \pm 2.25$ in the control. Overall,

Rubisco carboxylation efficiency decreased slightly during the initial drought stress, but carboxylation ultimately increased to nearly 100% as SWC declined to 0% (Figure 2.3).

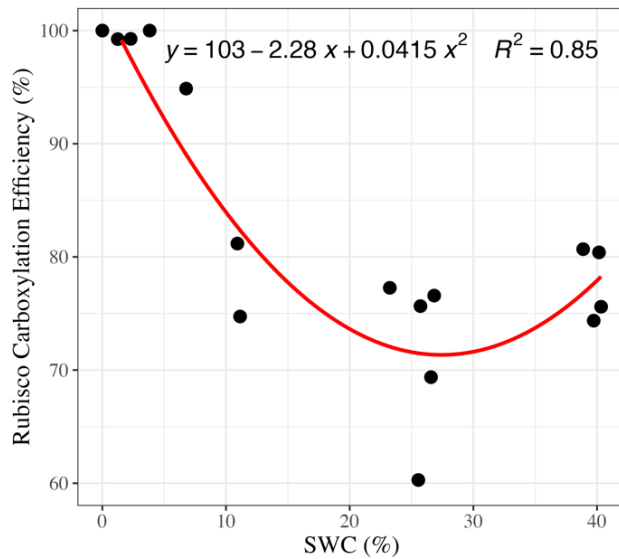


Figure 2.3: Rubisco carboxylation efficiency in response to soil water content (SWC) in silver fir. Data points present measured values collected on individual drought treatment seedlings (n = 4-6 per measurement campaign) at the experimental start, mid-drought, and end-drought. The provided equation represents a second-degree polynomial regression model, where Rubisco carboxylation efficiency is modeled as a function of SWC.

During the one-day heat event, relative PR in the control + heat treatment increased greatly ($p < 0.001$, Figure 2.2b, Table 1), as Rubisco carboxylation efficiency decreased to $47.62\% \pm 8.66$. However, under combined drought and heat stress, A_{net} was near or below zero and relative PR no longer increased ($p = 0.689$, Figure 2.4b, Table 1), leaving Rubisco carboxylation similar to the control.

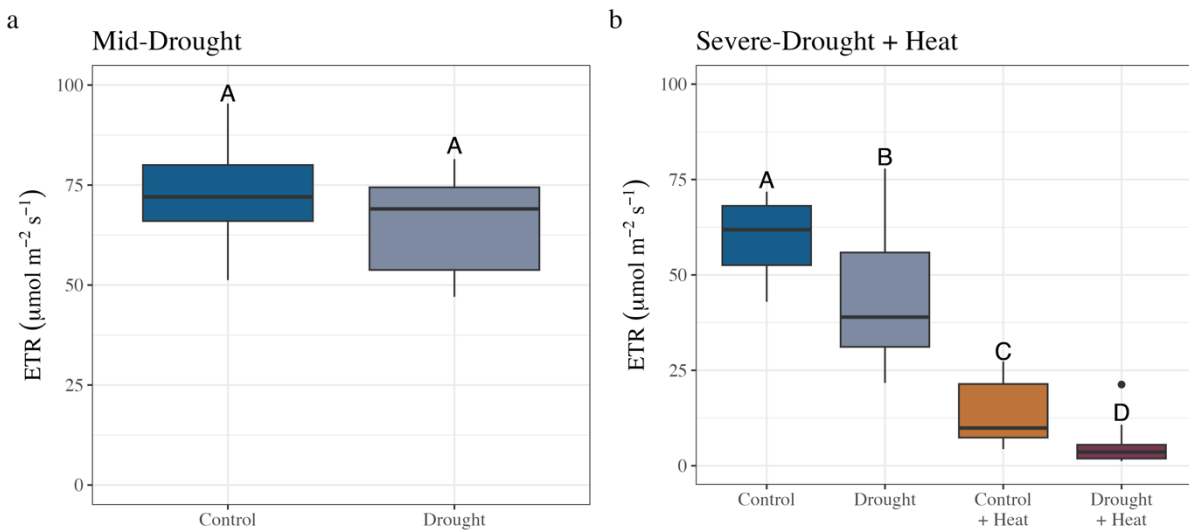


Figure 2.4: Treatment effects on electron transport rate (ETR) in silver fir. Shown are boxplots of ETR during mild-drought (a) and severe-drought plus a one-day heat event (b, $n=8$). Uppercase letters indicate significant pairwise differences determined post-hoc using Tukey's Honest Significant Difference.

Similarly, while ETR was unaffected during mild-drought, it largely declined during severe-drought ($p=0.008$, Figure 2.4b, Table 2.1). Additionally, we found ETR to increasingly explain the variation in A_{net} with drought progression (estimated using sums of squares ratio), suggesting an increase in photochemical limitations with increasing drought. Heat stress further decreased ETR ($p<0.001$, Table 2.1), with the greatest decrease in ETR occurring under drought + heat stress (Figure 2.4b), at which point A_{net} was near or below zero. Additional gas exchange data including stomatal conductance and transpiration are available in Figure S2.4.

2.3.3 Foliar hydrogen peroxide and peroxidase

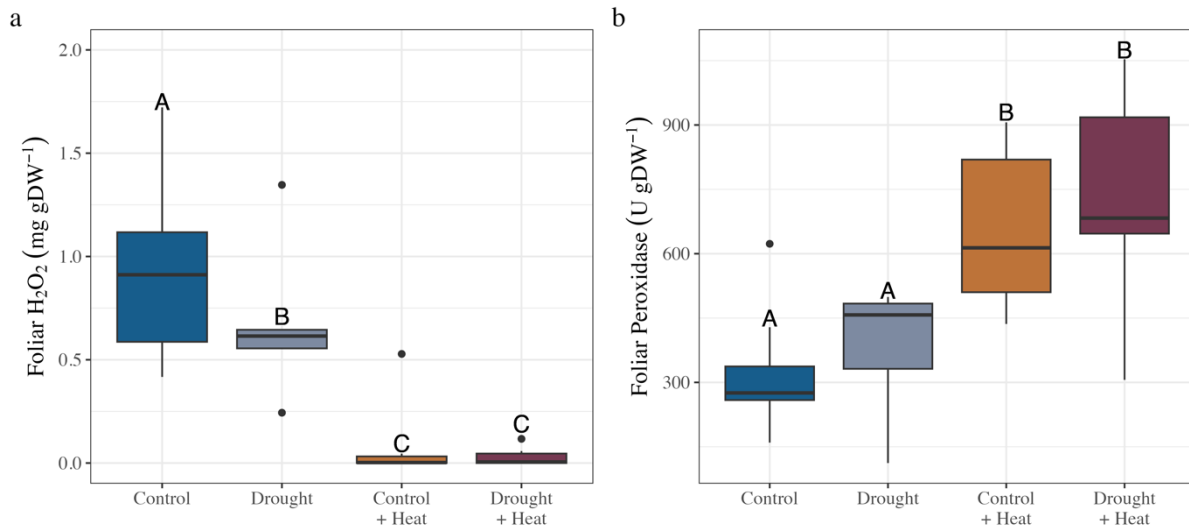


Figure 2.5: Treatment effects on foliar hydrogen peroxide (H_2O_2) and peroxidase levels in silver fir. Shown are boxplots of H_2O_2 concentration (a) and peroxidase (b) during severe-drought and a one-day heat stress in silver fir ($n = 8$). Uppercase letters indicate significant pairwise differences determined post-hoc using Tukey's Honest Significant Difference.

Foliar H_2O_2 concentration was sensitive to water-limitation as well as heat stress. We found drought to decrease foliar H_2O_2 concentration by $\sim 50\%$ ($0.68 \text{ mg gDW}^{-1} \pm 0.12$) compared to the control ($1.29 \text{ mg gDW}^{-1} \pm 0.18$; $p < 0.001$, Figure 2.5a, Table 2.1). Surprisingly, the one-day heatwave largely reduced foliar H_2O_2 to near zero in both control + heat as well as drought + heat ($p < 0.001$, Figure 2.5a, Table 2.1), indicating that H_2O_2 was quickly scavenged. While drought stress alone did not affect POD activity ($p = 0.419$, Figure 2.4b, Table 2.1), heat stress approximately doubled POD activity in both control + heat and drought + heat treatments ($635.33 \text{ U gDW}^{-1} \pm 57.59$) compared to the control ($320.33 \text{ U gDW}^{-1} \pm 40.17$; $p < 0.001$, Figure 4b, Table 1).

Table 2.1: Summary of mixed-effect models comparing the individual and interactive effects of drought (mild-drought, severe-drought) and heat treatment on leaf temperature (T_{leaf}), photorespiration, electron transport rate (ETR), hydrogen peroxide (H_2O_2), and peroxidase enzyme activity (POD). Reported values include estimated effect, t-value with degrees of freedom (not-applicable for H_2O_2 due to weighted analysis) and the respective p-value.

Mild-Drought		Drought			Heat			Drought*Heat		
Response	Estimate	t-value	P-value	Response	Estimate	t-value	P-value	Response	Estimate	P-value
Photorespiration	0.052	50.761 ₍₁₇₎	<.001							
ETR	-3.212	-0.489 ₍₁₈₎	0.631							
Severe-Drought + Heat	Drought			Heat			Drought*Heat			
Response	Estimate	t-value	P-value	Response	Estimate	t-value	P-value	Response	Estimate	P-value
T_{leaf}	2.404	3.735 ₍₁₈₎	0.002	T_{leaf}	15.056	39.500 ₍₄₈₎	<0.001	T_{leaf}	-0.507	-0.801 ₍₄₈₎ 0.427
Photorespiration	-.159	13.421 ₍₁₀₎	<0.001	Photorespiration	0.378	-6.219 ₍₁₀₎	<0.001	Photorespiration	-0.258	1.810 ₍₁₀₎ 0.100
ETR	-15.563	-2.906 ₍₂₃₎	0.008	ETR	-46.486	-10.206 ₍₁₂₎	<0.001	ETR	6.087	0.912 ₍₁₂₎ 0.377
H_2O_2	-.416	-7.759	<0.001	H_2O_2	-1.032	-19.262	<0.001	H_2O_2	.415	7.700 <0.001
POD	5.818	0.066 ₍₁₇₎	0.948	POD	324.661	8.657 ₍₁₂₎	<0.001	POD	95.327	1.536 ₍₁₂₎ 0.150

2.4 Discussion

We found that mild drought stress can increase PR when stomatal conductance primarily limits photosynthesis, but that severe drought stress may lead to decreases in PR as non-stomatal limitations of photosynthesis intensify, as observed with decreased ETR, ultimately decreasing photosynthetic CO_2 demand. We also found that heat stress can greatly increase PR, but in combination with drought this increase was no longer observed. Surprisingly, we found that foliar H_2O_2 concentrations were near zero under both heat and drought + heat treatments despite an increase in PR under heat. Analysis of POD activity suggests that heat stress led to rapid H_2O_2 scavenging, demonstrating a tight oxidative regulation independent of photosynthesis and thus also independent of water availability. Together, these results provide key insights into the response of the PR pathway and its stress-signaling potential to combined drought and heat stress. In the following we will further elaborate on the finding that the magnitude and direction of PR changes during drought and/or heat stress depend on the timing

and intensity of stress events, and that increased PR does not necessarily lead to accumulated H_2O_2 due to enzymatic scavenging.

2.4.1 PR depends on timing and interactions between drought and heat

We observed that PR slightly increased at mild drought, with declines in SWC from about 40% down to 25%, but only small changes in Ψ_{md} and radial growth indicating mild drought stress (Figure 2.1). PR is commonly assumed to increase during mild to moderate drought stress, as reduced CO_2 uptake from higher stomatal resistance increases the rate of Rubisco oxygenation relative to carboxylation (Bai et al. 2008; Voss et al. 2013; Tsonev et al. 2014). In contrast, more severe drought stress decreased relative PR, suggesting that reduced CO_2 uptake was no longer the main limiting factor of photosynthesis. As drought stress progresses, other factors such as reduced photochemical efficiency and/or limited regeneration of RuBP can additionally limit photosynthesis (Dias and Brüggemann 2010), demonstrated in our results by reduced ETR at severe-drought. Under severe drought stress, stomatal closure may not necessarily lead to decreased intercellular CO_2 as non-stomatal limitations may instead limit the ability of the Calvin-Benson cycle to utilize existing, resulting in intercellular CO_2 accumulating due to cellular respiration and cuticular permeability (Cornic and Briantais 1991; Flexas and Medrano 2002a; Pirasteh-Anosheh et al. 2016). As such, while Rubisco efficiency may approach 100%, reduced net gas exchange limits the benefit of increased carboxylation efficiency.

Thus, the presented results demonstrate that PR may increase or decrease during drought depending on the influence of non-stomatal limitations such as the slowdown of photosynthetic light reactions, and indicate that any ability of PR to mitigate stress may decrease with drought progression (Noctor et al. 2002; Lawlor and Tezara 2009). Additionally, this likely represents an inaccuracy in models of GPP which do not consider non-stomatal limitations of photosynthesis (Rödig et al. 2017; Yin and Struik 2017; Nadal-Sala et al. 2021; Asargew et al. 2024), despite being coordinated with stomatal control to maximize photosynthesis during drought (Salmon et al. 2020). Such models of GPP therefore do not account for potential fluctuations of PR's contribution to net carbon assimilation with soil dehydration, and may therefore be less accurate predicting GPP during drought events (Zhou et al. 2013). As stomatal and non-stomatal coordination during drought varies across forest species (Dewar et al. 2022), a better species-level understanding of such coordination is needed to improve models of GPP.

We observed the largest increase in PR relative to A_{net} following six hours of 40°C T_{air} , decreasing average Rubisco carboxylation efficiency by nearly half. Individual photorespiration responses to heat stress had increased variance than under other treatments, particularly with higher A_{net} values. Heat stress often increases PR despite constant atmospheric CO₂ due to an increased relative solubility of O₂ at higher temperatures, by decreasing Rubisco CO₂ affinity, and/or by increasing Rubisco misfire (Zhang and Sharkey 2009; Bracher et al. 2017). This increase in PR during heat stress could potentially be amplified by mild drought, when the ratio of O₂:CO₂ can be further increased by limited CO₂ uptake. However, we did not observe an amplification of PR under combined severe drought and heat stress when most plants had stomata closed and A_{net} was close to zero (Fig. S4), instead finding that severe drought stress eliminated the heat induced increase in PR. This suggests that despite changes in O₂:CO₂ solubility or Rubisco kinetics during heat that would otherwise favor PR, intercellular CO₂ may no longer limit photosynthesis during severe drought when non-stomatal limitations are increased, such as reduced ETR and greater NPQ (Flexas and Medrano 2002a; Zhou et al. 2013). Studies combining drought and heat stress also suggest a greater role of biochemical limitations rather than stomatal limitations on photosynthesis, supporting our observations (Flexas and Medrano 2002a; Ruehr et al. 2016; Perdomo et al. 2017). Additionally, drought stress can lower the optimal temperature of photosynthesis, meaning heat stress combined with drought is more likely to reach temperatures beyond this optimal photosynthesis threshold than just heat alone, increasing biochemical limitations (Fang et al. 2023). Taken together, our results demonstrate that while heat alone can increase PR, compounding non-stomatal limitations in the light-dependent reactions from additional drought stress may eliminate this increase.

2.4.2 H₂O₂ accumulation is tightly regulated despite variable PR during stress

Drought stress tended to reduce foliar H₂O₂ by c. 50% on average, suggesting either lower production and/or an increase in enzymatic scavenging from stress. Drought stress often leads to an accumulation in H₂O₂ due to increased PR which can outpace upregulated scavenging enzyme activity (Luna et al. 2005; Pan et al. 2017). Other studies demonstrate that drought stress instead reduces scavenging enzyme activity, resulting in a greater accumulation of H₂O₂ from PR (Silva et al. 2012). As we observed no significant changes in POD activity of silver

fir leaves in the drought treatment, we attribute lower foliar H₂O₂ concentration either to nearly-eliminated PR at severe-drought, and/or to increased activity of other scavengers like peroxisomal catalases. The remaining H₂O₂ concentration in the drought treatment may originate in cellular compartments not associated with PR, including in the thylakoid membrane during the light-dependent reactions of photosynthesis (Khorobrykh et al. 2015). With ETR reduced during drought stress, electrons may increasingly transfer to O₂ forming superoxide radicals, which are then quickly converted to H₂O₂. However, increased Non-Photochemical Quenching (NPQ) can mitigate this by dissipating excess excitation energy as heat, reducing H₂O₂ accumulation in the chloroplast. Our observation of small concentrations of H₂O₂ and increased leaf temperatures (Figure S2.3) under stress conditions additionally suggest increased NPQ under our severe stress conditions. While the expectation that the proportion of total H₂O₂ originating from PR increases during drought (Noctor et al. 2002; Silva et al. 2012), this likely is only true under mild-to moderate-drought stress when stomatal closure primarily limits photosynthesis.

Heat stress reduced H₂O₂ to near-zero concentration while greatly increasing POD activity, suggesting an efficient scavenging of H₂O₂ despite likely higher production from increased PR. The potential of H₂O₂ from PR as a stress-signaling molecule is dependent on the balance between accumulation and scavenging (Petrov and Van Breusegem 2012). H₂O₂ accumulated in the peroxisome during PR can diffuse into the cytosol, where it can be converted to hydroxyl radicals and cause cellular membrane damage, DNA mutations, and cell death (Richards et al. 2015; Carvalho and Silveira 2020). In addition to the measured POD enzymatic increase, increased H₂O₂ scavenging by catalases in the peroxisome, or enhanced regulation by the glutathione-ascorbate cycle in various cellular compartments such as chloroplasts, mitochondria, peroxisomes, and the cytosol, could have also contributed to the decreased H₂O₂ we observed. Quick scavenging of ROS like H₂O₂ during abiotic stress mitigates oxidative stress and maintains cell function, but may reduce the potential of ROS stress-signaling. Our results show that H₂O₂ can be effectively scavenged despite increases in PR during short-term heat stress, likely attributable to the high temperature stability of POD enzymes (Plieth and Vollbehr 2012). Furthermore, POD increases under combined drought and heat stress demonstrate tight regulation of H₂O₂ despite compounding stress, reducing H₂O₂ stress-signaling potential during abiotic stress. This regulation may limit the induction of stress responsive genes by H₂O₂ as well as limit the effectiveness of H₂O₂-mediated hormonal pathways. As prolonged heat stress may ultimately reduce the production of ROS

enzymatic scavengers (Foster et al. 2015), stress-signaling via H₂O₂-accumulation may have an increased role during longer-term heat events.

2.5 Conclusion

This study demonstrates that the effects of drought and heat stress on PR as well as foliar H₂O₂ in silver fir strongly depend on the timing and intensity of the stress event. We found that PR increased during mild drought stress but ultimately decreased during severe drought stress, likely due to intensifying non-stomatal limitations of photosynthesis such as reduced ETR. Additionally, while heat stress alone increased PR, greater non-stomatal limitations during severe drought corresponded to lower PR under combined stress. H₂O₂ accumulation was limited by scavenging enzyme activity during heat stress despite increases in PR. This demonstrates a tight regulation of ROS production during abiotic stress while limiting the potential for cellular stress-signaling. To understand tree-level stress signaling, it is necessary to consider photorespiration and the underlying physiological processes which determine its dynamic nature.

2.6 Supplementary Materials

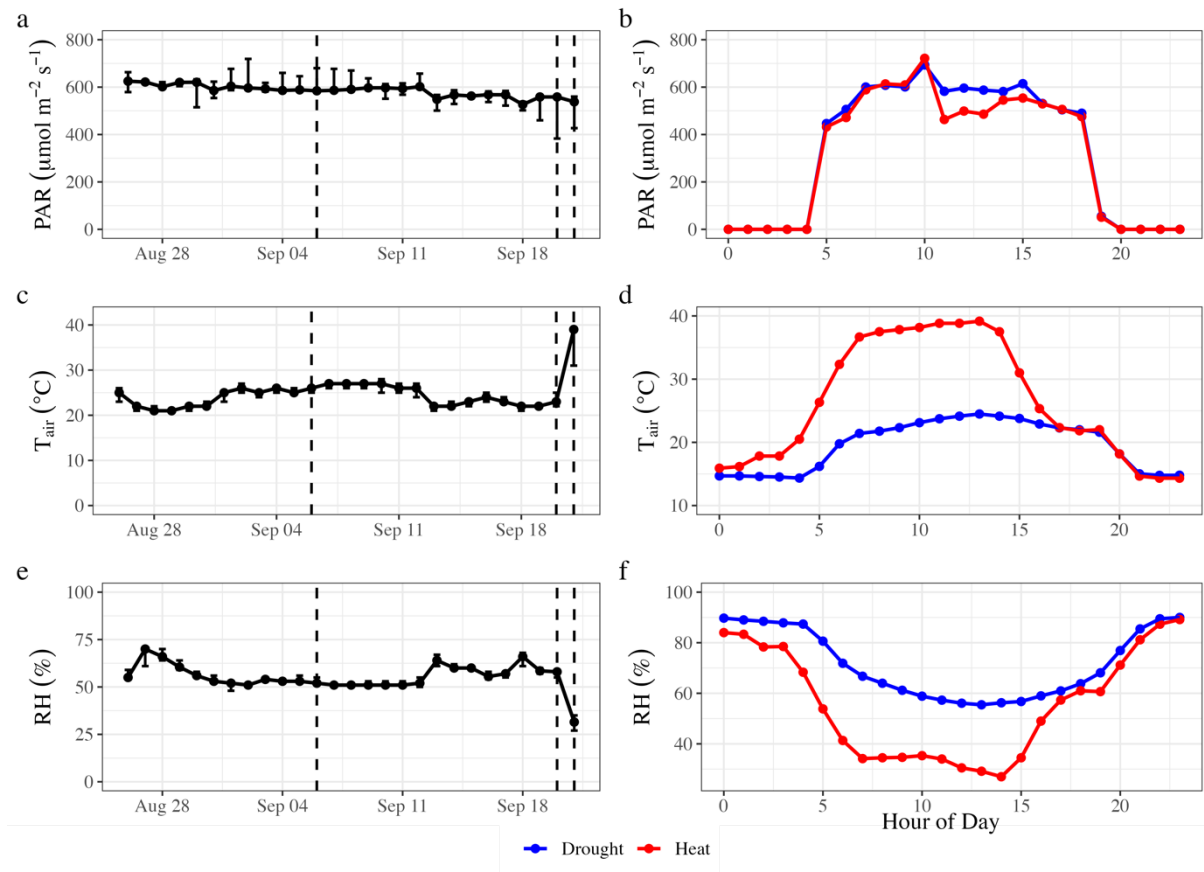


Figure S2.1: Time series visualization of greenhouse photosynthetic active radiation (PAR, a), air temperature (T_{air} , c), and relative humidity (RH, e) during the experimental drought and subsequent heat stress. Vertical dashed lines represent mild-drought, severe-drought, and heat treatment timepoints, respectively. Error bars represent daytime max and minimum values. Diurnal cycles are reported for each parameter (PAR, b; T_{air} , d; RH, f) by hour of day during both the drought (blue) and heat (red) periods.

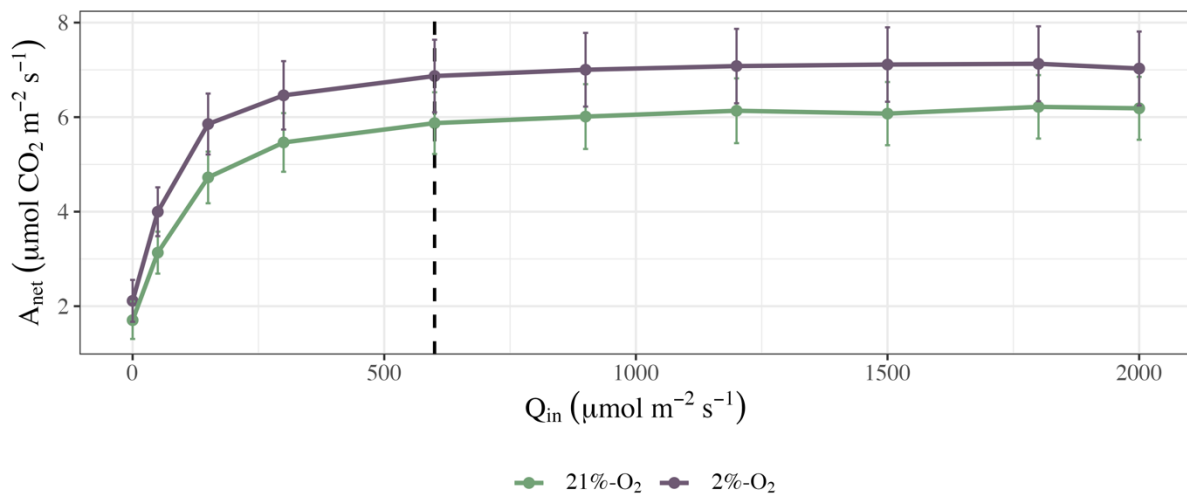


Figure S2.2: Light response curves displaying response of mean net carbon assimilation (A_{net}) to variable light conditions (Q_{in}) under both ambient (21%-O₂) and photorespiration-suppressed (2%-O₂) conditions. Data points are displayed with standard error ($n = 10$), while vertical dashed line is at $Q_{\text{in}} = 600$, estimated as the light-saturation point and utilized in all experimental measurements of A_{net} .

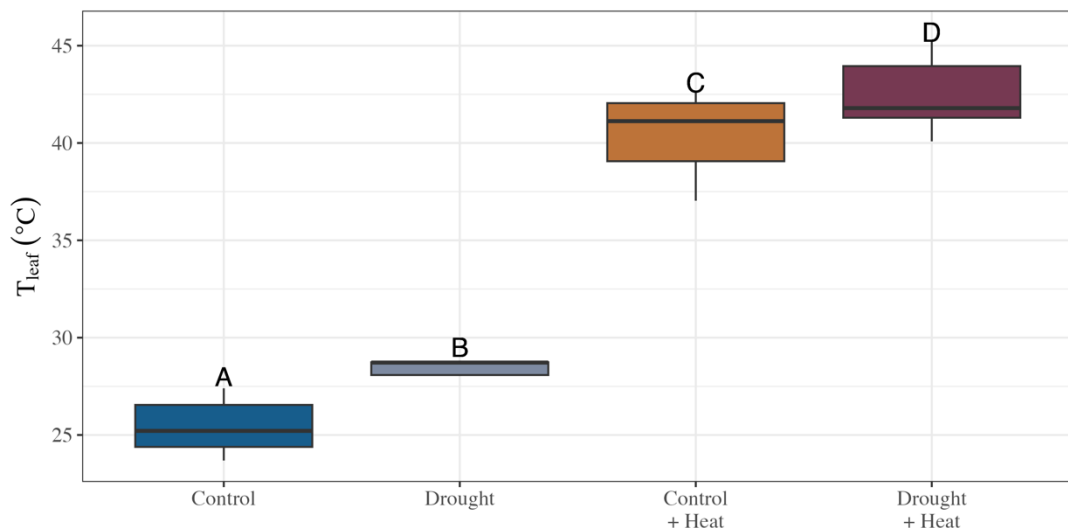


Figure S2.3: Boxplots displaying leaf temperature (T_{leaf}) determined using thermal imaging during severe-drought and a one-day heat stress. Uppercase letters indicate significant pairwise differences determined post-hoc using Tukey's Honest Significant Difference.

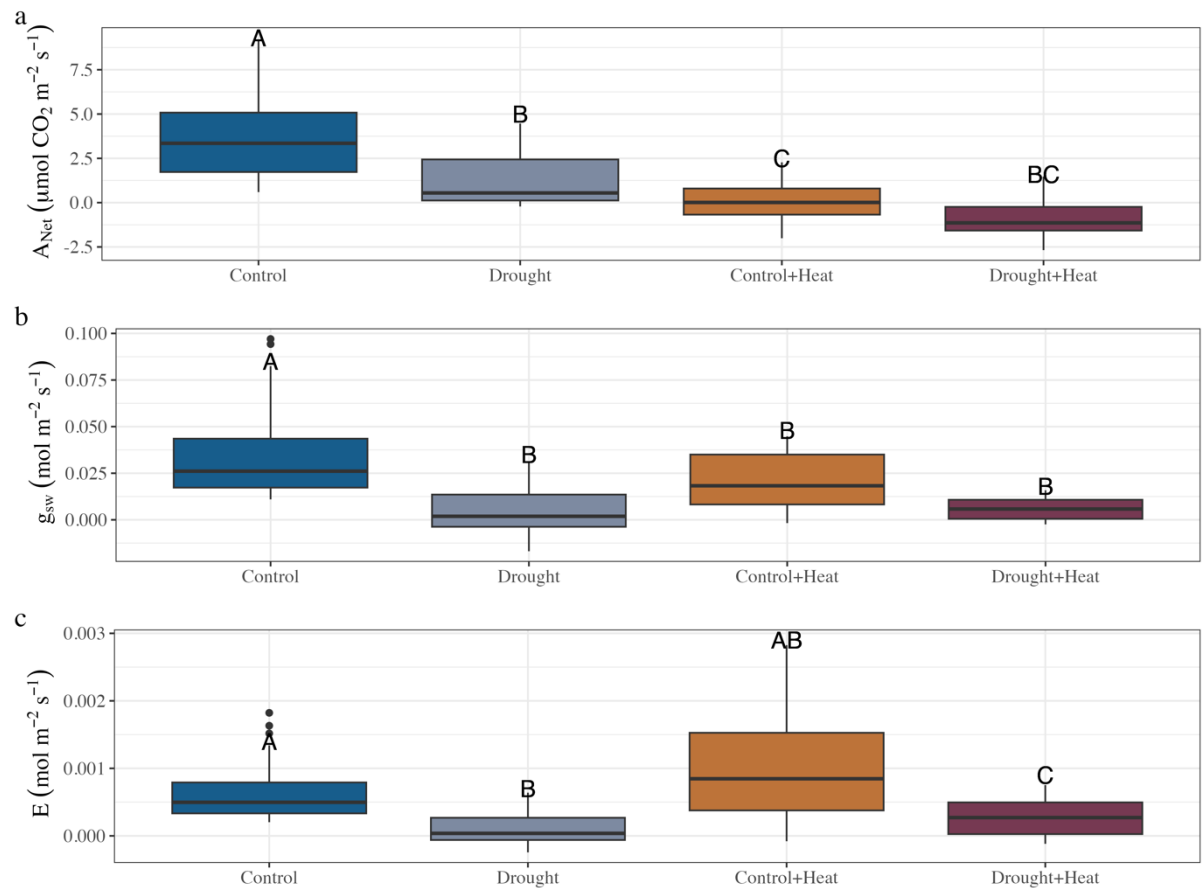


Figure S2.4: Boxplots displaying net photosynthetic assimilation (A_{net} , a), stomatal conductance to water vapor (g_{sw} , b), and transpiration (E , c) during severe-drought and a one-day heat stress. Uppercase letters indicate significant pairwise differences determined post-hoc using Tukey's Honest Significant Difference.

3 Drought-induced delays in stem hydraulic development shape gas exchange and growth recovery in Douglas fir

At the time of thesis submission, this chapter is accepted for publication as:

Alongi, F.; Knüver, T.; McAdam, S.A.M.; Ziegler, Y.; Gast, A.; Ruehr, N.K., 2025. Drought-induced delays in stem hydraulic development shape gas exchange and growth recovery in Douglas fir. *Plant Physiology*. *Plant Physiology - Accepted*.

Abstract

The limiting factors of tree recovery from drought, particularly the coordination between carbon sources and sinks, remain poorly understood. In this study, juvenile Douglas fir (*Pseudotsuga menziesii*) were exposed to 28 days of mild or severe drought, followed by 35 days of recovery. We continuously monitored CO₂ and H₂O fluxes in shoots and roots to derive gas exchange and carbon accumulation, while measuring basal area to estimate stem growth and sapwood development. To identify underlying mechanisms of drought recovery, we periodically measured nonstructural carbohydrates (NSC), midday water potential (Ψ_{md}), and foliar abscisic acid (ABA). We found no evidence that ABA or Ψ_{md} limited gas exchange recovery, with stomatal conductance recovery instead related to drought-induced reductions in sapwood development. While carbon accumulation ultimately recovered to control levels following mild stress, severe stress caused persistent impairments, ultimately reducing carbon accumulation by 51%, with stem growth similarly affected. We found no evidence of growth being limited by NSC, which remained abundant. However, we suggest that drought-induced limitations to stem development governed this pattern. This became clear when considering the diurnal growth cycle, where daytime growth was largely absent in severe trees post-drought while accounting for up to 30% of total growth in control trees. Daytime growth appeared to depend on sufficient sapwood area, which likely buffered xylem tension to support growth conditions. Our findings suggest drought-induced reductions of stem hydraulic development constrain the recovery of gas exchange and growth. Further, altered diurnal growth patterns may explain prolonged productivity declines in forests following drought.

3.1 Introduction

Forests are major carbon (C) sinks, but their capacity to accumulate C is increasingly threatened by the growing intensity of drought events (Liu et al. 2024). Severe drought events impose physiological constraints that alter C source and sink coordination, leading to delayed or limited recovery (Ruehr et al. 2019). While impaired forest productivity following drought is well documented in observational field studies (Serra-Maluquer et al. 2018), these studies struggle to identify the physiological mechanisms limiting recovery. In contrast, experimental studies can isolate physiological responses to drought, but few examine recovery—leaving a critical gap in understanding how impairments such as reduced photosynthesis, nonstructural carbohydrate (NSC) reserves, and tissue damage persist beyond drought and affect long-term carbon accumulation. Physiological impairment and damage are known to scale with drought intensity (Ruehr et al. 2019), but the extent to which drought-induced damage affects tree recovery potential is still largely unexplored. Understanding how drought severity mechanistically alters tree resilience during recovery is essential, as it directly affects long-term C storage efficiency and ultimately the role of forests as C sinks.

Effective stomatal regulation is crucial for minimizing water loss and maintaining hydraulic function during drought so that hydraulic impairment does not delay recovery. Stomatal conductance (g_{sw}) is tightly regulated by tree water status, with stomatal closure initiated by mild water stress and further suppressed under severe drought by elevated foliar abscisic acid (ABA) (McAdam and Brodribb 2014). Persistent reductions in g_{sw} during drought recovery have been attributed to delayed hydraulic restoration, assessed through measures of water potential (ψ), as well as continued signaling from ABA (Brodribb and McAdam 2013; Rehschuh et al. 2020). However, it is important to distinguish that ψ reflects the plant water status as indicated by xylem tension, whereas overall hydraulic conductance also depends on the extent of functional xylem present in the sapwood. The sapwood determines the tree's capacity to transport water to the canopy, and thus, its potential for recovering stomatal conductance (Matthaeus et al. 2022). Metrics such as the ratio of sapwood area to leaf area (Huber value, H_v) assess the hydraulic supply-demand balance. H_v values are closely linked to stem hydraulic conductance across species (Mencuccini et al. 2019), with higher H_v associated with greater g_{sw} , as the hydraulic system is better equipped to maintain guard cell turgor (Zlobin et al. 2024). Due to the formation of embolized xylem conduits during severe drought stress, g_{sw} recovery is likely dependent on new xylem formation. As a result, an

increase in H_v may be necessary to restore hydraulic capacity, enabling trees to recover g_{sw} and ultimately photosynthetic function.

Reduced g_{sw} limits CO_2 uptake and photosynthetic assimilation (A_{net}), restricting C availability for secondary metabolism and leading to shifts in C allocation. These shifts often reduce respiration and minimize growth, ultimately conserving C for primary metabolic function (Rodríguez-Calcerrada et al. 2021). Furthermore, slight reductions in water potential under drought stress can limit growth by imposing turgor constraints on cellular expansion and differentiation (Körner 2015; Peters et al. 2021), indicating a sink-driven control of growth during drought. As such, turgor-sensitive “resting” sink tissues can simultaneously experience an accumulation of carbohydrates and a reduced input from recent assimilates during drought (Hagedorn et al. 2016), assuming C input remains above respiratory demand. Therefore, drought-induced carbohydrate accumulation in sink tissues may lead to feedback inhibition of photosynthesis (Paul and Foyer 2001; M. Tian et al. 2024), decoupling the limitations of photosynthesis from stomatal control. Thus, the non-instantaneous recovery of A_{net} , and ultimately carbon uptake and growth is not readily attributed to either persistent hydraulic impairment or metabolic inhibition alone, highlighting the challenge of disentangling their relative contributions in limiting post-drought recovery.

Physiological damage sustained during drought stress may increase the C cost of recovery due to the need to repair or replace damaged tissues (Ruehr et al. 2019), ultimately delaying the resumption of growth. Cellular and hydraulic damage sustained under severe drought stress can directly impair the post-drought recovery of gas exchange (Rehschuh et al. 2020). This may be particularly relevant in conifers, which tend to maintain higher hydraulic safety margins and are therefore more embolism avoiding than angiosperm forest species (Johnson et al. 2011). Additionally, conifers have comparatively little parenchyma in their woody tissues compared to angiosperms (Morris et al. 2016), which store NSC that could aid in embolism refilling. However, whether embolism dissolution naturally occurs at all following drought-induced cavitation remains disputed (Choat et al. 2019). As such, conifers likely rely on the formation of new xylem tracheids via new sapwood area to overcome losses of hydraulic function sustained during drought stress, constituting a high C cost during recovery (Brodribb and Cochard 2009). This high C demand of tissue replacement and repair following stress-release may be why tree growth recovery often takes longer than the recovery of gas exchange (Kannenberg et al. 2022), and could explain why the lag in growth

recovery in conifers directly scales with the intensity of drought (Sargent et al. 2014). However, drought severity-induced shifts in tree C allocation during stress recovery are poorly understood due to difficulties in assessing whole-tree C status. This knowledge gap complicates our ability to assess C costs associated with drought stress, and how these ultimately translate to long-term reductions in C accumulation and growth ability.

NSCs represent a major C sink in conifers and play a critical role in sustaining tree function during drought stress. As drought intensifies and photosynthesis (A_{net}) declines, stored NSC are mobilized to support cellular respiration and lower osmotic potential (Long and Adams 2023). NSC depletion during drought is more frequent in gymnosperms than in angiosperms, and is closely related to xylem hydraulic vulnerability (Adams et al. 2017). Similarly, sustaining high NSC levels during drought is linked to increased drought survival in conifers (Garcia-Forner et al. 2016), suggesting that NSC retention may be prioritized over other metabolic processes like growth (Stefaniak et al. 2024). However, whether NSC accumulation is actively or passively regulated during drought remains widely debated, as growth typically ceases before photosynthesis due to turgor limitations on cell expansion, which could passively facilitate NSC accumulation for as long as C assimilation remains above respiratory demand (Hartmann and Trumbore 2016).

During post-drought recovery, NSC influence the ability of trees to regain optimal function and growth. In *Picea abies* it has been observed that NSCs in xylem parenchyma that were maintained during drought stress were depleted one week following recovery, which corresponded to increased xylem conductance (Tomasella et al. 2017). Similarly, accumulated NSCs during drought are linked to the rapid xylem cell formation upon recovery (Martínez-Sancho et al. 2022), allowing trees to develop functional new xylem to compensate for non-functional, embolized xylem. Due to the critical role of NSCs in tree survival during drought and in supporting recovery, prioritization of NSC maintenance may limit long-term growth (Kannenberg and Phillips 2020; Guo et al. 2021). Determining the prioritization between NSC maintenance and growth requires an understanding of whole-tree C balance during both drought and recovery; however, few studies integrate NSC responses to stress with whole-tree C exchange measurements (Hartmann et al. 2015; Hartmann and Trumbore 2016). Simultaneous measurements of gas exchange and NSC dynamics can clarify how trees allocate between storage and growth following stress-induced changes in carbon balance,

providing critical insights into the physiological mechanisms that govern stress recovery and long-term forest resilience.

In this study, we aimed to identify how drought severity mechanistically limits the recovery of key physiological processes related to C acquisition and allocation in Douglas fir (*Pseudotsuga menziesii*) seedlings. This study builds on existing conceptual frameworks that describe the dual impacts of drought severity on hydraulic function and metabolic C dynamics during recovery (Ruehr et al. 2019). Douglas fir was selected because of its widespread distribution across North America, as well as its increasing role in European forestry due to its higher drought tolerance and growth resilience than many native species (Stangler et al. 2022). Specifically, this study uses whole-tree gas flux chambers to examine the effects of mild and severe drought on C assimilation, accumulation, and growth during recovery, while foliar ABA and branch NSC concentrations were periodically sampled to identify phytohormone regulation and C reserve status. We addressed the following hypotheses:

- (1) Foliar ABA and Ψ_{md} will increasingly limit gas exchange during drought and initial post-drought recovery.
- (2) C assimilation and C accumulation will acclimate to mild stress and quickly recover, while severe drought stress will more greatly limit recovery.
- (3) NSC will accumulate following growth cessation and ultimately decrease during severe stress (due to higher respiration relative to photosynthesis), while stem growth will partially recover only after NSC reserves are restored.

3.2 Results

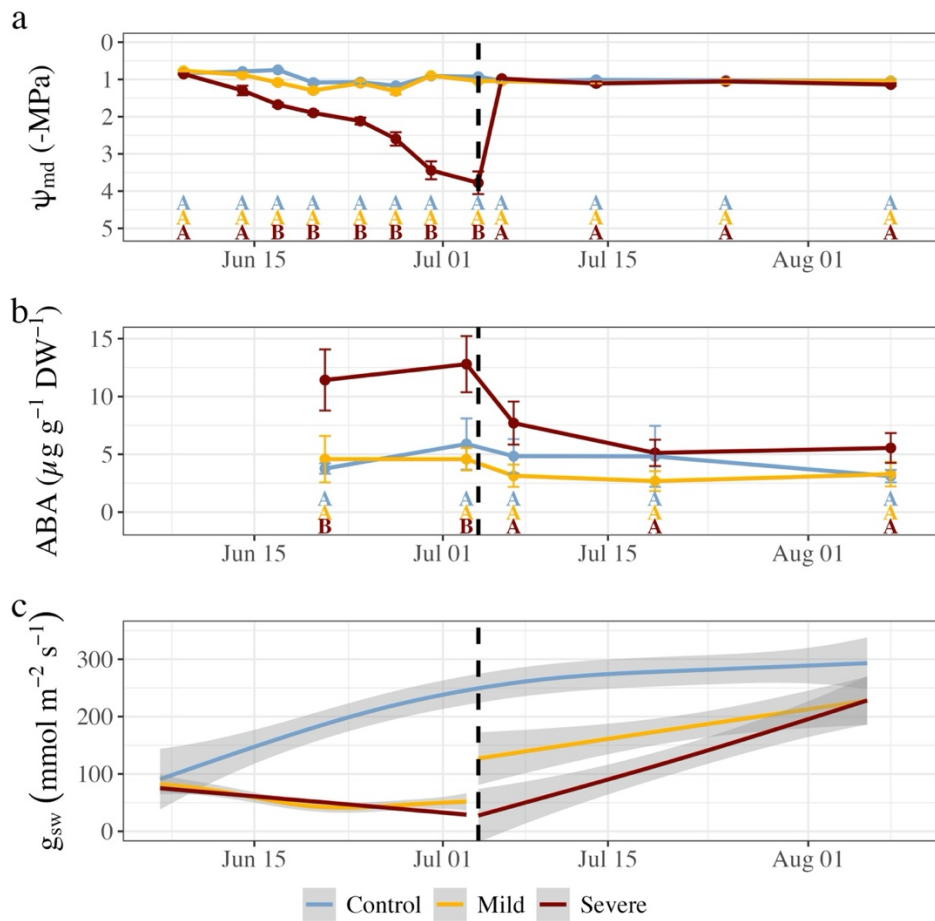


Figure 3.1: Dynamics of water potential, abscisic acid levels, and stomatal conductance during drought and recovery in Douglas-fir juveniles. Midday branch water potential (a, Ψ_{md}) was measured periodically on pilot trees ($n = 5$ per treatment). Foliar abscisic acid (b, ABA) concentrations were measured periodically in pilot trees ($n = 5-7$ per treatment). Error bars are $\pm SE$ between individual mean values. Uppercase letters indicate significant pairwise differences at each timepoint determined post-hoc using Tukey's Honest Significant Difference. Mean daytime (09.00 – 14.00) stomatal conductance (c, g_{sw}) rates for chamber seedlings ($n = 4-6$ per treatment). Generalized additive models were fit to produce smoothing lines for panel c, with shaded gray representing $\pm SE$. The vertical black dashed line in all panels indicates the transition from drought to recovery.

3.2.1 Dynamics of water potential, abscisic acid, and stomatal conductance

Midday water potential (ψ_{md}) in the mild drought treatment plants remained close to or at control levels (-1.0 ± 0.1 MPa) throughout the drought period (Figure 3.1a), despite lower volumetric soil water content (SWC). In the severe treatment plants, ψ_{md} progressively decreased throughout the drought period. The severe drought treatment plants reached -3.8 ± 0.3 MPa by the end of drought stress, corresponding to 70-85 % loss of conductivity for this species (Chauvin et al. 2019). Following the release of drought stress, ψ_{md} in the severe treatment plants returned to levels of the control treatment plants within two days.

Foliar ABA levels in the severe drought treatment plants more than doubled by day 14 of drought stress ($p = 0.016$, $t_{12} = -2.801$, Figure 3.1b), and remained through the end of drought ($p = 0.024$, $t_{12} = 2.467$), corresponding to a strong decrease in ψ_{md} . We observed no differences in ABA levels between the control and mild drought treatment plants during either drought or recovery, corresponding to the lack of a detectable difference in ψ_{md} . Within two days of recovery, ABA levels declined in the severe treatment to levels measured in control treatment plants as ψ_{md} recovered, and were maintained throughout the recovery period.

Stomatal conductance (g_{sw}) responded according to drought severity (Figure 3.1c). Mild stress plants moderately decreased g_{sw} values by the end of drought stress to 45.02 ± 7.11 $\text{mmol m}^{-2} \text{ s}^{-1}$, which was 81 % lower than the control treatment ($p = 0.004$, $t_{12} = -3.526$), as the control treatment plants instead continuously increased g_{sw} . This increase in g_{sw} in control treatment plants over the course of the experiment was strongly related to increases in Huber value (stem sapwood:leaf area; H_v), suggesting increases in hydraulic supply occurred due to continual stem growth (Figure 3.2a), until a H_v of ~ 0.08 was reached, at which point maximal g_{sw} was sustained. In individuals exposed to severe stress, g_{sw} consistently decreased throughout the drought period, reaching 31.52 ± 2.35 $\text{mmol m}^{-2} \text{ s}^{-1}$, or 86 % lower than the control by the end of drought ($p = 0.004$, $t_{12} = -3.547$). An exploratory model to determine the contributing factors to g_{sw} during the experimental period revealed that g_{sw} was negatively related to VPD ($p < 0.001$, $t_{904.64} = -9.03$), with the effect of VPD weakened by increasing H_v ($p < 0.001$, $t_{908.81} = 5.25$; Figure 3.3). The highest VPD was recorded in the severe treatment at the end of the drought period ($\sim 2.4 \pm 0.2$ kPa), while the VPD in the control treatment remained consistent ($\sim 1.5 \pm 0.1$ kPa, Figure S3.2d).

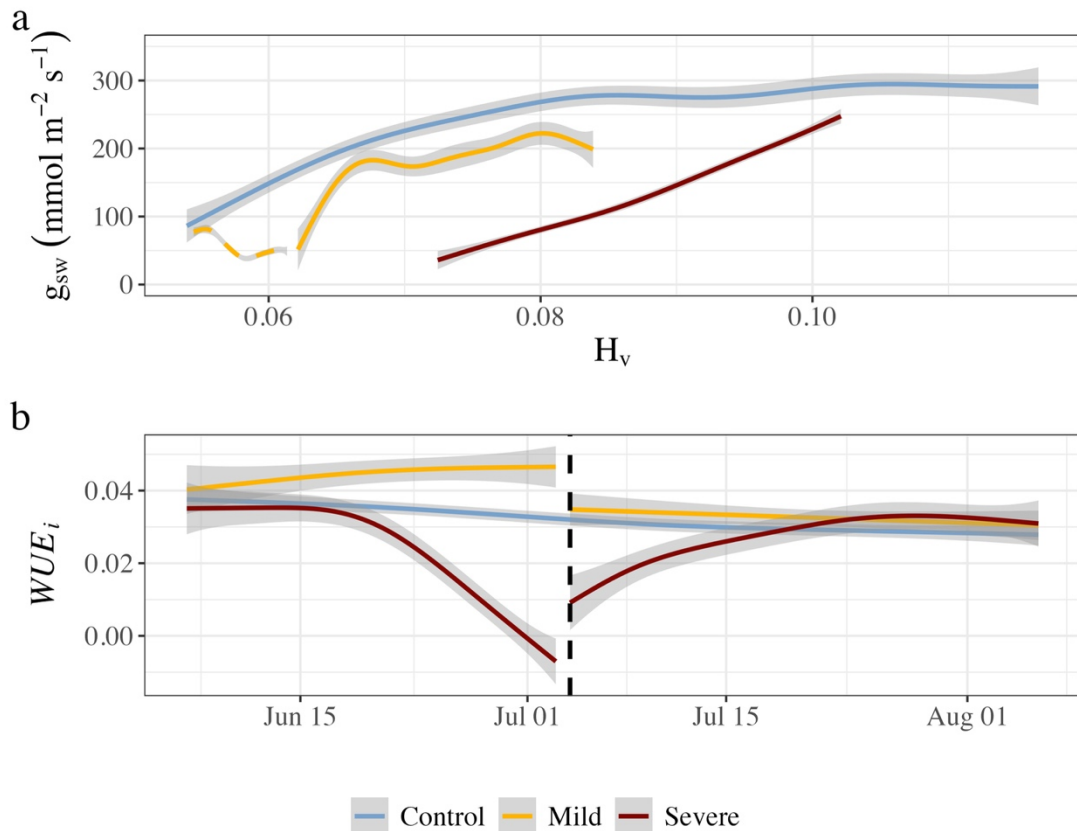


Figure 3.2: Development of daytime g_{sw} with Huber value (sapwood area : leaf area; H_v) throughout the experimental period (a, $n = 4-6$). The drought period for the mild treatment is denoted by a dashed line, while it is omitted for the severe treatment due to observed effects of abscisic acid on g_{sw} , as well as stem contraction due to dehydration. Time series of daytime (09.00 – 14.00) intrinsic water use efficiency (b, WUE_i). The vertical dashed black line indicates the transition from drought to recovery. Generalized additive models are fit to produce smoothing lines in both panels, with the shaded gray area representing ±SE.

Within two days of recovery, the mild stress treatment immediately increased g_{sw} to 90.42 ± 19.13 mmol m⁻² s⁻¹, which was above pre-stress levels. g_{sw} continued to recover in the mild stress treatment, corresponding to increases in H_v (Figure 3.2a), ultimately reaching 204.9 ± 67.3 mmol m⁻² s⁻¹, 30 % below that of the control (n.s. due to high SE). Interestingly, this g_{sw} was associated with a H_v of ~ 0.08 , a similar value to that which facilitated the highest g_{sw} in the control group (Figure 3.2a, Figure 3.3). In contrast, there was no immediate recovery of g_{sw} following severe stress despite an immediate reduction in foliar ABA, with pre-stress levels not reached until five days into recovery. Despite this, g_{sw} ultimately recovered to similar levels as the mild stress treatment, reaching 234.6 ± 119.2 mmol m⁻² s⁻¹ by the end of recovery, or 20 % below that of the control (n.s. due to high SE). Transpiration (E) was lower than the control in both stress treatments; however, a higher E was observed in the severe

treatment than the mild treatment during both drought and recovery (Figure S3.1), likely due to the generally higher VPD in the severe treatment chambers (Figure S3.2d).

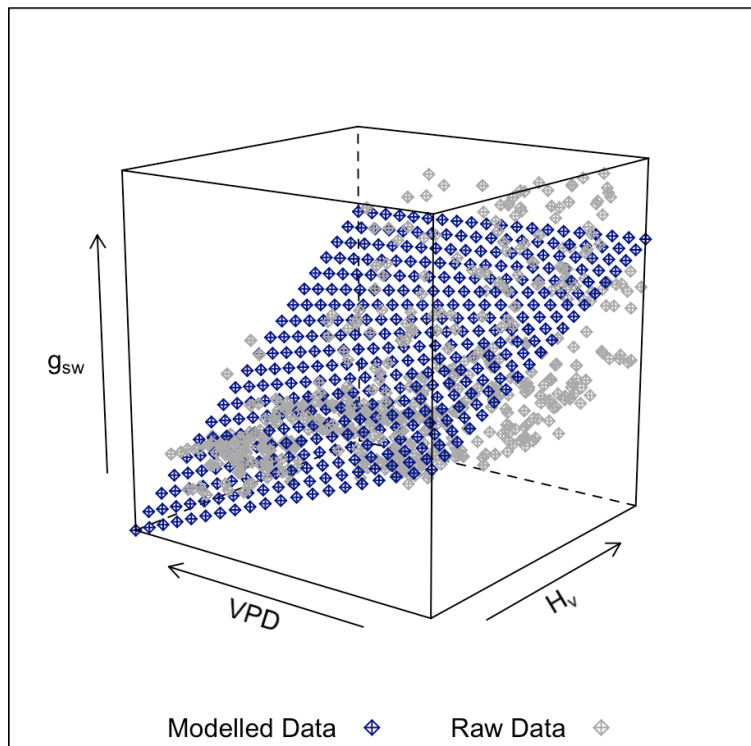


Figure 3.3: 3D representation of the influence of vapor pressure deficit (VPD) and Huber value (sapwood area : leaf area; H_v) on stomatal conductance (g_{sw}). The direction of increase for each variable is indicated with an arrow. Gray points represent the raw data, while the blue surface represents model-predicted values from a linear mixed-effects model. The model included additive and interactive effects of VPD and H_v , along with treatment as a fixed effect, and plant identity (PlantID) as a random intercept to account for repeated measures. Model predictions were generated by creating a regular grid of H_v and VPD values across their observed. The `predict()` function was used to compute predicted g_{sw} values across this grid. Raw and modeled data were merged and visualized using the `cloud()` function from the *lattice* package, with symbol shapes and colors differentiating observed and predicted data. This modeling approach was exploratory and aimed to assess potential interactions between structural and environmental controls on stomatal conductance, not to produce causal inference.

3.2.2 Carbon assimilation and accumulation

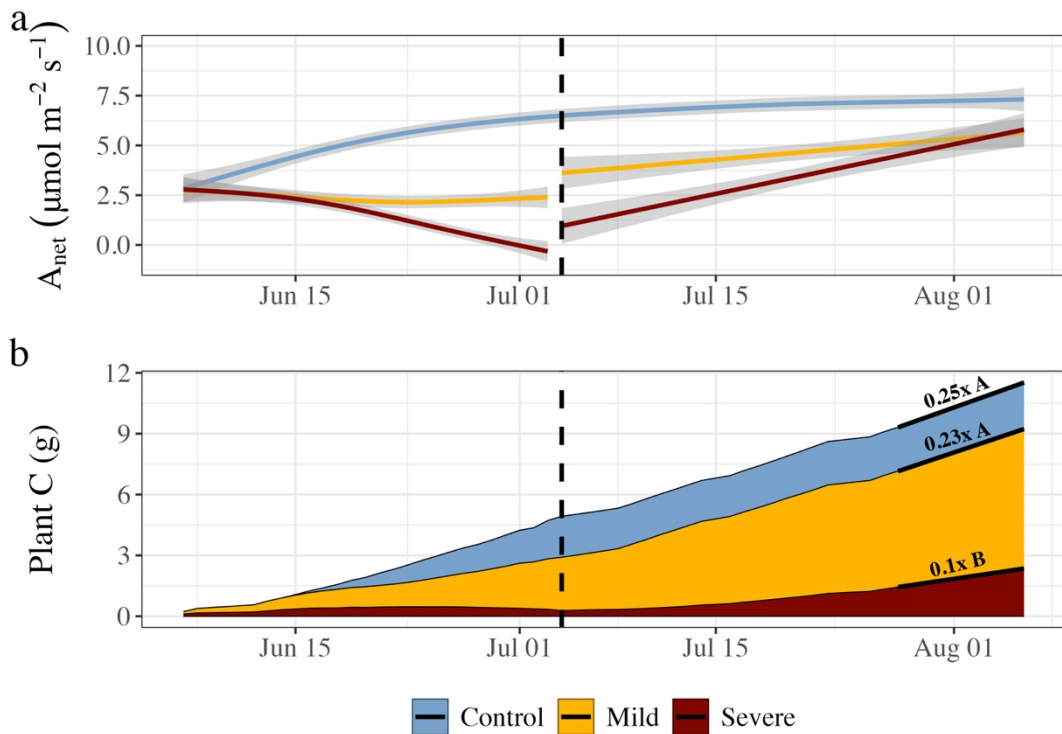


Figure 3.4: Net carbon (C) assimilation and accumulation from Douglas fir seedlings in gas exchange chambers. Mean daytime (09.00-14.00) net photosynthesis rates (a, A_{net}) for each individual tree were fit with generalized additive models to produce smoothing lines, with the shaded gray area representing $\pm\text{SE}$. Carbon accumulation is reported in grams of carbon from chamber seedlings (b). Data reflect daily sums of CO_2 gas exchange of shoot and root sections indicating the whole-seedling net carbon accumulation over the course of the experiment. In panel b, linear models are fit for the final 10 days of recovery for each treatment (black lines) with the slope reported to indicate daily C accumulation rates. Significant differences of the slopes (uppercase letters) were calculated using Tukey's Honest Significant Difference. The dashed black line indicates the transition from drought to recovery in both panels.

Net photosynthetic assimilation (A_{net}) largely mirrored drought intensity throughout the experimental period (Figure 3.4a). During the experimental drought, control plants continuously increased daytime A_{net} in coordination with g_{sw} , reaching $6.56 \pm 0.74 \mu\text{mol m}^{-2} \text{s}^{-1}$ by the end of drought stress. A_{net} in the mild drought treatment plants fluctuated around initial values, with an A_{net} of $2.25 \pm 0.55 \mu\text{mol m}^{-2} \text{s}^{-1}$ by the end of drought, 66 % below that of the control ($p < 0.001$, $t_{12} = -5.174$). As a result, intrinsic water use efficiency (WUE_i) remained higher than the control during mild stress (Figure 3.2b). WUE_i during severe stress ultimately decreased below control levels, and turned negative due to net daytime respiration (Figure 3.4b), suggesting metabolic and non-stomatal limitations to photosynthesis.

As with g_{sw} , A_{net} in the mild stress treatment immediately recovered to higher rates than pre-stress, and continued to increase through recovery in-line with increases in H_v , ultimately reaching an A_{net} of $5.53 \pm 1.25 \text{ } \mu\text{mol m}^{-2} \text{ s}^{-1}$ at the end of recovery, 26 % less than the control on average (n.s.). As a result, WUE_i in the mild stress trees immediately returned to control levels upon recovery (Figure 3.2b), reflecting the release of stomatal limitations to photosynthesis. A_{net} in the severe stress treatment immediately increased upon recovery; however, unlike the mild stress treatment, remained below pre-drought levels for ~ 10 days, five days longer than g_{sw} . This corresponded to WUE_i temporarily remaining below control levels during the first two weeks of recovery. As with g_{sw} , A_{net} ultimately recovered to similar levels following severe stress as after mild stress, approximately 26 % below control levels on average (n.s.). This delayed recovery of both A_{net} and g_{sw} was associated with a higher H_v , suggesting that new basal area was necessary to regain the hydraulic supply required to facilitate maximal gas exchange. In support of this, the intercorrelations between g_{sw} , A_{Net} , and H_v were strongest in the mild and severe treatments (Table S3.1), as the control treatment reached sufficient H_v to support maximal gas exchange earlier in the season (Figure 3.2a).

Net C accumulation was limited by drought stress during both the drought and recovery period. While control plants accumulated $4.93 \pm 0.88 \text{ gC}$ during the drought period, accumulated C was on average 41 % lower under mild stress ($p = 0.040$, $t_{12} = -1.92$), and 94 % lower under severe stress ($p = 0.001$, $t_{12} = -4.07$). These trends were similar in both above- and below-ground compartments (Figure S3.3), with both aboveground net C assimilation and belowground respiration rates decreasing with drought intensity (Table 3.1, Figure S3.4). During the recovery period, control trees accumulated an additional $6.61 \pm 1.31 \text{ gC}$, with a C accumulation rate of $0.25 \pm 0.01 \text{ g C d}^{-1}$ during the final week of recovery, similar to the mild treatment ($p = 0.76$). The severe stress treatment plants accumulated 69 % less carbon than the control treatment plants during recovery ($p = 0.011$, $t_{11} = -3.075$). Daily C accumulation rates at the end of recovery were similar between the control and mild treatment, but were 51 % lower in the severe treatment (Figure 3.4b, TukeyHSD).

3.2.3 Nonstructural carbohydrates (NSC)

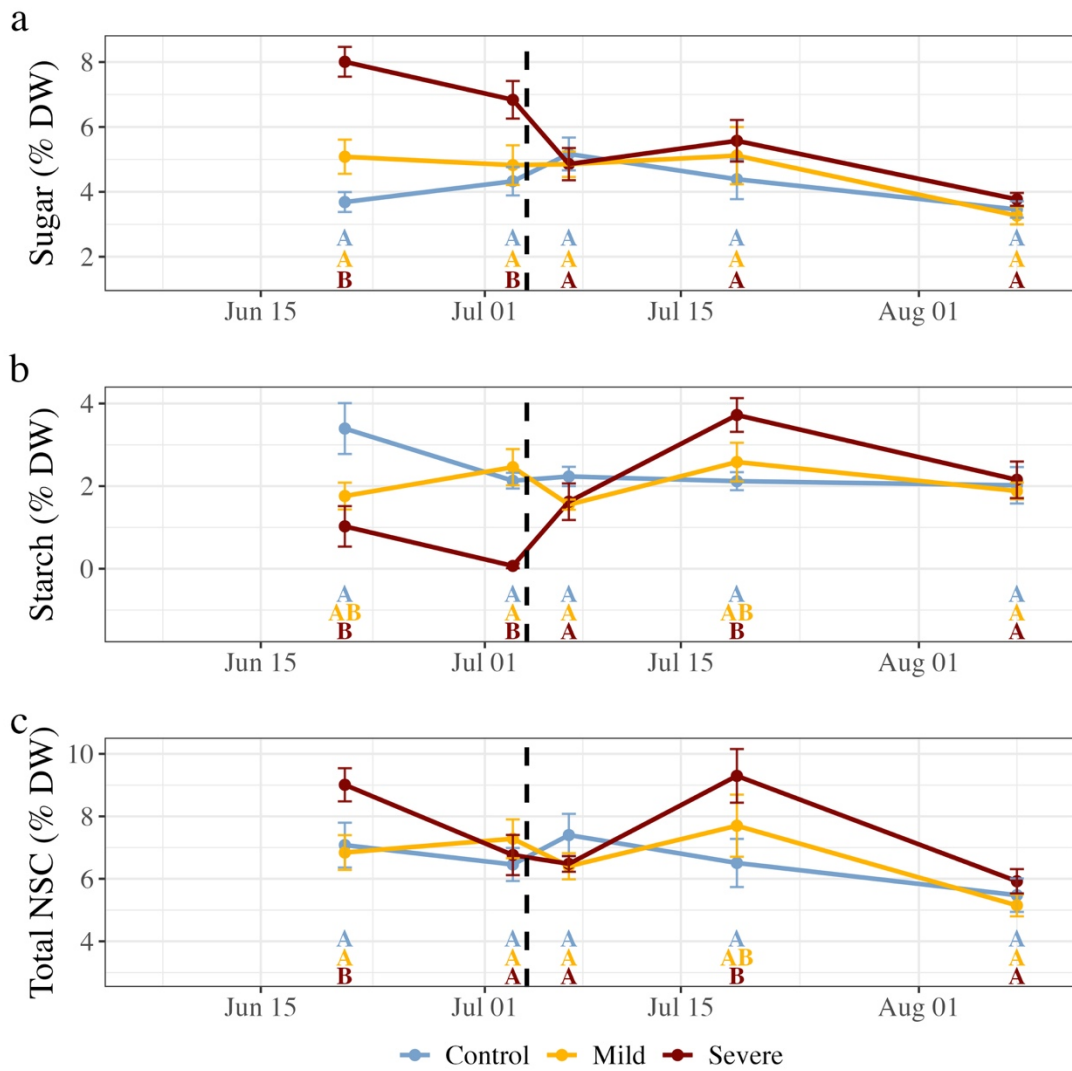


Figure 3.5: Non-structural carbohydrate (NSC) concentrations in axial branch tissues of Douglas fir pilot seedlings ($n = 5-7$ per drought treatment). Displayed are free sugar (a, glucose + fructose + sucrose), starch (b) and total NSC (c, free sugar + starch). Error bars indicate standard error, while the dashed black line in all panels indicates the transition from drought to recovery. Uppercase letters indicate significant pairwise differences per timepoint determined post-hoc using Tukey's Honest Significant Difference.

Branch free sugar concentrations were highly dynamic during the drought period (Figure 3.5a), more than doubling under severe drought stress to 8.01 ± 0.49 % DW after 14 days compared to the control ($p < 0.001$, $t_{12} = 6.942$). By the end of the drought period (28 days), free sugar concentrations were still 58 % greater than the control treatment plants ($p = 0.004$, $t_{18} = 2.962$). In mild stress treatment plants axial branch free sugar concentration remained unchanged throughout the drought. Within two days of recovery, sugar concentrations in the

severe treatment individuals returned to concentrations measured in control treatment plants, and did not vary at any timepoint in the 35-day recovery.

Axial branch starch concentrations responded inversely to free sugar during drought stress (Figure 3.5b). By 14 days into drought stress, starch decreased by 70 % to 1.03 ± 0.49 % DW in the severe treatment individuals, and was no longer detectable by the end of drought. As was the case with free sugars, starch concentrations did not differ at any timepoint between the mild drought treatment plants and the control treatment plants. Within two days of recovery, starch concentrations in the severe drought treatment plants quickly increased to levels measured in control treatment plants and were higher than the control 15 days into recovery ($p = 0.015$, $t_{17} = 2.689$). Starch concentrations ultimately returned to levels measured in control treatment plants by the end of the 35-day recovery.

Total NSCs (sum of sugar and starch) differed between treatments only at the mid-drought timepoint (Figure 3.5c), where total NSC reached 9.03 ± 0.52 % DW, or was 28 % higher in the severe drought stressed plants than the control treatment plants ($p = 0.041$, $t_{12} = 2.289$). Of this, about 90 % of NSC was allocated in free sugars. Total NSC no longer differed by treatment by the end of drought, and did not differ at any time during recovery.

3.2.4 Growth and Biomass accumulation

Stem basal growth proportionally reflected drought intensity throughout the drought and recovery period (Figure 3.6a). While control plants increased basal area on average by 0.58 ± 0.05 $\text{mm}^2 \text{ d}^{-1}$ during drought, growth decreased by 47 % under mild stress to 0.28 ± 0.03 $\text{mm}^2 \text{ d}^{-1}$ ($p = 0.038$, $t_{12} = -1.95$). In the severe drought treatment plants, basal area growth ultimately stopped and began shrinking due to stem dehydration (Figure 3.6a), with an average growth rate of only 0.04 ± 0.02 $\text{mm}^2 \text{ d}^{-1}$. Basal area growth in the mild stress treatment immediately accelerated upon rewetting; however, was on average 25 % (0.61 ± 0.06 $\text{mm}^2 \text{ d}^{-1}$) than the control (0.80 ± 0.05 $\text{mm}^2 \text{ d}^{-1}$), although not statistically different ($p = 0.351$). Following rewetting, severely stressed plants quickly regained their previous maximum diameter; however, further growth (and therefore stem hydraulic development) did not resume until the second week of recovery (Figure 3.6b). Basal area expansion rates remained below the control, leading to a 42 % lower stem growth on average during recovery

$(0.40 \pm 0.02 \text{ mm}^2 \text{ d}^{-1})$ than the control treatment plants, though not statistically significant ($p = 0.085$, $t_{12} = -1.88$).

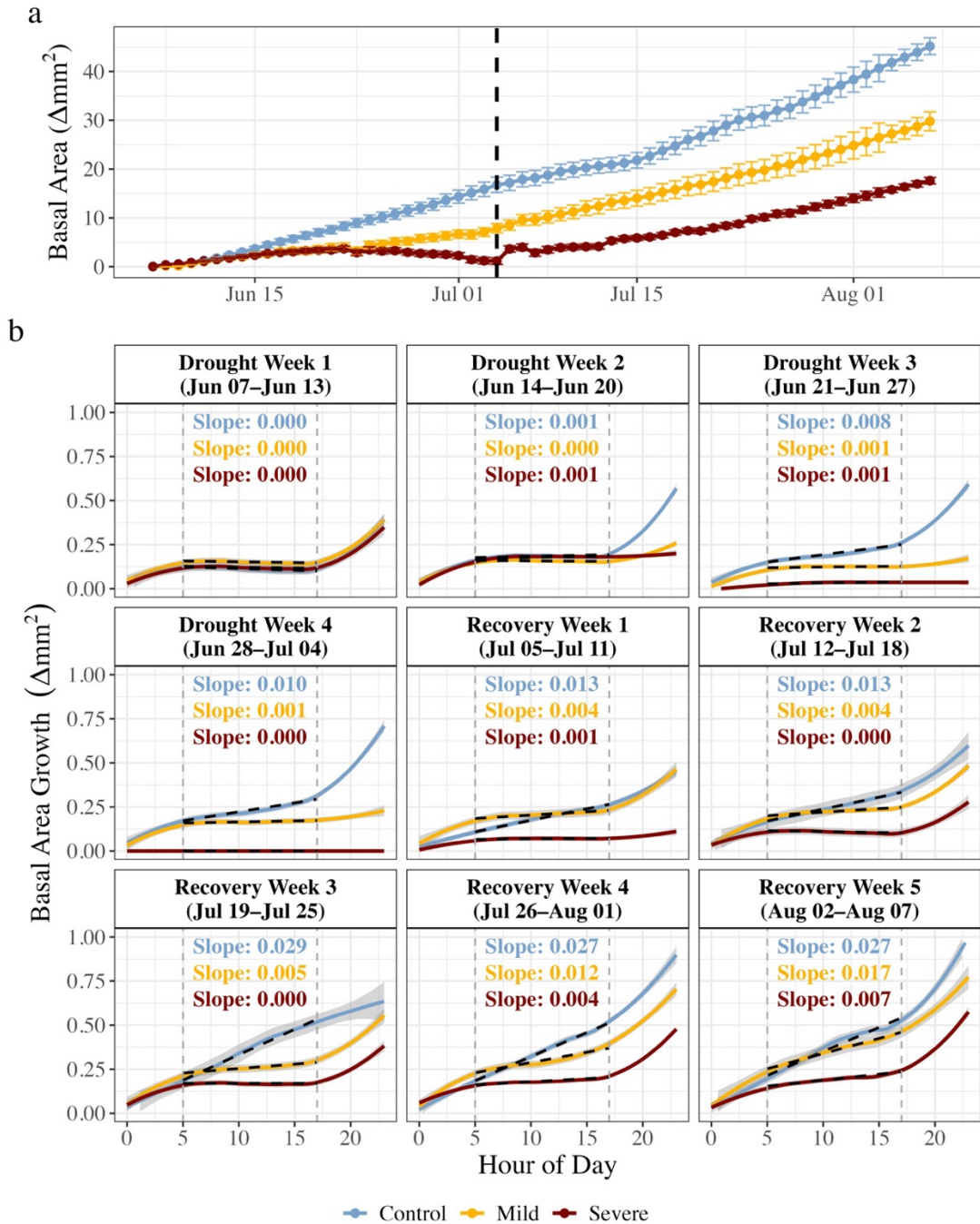


Figure 3.6: Basal area and growth metrics of Douglas fir chamber seedlings during the experimental (drought and recovery) period. Displayed are daily changes in stem basal area (a, $n = 4-6$ per treatment), with error bars indicating standard error and the dashed black line indicating the transition from drought to recovery. Diurnal growth dynamics during each week of the experimental period are reported with growth calculated following the zero-growth concept (b), whereby no growth is assumed during periods of stem dehydration. The shaded error indicating standard error. Linear regression lines and the corresponding slopes represent the midday growth rate (between 5.00 and 17.00).

Notably, differential growth patterns were apparent on a diurnal scale, whereby daytime basal area growth appeared in the control trees by the third week of the drought period, while growth remained restricted to nighttime in the mild and severe treatments throughout drought (Figure 3.6b). Daytime growth appeared in the mild treatment by the third week of recovery, and by the final week of recovery in the severe treatment. An exploratory model to determine the contributing factors to daytime growth revealed daytime growth rate was positively related to H_v at the start of the day ($p=0.001$, $t_{682.06}=2.62$) and negatively related to VPD ($p=0.001$, $t_{290.33}=-2.28$). Net daytime growth appeared possible once trees reached an H_v of ~ 0.08 or greater in mild and control trees (Figure 3.6b, Figure S3.5), but occurred at a slightly higher H_v in the severe treatment (~ 0.09).

Root-to-shoot ratios revealed drought-dependent carbon distribution between biomass compartments (Figure S3.6). The root:shoot ratio was highest in control plants (0.67 ± 0.04) despite having the largest diameter expansion, reflecting elevated allocation to belowground tissues. The root:shoot ratios of mild and severe treatment plants were both below that of the control (mild: 0.42 ± 0.06 , $p = 0.001$, $t_{13}=-4.134$; severe: 0.37 ± 0.06 , $p<0.001$, $t_{13}=-4.323$), indicating lower allocation to belowground tissues relative to above ground tissues, in line with reduced belowground respiration (Figure S3.4a). A summary of biomass between belowground woody biomass, aboveground woody biomass, and needle tissues can be found in Table S3.2.

3.3 Discussion

3.3.1 Drought severity-induced hydraulic and ABA control of stomatal conductance

We found that drought stress impacted g_{sw} in an intensity-dependent manner; however, this was not solely attributable to Ψ_{md} or phytohormone status. Stomatal closure during drought is regulated both passively and actively in gymnosperms, whereby water stress passively decreases guard cell turgor early in drought, while active accumulation of ABA further reduces g_{sw} (McAdam and Brodribb 2014; Tombesi et al. 2015; Manandhar et al. 2024). In agreement, branch Ψ_{md} gradually decreased, triggering an increase in foliar ABA levels as the severe drought progressed, corresponding to gradual and near complete stomatal closure in these plants (Fig. 1c). Under mild drought stress, g_{sw} remained around initial values while Ψ_{md} and ABA levels were maintained. While this could be interpreted as g_{sw} not responding

to the mild drought treatment, the control individuals contrastingly increased g_{sw} over the same time period. Considering leaf-out was complete by the start of the drought period, we attribute the increasing g_{sw} in the control treatment plants to greater hydraulic supply from sapwood growth, indicating that g_{sw} was hydraulically limited in all treatments during the early growing season by inadequate stem hydraulic supply (Song et al. 2024). This is supported by the positive relationship between H_v (stem sapwood area : leaf area) and g_{sw} (Figure 3.2a), with H_v and chamber VPD identified as key factors contributing to g_{sw} throughout the experimental period (Figure 3.3). Thus, the lack of g_{sw} increase in the mild stress treatment plants may be due to minimal sapwood growth during the drought treatment, suggesting that g_{sw} remained low due to stem hydraulic supply. This effect of stem hydraulic supply; however, was not reflected in our measurements of Ψ_{md} . It is important to distinguish that Ψ_{md} represents the plant water status, i.e., xylem tension, whereas hydraulic supply refers to the xylem water transport capacity, which closely depends on the functional sapwood area. Diurnal traces of whole plant gas exchange and water potential in conifers during a drought have demonstrated that the critical water potential thresholds conferring reductions in gas exchange can be subtle given the passive regulation of stomatal control in these species under mild drought stress (McAdam and Brodribb 2014; Manandhar et al. 2024). Thus, small yet physiologically relevant differences in water potential likely existed between the mild and control treatments, but appeared to be below our detection threshold or were present outside of our sampling timeframe.

After rewetting, we observed an immediate partial recovery of g_{sw} in mild-stressed plants, and a gradual increase in g_{sw} in the severely drought-stressed plants. While high levels of ABA contributed to greatly reducing g_{sw} during severe stress, ABA recovered to control levels within two days of recovery (Figure 3.1b). Accumulation of foliar ABA has been linked to delayed g_{sw} recovery on rewetting in *Cinnamomum camphora* and in conifers such as *Pinus radiata* (Brodribb and McAdam 2013; Duan et al. 2020); however, this was not observed in *Pinus sylvestris* (Zlobin et al. 2023), nor in field studies (Skelton et al. 2017). While drought-induced xylem embolism can limit g_{sw} recovery in conifers (Brodribb and Cochard 2009; Rehschuh et al. 2020), we found Ψ_{md} immediately returned to control values following rewetting (Figure 3.1a), despite Ψ_{md} reaching ~ 3.8 MPa during severe stress, corresponding to an estimated loss of conductivity between 70 and 85% (Chauvin et al. 2019). This indicates that the recovery of water status (Ψ_{md}) occurred rapidly, while full hydraulic recovery was more gradual and likely dependent on new xylem formation. The

gradual increase of g_{sw} in the drought-treated plants during recovery was likely related to drought-induced limits of stem hydraulic supply (estimated via H_v) and embolized conduits both being relieved by new sapwood growth (Song et al. 2024). Greater H_v reflects a larger potential hydraulic conductivity relative to leaf area, which reduces the xylem tension necessary to supply the evaporative demand from the foliage (Gattmann et al. 2023), thereby sustaining the delivery of water to the guard cells, maintaining their turgor pressure, and allowing stomata to remain open to support maximal g_{sw} . It is important to note that slightly higher VPD during recovery in the drought treatments contributed to reduced g_{sw} in addition to H_v , as both of these factors were related to g_{sw} (Figure 3.3). Reduced growth rates during mild drought stress likely led to the formation of fewer or smaller xylem tracheids (Olano et al. 2014), leading to lower hydraulic conductivity per area of new growth than the control. As such, g_{sw} remained below control levels during stress recovery in trees with a similar H_v (Figure 3.2a). Reduced xylem conductivity per area of growth suggests that previously drought-stressed trees may require a greater stem basal area to achieve the same g_{sw} as unstressed trees, particularly in plants exposed to severe drought which develop embolism. Taken together, these results emphasize how stem anatomical constraints on hydraulic supply strongly regulate gas exchange in conifers (Gattmann et al. 2023; Knüver et al. 2025), and may ultimately limit the recovery of gas exchange following any intensity of drought stress.

3.3.2 Drought severity increasingly limits recovery of C accumulation

Recovery of C assimilation was limited according to drought severity. During recovery from mild drought stress, photosynthesis gradually increased in-step with g_{sw} , suggesting the non-immediate photosynthesis recovery from mild stress was due to stomatal limitations. In contrast, following severe stress, the recovery of A_{net} was initially decoupled from g_{sw} . This occurred despite an immediate increase in A_{net} , but not g_{sw} following rewetting, indicating A_{net} was initially more sensitive to rewetting. However, A_{net} required longer than g_{sw} to reach pre-drought levels, meaning WUE_i remained below control levels during this time period. This suggests that A_{net} was ultimately less sensitive to the recovery of soil water availability than g_{sw} following severe stress. To balance ATP and NADPH regeneration to lower Rubisco demand during drought, plants actively minimize electron flow through photosystems I and II (Pandey et al. 2022; Alongi et al. 2024), and down-regulate Rubisco activity and content (Parry et al. 2002). While reduced photosynthesis can occur due to NSC feedback inhibition

during periods of reduced sink-activity (M. Tian et al. 2024), we did not observe evidence of NSC accumulation during recovery. Our observed decoupling of g_{sw} and photosynthesis following stress release indicates that short-term recovery of C assimilation may be less limited by hydraulic constraints than by persistent metabolic inhibition of the photosynthetic apparatus following severe stress. In addition to metabolic downregulation, other mechanisms could explain the observed initial non-stomatal limitation of photosynthesis. Photoinhibition, particularly damage to photosystem II due to the production of reactive oxygen species, may impair recovery until repair processes restore photosystem functionality (Schönbeck et al. 2022). Furthermore, reduced mesophyll conductance can persist independently of g_{sw} , thereby increasing the resistance of CO₂ diffusion (Galle et al. 2010). These alternative mechanisms may act independently or in concert with biochemical downregulation to limit initial photosynthesis recovery following severe drought events.

These drought-severity dependent limitations to C assimilation recovery were clearly reflected in whole-tree C accumulation. While mild-stressed plants accumulated on average 45 % less C per day than the control plants throughout the drought period, net C accumulation rates were close to control levels during the recovery period. This occurred despite generally lower A_{net} in mild compared to control trees being compensated for by lower root respiration (Figure S3.4). In agreement with hypothesis (2), severe drought-stress-treated plants accumulated 69 % less C per day than the control-treated plants throughout the entire recovery period, with final daily accumulation rates still 51 % lower. This largely confirms other work demonstrating strong negative relationship between drought severity and recovery of C accumulation rates (Martínez-Sancho et al. 2022). Moreover, these results emphasize that the recovery potential following droughts of varying severities are directly related to the degree and mechanisms of physiological limitation that occur in response to the stress event (Ruehr et al. 2019).

3.3.3 *Reduced recovery of growth not limited by NSC*

Drought-induced reductions in growth persisted through recovery, with 25 % less basal growth during recovery from mild stress and 42 % less from severe stress. The stronger limitation of growth by severe stress can be partially attributed to a delay in the resumption of growth, as growth was minimal during the first week of recovery, suggesting a temporary

delay due to cellular repair (Kannenberg et al. 2022; Lv et al. 2022) or due to regaining phloem functionality (Rehschuh et al. 2020). Our observed growth rate reductions following both mild and severe drought stress are difficult to explain under the sink-driven model of C accumulation. In a sink-driven model of C accumulation, the capacity for growth, as determined mostly by nighttime cell turgor conditions, regulates the amount of C intake via photosynthesis during the day (Körner 2015). While we did not observe differences in branch Ψ_{md} across our stress treatments during recovery, it is possible that small but physiologically relevant differences in Ψ were present, but remained below our detection threshold or sampling timeframe.

Reduced growth following either stress treatment could not be attributed to increased C allocation to storage, as NSC concentrations were maintained at or above nominal levels throughout drought and recovery periods. However, it is important to acknowledge that our severe drought treatment was relatively intense, as Ψ_{md} rapidly decreased, leading to individuals having a net negative C balance during the final eight days of drought on average (Figure 3.4b), during which NSC decreased (Figure 3.5c). It is likely that a more gradual drought would extend the period of a negative C balance and ultimately lead to NSC depletion below control levels. As total NSC concentrations did not deplete below control levels in either the mild or severe treatment, refilling of NSC did not appear to limit growth recovery as some studies suggest (Kannenberg and Phillips 2020; Guo et al. 2021), in contrast to hypothesis (3). We did observe an increase in stem starch concentration around two weeks into recovery; however, starch ultimately returned to control levels, representing only a temporary increase in C allocation to storage, and likely was a result of reduced growth sink strength.

Nonetheless, we recognize that stem NSC concentrations alone likely oversimplify the available carbon for metabolic and structural demands. Drought events can additionally constrain NSC accessibility by tissue compartmentalization, as well as limitations to transport and remobilization (Hartmann and Trumbore 2016). While stem NSC concentrations remained stable, it is possible that other large NSC pools, such as those in root tissue, remained physiologically inaccessible. Therefore, we conclude that the recovery of stem growth is unlikely to be limited by NSC availability following stress (Palacio et al. 2014), but cannot rule out constrained NSC mobilization as a contributing factor to delayed growth resumption.

3.3.4 Modified diurnal patterns restrict growth recovery

A further investigation into the timing of growth revealed key diurnal differences between the control and drought treatment plants. Specifically, the higher daily growth rate in control plants appeared to be largely due to daytime growth, which progressively increased throughout the experimental period (Figure 3.6b). In contrast, daytime growth was absent in the mild and severe stress treatments during the drought period. Daytime growth appeared in the mild treatment by the third week of recovery, but was delayed until the final week of recovery in the severe treatment (Figure 3.6b). As with g_{sw} , the appearance and degree of daytime growth was strongly related to sapwood development (estimated via H_v) at the beginning of each day (Figure S3.5). This was likely due to a greater stem hydraulic supply from increases in sapwood area buffering against daytime changes in xylem tension (Zheng et al. 2022; Ziegler et al. 2024), allowing for growth-favorable turgor conditions to be maintained during the day. This contrasts with the general understanding of tree diurnal growth patterns, where high daytime VPD is expected to restrict growth processes to night (Zweifel et al. 2021). In agreement with this, we found that increasing daytime VPD did negatively affect daytime growth (Figure S3.5). Interestingly, daytime growth appeared possible once H_v reached ~ 0.08 under moderate VPD (Figure S3.5), corresponding to the point in which the seasonal max g_{sw} was reached in both the control and mild stress treatments (Figure 3.2a). Daytime growth in the severe treatment, however, did not occur until the final week of recovery (Figure 3.6b), corresponding to a notably higher H_v (Figure 3.2a). This likely was due to the presence of embolism formed during severe drought stress (Figure 3.1a), which would reduce stem hydraulic conductance of the existing stem basal area (Rehschuh et al. 2020).

Taken together, our findings suggest that drought-induced modifications to sapwood development largely regulate the capacity for juvenile trees to optimize growth patterns across a greater diurnal scale. With daytime growth constituting up to 30% of daily growth in control trees, drought-induced delays in stem hydraulic development may lead to substantial reductions in seasonal biomass accumulation. Furthermore, these results highlight the importance of the drought timing within the growing season. Drought events occurring early in the growing season, before sufficient sapwood has developed to support and canopy gas

exchange, may be particularly disruptive (Ruehr and Nadal-Sala 2025). By limiting the formation of hydraulic capacity needed to sustain photosynthesis and growth, such early-season droughts are likely to lead to prolonged recovery periods, and have the potential to carry-over into the next season.

3.4 Conclusion

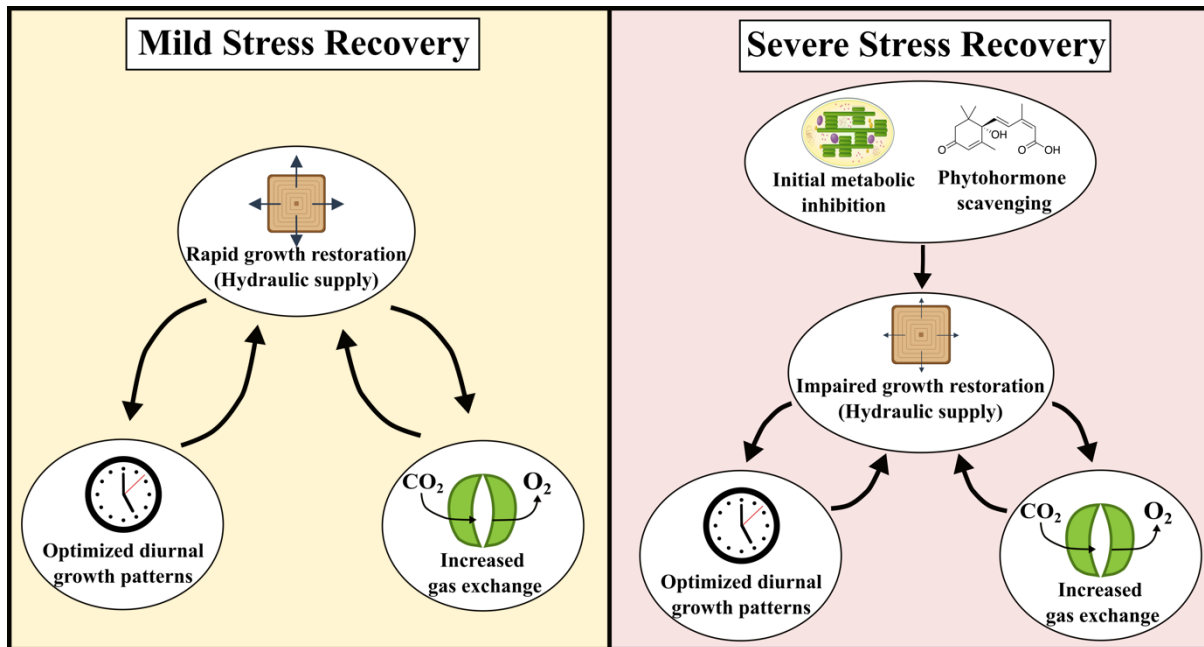


Figure 3.7: Schematic overview of the mechanistic recovery pathways following mild stress (left) and severe stress (right). The restoration of stem hydraulic development positively influenced both the restoration of gas exchange as well as the expansion of diurnal growth patterns, with this pathway substantially delayed following severe stress.

Our findings demonstrate that tree recovery following drought is primarily governed by stem hydraulic constraints, with reduced sapwood development limiting the recovery of both gas exchange and growth in juvenile *Pseudotsuga menziesii* (Figure 3.7). While carbon assimilation declined with drought intensity, severe stress induced an initial metabolic inhibition of assimilation, yet recovery was ultimately constrained by limited sapwood development. Similarly, nonstructural carbohydrate reserves in the stem remained abundant, indicating that carbon likely did not limit growth. Instead, reduced sapwood development delayed the seasonal appearance of daytime growth particularly under severe stress, where daytime basal expansion was largely absent. These drought-induced constraints on stem hydraulic development not only slowed gas exchange recovery, but also suppressed seasonal

carbon accumulation. As this relationship was identified in a singular conifer species with strong stomatal regulation, these mechanisms may not generalize to angiosperms or species with anisohydric hydraulic strategies. Nonetheless, our findings highlight the importance of drought seasonality, as drought events occurring earlier in the year, before sufficient sapwood area has developed to sustain the newly developed leaf area, may disproportionately affect gas exchange and growth, and ultimately lead to extended recovery periods. Together, these results provide a process-based explanation for the observance of prolonged reductions in forest productivity following drought events.

3.5 Materials & Methods

3.5.1 *Plant material and environmental conditions*

We obtained 72 bare-root three-year old *Pseudotsuga menziesii* seedlings (HkG 85305) from a tree nursery in March 2023 (Forstbaumschulen Gracklauer, Gunzenhausen, Germany). Seedlings were placed in individual 5.7 L pots containing an inorganic substrate mixture of fine quartz sand (0.1 – 1.2 mm), medium grain sand (1 – 2.5 mm), perlite, and vermiculite (2:2:2:1), with 12 g extended-release fertilizer and 2 g micronutrient mix (Osmocote® 5 8-9M, Micromax® Premium; ICL Specialty Fertilizers, Geldermalsen, Netherlands).

In May 2023, seedlings were moved into an experimental greenhouse facility in Garmisch-Partenkirchen, Germany (708 m a.s.l., 47°28'32.9" N, 11°3'44.2" E) to acclimate for four weeks. Seedlings were automatically drip irrigated with 150 mL water twice daily (07:00, 21:00; Rain Bird, Azusa, USA), with LED grow lamps maintaining a 15-h photoperiod (LED-KE 400 VSP, DHLicht, Wuelfrath, Germany). Throughout the acclimation and experimental period, continuously measured photosynthetic active radiation (PAR; PQS 1, Kipp & Zonen, Delft, The Netherlands) reached daytime averages of 600 $\mu\text{mol m}^{-2}$ while air temperature and relative humidity were maintained at 23 °C and 60 % respectively (see Figure S3.7 for greenhouse growth conditions).

3.5.2 *Experimental conditions*

The seedlings were randomly assigned to either a well-watered control ($n = 24$), mild-drought ($n = 24$), or severe-drought ($n = 24$) treatment. Six seedlings from each treatment were placed

in custom-built tree gas flux chambers (referred to as chamber seedlings); however, three individuals were ultimately removed due to exceptionally high initial transpiration rates (outliers), resulting in a sample size of $n = 6$ for control, $n = 5$ for mild, and $n = 4$ for severe treatments. The remaining seedlings were placed on separate benches by treatment (referred to as pilot seedlings), and were utilized for destructive samples as to not influence gas-exchange measurements.

On June 6th 2023 following leaf out, irrigation was withheld completely from the severe-drought treatment (0 mL daily), reduced in the mild-drought treatment (60 mL daily), while the control treatment continued to receive drip irrigation (300 mL daily). SWC was measured throughout the experimental period in all gas flux chamber pots, and in four pilot pots per treatment (10HS, Meter Group, USA), and informed drip-irrigation modifications to minimize variation within and between the pilot and corresponding chamber treatments. Targeted soil volumetric water content (SWC) by the end of drought were 0 % in severe, 10 % in mild, and >20 % in the control. SWC progressively decreased throughout the drought period in the non-control treatments. The mild drought treatment attained the targeted 10 % SWC halfway through drought stress and was maintained, reaching 10.3 ± 1.3 % in chamber seedlings and 9.6 ± 0.7 % in pilot seedlings by the end of drought stress. The severe drought treatment continuously dehydrated throughout the drought period, with chamber and pilot seedlings reaching values close to zero by the end of drought stress.

All gas flux chamber pots were equipped with dendrometers installed ~5cm above the soil to continuously measure relative changes in diameter (DD-S, Ecomatik, Germany, 1.5 μ m resolution). Absolute diameters were calculated in comparison to the initial diameter measured by a caliper, and were transformed into basal area. These measurements of basal area were used to infer sapwood area, which we utilized to calculate the Huber value (H_v , estimated as the sapwood area to leaf area ratio).

Growth was determined based on the zero growth concept (Zweifel et al. 2016), which assumes no growth during periods of stem dehydration when the stem diameter is below the previously recorded maximum (Ziegler et al. 2024). Growth data during recovery was reported starting the second day of recovery to account for immediate stem rehydration. Midday branch water potential (Ψ_{md}) was frequently measured on axial branches of randomly selected pilot seedlings ($n=3-5$ per treatment) using a Scholander-type pressure chamber

(Model 1505D, PMS Instruments, Oregon, USA). Midday branch water potential was selected to identify the highest daily xylem tension experienced during treatment progression. An end-drought target Ψ_{md} of ~ 4 MPa in the severe drought treatment was chosen to induce hydraulic damage but not mortality, corresponding to a percent loss of conductivity of 70 – 85 % (Chauvin et al. 2019).

On July 4th 2023, mild and severe drought treatment irrigation returned to 300 mL daily, while all parameters continued to be measured until the end of recovery on August 9th 2023. Following release of drought stress, mild and severe drought treatment SWC quickly increased to control values (>20 %) and were maintained throughout the recovery period (Figure S3.8).

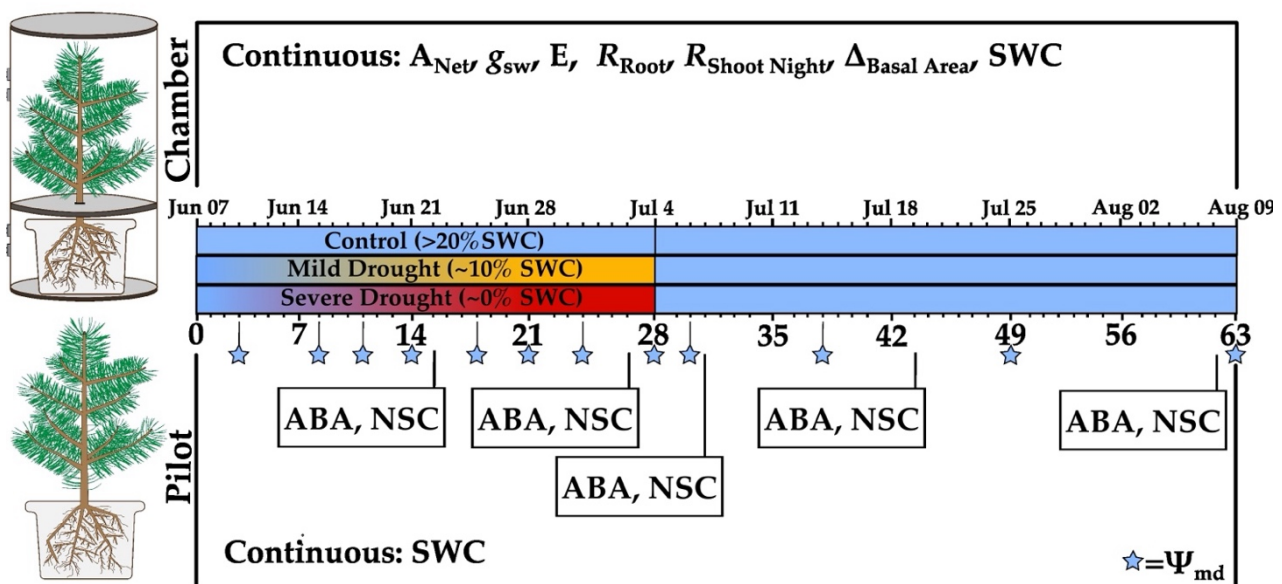


Figure 3.8: Experimental design overview and sampling timeline, indicated by both calendar date (upper timeline) and experimental day (lower timeline). Seedlings were divided between custom-built gas exchange chambers (upper left, $n = 4-6$ per treatment) and pilot seedlings for destructive harvest (lower left, $n = 17-18$ per treatment). Chamber seedlings were measured hourly for net photosynthesis (A_{Net}), stomatal conductance (g_{sw}), transpiration (E), root respiration (R_{Root}), shoot respiration (R_{Shoot} , nighttime only), with continuous measurements of stem basal area ($\Delta_{Basal\ Area}$) and volumetric soil water content (SWC). Pilot seedlings were destructively harvested at the indicated timepoints for midday branch water potential (Ψ_{md}), foliar abscisic acid (ABA), and branch non-structural carbohydrate (NSC), with SWC being continuously measured ($n = 3-4$ per treatment).

Following the end of the recovery period, all chamber seedlings were harvested for biomass and separated into leaf, above ground woody tissue (stem + branch), and belowground woody

tissue (root). Root:shoot is defined as the ratio of belowground biomass (root) to aboveground biomass (leaf + stem + branch). Biomass was then dried for 72 hours at 60 °C, with dry weight recorded thereafter. Total leaf biomass was then used to calculate leaf area for gas exchange standardization. Leaf area was measured on a subset of fresh leaves, with those leaves subsequently dried to determine the leaf area to dry weight ratio, which was then used to transform total leaf biomass into leaf area. We assume that leaf area for each individual was constant throughout the duration of the experiment, as leaf-out and needle elongation was complete at the onset of gas-exchange measurements. Minor leaf shedding and lammas growth occurred on a few individuals under drought treatment; however, this growth was visually estimated to contribute very little to the total leaf area (< 5%). An experimental overview including the measurement timeline is available in Figure 3.8.

3.5.3 Tree gas flux chamber system

Gas exchange (H_2O and CO_2) was continuously measured in above- (shoot) and belowground (root) compartments using a custom-built tree gas flux chamber system (for details see Birami et al. 2020 and Rehschuh et al. 2022). Chambers were continuously supplied predefined 445.6 ± 0.2 ppm CO_2 and 8.0 ± 0.0 mmol H_2O concentration air, with both the provided airstream (reference) and returned airstream (sample) measured for absolute and differential CO_2 and H_2O (Li-840, Li-7000; Li-Cor, Lincoln, NE, USA). CO_2 was supplied above ambient levels to partially offset reductions in individual chamber CO_2 which occur during photosynthesis. Additionally, two empty chambers containing the same C-free potting substrate were utilized to account for background fluxes, and were accordingly subtracted from their respective sample chamber sections. We note that these offsets were relatively minor across chamber sections ($+0.15 \pm 0.09$ ppm CO_2 and 0.03 ± 0.11 mmol H_2O on average). Licor devices were calibrated every two weeks using zero CO_2 and H_2O air. Air temperature (T_{air}) of shoot compartments was regulated by fast-response thermocouples (5SC-TTTI-36-2 M, Newport Electronics GmbH, Deckenpfronn, Germany). Air measurements were at 10 second intervals, with one measurement cycle through all chambers lasting ~80 minutes. For environmental conditions in the gas exchange chambers, see Figure S3.2. Net photosynthetic assimilation per leaf area (A_{net}), root respiration (R_{root}), stomatal conductance per leaf area (g_{sw}), and transpiration per leaf area (E) were calculated as in Rehschuh and Ruehr 2022. Carbon fluxes were calculated separately for each chamber

compartment (root and shoot) without normalizing by leaf area in order to capture the whole-tree carbon budget.

Molar CO₂ fluxes for each chamber compartment were derived from the difference in dry-air CO₂ mole fractions between sample and reference air streams:

$$F_{CO_2,comp} = -\dot{m}_{comp}(C_{sample,comp} - C_{reference,comp})$$

Eq. 1

Where:

$F_{CO_2,comp}$: molar CO₂ flux of the chamber compartment *comp* (mol CO₂ s⁻¹)

\dot{m}_{comp} : molar flow rate through the chamber compartment (mol s⁻¹)

$C_{sample,comp}$: CO₂ mole fraction in the chamber sample air after correction for water dilution (mol CO₂ mol⁻¹ dry air)

$C_{reference,comp}$: CO₂ mole fraction in the reference airstream after correction for water dilution (mol CO₂ mol⁻¹ dry air)

Daily net carbon exchange for each individual (C_{daily}) was then obtained by integrating average molar fluxes (mol CO₂ s⁻¹) from each compartment throughout the day and then multiplying by the molar mass of C and seconds in a day:

$$C_{daily} = (\overline{F_{CO_2,shoot}} + \overline{F_{CO_2,root}}) * M_C * s_{day}$$

Eq. 2

Where:

C_{daily} : daily net C exchange for the study individual (g C day⁻¹)

$\overline{F_{CO_2,shoot}}$ and $\overline{F_{CO_2,root}}$: daily average molar CO₂ flux (mol CO₂ s⁻¹) from the shoot and root compartments, respectively

$M_C = 12.01$ g mol⁻¹: molar mass of carbon

s_{day} : 86400 s day⁻¹

Cumulative carbon accumulation over the course of the experiment was then calculated as the sum of daily values:

$$Plant\ C(d) = \sum_{i=1}^d C_{daily,i}$$

Eq.3

Where:

Plant C(d): cumulative carbon accumulation up to day *d* (g C)

C_{daily,i}: net daily carbon accumulation on day *i* (g C day⁻¹)

d: day index (1≤ *d* ≤ total number of days in the experiment)

3.5.4 Nonstructural carbohydrate quantification

Axial stems (~8 cm) were harvested from randomly selected pilot trees of all treatments (n= 5-7) and microwaved for three 60s increments to halt metabolic activity. Tissues were then dried for 72 hours at 60 °C and ground to a fine powder. Stems were analyzed for starch and sugar (sucrose + fructose + glucose) concentration using a standardized enzymatic method (Landhäuser et al., 2018). Free sugar concentrations were determined after conversion to glucose-6-P via invertase and isomerase. Starch concentration was determined by hydrolyzing α-amylase and amyloglucosidase to convert starch to glucose-6-P. Dehydrogenase was used to oxidize glucose-6-P to gluconate-6-P and absorbance was read at 340 nm on a 96-well microplate photometer (Epoch 2, Agilent, Santa Clara, CA, USA). Total NSC is considered the sum of free sugar and starch, with all NSC reported in % dry weight.

3.5.5 Abscisic acid quantification

Needles were collected from the harvested axial stems and immediately frozen in liquid nitrogen until ABA quantification at the destructive timepoints (n= 5-7/ treatment). Foliar ABA levels were determined via physicochemical methods (McAdam and Brodribb, 2015), where samples were fully homogenized and 15 ng of [²H₆]ABA internal standard was added to each sample. Endogenous ABA was extracted from the homogenized foliar tissue, with an aliquot taken and dried under vacuum until completion. Samples were then resuspended in 200 µL of 2 % acetic acid, with ABA levels then quantified using liquid chromatography–mass spectrometry (Agilent 6400 LC/MS, USA).

3.5.6 Statistical methods

Statistical analysis was conducted in the R statistical programming environment v4.3.2 (R Core Team 2022). Linear fixed-effect models were used to identify fixed treatment differences for all measured parameters at single timepoints (Ψ_{md} , ABA, NSC, biomass metrics, gas exchange, as well as cumulative C uptake and growth for the drought, recovery, and total experiment timeframes). For timeseries regression analysis (daytime growth and final C accumulation rates), mixed-effect models were used to account for repeated measures by including individuals as a random effect, while treatment remained as a fixed effect (*lme4* package, Bates et al. 2014). Exploratory mixed-effect models describing g_{sw} and daytime growth throughout the experimental period were fit using an interaction term between VPD and H_v with treatment as an additive effect, while including individuals as a random effect. All models were analyzed via diagnostic plots to verify parametric modeling assumptions of normality, equal variance, and influential points, with log-response transformations used for data which violated assumptions. Post-hoc differences between treatments were determined using Tukey's Honest Significant Distance with the Kenward-roger degree of freedom method with a 95 % confidence interval and a 0.05 significance level (*emmeans* package; Lenth et al. 2024). Standard error is reported for all included measurements. For daytime (09.00-14.00) and nighttime (00.00-05.00) averages, parameters were first averaged for each individual, with standard error then calculated per treatment.

3.6 Supplementary Materials

Table S3.1: Correlation matrices of average daytime (09.00 – 14.00) net photosynthesis (A_{Net}), stomatal conductance (g_{sw}), and the stem sapwood area : leaf area ratio (H_v) for each treatment throughout the course of the experiment. We computed Pearson correlations after adjusting for the effect of vapor pressure deficit and repeated measures using linear mixed-effects models. Correlation matrices with associated p-values were generated separately for each treatment group.

Treatment	Variable	A_{Net}	g_{sw}	H_v
Control	A_{Net}	1.00 (—)	0.32 (p<0.001)	0.42 (p<0.001)
	g_{sw}	0.32 (p<0.001)	1.00 (—)	0.18 (p=0.001)
	H_v	0.42 (p<0.001)	0.18 (p=0.001)	1.00 (—)
Mild	A_{Net}	1.00 (—)	0.66 (p<0.001)	0.56 (p<0.001)
	g_{sw}	0.66 (p<0.001)	1.00 (—)	0.59 (p<0.001)
	H_v	0.56 (p<0.001)	0.59 (p<0.001)	1.00 (—)
Severe	A_{Net}	1.00 (—)	0.51 (p<0.001)	0.37 (p<0.001)
	g_{sw}	0.51 (p<0.001)	1.00 (—)	0.51 (p<0.001)
	H_v	0.37 (p<0.001)	0.51 (p<0.001)	1.00 (—)

Table S3.2: Biomass (g DW) measured during destructive harvest at the end of the experimental period. Reported are tissue means across treatment with standard error. Bold letters indicate significant differences calculated using TukeyHSD.

Treatment	Total biomass	Belowground woody biomass	Aboveground woody biomass	Needle
Control	$49.2 \pm 7.4 \text{ A}$	$19.8 \pm 2.9 \text{ A}$	$20.1 \pm 2.3 \text{ A}$	$9.2 \pm 0.7 \text{ A}$
Mild	$45.5 \pm 10.5 \text{ AB}$	$13.1 \pm 3.0 \text{ AB}$	$20.5 \pm 4.7 \text{ AB}$	$11.8 \pm 3.2 \text{ A}$
Severe	$24.8 \pm 11.8 \text{ B}$	$7.1 \pm 1.6 \text{ B}$	$10.8 \pm 1.6 \text{ B}$	$7.0 \pm 0.7 \text{ A}$

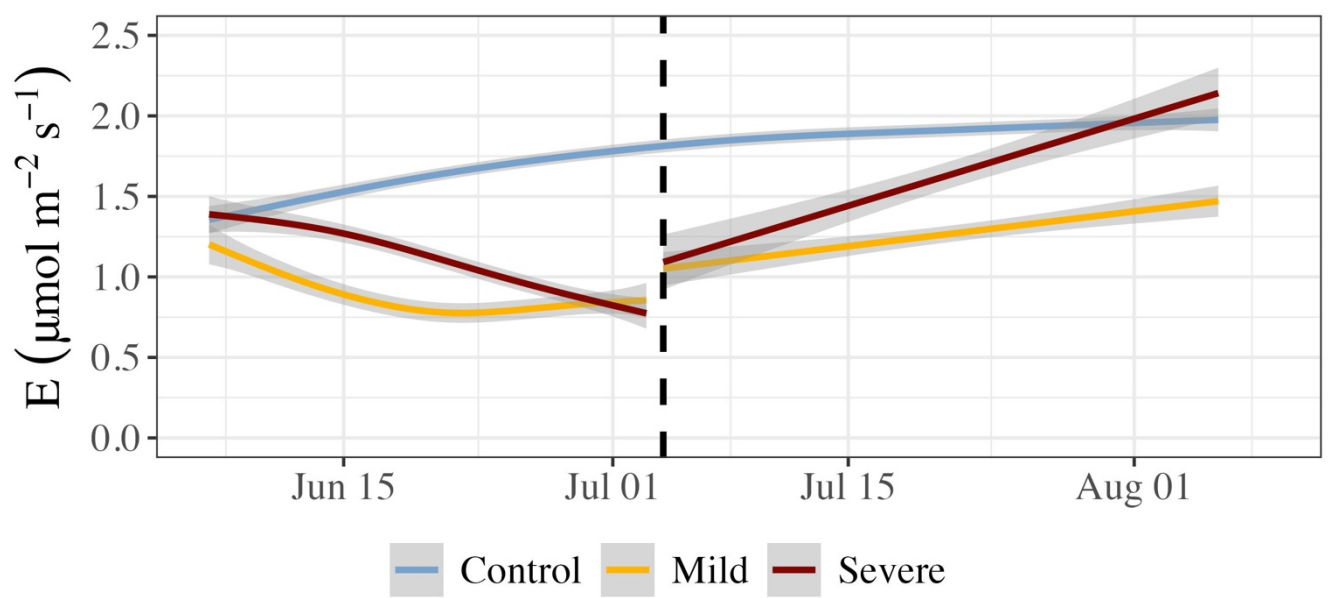


Figure S3.1: Time series of daytime (09.00 – 14.00 transpiration (E) throughout the experimental period ($n = 4-6$ per treatment). Generalized additive models were fit to produce smoothing lines, with the gray shaded area representing $\pm\text{SE}$. The dashed black line in both panels indicates the transition from drought to recovery.

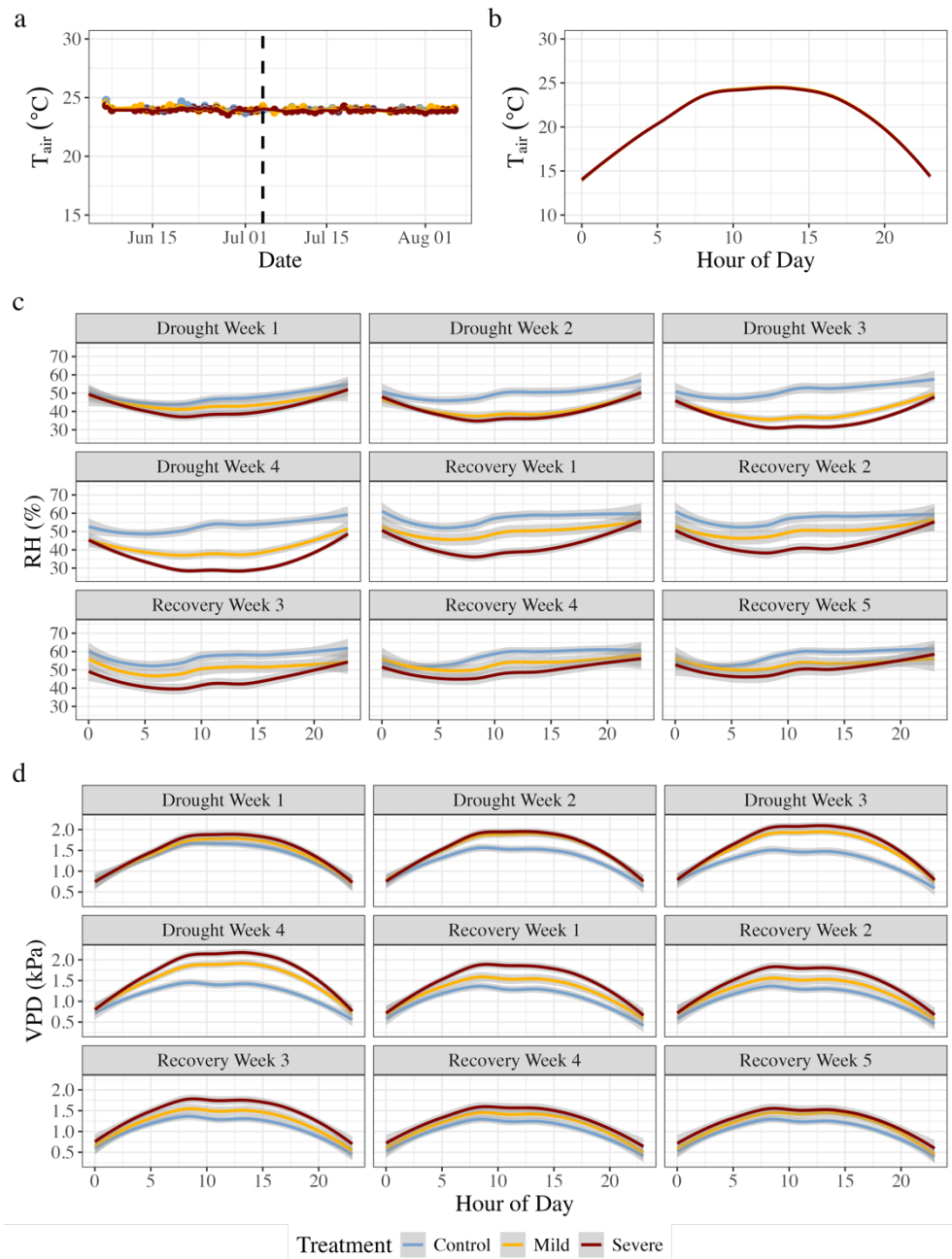


Figure S3.2: Environmental conditions for chamber seedlings during the experimental period. Reported are mean daytime (09.00 – 14.00) air temperature (T_{air} , a), and the diurnal cycle of air temperature (b) throughout the experiment. Due to drought-induced changes in transpiration, relative humidity (RH, c) and therefore vapor pressure deficit (VPD, d) varied between chamber treatments with drought development, and therefore are displayed for each week in the experimental period. All diurnal cycles are shown with standard error. Note, while photosynthetic active radiation is not reported for chamber seedlings, this can be assumed to be equivalent to the greenhouse PAR shown in Figure S3.1.

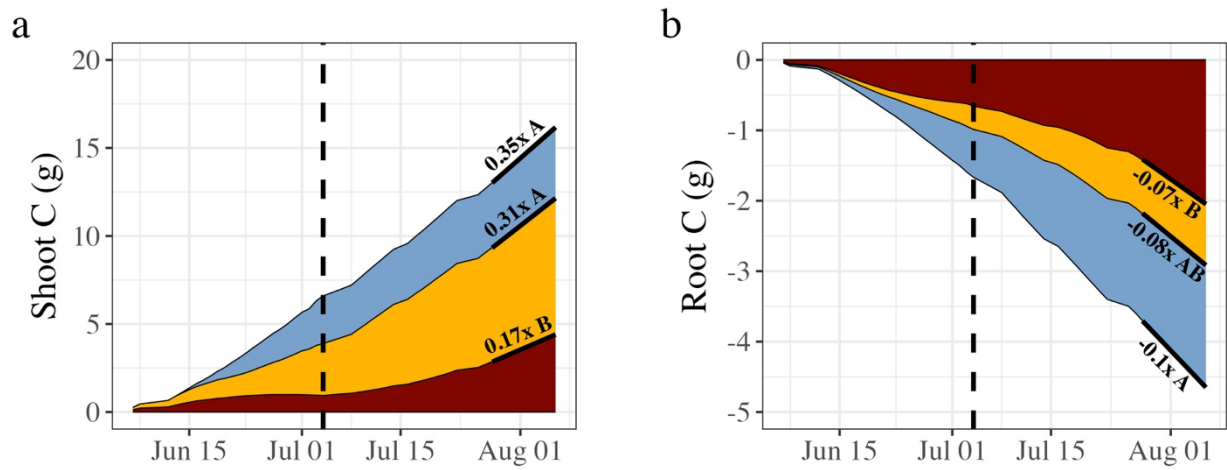


Figure S3.3: Carbon accumulation is reported in grams of carbon from Douglas fir seedlings in gas exchange chambers. Reported are daily net C accumulation from shoot chamber sections (a) and daily net respiration from root chamber sections (b) over the course of the experiment. The dashed black line indicates the transition from drought to recovery. Linear models are fit for the final 10 days of recovery for each treatment (black lines) with the slope reported to indicate daily C accumulation rates. Significant differences of the slopes (uppercase letters) were calculated using Tukey's Honest Significant Difference.

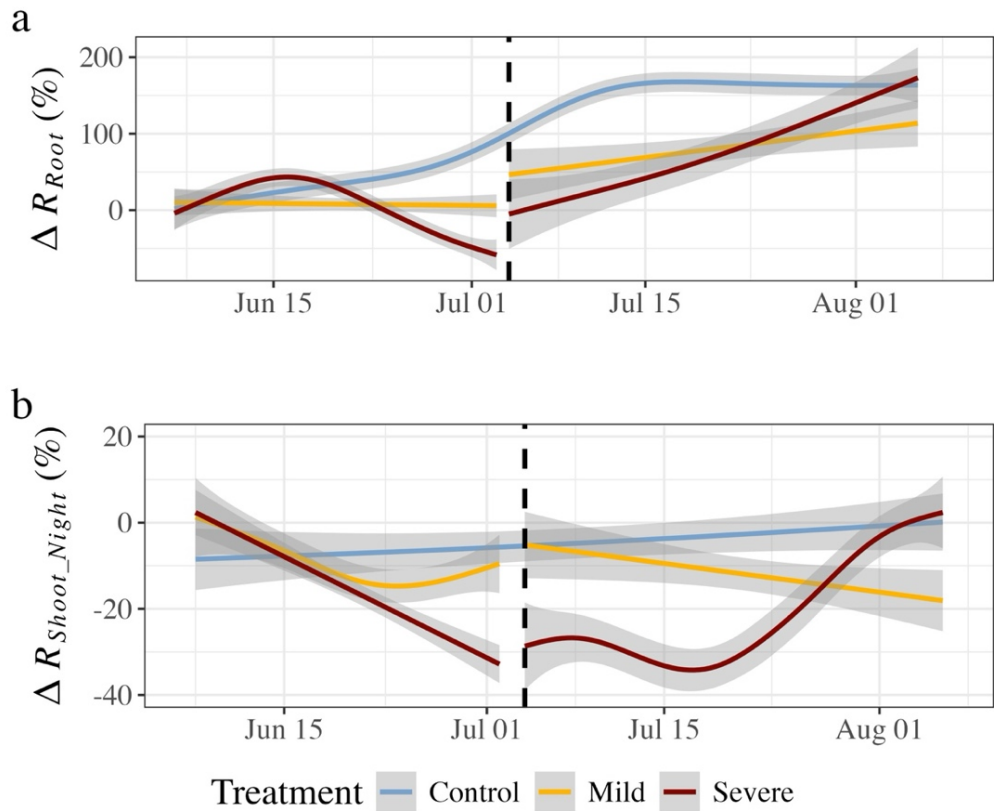


Figure S3.4: Change in Douglas fir seedling respiration throughout the experimental period (drought and recovery). Due to growth of woody tissues, data is standardized to percent change from the experimental start rather than biomass. Generalized additive models were fit on individual daily mean belowground respiration rates (R_{Root} , a), as well as nighttime aboveground respiration (R_{Shoot_Night} , b). The gray area represents \pm SE while the dashed black line in both panels indicates the transition from drought to recovery.

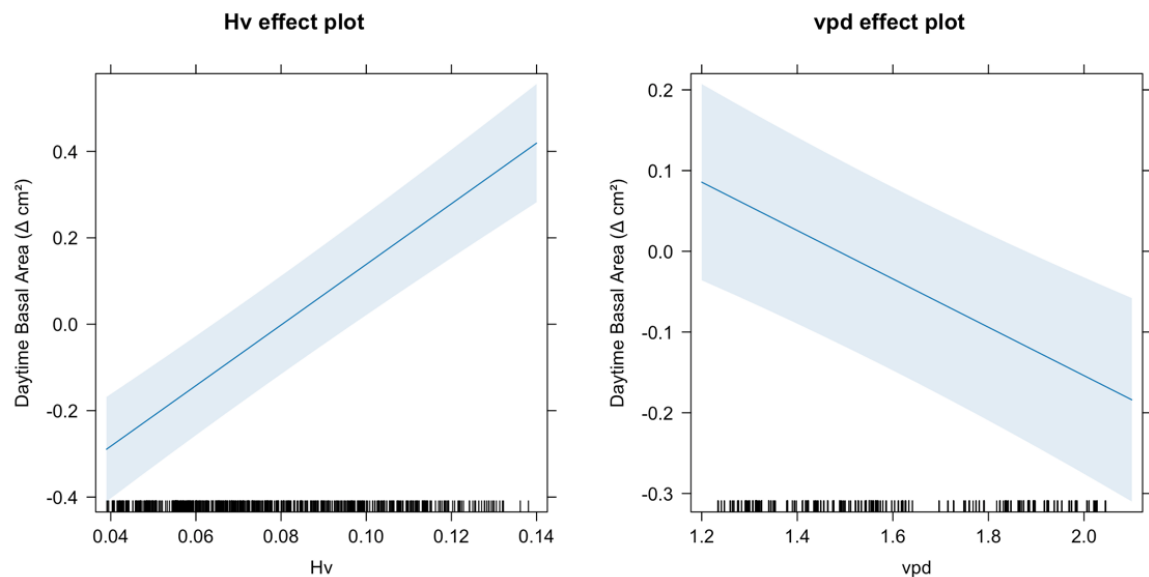


Figure S3.5: Effect plots from an exploratory model evaluating the effects of stem hydraulic supply at the start of the day (Huber value; H_v) and vapor pressure deficit (vpd) on daytime change in basal area, calculated as the difference in basal area between 5.00 and 17.00. The model did not reveal an interaction between H_v and vpd, with no additional variation explained by treatment.

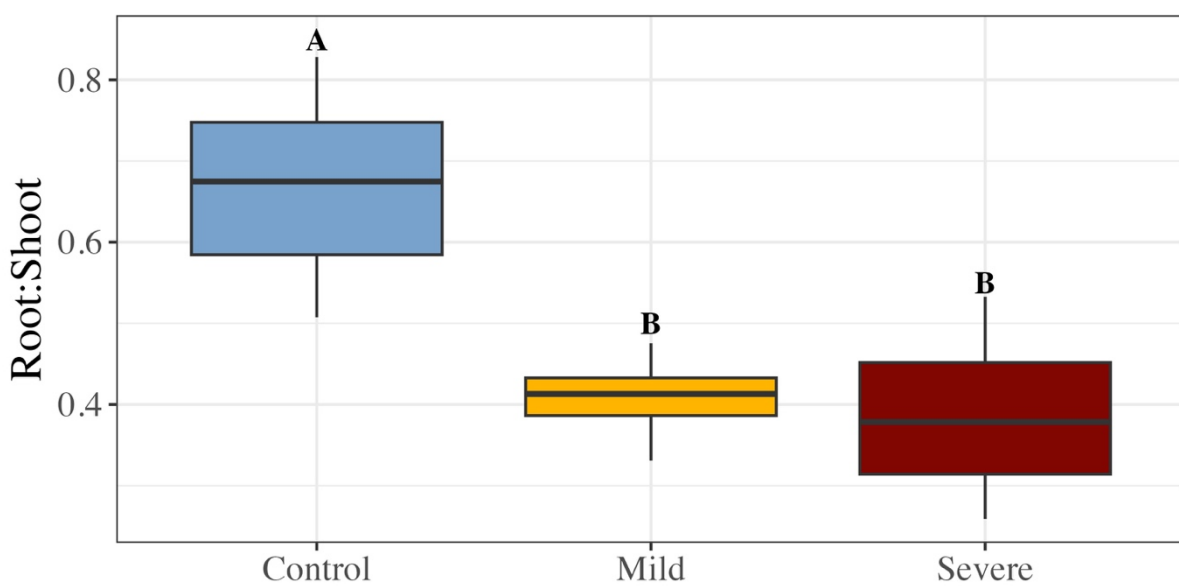


Figure S3.6: The root:shoot ratio is reported for all seedlings utilized in the gas exchange chambers at the end of the experiment (c, $n = 4-6$ per treatment). Uppercase letters indicate significant pairwise differences determined post-hoc using Tukey's Honest Significant Difference.

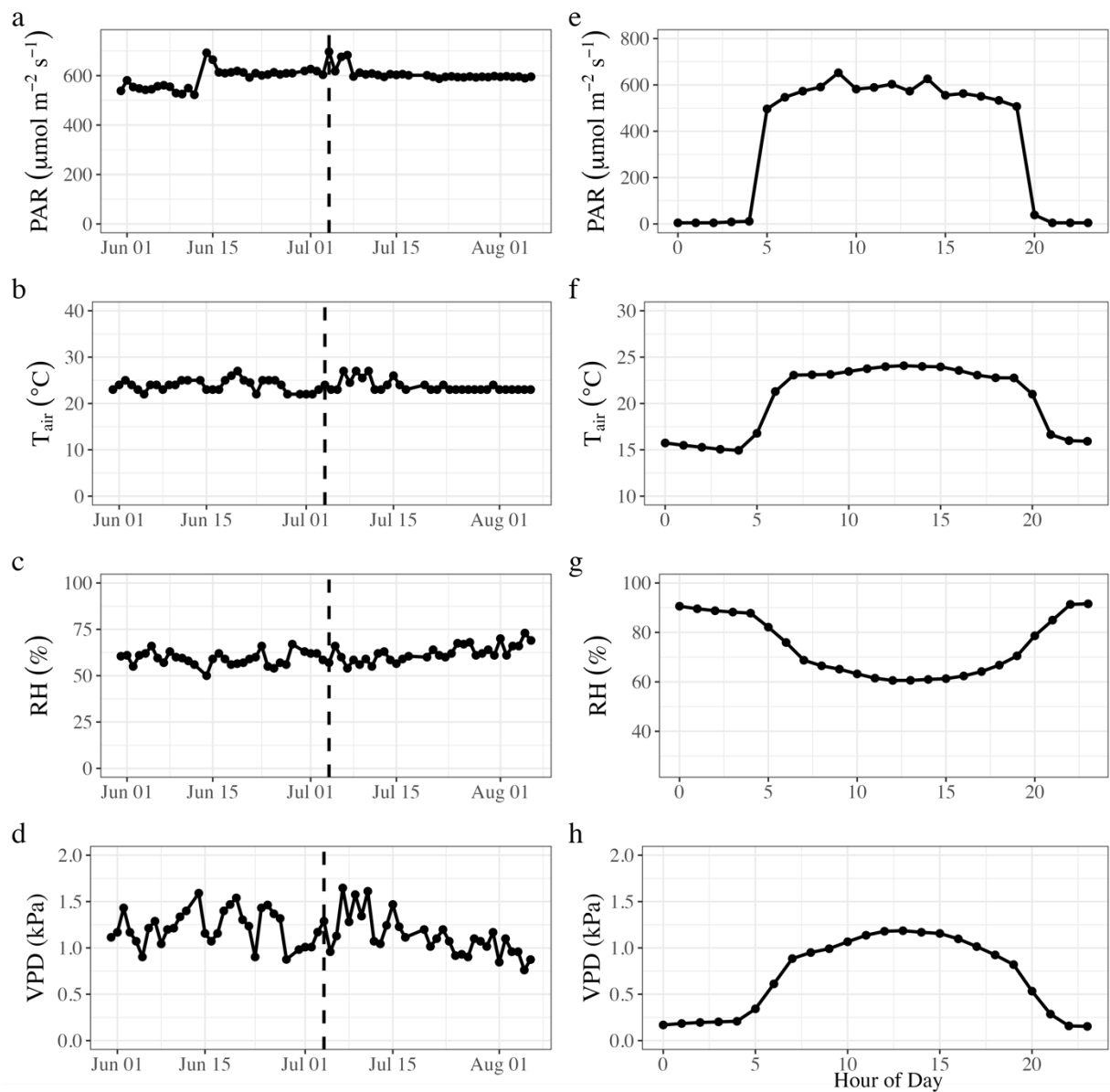


Figure S3.7: Time series visualization of mean daytime (09.00 – 14.00) greenhouse photosynthetic active radiation (PAR, a), air temperature (T_{air} , b), relative humidity (RH, c), and vapor pressure deficit (VPD, d) during the experimental drought and subsequent recovery period for pilot seedlings. The dashed black line indicates the transition from drought to recovery. Diurnal cycles of the environmental conditions are reported (e-h).

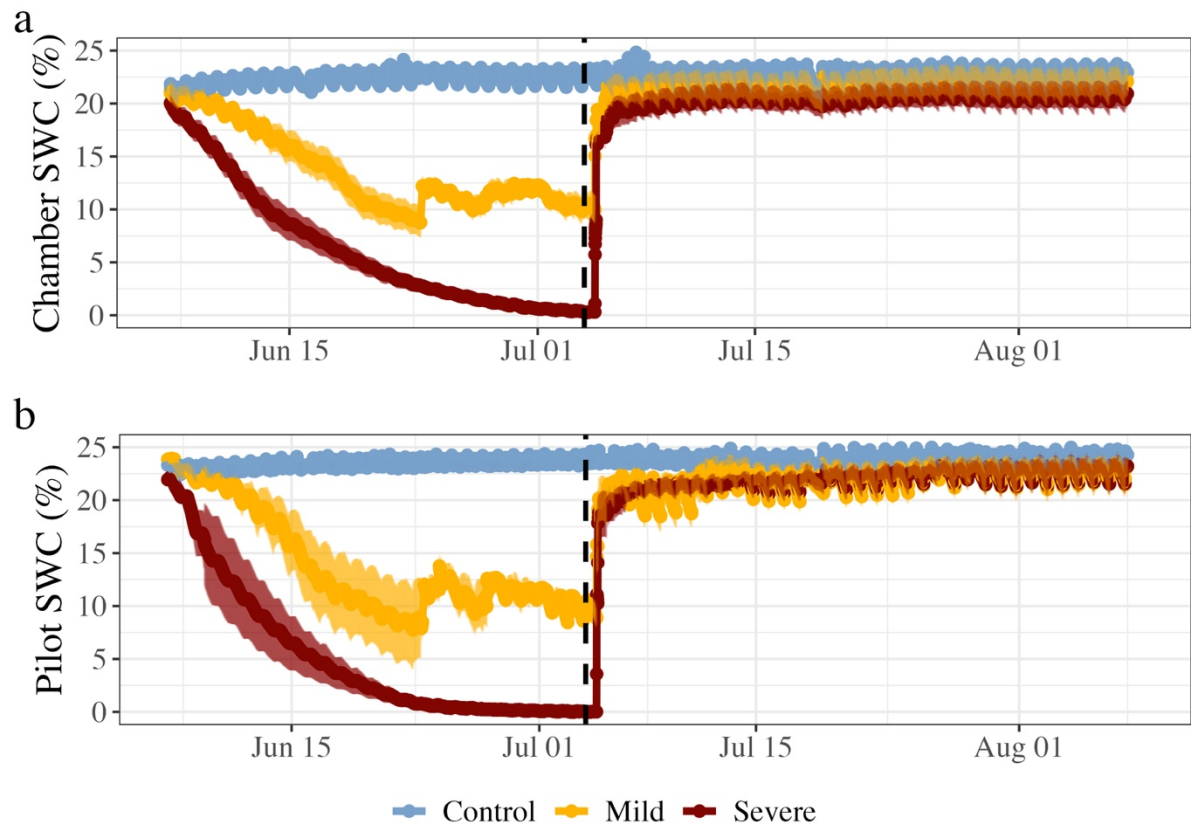


Figure S3.8: Soil water limitation imposed on seedlings by drought treatments (Control, Mild, Severe) throughout the experiment. Volumetric soil water content (SWC) is shown for gas exchange chamber seedlings (a, $n = 4-6$ per treatment) and pilot seedlings (b, $n = 3-4$ per treatment). Shaded area represents \pm SE for each timepoint, while the dashed black line indicates the transition from drought to recovery.

4 Carbon-mediated drought legacy effects differ between two forest species with contrasting leaf habit

This chapter has been submitted (2026) to *Journal of Experimental Botany* as:

Alongi F.; Knüver T.; Blumstein M.; Sontheim A.; Zeppan J.; Reddy S.; Brandfonbrener J.; and Ruehr N.K. Carbon-mediated drought legacy effects differ between two forest species with contrasting leaf habit.

Abstract

Drought events induce long-lasting physiological changes in trees. These “legacy effects” continue to alter forest productivity during subsequent growing seasons. Due to often confounding hydraulic and carbon-related drought impacts, the underlying mechanisms causing legacy effects remain poorly understood. To assess carbon-mediated legacy effects, we exposed two temperate species of contrasting leaf habit to extended drought, reducing photosynthesis while maintaining hydraulic integrity. We quantified bud and branch nonstructural carbohydrates (NSC) between two growing seasons, monitored autumn and spring leaf phenology, and assessed new tissue function and morphology during the subsequent growing season. New tissue development following drought retained physiological function, but exhibited significantly reduced biomass, demonstrating pronounced legacy effects. These patterns were widely correlated with drought-induced reductions in NSC content and dormancy remobilization. Legacy effects were more pronounced in the deciduous *L. decidua* which experienced greater NSC limitations, disrupted spring budburst, and larger reductions in tissue production than the evergreen *P. sylvestris*. Our findings establish a carbon-mediated pathway of drought legacy, resulting in reduced tissue production while preserving tissue function. Deciduous species, which rely predominantly on stored NSC for spring growth, may be particularly vulnerable to this carbon-mediated pathway, suggesting leaf habit as a determinant of legacy sensitivity.

4.1 Introduction

Drought events are expected to increase in frequency and severity, particularly in temperate and boreal forests (Adams et al. 2017; Naumann et al. 2018). Beyond the immediate physiological impacts of drought in trees like reduced carbon (C) assimilation and impaired hydraulic conductance, there is growing recognition that drought induces persistent legacy effects, which modify plant function during subsequent growing seasons (Hartmann et al. 2018; Ruehr et al. 2019; Sterck et al. 2024). These legacy effects often manifest as disrupted seasonal leaf phenology (Vander Mijnsbrugge et al. 2016), reduced productivity (Kannenberg et al. 2022), and through structural modifications in newly developed tissues (Petrik et al. 2022). Despite the growing recognition of legacy effects as drivers of forest function following drought events, the underlying physiological mechanisms that enable these effects to persist into subsequent growing seasons remain largely unresolved (Kannenberg et al. 2020). Proposed mechanisms include both hydraulic and C-mediated pathways; however, it is often difficult to separate these mechanisms as they typically co-occur. This lack of a mechanistic understanding regarding the causes of legacy effects impairs our ability to project ecosystem responses to increasingly severe drought events. Addressing this gap requires experimental studies that can isolate the physiological effects of drought.

The physiological effects of drought can vary by the intensity, duration, and affected forest species (McDowell 2011). Intense drought events induce xylem embolism, impairing hydraulic conductance until the formation of sufficient new sapwood (Rehschuh et al. 2020). In contrast, mild drought events are less likely to induce permanent hydraulic damage, but can still reduce or halt photosynthesis, leading to periods of reduced growth (Ruehr and Nadal-Sala 2025) and substantial C losses (Hartmann and Trumbore 2016). While these C imbalances are often reversible following short drought events, prolonged drought periods can exacerbate C depletion, increasing the recovery time required to replenish C reserves (Ruehr et al. 2019). This may pose a significant challenge for temperate tree species, in which the post-drought recovery window is ultimately constrained by autumn leaf senescence and the onset of winter dormancy.

Temperate tree species experience seasonal cycles of growth, senescence, and dormancy, during which the balance between C acquisition and utilization fluctuates. To buffer against periods of low C assimilation like dormancy, trees rely on internal C reserves in the form of nonstructural carbohydrates (NSC), which support winter respiration and provide substrate for new tissue growth in spring (Tixier et al. 2018; Furze et al. 2019). Drought may be disruptive to this seasonal C budget particularly during late summer and early autumn, when temperate perennials typically shift C allocation away from growth and toward NSC accumulation and bud development in preparation for dormancy (Strømme et al. 2017; Chen et al. 2023). These impacts may be further exacerbated if drought advances autumn leaf senescence, effectively limiting late-season photosynthetic gain (Estiarte and Peñuelas 2015; Wu et al. 2022). However, delayed autumn leaf senescence has also been reported, interpreted as an effort to compensate for drought-reduced growth and NSC storage (Arend et al. 2016; Vander Mijnsbrugge et al. 2016; 2025). Because autumn senescence and subsequent spring budburst define the bounds of the growing season, drought induced shifts in these events directly impact the temporal window for C recovery.

As with autumn senescence, another observed drought legacy effect is either advanced or delayed onset of spring budburst (Kuster et al. 2014; Vander Mijnsbrugge et al. 2016; Čehulić et al. 2019). Budburst depends on the mobilization of NSC from proximal branches toward bud tissues to support new tissue development (Tixier et al. 2018; Blumstein et al. 2024). As such, insufficient NSC accumulation during the previous growing season may delay or slow budburst (Pérez-de-Lis et al. 2016; Amico Roxas et al. 2021), or even result in aborted buds (Misson et al. 2011). Similarly, reduced NSC content in branch tissues are thought to contribute to lower productivity and biomass development in the next growing season (Klein et al. 2014; Löiez and Piper 2022), as early tissue development is highly dependent on the presence of sufficient NSC reserves (Klein et al. 2016, Furze et al. 2019). However, additional legacy effects, namely functional trait modification in new tissues, can lead to longer-term reductions in C acquisition. Specifically, new growth following drought years often displays water-conservative traits, such as lower specific leaf area (SLA) and reduced rates of stomatal conductance (Petrik et al. 2022; Thomas et al. 2024), which can limit seasonal C gain while simultaneously rendering individuals more resilient to recurrent drought events. Understanding drought legacy mechanisms requires linking immediate impacts, such as reduced NSC reserves, with delayed responses in leaf phenology, tissue

function, and morphology, since these combined effects influence plant productivity and resilience in following seasons.

Our understanding of how drought legacy effects are mediated is complicated by the variable strategies across forest species. Deciduous species may be particularly sensitive to drought legacy effects as they rely exclusively on NSC accumulated during the previous year to complete spring leaf-out. In contrast, evergreen species may be able to extend their period of C gain both later in autumn and earlier in spring by utilizing persistent leaf tissue (Parazoo et al. 2018), thereby rendering them less reliant on previous-year NSC to support leaf out and new tissue development (Furze et al. 2019). This dynamic may partially explain the recent observation of greater drought resilience in evergreen species (Marchand et al. 2025); however, the opposite trend has also been observed (Anderegg et al. 2015). How species of contrasting leaf habit regulate their NSC budgets after drought will influence species competition and community composition, underscoring the need for comparative studies that integrate physiological and phenological responses to identify the mechanisms driving drought legacies.

In this study, we experimentally assess how an extended summer drought which maintains hydraulic integrity directly and indirectly affects the plant C budget into the next growing seasons, and how this relates to legacy changes in phenology and subsequent new tissue development. We subjected juveniles of two temperate tree species of contrasting leaf habit (*Larix decidua*, gymnosperm-deciduous; *Pinus sylvestris*, gymnosperm-evergreen) to an experimental drought. Specifically, we explore the immediate and indirect effects of drought on bud and branch NSC content and its relationship to autumn leaf phenology, spring budburst phenology, and new tissue growth and function in the following growing season. We hypothesize that:

H1: Summer drought will decrease NSC content in bud and branch tissues, with these reductions persisting into the following growing season.

H2: Drought will advance autumn leaf senescence, further limiting autumn NSC recovery, with lower NSC correlated with delayed and slower spring budburst.

H3: Drought-reduced NSC reserves will be linked to reduced tissue production in the following growing season, with this tissue exhibiting more conservative water use traits and decreased photosynthetic capacity.

H4: The extent of drought-related NSC reduction, and therefore legacy effects, will differ between species with contrasting leaf habits, with the deciduous *L. decidua* expected to show lower NSC recovery by the start of the following growing season than the evergreen *P. sylvestris*.

4.2 Materials and Methods

4.2.1 Plant material and environmental conditions

We obtained 80 three-year old trees (*L. decidua*, $n = 40$; *P. sylvestris*, $n = 40$) from a tree nursery in March 2023. (Forstbaumschulen Gracklauer, Gunzenhausen, Germany). These individuals were immediately placed in individual 5.7 L plots containing an organic substrate mixture of peat substrate and perlite (5:1), with Osmocote[©] 5 8-9 month slow-release fertilizer (16-8-12 + 2.2MgO + TE; ICL Specialty Fertilizers) added to each pot at a rate of 1g/L. All trees were kept outside at an experimental greenhouse facility in Garmisch-Partenkirchen, Germany (708 m a.s.l., $47^{\circ}28'32.9''$ N, $11^{\circ}3'44.2''$ E). In March 2024, all trees were transplanted into larger 11L pots containing the same soil and fertilizer ratios. In July 2024, all trees were moved inside the greenhouse facility to acclimate to greenhouse conditions for two weeks. Sodium vapor lamps (T-agro 400W; Philips) supplemented natural light to maintain a 14-hour photoperiod. Air temperature, relative humidity, and photosynthetic active radiation were continuously monitored at the mid canopy height (CS215; Campbell Scientific; PQS 1; Kipp & Zonen). For a summary of measured greenhouse environmental conditions throughout the drought period, see Figure S1. Individuals of each species were randomly assigned to either a control or drought treatment ($n=20$ per species per treatment), and placed on respective greenhouse benches (one per treatment/species combination) with dedicated irrigation lines. All individuals were automatically drip irrigated twice daily (07:00, 19:00; Rain Bird, Azusa, USA) to maintain volumetric soil water content (SWC) greater than 30%. We continuously measured SWC (10HS, Meter Group, USA), with five sensors equipped per species in the control treatment, and ten sensors equipped per species in the drought treatment.

4.2.2 Experimental design

The drought treatment started on July 15th 2024 by withholding irrigation from the drought individuals until targeted SWC were reached. Target SWC (5%) was determined by a decline of photosynthesis (A_{net}) $> 50\%$ from control values in order to substantially reduce C input without inducing hydraulic damage (for gas exchange measurement conditions, see section *Assessment of new leaf photosynthetic function*). For drought individuals without an installed SWC sensor, SWC was manually measured twice weekly with an additional 10HS unit. All trees were provided water as needed to maintain the 5% SWC target. We measured both pre-

dawn and midday branch water potential (Ψ) using a pressure chamber (Model 600D, PMS Instruments, Corvalis, USA) on a random subset of each species-treatment combination during peak drought (August 26th, $n=6$) to assess the extent of hydraulic stress, with measurements repeated at the end of the drought period (September 17th, $n=5$). For an overview of the experimental design, see Figure 4.1.

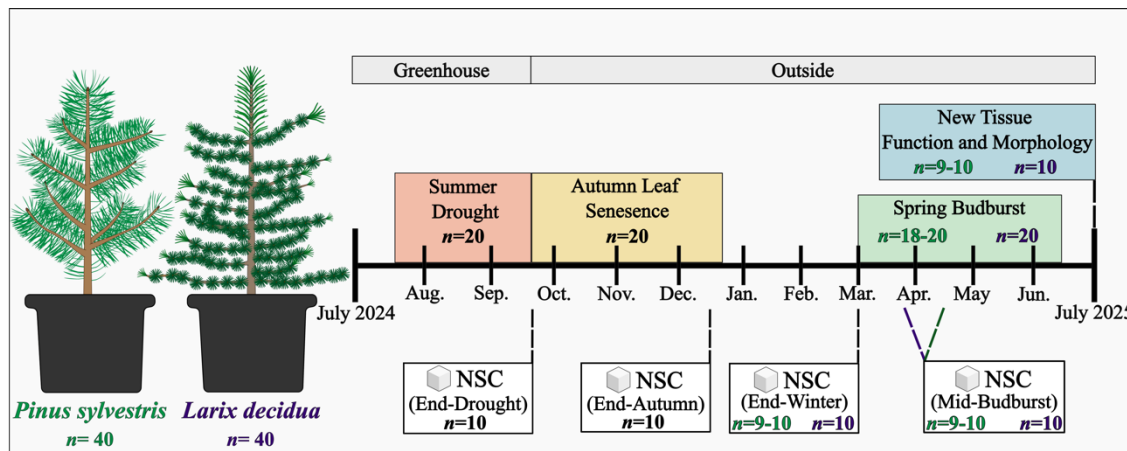


Figure 4.1: Experimental design. Potted juveniles of either *Pinus sylvestris* (green) or *Larix decidua* (purple) were subjected to an extended mild drought (preserving hydraulic integrity) in an experimental greenhouse facility. Following drought, juveniles were moved outside and subsequently monitored throughout autumn leaf senescence using leaf spectral indices, as well as during spring budburst using a phenological scale. New leaf function and new tissue morphology was assessed in July 2025 (one year following drought). Bud and branch samples for non-structural carbohydrate (NSC) analysis were collected at four timepoints. Juveniles of both species ($n=40$ per species) were divided equally into drought and control treatment groups ($n=20$ per treatment per species). Random subsets ($n=10$ per treatment per species) were selected for NSC analysis and legacy trait assessment, with the same subsets used at each sampling point. Two *Pinus sylvestris* drought-treatment individuals did not complete budburst, and were subsequently removed from analysis (deviations in sample size are denoted using each species' respective color).

On September 18th, all trees were watered to field capacity and arranged outside in a randomized design. All studied individuals remained outside through July 2025, and were monitored for autumn and spring leaf phenology, with functional and morphological traits of new growth measured during the following growing season (Spring 2025). Environmental conditions outside the experimental greenhouse were monitored using a ClimaVue 40 (Campbell Scientific, Logan, Utah, US; Figure S4.2). No mortality occurred throughout the experimental and subsequent monitoring period in any *L. decidua* individuals, while two *P.*

sylvestris drought-treatment individuals did not survive into the following growing season and were subsequently removed from all analyses.

4.2.3 Leaf phenology determination

To quantify autumn leaf senescence while accounting for both deciduous and evergreen leaf habit, we measured spectral reflectance in the visible spectrum (380 nm – 790 nm) on all study individuals three times per week between the 19th of September 2024 and the 22nd of December 2024 using a PolyPen RP 410 (Photon System Instruments, Drásov, Czech Republic). For the deciduous *L. decidua*, leaf spectral measurements for each individual continued until >80% leaf shedding occurred (assessed visually), while all evergreen *P. sylvestris* individuals were measured until December 22nd 2024. For each measurement timepoint, 26 commonly used reflectance indices for assessing photosynthetic pigment status were calculated (Table S1). To identify a common spectral index for analysis of autumn leaf senescence, linear correlations were determined between each spectral index and the day of year for both species. Numerous spectral indices were found to be highly correlated with DOY across the autumn senescence period in both conifer species. As expected, these correlations were stronger in the deciduous *L. decidua*, with the top three correlated spectral indices being ZMI (-0.90), GM2 (-0.90), and SR (-0.88) (Figure S4.3). While correlations were slightly lower for the evergreen *P. sylvestris*, we nonetheless identified strong phenological signals in the spectral indices PRI (-0.81), ZMI (-0.79), and GM2 (-0.73). Due to the high negative correlation in both species, ZMI was selected to evaluate autumn leaf phenology. The ZMI index is derived as the ratio between reflectance in the near infra-red (R750 nm) and red-edge (R710 nm) region, and is well documented to serve as a proxy for leaf chlorophyll content (Zarco-Tejada et al. 2001).

We visually assessed spring leaf phenology (budburst) on the shoot apex on all study individuals every other day between March 3rd 2025 and June 20th 2025 using a six-stage visual scale (Figure S4.4). For *L. decidua*, the stages were stage 1 = dormant bud, stage 2 = bud swelling, stage 3 = leaf emergence (scale attached), stage 4 = leaf emergence (scale detached), stage 5 = leaf separation, and stage 6 = leaf elongation. For *P. sylvestris*, the stages were stage 1 = dormant bud, stage 2 = bud swelling, stage 3 = bud elongation, stage 4 = needle sheath emergence, stage 5 = needle emergence, and stage 6 = needle elongation.

4.2.4 Tissue sampling

Tissue sampling occurred at four timepoints to capture both drought and seasonally induced variations in NSC concentrations of branches and buds. Specifically, the sampling occurred at the end of the drought period before rewatering (September 15th 2024; “end-drought”), following the end of the autumn senescence period (December 15th 2024; “end-autumn”), at the end of winter (March 2nd 2025; “mid-budburst”), and finally during active budburst (March–April 2025). Sampling during budburst occurred for each species when the control group of that species reached budburst phenophase three (50% complete), which occurred March 20th 2025 in *L. decidua* and April 22nd 2025 in *P. sylvestris*. Each sampling campaign consisted of removing an axial branch which developed during the 2024 growing season from the 2023 apical shoot. While only a subset of individuals was used for NSC analysis, tissue removal was performed on all individuals to maintain consistent harvest effects. NSC concentrations were quantified in branch and bud tissues produced during the 2024 growing season on a randomly-selected subset of individuals ($n = 9-10$ per treatment per species), with buds separated from branch tissue and separately microwaved for three minutes to halt metabolic activity. NSC samples were then dried for 72h at 60°C and ground to a fine powder using a ball-mill. Prior to grinding, buds were counted and weighed to calculate the average bud dry mass at both the end-drought and end-autumn destructive harvest timepoints.

4.2.5 Nonstructural carbohydrate quantification

The concentration of starch and sugars (sucrose, fructose, and glucose) in the ground branch and bud samples was measured using a well-established enzymatic protocol (Landhäusser et al., 2018). In short, 15 mg of ground tissue was weighed into tubes, with the specific mass for each sample recorded. Samples were boiled in 80% ethanol for 10 minutes, with the resulting supernatant used for soluble sugar quantification following their conversion to glucose-6-phosphate (G6P) through the action of invertase, hexokinase, and phosphoglucose isomerase. The remaining pellet was gelatinized in water and then utilized for quantification of starch. The starch pellet was first treated with α -amylase (Sigma-Aldrich, Darmstadt, Germany) to convert starch into water-soluble glucans. Following separation of the solids with a centrifuge, the glucans were hydrolyzed into glucose using amyloglucosidase (Sigma-

Aldrich, Darmstadt, Germany), which was then converted to G6P by hexokinase. For both sugar and starch quantification, G6P was oxidized to gluconate-6-phosphate by G6P dehydrogenase (Sigma-Aldrich, Darmstadt, Germany), and absorbance was recorded at 340 nm using a 96-well microplate photometer (Epoch 2, Agilent, Santa Clara, CA, USA), with sample absorbances compared to those from a standard curve. The total NSC were determined by summing the concentrations of soluble sugars and starch, with results expressed as a percentage of dry weight.

4.2.6 Assessment of new leaf photosynthetic function

We assessed new leaf photosynthetic function using a combination of leaf spectral reflectance indices, gas exchange, and chlorophyll fluorescence measurements. Spectral indices (see section *Leaf Phenology Determination*) were calculated for all individuals of *P. sylvestris* (n=18-20 per treatment) on new crown foliage, and for *L. decidua* on long “single” leaves emerging from new branch growth (n=20 per treatment). Gas exchange and chlorophyll fluorescence were measured using a Li-6800 portable photosynthesis system equipped with the 6800-01A multiphase flash fluorometer (LI-COR Biosciences, Lincoln, Nebraska, USA). The 2-cm² cuvette conditions were set to 420 ppm CO₂, 1000 $\mu\text{mol m}^{-2} \text{s}^{-1}$ photosynthetic photon flux density, and a 750 $\mu\text{mol s}^{-1}$ flow rate at 25°C using ambient relative humidity. Gas exchange measurements were corrected for actual leaf area within the 2-cm² cuvette on all individuals. Gas exchange and chlorophyll fluorescence measurements were conducted on newly developed foliage in the same subset of individuals selected for NSC analysis (n = 9-10 per treatment per species). In *P. sylvestris*, measurements were performed on new crown foliage, while in *L. decidua*, measurements were taken on long “single” leaves from current-season branches.

4.2.7 Growth and new tissue morphology

Total plant height and stem basal area (measured at pot height) were recorded for all individuals in July 2025, and were compared to initial measures of height and diameter to quantify annual growth. In addition, we quantified new axial branch growth by counting the number, length, and dry mass of all newly emerged branches extending from the previous year’s apical shoot in *L. decidua* (n = 20) and in *P. sylvestris* (n = 19), following the

separation of all foliage. These individuals were the same subset selected for NSC quantification to allow for correlation analysis.

Leaf surface area was calculated prior to drying on fresh leaf subsets. In *L. decidua*, a new branch foliage was scanned to determine one-sided projected leaf area; total leaf surface area was estimated by doubling this value to account for both sides of the flattened leaves. For *P. sylvestris*, needles were modeled as half-cylinders to account for both the curved and flat surfaces. Each fascicle, containing two needles of uniform length and width, was treated as follows:

$$A_i = 2 \cdot L_i \cdot W_i \cdot (\pi/2 + 1)$$

Where A_i is the total surface area of fascicle i , L_i is needle length (mm), and W_i is the needle diameter (mm). Following the determination of leaf area to derive specific leaf area (SLA), all samples were dried at 60°C for 72h and dry mass determined.

4.2.8 Statistical methods

All statistical analyses were conducted in R version 4.4.1. (R Core Team 2022; Posit Team 2025). For gas exchange parameters measured throughout the drought treatment period, we used linear mixed-effect models (LME; *lme4* package, Bates et al. 2014) with individual tree identity included as a random effect to account for repeated measurements.

To evaluate changes in tissue NSC content between seasons, we fit linear mixed-effect models separately for each species, including the interaction between treatment and harvest timepoint, and with the individual plant included as a random effect to account for repeated sampling.

Treatment effects on single-timepoint response variables—including non-structural carbohydrate (NSC) concentrations, phenological timing (start, end, and duration), as well as growth and new tissue measurements—were assessed using linear models at each timepoint with species and treatment as interactive effects. Model assumptions of normality and homoscedasticity were evaluated using diagnostic plots and formal tests. Where necessary,

response variables were log-transformed to better meet parametric assumptions of normality and equal variance (evaluated again via diagnostic plots). Analysis of variance (ANOVA) tables derived from these linear models were used to test the significance of main and interaction effects. A main effect of treatment, when no significant interaction was detected, was interpreted as a consistent response across each species. In cases where a significant treatment by species interaction was observed, post-hoc pairwise comparisons were performed within each species using estimated marginal means (*emmeans*, Lenth et al. 2024). These contrasts informed the assignment of significance markers in visualizations. If assumptions were still violated after transformation, non-parametric Kruskal-Wallis tests were conducted within each species to assess treatment effects.

To evaluate the legacy effects of drought treatment, species identity, and their interaction on leaf function, we conducted a permutational multivariate analysis of variance (PERMANOVA) using the *adonis2()* function from the *vegan* package in R (Oksanen et al. 2025). The response matrix consisted of standardized pigment indices, gas exchange traits, and chlorophyll fluorescence parameters, and Euclidean distance was used as the dissimilarity metric. The model included treatment, species, and their interaction as fixed effects, and terms were evaluated sequentially using Type I sums of squares (by = "terms"). Statistical significance was assessed using 999 permutations.

To assess the relationship between tissue NSC and legacy response variables (e.g., phenology timing and new tissue development), we calculated correlation matrices using the Pearson correlation coefficient. Analyses were conducted separately for each species, with data pooled across treatments. Correlations for which we interpret relationships were restricted to variables previously determined to have varied by the drought treatment, while all correlations are visualized and reported in the supplementary materials.

Model results for NSC dynamics, new tissue morphology, and correlation analyses are provided in the Supplementary Materials, whereas all other model results are reported in-text with their corresponding test statistic, degrees of freedom, and type of test performed.

4.3 Results

4.3.1 Drought Treatment Effects

The imposed drought led to gradual declines in soil water content during the first month of treatment, reaching targeted SWC values of c. 5%, which were maintained throughout the second month of drought (Figure S4.5a). Drought decreased net photosynthesis by $4.71 \pm 1.23 \mu\text{mol m}^{-2} \text{s}^{-1}$ on average ($\chi^2 = 72.97$, $\text{df} = 1$, $p < 0.001$, linear mixed-effects model), or by $\sim 63\%$, with this effect consistent across both species ($p = 0.567$), with similar reductions observed for transpiration (E) and stomatal conductance (g_{sw} , Table 1). Measurements of predawn and midday leaf water potential (Ψ) taken during the peak drought period revealed lower Ψ_{pd} ($F_{1,28} = 39.59$, $p < 0.001$, Two-way ANOVA) and Ψ_{md} ($F_{1,28} = 68.65$, $p < 0.001$, Two-way ANOVA) in drought individuals of both species (Table 1, Figure S4.5c). Despite these decreases, Ψ_{md} remained above -1.5 MPa in both species, above levels typically associated with complete stomatal closure and embolism formation in these species (Ziegler et al. 2024). In addition, drought reduced stem basal growth in both species by 74.2% during the treatment period ($F_{1,78} = 21.57$, $p < 0.001$, Two-way ANOVA; Figure S4.5d).

Table 4.1: Summary of photosynthetic, hydraulic, and growth parameters during the two-month drought treatment in *Larix decidua* and *Pinus sylvestris* juveniles. Provided are treatment averages $\pm \text{SE}$, and the resulting p-value from mixed effect (A_{net} , g_{sw} , E , ETR), and one-way ANOVA (Ψ_{predawn} , Ψ_{midday} , Basal Area Growth) models.

Variable	<i>Larix decidua</i>			<i>Pinus sylvestris</i>		
	Control	Drought	p	Control	Drought	p
A_{net} ($\mu\text{mol m}^{-2} \text{s}^{-1}$)	11.5 ± 0.7	6.1 ± 0.5	<0.01	10.6 ± 0.6	4.49 ± 0.5	<0.01
g_{sw} ($\text{mmol m}^{-2} \text{s}^{-1}$)	204.7 ± 18.6	69.5 ± 6.6	<0.01	121.2 ± 9.7	39.3 ± 5.4	<0.01
E ($\text{mmol m}^{-2} \text{s}^{-1}$)	3.18 ± 0.3	1.12 ± 0.1	<0.01	2.0 ± 0.2	0.7 ± 0.1	<0.01
ETR ($\mu\text{mol m}^{-2} \text{s}^{-1}$)	81.8 ± 2.5	67.9 ± 3.10	<0.01	93.2 ± 2.62	68.4 ± 3.35	<0.01
Ψ_{predawn} (MPa)	-0.14 ± 0.04	-0.34 ± 0.05	$=0.01$	-0.26 ± 0.02	-0.47 ± 0.04	$=0.02$
Ψ_{midday} (MPa)	-0.46 ± 0.04	-0.99 ± 0.09	<0.01	-0.40 ± 0.02	-0.75 ± 0.02	$=0.04$
Basal Area Growth (mm^2)	60.5 ± 9.6	13.9 ± 7.2	<0.01	68.7 ± 9.1	37.9 ± 6.9	$=0.01$

4.3.2 Bud Morphological Development

We observed minimal effects of drought treatment on bud morphological development in the studied species. While drought stress caused an immediate 20% reduction in average bud dry mass in *L. decidua* ($F_{1,18} = 11.56, p = 0.003$, Two-way ANOVA), this deficit recovered by the end of the autumn senescence period (Table S2), and was not observed in *P. sylvestris*. There were no treatment effects observed on the total NSC mass per bud, the total bud NSC mass per branch, nor the count of buds at either the end-drought or end-autumn timepoints in either species (Table S2).

4.3.3 Autumn Leaf Phenology

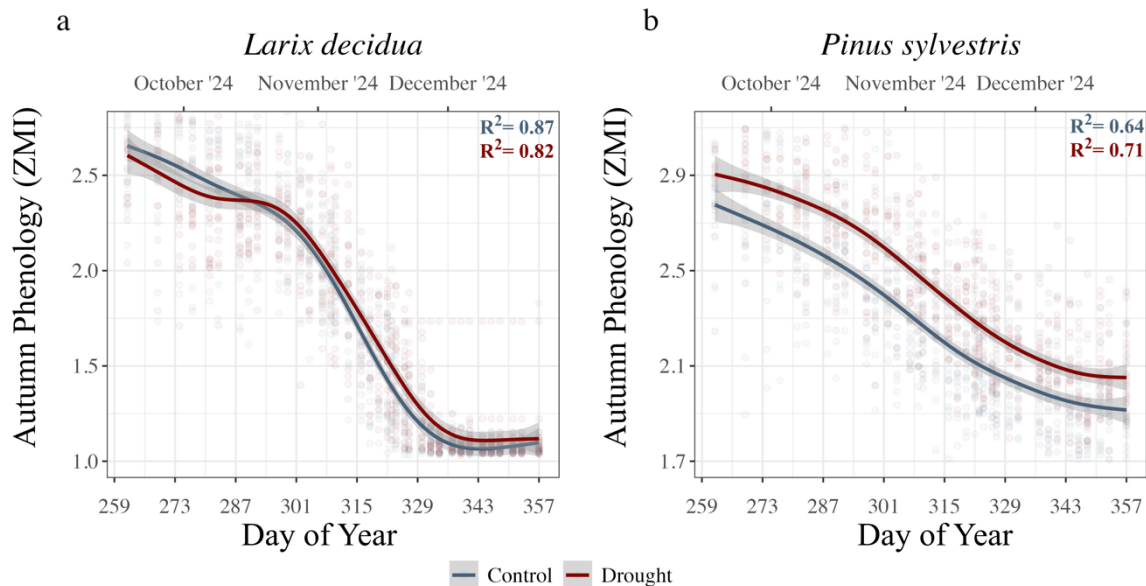


Figure 4.2: Seasonal progression of autumn leaf phenology following an experimental summer drought in *Larix decidua* (a) and *Pinus sylvestris* (b). Phenological dynamics were quantified on all individuals ($n = 40$ per species) using the Zarco-Tejada & Miller Index (ZMI; Zarco-Tejada et al. 2001), a spectral index highly sensitive to changes in chlorophyll content. Spectral scans were performed every two days on the upper foliage between day of year 259 and 357. Generalized Additive Models were fit to produce smoothed phenological trajectories for each species and treatment combination, with the shaded area indicating standard error, and the respective R^2 reported.

Drought stress did not alter foliar ZMI in *L. decidua* during the monitoring period (Figure 4.2a), and both control and drought-treated individuals reached similar ZMI values prior to leaf shedding ($ZMI = 1.11 \pm 0.02$). By the end of the drought treatment, drought-stressed *P.*

sylvestris individuals exhibited minor discoloration and shedding of older needle tissues, particularly around the bole. Despite this, ZMI values measured on current-season foliage were consistently higher in drought-treated than control trees (Figure 4.2b), suggesting greater chlorophyll content. By the end of the monitoring period, the rate of decrease in ZMI had largely slowed, and a subsequent measurement in January identified the persistence of higher ZMI in drought-treated individuals ($F_{1,39} = 10.57, p = 0.002$, One-way ANOVA). However, this difference was no longer observed during the following growing season in either new or previous year leaves (both $p > 0.05$).

4.3.4 Spring Budburst Phenology

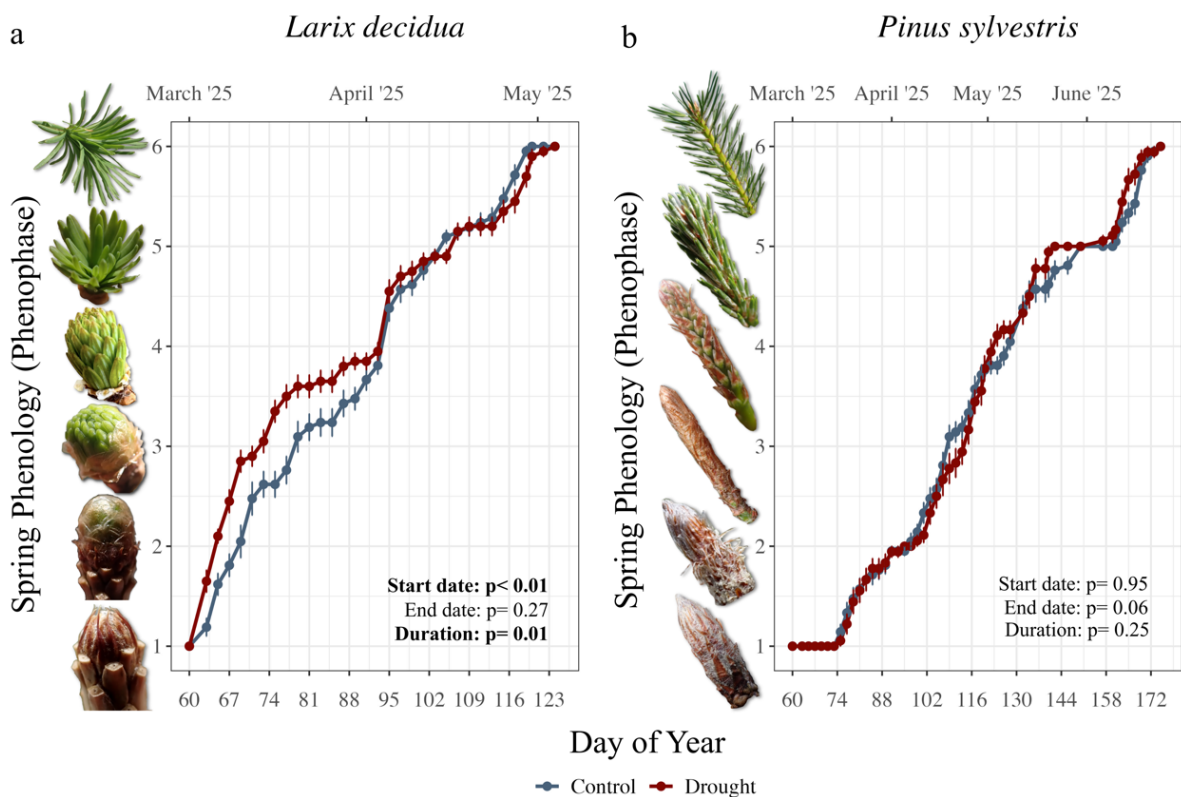


Figure 4.3: Seasonal progression of spring leaf phenology (budburst) following an experimental summer drought in *Larix decidua* (a) and *Pinus sylvestris* (b). Budburst phenophase was visually assessed every two days using a six-step scale (reference images along the y-axis) on all study individuals (*Larix decidua* $n = 40$, *Pinus sylvestris* $n = 38$). Each data point represents the mean budburst stage (phenophase) per date, with error bars indicating the standard error. Statistical comparisons between control and drought treatments were conducted for (1) the onset of budburst (stage 2), (2) budburst completion (stage 6), and (3) the duration of budburst (number of days between stages 2 and 6) separately for each species using a Kruskall-Wallis test.

Drought stress modified spring budburst phenology in *L. decidua* but not in *P. sylvestris*. Specifically, drought advanced the start of spring budburst in *L. decidua* by 5.2 ± 0.8 days on

average ($\chi^2 = 12.13$, $df = 1$, $p < 0.001$, Kruskall-Wallis; Figure 4.3a), while budburst completion appeared slightly delayed by 0.8 ± 0.8 days, although this effect was not significant ($p > 0.05$). As a result, drought ultimately led to slower phenophase progression in the following year, with budburst duration extended by 4.8 ± 1.7 days on average in previously drought stressed *L. decidua* ($\chi^2 = 8.74$, $df = 1$, $p = 0.003$, Kruskall-Wallis). For *P. sylvestris*, we did not observe drought effects on the start of budburst, budburst completion date, or the duration of budburst (all $p > 0.05$; Figure 4.3b).

4.3.5 Bud nonstructural carbohydrates (NSC)

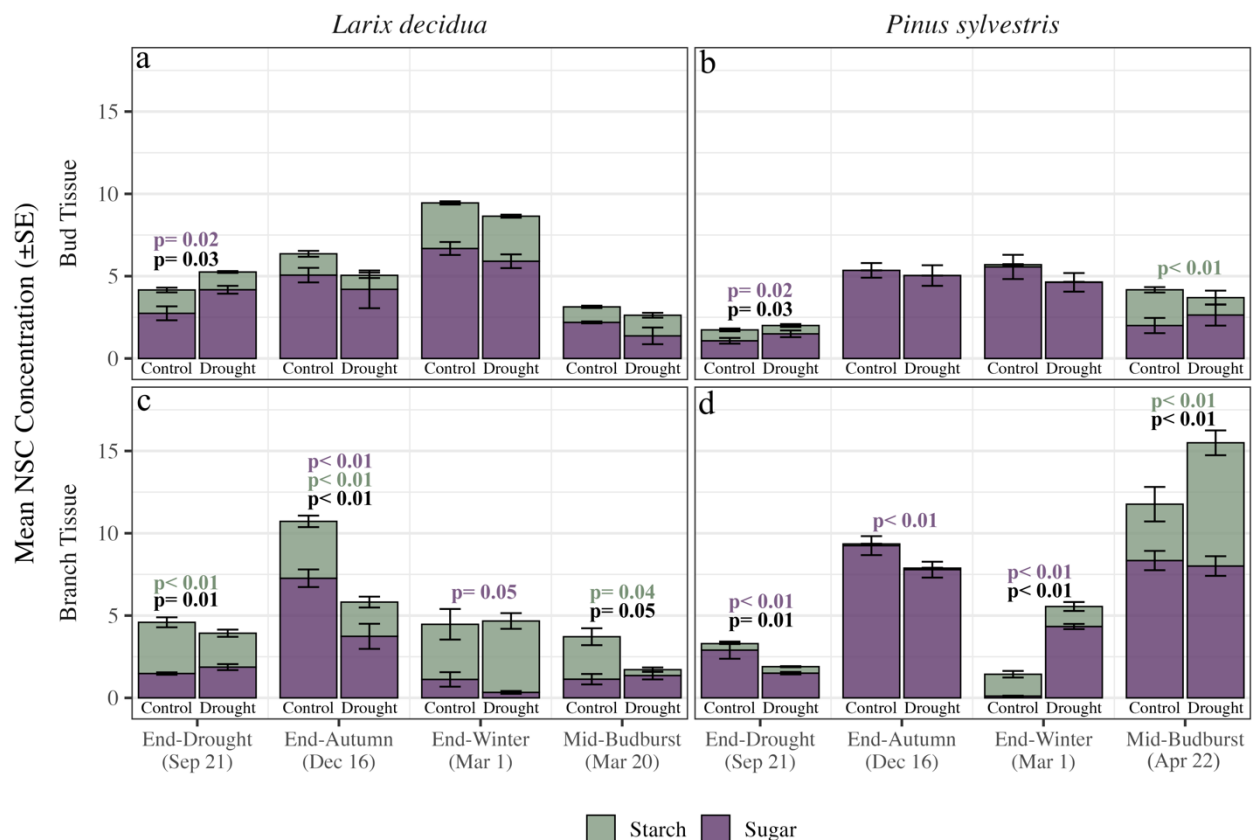


Figure 4.4: Seasonal dynamics of non-structural carbohydrates (NSC) concentrations in bud (top) and branch (bottom) tissues of *Larix decidua* (left) and *Pinus sylvestris* (right) following an experimental summer drought. Bar plots show the mean concentration (% dry weight) for both starch (green) and soluble sugars (glucose + fructose + sucrose; purple), with error bars indicating \pm SE. NSC were measured at four timepoints: end of drought, end of autumn, end of winter, and during active budburst in the following spring. Reported p-values indicate significant effects of drought treatment on NSC concentrations, where green text denotes differences in starch, purple denotes differences in sugar, and black denote differences in total NSC concentration. Full two-way ANOVA results and pairwise contrasts are provided in Supplementary Table S3.

Drought induced an immediate increase in bud NSC concentrations of both species (*L. decidua*: $+22.2 \pm 6.7\%$; *P. sylvestris*: $+22.1 \pm 12.3\%$), driven by soluble sugar (Figure 4.4). Despite this immediate increase, differences in total bud NSC were no longer detected by the end of autumn, nor at either the end-winter or mid-budburst timepoints in either species. We note that previously drought-stressed individuals had lower bud total NSC concentrations on average, although this difference was consistently small (Figure 4.4). Changes in bud NSC concentration between sampling timepoints were generally consistent regardless of treatment but differed between the two species. We found bud NSC concentrations in *L. decidua* to increase through autumn and winter, but depleted during budburst (Figure 4.5a). While in *P. sylvestris* the greatest increase in bud NSC concentrations occurred during autumn, with only a minimal change over winter and just a slight decrease by mid-budburst (Figure 4.5b).

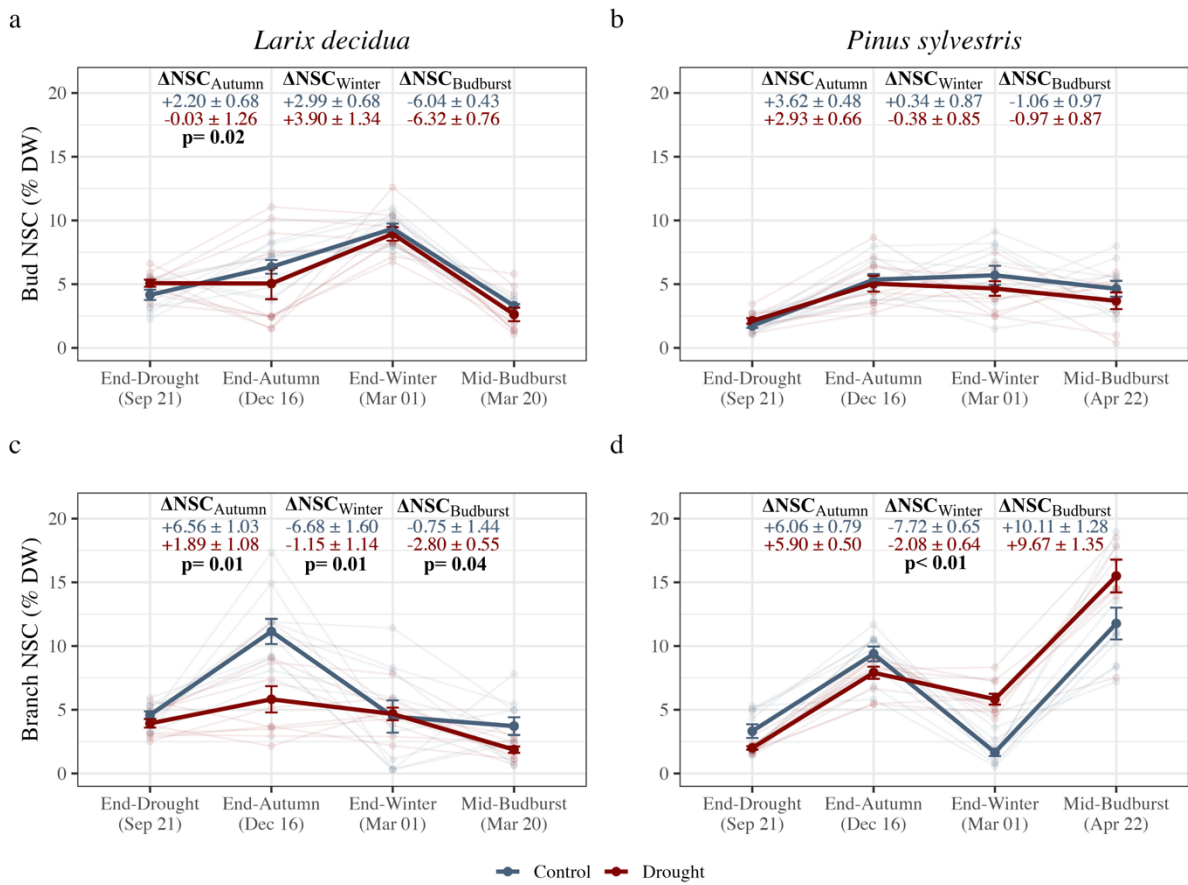


Figure 4.5: Seasonal total NSC dynamics in bud and branch tissues for *Larix decidua* and *Pinus sylvestris* subjected to an experimental summer drought. Given are treatment averages \pm SE as well as individual measurements (lighter color background). In addition, average changes in total NSC (% DW, Δ NSC) \pm SE are given for the autumn, winter and spring period. Printed p-values represent a significant treatment interaction term between two dates from linear mixed effect models.

4.3.6 Branch nonstructural carbohydrates (NSC)

In contrast to NSC bud dynamics, branch NSC concentrations showed a much higher sensitivity to drought, with treatment effects apparent across all timepoints but varying substantially between species (Figure 4.4). While drought immediately reduced total branch NSC in both species (*L. decidua*: $-14.4 \pm 7.3\%$; *P. sylvestris*: $-39.6 \pm 12.3\%$), this decrease was driven by starch in *L. decidua* and by sugar in *P. sylvestris*. These treatment differences were exacerbated by the end of autumn in *L. decidua*, with total branch NSC $47.8 \pm 9.2\%$ lower in previously drought-treated trees (Figure 4.5c). However, summer drought did not limit autumn NSC accumulation in *P. sylvestris* (Figure 4.5d), resulting in similar branch NSC concentrations as the control by the end of autumn, although 15.8% less soluble sugar on average (Figure 4.4).

Drought largely affected branch over winter changes in NSC content. Control trees of both species greatly reduced branch NSC concentration, with smaller decreases occurring in the previously drought-stressed trees (Figure 4.5c, d). Despite different net NSC changes over winter, *L. decidua* individuals entered spring with similar branch NSC concentrations, while previously drought-stressed *P. sylvestris* had $251.8 \pm 25.6\%$ higher branch NSC concentrations than controls, driven by accumulation of soluble sugar (Figure 4d). These species-specific NSC responses further diverged by mid-budburst, with branch NSC $49.7 \pm 6.7\%$ lower than the control in drought-treated *L. decidua* (Figure 4.5c). In contrast, drought-treated *P. sylvestris* had $31.7 \pm 6.7\%$ higher branch NSC than the control by mid-budburst, with similar spring NSC accumulation in each treatment. Statistical model output including ANOVA and relevant contrasts are available in Table S3.

4.3.7 New Leaf Function in the Following Growing Season

We assessed physiological legacy effects on newly developed tissue in the year following the drought event. For the multivariate analysis 26 leaf spectral indices (Table S1), gas exchange (A_{net} , g_{sw} , E), and chlorophyll fluorescence parameters (ETR, NPQ) were assessed. We found a strong effect of species, which explained the majority of total variance ($R^2 = 0.664$, $p = 0.001$, PERMANOVA). In contrast, the drought treatment explained little additional variance ($R^2 = 0.002$, $p = 0.675$, PERMANOVA), with the species effect consistent across both

drought and control groups ($R^2 = 0.007$, $p = 0.393$, PERMANOVA). These results indicate little to no drought legacy effect on new leaf function in the following year (Figure 4.6a).

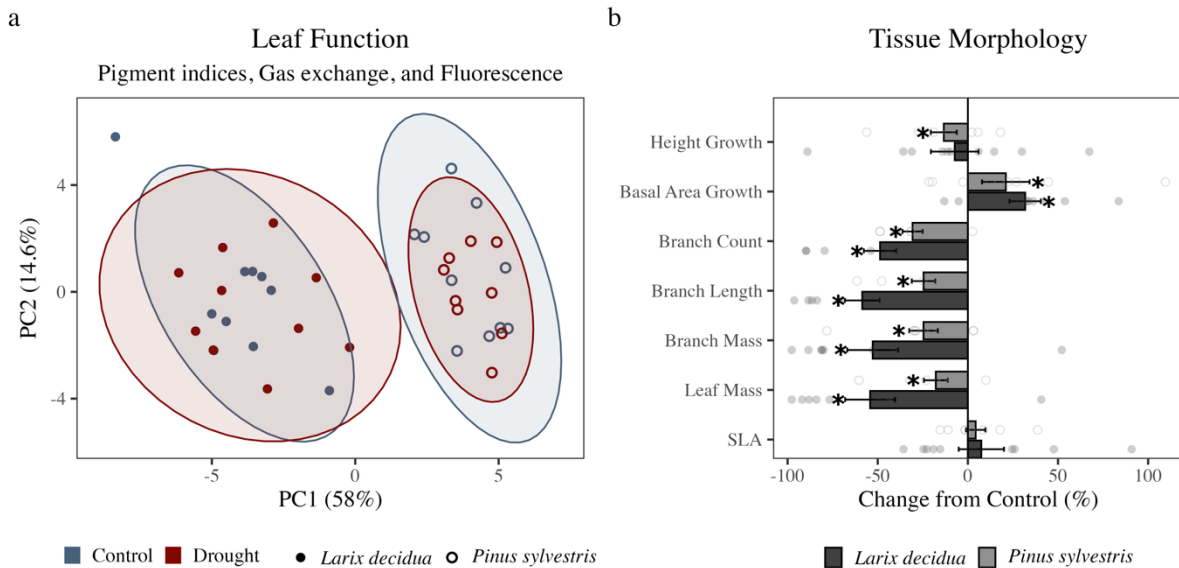


Figure 4.6: Changes in leaf function and tissue morphology in newly developed growth during the growing season following an experimental summer drought. (a) Principal component analysis (PCA) of new leaf functional traits based on 26 spectral indices (see Table S1), gas exchange (A_{net} , g_{sw} , E), and chlorophyll fluorescence parameters (ETR and NPQ). Shaded ellipses represent 95% confidence intervals around treatment groups. (b) Percent change from control in new tissue morphology, including height and basal growth, new branch development (count, total length, total mass), total leaf mass, and specific leaf area (SLA). Bars represent the mean % change from control, with error bars denoting standard error. Asterisks indicate significant effects of the drought treatment. Full two-way ANOVA model results and pairwise contrasts are provided in Supplementary Table S4.

4.3.8 New Tissue Morphology in the Following Growing Season

We observed substantial morphological changes in new tissue development during the growing season following drought, with effects generally more pronounced in *L. decidua* than in *P. sylvestris* (Figure 4.6b). Specifically, drought treatment led to fewer new axial branches (*L. decidua*: $-48.7 \pm 9.0\%$; *P. sylvestris*: $-30.7 \pm 5.6\%$), despite no differences in bud quantity between treatments (Table S2). As a result of fewer new branches, this total branch length was reduced (*L. decidua*: $-58.6 \pm 9.6\%$; *P. sylvestris*: $-24.6 \pm 6.6\%$) as well as total branch mass (*L. decidua*: $-52.8 \pm 14.1\%$; *P. sylvestris*: $-24.6 \pm 7.9\%$). Drought similarly decreased new leaf mass in the following growing season (*L. decidua*: $-54.2 \pm 14.9\%$; *P. sylvestris*: $-17.8 \pm 6.6\%$), without altering specific leaf area (SLA, Figure 4.6b).

Shoot height growth in the following growing season responded differently between species, with no change observed in *L. decidua*, but with slightly less height growth in drought-treated *P. sylvestris* ($-13.4 \pm 7.2\%$). Basal area growth of both species increased between the end of drought stress and the peak of the following growing season (*L. decidua*: $+31.8 \pm 8.6\%$; *P. sylvestris*: $+21.0 \pm 13.2\%$), effectively compensating for the lower basal area growth observed during the drought treatment. As a result, differences in stem basal area between treatments were no longer apparent in the following growing season ($p = 0.639$, Two-way ANOVA). Detailed statistical model results for new tissue morphological data are available in Table S4.

4.3.9 Relationships between legacy NSC, phenology, and morphology

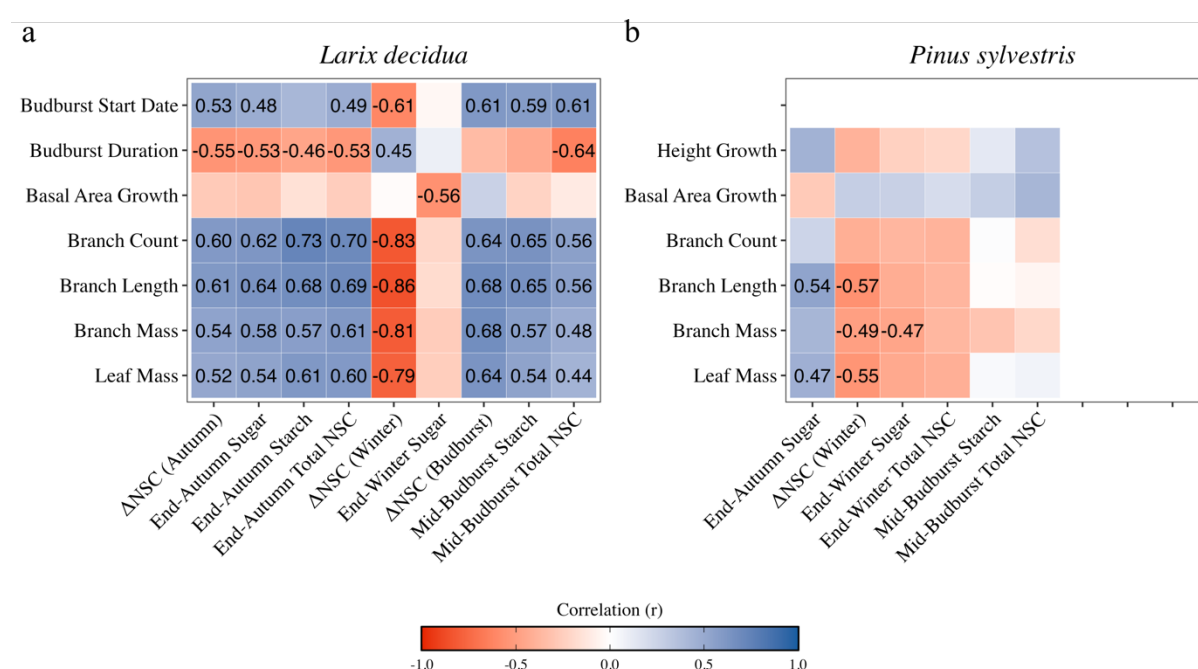


Figure 4.7: Correlation heatmap showing the relationship between legacy non-structural carbohydrate (NSC) effects in branch tissue (x-axis) and phenological or morphological legacy effects (y-axis) in two conifer species of contrasting leaf-habit (*Larix decidua*, a; *Pinus sylvestris*, b). Only variables found to be significantly affected by the drought treatment are displayed for each species. Pearson correlation coefficients (r) are displayed for significant correlations ($p < 0.05$). The color scale represents the strength of the correlation, ranging from -1 (strong negative, red) to +1 (strong positive, blue).

To derive distinct relationships, we conducted correlation analyses between identified drought legacy NSC dynamics, phenology, and new tissue development. A striking difference

between the two species became apparent (Figure 4.7), indicating more pronounced relationships in *L. decidua* than in *P. sylvestris*.

In *L. decidua*, we found lower NSC concentrations in branch tissues at the end of autumn and mid-budburst to be moderately associated with earlier budburst timing and slower budburst progression. These reduced NSC levels were also linked to reduced branch and leaf biomass in the following growing season. The strongest correlations were observed with the calculated change in winter branch NSC, whereby a greater winter decline in NSC was strongly associated with greater growth. A full correlation matrix including non-drought-affected variables as well as bud NSC concentrations is shown in Figures S4.6 and S4.7.

In *P. sylvestris*, correlations among drought legacy NSC, phenology, and morphology effects were fewer and generally weaker than in *L. decidua* (Figure 4.7b). However, these correlations were generally aligned with those found in *L. decidua*, where greater NSC status in the control treatment at the end of autumn associated with greater branch and leaf growth. As in *L. decidua*, the change in winter branch NSC displayed the strongest correlations with new tissue morphology, where greater winter NSC decline (as observed in the control) was related to greater branch length, as well as new branch and leaf mass. The broader lack of correlation was also observed when including bud NSC concentrations and insignificant variables (Figure S4.6, S4.7).

4.4 Discussion

We imposed an extended, mild summer drought to investigate how carbon legacies from stress affect tissue phenology, function, and morphology during the following growing season. Critically, while photosynthesis was strongly reduced, xylem water potential remained well above embolism thresholds in both species, allowing us to assess carbon-mediated legacy effects without the confounding influence of hydraulic damage. Within this framework, drought legacy effects were characterized by altered NSC composition that carried across growing seasons and corresponded with shifts in phenology, as well as reduced tissue production. The two studied species also varied greatly in their legacy response, with leaf habit providing a clear framework to explain these divergent responses.

4.4.1 Drought affects NSC composition into the following growing season

Carbon allocation to bud tissues remained unaffected by drought, both during and after stress. At the end of drought, both species' bud tissues contained higher soluble sugar concentrations than the control, consistent with osmotic adjustment, while adjacent branches had reduced total NSC. Importantly, bud NSC did not vary strongly between treatments at subsequent timepoints, even as branch reserves diverged substantially (Figure 4.5). Bud counts and bud mass were also similar across treatments by winter (Table 1), suggesting that C investment into meristems was maintained, likely at the expense of radial growth or woody NSC accumulation (Figure 4.4). This pattern supports the view that buds are prioritized sinks (Sala et al. 2012; Martínez-Vilalta et al. 2016), and shows that buds are preferentially maintained into dormancy despite extended periods of limited C.

In contrast with buds, branch NSC dynamics diverged strongly between species following drought. During autumn NSC accumulation was reduced by more than 70% in *L. decidua*, while accumulation in *P. sylvestris* remained unaffected. Considering that autumn photosynthetic capacity appeared undisrupted in *L. decidua* (Figure 4.2a), the lower NSC accumulation may be related to compensation for the initial bud mass deficit (Table 1), or potentially toward increased root allocation (Karlowsky et al. 2018). However, both species displayed similar drought-induced NSC patterns during winter dormancy: control trees showed substantial NSC depletion over winter, while drought trees exhibited little to no decline. Considering that overwinter losses in NSC are typically driven by respiratory demand (Tixier et al. 2019), and that the individuals in each treatment were of similar mass, we would expect similar winter NSC use. Therefore, it is likely that drought trees mobilized compensatory NSC from distal storage pools, such as stem or root parenchyma, to support winter respiration (Hoch et al. 2003; Godfrey et al. 2020). Although we did not quantify NSC in these distal tissues, such instances of remobilization have been observed following girdling (Amico Roxas et al. 2021), which along with our study supports the ability of woody perennials to rebalance NSC across tissues during winter in response to C-limitations.

Despite similar winter mobilization patterns, the two species entered spring with largely different NSC status. Winter NSC mobilization left *L. decidua* branch NSC temporarily rebalanced, but deficient again by mid-budburst. In stark contrast, winter NSC mobilization left *P. sylvestris* with greater branch NSC, with further accumulation by mid-budburst

presumably due to C assimilation by the persisting foliage (Moser et al. 2010). In partial disagreement with H1, drought legacy manifested not through persistent NSC deficits in our measured tissues, but instead through altered seasonal mobilization patterns, with the ultimate ability to recover local NSC levels dependent upon species-specific leaf habit.

4.4.2 *Altered autumn and spring leaf phenology as drought legacy effects*

In disagreement with H2, autumn senescence remained largely unaffected by drought in either species. Species displayed similar temporal patterns of pigment remobilization between treatments (Figure 4.2), with reduced photosynthetic capacity therefore not explaining inhibited autumn NSC accumulation in *L. decidua*. This contrasts with many observations of drought advancing autumn leaf senescence (Estiarte and Peñuelas 2015; Jan et al. 2019; Vander Mijnsbrugge et al. 2025). In these cases, early leaf senescence can be attributed to drought-induced dehydration of leaf mesophyll, with compromised cells unable to maintain cell turgor (Radermacher et al. 2019). The lack of phenological shift in our study therefore can be explained by the uncompromised tissue hydraulics, meaning signaling pathways involved in regulating leaf senescence were likely not initiated (Vander Mijnsbrugge et al. 2016; 2025). Drought-treated *P. sylvestris*; however, displayed higher pigment content throughout the fall period, although the phenological pattern remained unchanged. While this may reflect an active mechanism to extend photosynthetic gain in the late season, this shift occurred alongside senescence of the oldest (four-year-old) foliage—a common response to drought in the species thought to reduce water loss while facilitating nutrient recycling (Galiano et al. 2011). To this effect, autumn NSC accumulation remained unaffected, and the elevated leaf pigment content subsided by the following growing season, supporting this as a temporary shift for the purpose of resource (N) storage.

Drought effects on spring phenology differed between species and were closely linked to C status, supporting H3. Drought-treated *L. decidua* initiated budburst earlier yet progressed slower through bud development, resulting in an extended budburst period. This slower development was moderately correlated with lower branch NSC levels and the drought-modified winter mobilization, adding to the body of evidence that stress-induced changes in NSC can disrupt phenological timing (Corot et al. 2017; Monteiro et al. 2022). As sugars serve as signaling molecules to promote bud outgrowth in woody species (M. Wang et al. 2022), reduced NSC may have cued earlier dormancy release, consistent with recent evidence that carbohydrate status may function as a “molecular clock” for leaf-out (Blumstein et al.

2024). This mechanism may explain why warming temperatures advance spring budburst, as higher rates of respiration more rapidly deplete NSC (Dixit et al. 2020), resulting in critical NSC thresholds occurring earlier in the year (Vitasse et al. 2018). Our results support the role of NSC in regulating both the timing and speed of budburst development, and demonstrate how C-mediated legacy effects can manifest as disrupted spring phenology.

4.4.3 NSC legacy effects are largely correlated with reduced tissue production in the following year

Against our expectations, foliage developed in the year following drought displayed no adjustments to leaf functioning in either species, with photosynthetic rates, pigment spectral reflectance, and chlorophyll fluorescence unchanged. This contrasts with studies reporting increased water use efficiency, largely through reductions in stomatal conductance (Petrik et al. 2022; Herrera et al. 2024) or SLA (Thomas et al. 2024), and agrees with studies not observing structural (Peltier et al. 2016; Gattmann et al. 2023). Phytohormonal signaling pathways are thought to mediate structural modifications to leaf architecture in response to environmental stress. For example, abscisic acid (ABA) is involved in triggering a cascade of hormonal responses involving auxin and cytokinin which can alter leaf architecture (Alongi et al. 2025); however, ABA is typically upregulated following severe water stress to ensure stomatal closure (McAdam and Brodribb 2014; Kane and McAdam 2023). Under the mild drought stress conditions here, which did not lead to full stomatal closure, the phytohormonal signaling pathways that trigger structural modifications likely were not initiated.

Despite no changes to leaf function, new biomass production was strongly reduced in previously drought-stressed trees. Specifically, both species produced fewer branches, decreasing total branch length, mass, and foliage (Figure 4.6b). This occurred despite similar bud counts and bud mass by the end of the previous season. Fewer new branches in *L. decidua*, despite similar initial bud counts, likely resulted from post-drought adjustments in bud development. Branch differentiation in this species is dependent upon the formation of the “axial” region (Frampton 1960), with buds lacking this region instead forming foliar fascicles. In contrast, a loss of bud vitality explains the similar pattern of reduced branch numbers in *P. sylvestris* (Thomas et al. 2024), observed visually through aborted buds during spring budburst. Despite occurring through different mechanisms, this observed pattern of reduced branching in both species suggests that active regulation of bud fate is likely a

common drought legacy effect to regulate new tissue production.

Correlative analyses underscore the tight connection between C reserves and new growth. In *L. decidua*, the markedly greater reductions in biomass production were moderately to strongly correlated with branch NSC deficits from autumn through budburst, consistent with direct C limitation of tissue production (Klein et al. 2016; Tixier et al. 2019). In contrast, *P. sylvestris* showed biomass reductions despite having greater branch NSC concentrations, a pattern also observed in field studies (Peltier et al. 2022), which taken together suggest that this legacy effect in *P. sylvestris* of reduced productivity is not necessarily due to NSC limitation. The strongest correlations in either species; however, involved the magnitude of overwinter NSC change, where we interpret the drought-modified NSC mobilization patterns as reflecting a whole-plant C limitation (discussed above). These findings indicate that the tree's total NSC reserve status, rather than local branch concentrations, is the critical constraint on new tissue development in the following season. Taken together, our results provide quantitative evidence that drought-driven NSC legacies limit subsequent-year tissue production.

The ecological implications of these morphological shifts likely hinge on drought recurrence. Under non-stress conditions, the observed marked reduction in new leaf area, particularly in the deciduous *L. decidua*, would likely limit the tree's ability to exploit optimal light and growth opportunities, and therefore could be interpreted as a loss of fitness. Conversely, a higher sapwood-to-leaf area ratio (Figure 4.6b) should reduce water loss and improve buffering in the case of recurrent drought conditions. This finding provides a mechanistic explanation for recent reports that prior drought exposure can enhance resilience to recurrent droughts (Marchand et al. 2025). In addition, the elevated branch NSC content observed during budburst in *P. sylvestris* may represent a form of 'drought priming' for the following growing season (Blumstein et al. 2023), providing a higher starting carbon-safety margin should C limitation reoccur (Mitchell et al. 2013). However, this elevated branch NSC in pine was achieved through extensive remobilization from distal tissues, which may represent a riskier strategy that could compromise whole-tree reserves. The two observed pine mortalities (10%), compared to zero larch mortalities, suggest that while pine's compensatory response enables greater short-term tissue production, it may come at the cost of reduced survival under severe or repeated stress.

4.4.4 Evidence for leaf-habit influencing the expression of drought legacy effects

In agreement with H4, our study provides evidence that leaf habit influences the mechanisms through which drought legacies are expressed. Although the immediate physiological responses to drought were comparable in *L. decidua* and *P. sylvestris*, including similar reductions in growth, gas exchange, and immediate NSC responses, their post-drought trajectories diverged sharply. In *L. decidua*, autumn NSC accumulation was strongly inhibited despite normal leaf senescence, budburst occurred earlier yet progressed slower, and NSC appeared limiting by mid-budburst, reflecting the species' complete reliance on stored C to fuel spring growth. In contrast, *P. sylvestris* maintained normal autumn NSC accumulation and even increased branch NSC during budburst, as persisting foliage appeared to be utilized for the temporary storage of remobilized nutrients (Figure 4.2b) as well as early season C gain (Figure 4.5d). This extended capacity to assimilate C makes *P. sylvestris*, and likely *other evergreens*, less dependent on previous-year NSC to support budburst. Such contrasting strategies provide a mechanistic explanation for observations that drought can induce highly dynamic, species-specific legacy responses (Peltier and Ogle 2020) and can explain why temperate deciduous trees, through greater reliance on NSC reserves for spring development, show steeper long-term declines in post-drought recovery than evergreens (Marchand et al. 2025). Although our observed species responses appeared aligned with leaf habit, these contrasting post-drought strategies likely represent different risk-reward trade-offs. Pine's extensive remobilization enabled greater tissue production but resulted in mortality in two individuals, suggesting a less conservative approach. Assessment of the relative fitness consequences of these strategies requires evaluation under repeated drought conditions to determine their costs and benefits across different drought regimes. As our results are derived from a singular deciduous and evergreen species, further studies utilizing a broader range of species and taxonomic groups are necessary to determine whether this leaf-habit pattern is generalizable, or instead represents species-specific strategies.

4.5 Conclusion

By imposing a drought event where hydraulic integrity was maintained, we were able to isolate C-related mechanisms of drought legacy and quantitatively link these to shifts in phenology and morphology during the following growing season. In both species, altered

NSC dynamics manifested through reduced branching and foliar production, underscoring how drought, through modifications to C availability, can induce legacy changes in tissue architecture in subsequent growing seasons. Nonetheless, *L. decidua* displayed more severe legacy effects, including greater NSC limitations, disrupted budburst phenology, and generally greater decreases in new tissue production. The divergent responses between the deciduous *L. decidua* and evergreen *P. sylvestris* highlight the role of stored C reserves, with the deciduous species more sensitive to carbon-mediated legacy effects due to their leaf habit. These findings establish NSC as a critical driver of drought legacy effects and demonstrate how species-specific differences in seasonal NSC utilization likely determine the extent of legacy morphological modifications.

4.6 Supplementary Materials

Table S4.1: Calculated spectral indices utilized for phenology and leaf function assessment.

Index	Name	Equation	Reference
NDVI	Normalized Difference Vegetation Index	NDVI = (R780 – R630)/ (R780+ R630)	Rouse et al. (1974)
SR	Simple Ratio Index	SR = R780/R630	Jordan (1969)
MCARI1	Modified Chlorophyll Absorption in Reflectance Index	MCARI1 = 1.2 * [2.5 * (R790 - R670) - 1.3 * (R790 - R550)]	Haboudane et al. (2004)
OSAVI	Optimized Soil-Adjusted Vegetation Index	OSAVI = (1 + 0.16) * (R790 - R670) / (R790 - R670 + 0.16)	Rondeaux et al. (1996)
G	Greenness Index	G = R554 / R677	Gitelson et al. (2002)
MCARI	Modified Chlorophyll Absorption in Reflectance Index	MCARI = [(R700 - R670) - 0.2 * (R700 - R550)] * (R700 / R670)	Daughtry et al. (2000)
TCARI	Transformed CAR index	TCARI = 3 * [(R700 - R670) - 0.2 * (R700 - R550) * (R700 / R670)]	Haboudane et al. (2002)
TVI	Triangular Vegetation Index	TVI = 0.5 * [120 * (R750 - R550) - 200 * (R670 - R550)]	Broge and Leblanc (2000)
ZMI	Zarco-Tejada & Miller Index	ZMI = R750 / R710	Zarco-Tejada et al. (2001)
SRPI	Simple Ratio Pigment Index	SRPI = R430 / R680	Peñuelas et al. (1995)
NPQI	Normalized Phaeophytinization Index	NPQI = (R415 - R435) / (R415 + R435)	Barnes et al. (1992)
PRI	Photochemical Reflectance Index	PRI = (R531 - R570) / (R531 + R570)	Gamon et al. (1992)
NPCI	Normalized Pigment Chlorophyll Index	NPCI = (R680 - R430) / (R680 + R430)	Carter (1994), Carter et al. (1996)
SIPI	Structure Intensive Pigment Index	SIPI = (R790 - R450) / (R790 - R650)	Peñuelas et al. (1995)
Lic1	Lichtenhaler Index 1	Lic1 = (R780- R680)/(R780+R680)	Lichtenthaler et al. 1996
Lic2	Lichtenhaler Index 2	Lic2 = R440/R690	Lichtenthaler et al. 1996
GM1	Gitelson and Merzlyak Index 1	GM1 = R750 / R550	Gitelson & Merzlyak (1997)
GM2	Gitelson and Merzlyak Index 2	GM2 = R750 / R700	Gitelson & Merzlyak (1997)

CRI1	Carotenoid Reflectance Index 1	$CRI1 = (1/R510) - (1/R550)$	Gitelson et al. (2002)
CRI2	Carotenoid Reflectance Index 2	$CRI2 = (1/R510) - (1/R700)$	Gitelson et al. (2002)
RDVI	Renormalized Difference Vegetation Index	$RDVI = (R780 - R670) / ((R780 + R670)^{0.5})$	Roujean & Breon (1995)
CCI	Chlorophyll Carotenoid Index	$CCI = (R532 - R630) / (R532 + R630)$	Gamon et al. 2016
ARI1	Anthocyanin Reflectance Index 1	$ARI1 = (1/R550) - (1/R700)$	Gitelson et al. (2001)
ARI2	Anthocyanin Reflectance Index 2	$ARI2 = R790 * ((1/R550) - (1/R700))$	Gitelson et al. (2001)
Ctr1	Carter Index 1	$Ctr1 = R695/R420$	Carter (1994)
Ctr2	Carter Index 2	$Ctr2 = R695/R760$	Carter (1994)

Table S4.2: Average bud dry mass and non-structural carbohydrate (NSC) content per bud at the end of drought and end of autumn for each species and treatment. Provided are treatment averages \pm SE, and the resulting p-value from one-way ANOVA models.

		<i>Larix decidua</i>			<i>Pinus sylvestris</i>		
		Control	Drought	<i>p</i>	Control	Drought	<i>p</i>
Bud Mass (mg DW bud ⁻¹)	End-Drought	1.48 \pm 0.09	1.12 \pm 0.06	<0.01	19.91 \pm 3.19	18.07 \pm 2.10	0.63
	End-Autumn	2.14 \pm 0.20	2.29 \pm 0.30	0.69	26.16 \pm 3.25	21.27 \pm 2.27	0.23
	Change	0.66 \pm 0.23	1.17 \pm 0.27	0.09	6.25 \pm 1.46	3.20 \pm 2.08	0.58
NSC (mg bud ⁻¹)	End-Drought	0.06 \pm 0.01	0.06 \pm 0.01	0.50	0.35 \pm 0.07	0.37 \pm 0.05	0.71
	End-Autumn	0.14 \pm 0.02	0.10 \pm 0.02	0.18	1.43 \pm 0.23	1.21 \pm 0.24	0.39
	Change	0.08 \pm 0.02	0.04 \pm 0.02	0.27	1.08 \pm 0.19	0.84 \pm 0.21	0.28
Bud NSC (mg branch ⁻¹)	End-Drought	3.15 \pm 0.43	4.16 \pm 0.55	0.16	2.32 \pm 0.40	2.32 \pm 0.35	0.99
	End-Autumn	4.75 \pm 0.53	3.68 \pm 0.91	0.33	7.46 \pm 1.26	5.89 \pm 1.17	0.37
	Change	1.60 \pm 0.89	-0.53 \pm 0.89	0.11	5.14 \pm 1.17	3.57 \pm 1.27	0.39
Buds (n)	End-Drought	30.5 \pm 1.8	30.2 \pm 1.1	0.89	4.6 \pm 0.2	4.6 \pm 0.2	>0.99
	End-Autumn	36.9 \pm 2.3	37.1 \pm 2.3	0.95	5.1 \pm 0.2	5.2 \pm 0.2	0.72
	Change	6.4 \pm 2.3	6.9 \pm 2.2	0.88	0.5 \pm 0.2	0.6 \pm 0.4	0.81

Table 4.3.1 ANOVA results for interactive models on non-structural carbohydrates.

Tissue	Date	Variable	Term	Df	Sum Sq	Mean Sq	F value	P value
Branch	21.09.24	Starch	Treatment	1	3.01	3.01	8.24	0.007
			Species	1	46.95	46.95	128.58	0.000
			Treatment:Species	1	2.54	2.54	6.95	0.012
			Residuals	35	12.78	0.37		
	21.09.24	Sugar	Treatment	1	1.56	1.56	1.86	0.181
			Species	1	3.88	3.88	4.64	0.038
			Treatment:Species	1	6.43	6.43	7.69	0.009
			Residuals	35	29.26	0.84		
Branch	21.09.24	Total	Treatment	1	8.89	8.89	6.93	0.013
			Species	1	23.84	23.84	18.58	0.000
			Treatment:Species	1	0.89	0.89	0.69	0.412
			Residuals	35	44.90	1.28		
	21.09.24	Starch	Treatment	1	0.12	0.12	0.75	0.394
			Species	1	4.11	4.11	24.69	0.000
			Treatment:Species	1	0.12	0.12	0.69	0.410
			Residuals	35	5.83	0.17		
Bud	21.09.24	Sugar	Treatment	1	5.35	5.35	5.49	0.025
			Species	1	41.38	41.38	42.41	0.000
			Treatment:Species	1	1.59	1.59	1.63	0.210
			Residuals	35	34.15	0.98		
	21.09.24	Total	Treatment	1	3.85	3.85	4.73	0.036
			Species	1	71.59	71.59	88.06	0.000
			Treatment:Species	1	0.85	0.85	1.04	0.314
			Residuals	35	28.45	0.81		
Branch	16.12.24	Starch	Treatment	1	8.37	8.37	8.19	0.007
			Species	1	80.65	80.65	78.89	0.000
			Treatment:Species	1	7.80	7.80	7.62	0.009
			Residuals	35	35.78	1.02		
	16.12.24	Sugar	Treatment	1	42.12	42.12	9.19	0.005
			Species	1	78.05	78.05	17.04	0.000
			Treatment:Species	1	4.32	4.32	0.94	0.338
			Residuals	35	160.34	4.58		
Branch	16.12.24	Total	Treatment	1	88.03	88.03	10.72	0.002
			Species	1	0.02	0.02	0.00	0.960
			Treatment:Species	1	23.72	23.72	2.89	0.098
			Residuals	35	287.35	8.21		
	16.12.24	Starch	Treatment	1	0.49	0.49	3.28	0.079
			Species	1	11.26	11.26	75.37	0.000
			Treatment:Species	1	0.50	0.50	3.32	0.077
			Residuals	35	5.23	0.15		
Bud	16.12.24	Sugar	Treatment	1	3.02	3.02	0.56	0.459
			Species	1	3.46	3.46	0.64	0.428
Bud	16.12.24	Sugar	Treatment:Species	1	0.97	0.97	0.18	0.674

			Residuals	35	188.28	5.38		
Bud	16.12.24	Total	Treatment	1	5.93	5.93	0.97	0.331
			Species	1	2.23	2.23	0.36	0.550
			Treatment:Species	1	2.85	2.85	0.47	0.500
			Residuals	35	214.18	6.12		
Branch	01.05.25	Starch	Treatment	1	1.66	1.66	0.21	0.651
			Species	1	33.67	33.67	4.22	0.047
			Treatment:Species	1	185.25	185.25	23.23	0.000
			Residuals	35	279.11	7.97		
Branch	01.05.25	Sugar	Treatment	1	0.02	0.02	0.01	0.917
			Species	1	468.70	468.70	231.85	0.000
			Treatment:Species	1	0.76	0.76	0.38	0.544
			Residuals	35	70.75	2.02		
Branch	01.05.25	Total	Treatment	1	2.06	2.06	0.17	0.684
			Species	1	753.60	753.60	61.39	0.000
			Treatment:Species	1	162.28	162.28	13.22	0.001
			Residuals	35	429.68	12.28		
Bud	01.05.25	Starch	Treatment	1	83.14	83.14	5.53	0.024
			Species	1	57.11	57.11	3.80	0.059
			Treatment:Species	1	120.02	120.02	7.98	0.008
			Residuals	35	526.36	15.04		
Bud	01.05.25	Sugar	Treatment	1	3.74	3.74	1.78	0.191
			Species	1	18.38	18.38	8.75	0.006
			Treatment:Species	1	10.70	10.70	5.09	0.030
			Residuals	35	73.54	2.10		
Bud	01.05.25	Total	Treatment	1	122.16	122.16	7.37	0.010
			Species	1	140.30	140.30	8.46	0.006
			Treatment:Species	1	59.06	59.06	3.56	0.067
			Residuals	35	580.35	16.58		

Table S4.3.2: Contrast results for significant interaction effects in nonstructural carbohydrates.

Tissue	Date	Variable	contrast	estimate	std.error	df	statistic	p.value
Branch	21.09.24	Sugar	Control - Drought	-0.39	0.41	35	-0.956	0.345
Branch	21.09.24	Sugar	Control - Drought	1.23	0.42	35	2.938	0.006
Bud	01.05.25	Sugar	Control - Drought	1.64	0.65	35	2.530	0.016
Bud	01.05.25	Sugar	Control - Drought	-0.46	0.67	35	-0.686	0.497
Branch	21.09.24	Starch	Control - Drought	1.05	0.27	35	3.897	0.000
Branch	21.09.24	Starch	Control - Drought	0.03	0.28	35	0.112	0.911
Branch	01.05.25	Starch	Control - Drought	4.66	1.26	35	3.688	0.001
Branch	01.05.25	Starch	Control - Drought	-4.07	1.30	35	-3.136	0.003
Branch	16.12.24	Starch	Control - Drought	1.80	0.45	35	3.976	0.000
Branch	16.12.24	Starch	Control - Drought	0.01	0.46	35	0.017	0.987
Bud	01.05.25	Starch	Control - Drought	-0.50	1.73	35	-0.285	0.777
Bud	01.05.25	Starch	Control - Drought	6.53	1.78	35	3.664	0.001
Branch	01.05.25	Total	Control - Drought	4.43	1.57	35	2.830	0.008
Branch	01.05.25	Total	Control - Drought	-3.73	1.61	35	-2.319	0.026

Table S4.4.1: ANOVA results for interactive models regarding legacy morphological variables.

Variable	Term	Df	Sum Sq	Mean Sq	F value	P value
SLA	Treatment	1	0.04	0.04	0.71	0.405
	Species	1	8.07	8.07	158.98	1.42E-14
	Treatment × Species	1	0	0	0	0.987
	Residuals	35	1.78	0.05		
Branch number	Treatment	1	400.41	400.41	9.56	0.00389
	Species	1	311.87	311.87	7.45	0.00987
	Treatment × Species	1	88.87	88.87	2.12	0.154
	Residuals	35	1465.62	41.87		
Total branch length	Treatment	1	204129.8	204129.8	9.65	0.00375
	Species	1	104594.3	104594.3	4.94	0.0327
	Treatment × Species	1	83381.05	83381.05	3.94	0.055
	Residuals	35	740523	21157.8		
Branch dry weight	Treatment	1	93.15	93.15	7.73	0.00867
	Species	1	483.03	483.03	40.1	2.83E-07
	Treatment × Species	1	0.27	0.27	0.02	0.883
	Residuals	35	421.64	12.05		
Leaf dry weight	Treatment	1	382.92	382.92	6.77	0.0135
	Species	1	5537.91	5537.91	97.89	1.12E-11
	Treatment × Species	1	2.17	2.17	0.04	0.846
	Residuals	35	1979.98	56.57		
Leaf mass per branch length	Treatment	1	0	0	0.08	0.782
	Species	1	0.21	0.21	298.46	1.04E-18
	Treatment × Species	1	0	0	0.34	0.564
	Residuals	35	0.03	0		
Height growth	Treatment	1	0.85	0.85	5.08	0.0271
	Species	1	8.01	8.01	48.08	1.23E-09
	Treatment × Species	1	0.72	0.72	4.32	0.041
	Residuals	75	12.49	0.17		
Basal area growth	Treatment	1	3.19	3.19	8.34	0.00505
	Species	1	4.54	4.54	11.86	0.000936
	Treatment × Species	1	0.31	0.31	0.81	0.372
	Residuals	76	29.12	0.38		

Table S4.4.2: Contrast results of significant interactive terms for legacy morphological variables.

Variable	Species	contrast	estimate	SE	df	t.ratio	p.value
Height growth	<i>Larix decidua</i>	Control - Drought	0.387	0.129	75	3.00	0.004
Height growth	<i>Pinus sylvestris</i>	Control - Drought	0.005	0.131	75	0.04	0.972

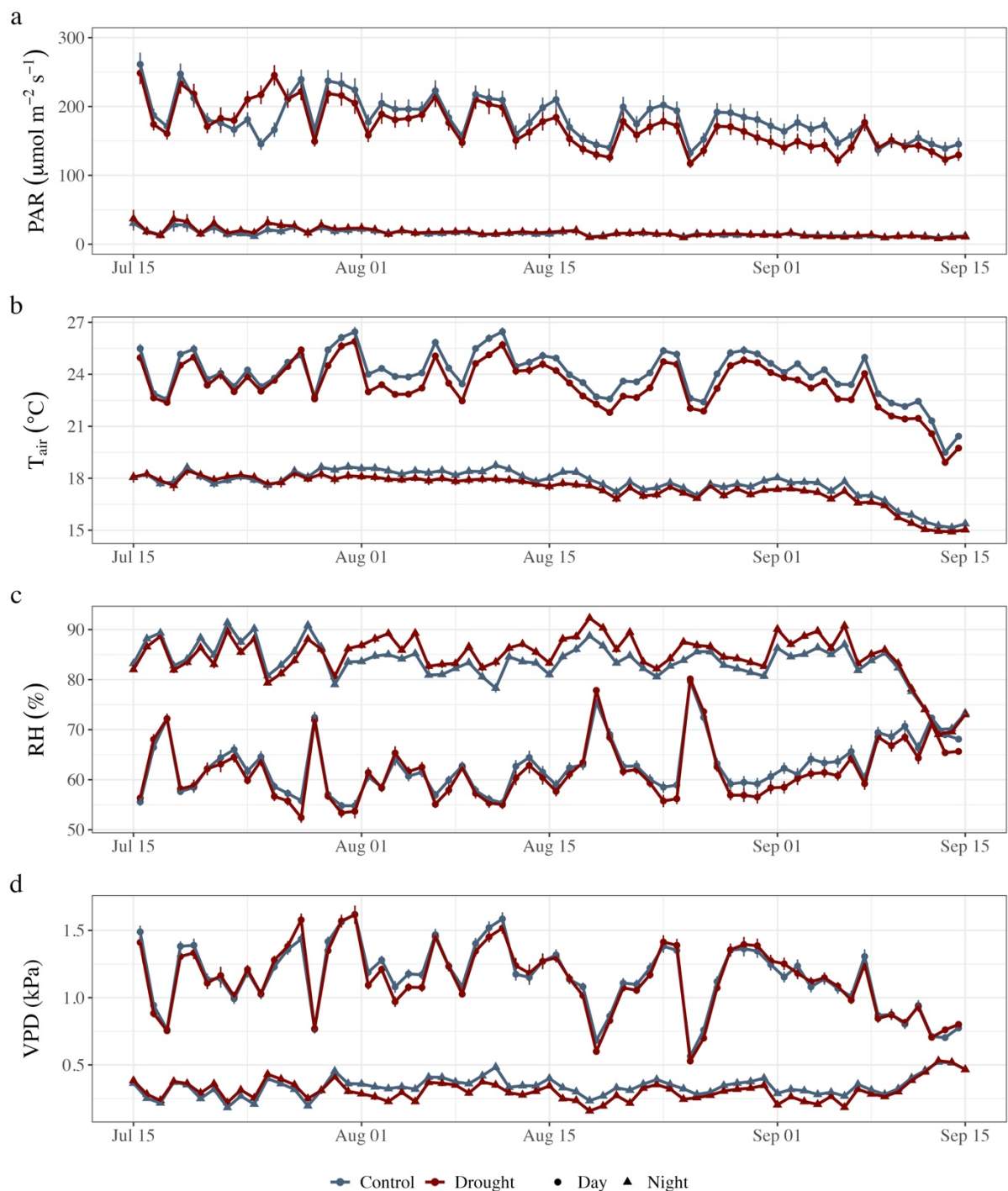


Figure S4.1: Meteorological conditions inside the greenhouse during the experimental drought period. Displayed are daytime (08:00-20:00; circle) and nighttime (20:00-08:00; triangle) averages for photosynthetic active radiation (PAR; a), air temperature (T_{air} ; b), relative humidity (RH, c), and vapor pressure deficit (VPD; d). As study individuals were spatially separated by treatment, meteorological conditions are reported separately for control (blue) and drought (red).

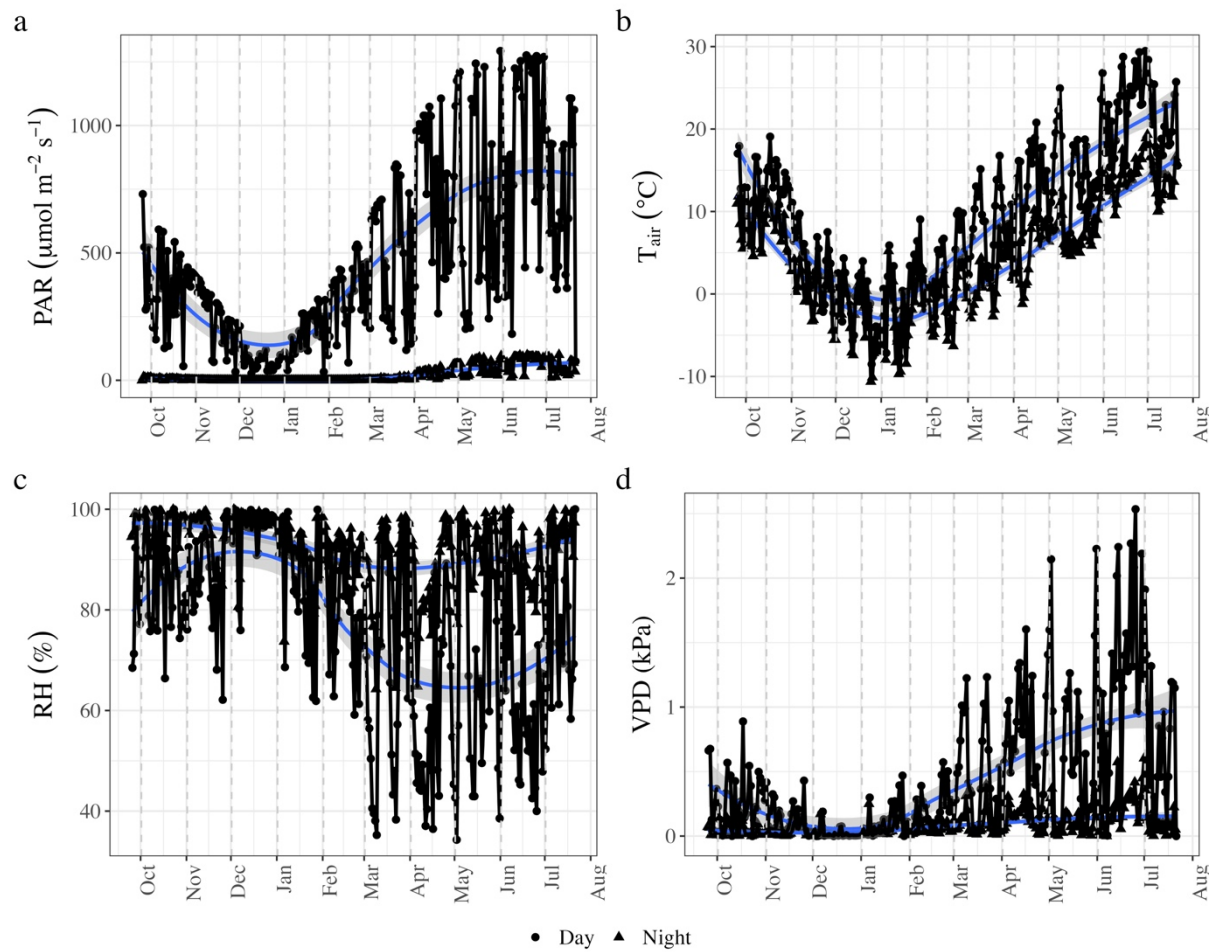
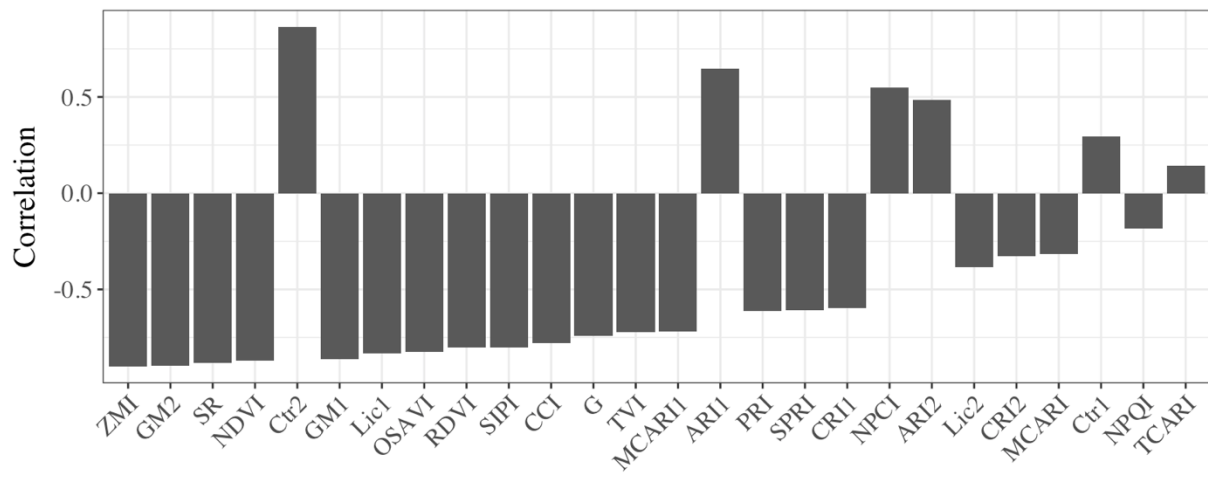


Figure S4.2: Meteorological conditions outside the experimental greenhouse facility during the post-drought period (between mid-September 2024 and mid-July 2025). Displayed are daytime (08:00-20:00; circle) and nighttime (20:00-08:00; triangle) averages for photosynthetic active radiation (PAR; a), air temperature (T_{air} ; b), relative humidity (RH, c), and vapor pressure deficit (VPD; d).

Larix decidua



Pinus sylvestris

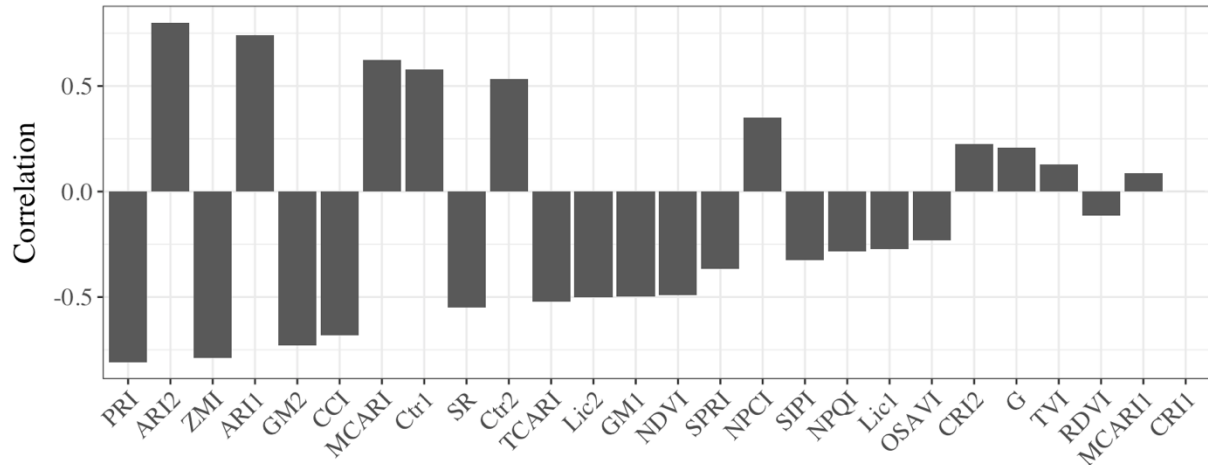


Figure S4.3: Correlations of calculated spectral indices with day of year throughout the autumn senescence monitoring period. Indices are ordered by species from greatest to lowest correlation. Correlation results were used to inform the selection of a common spectral index to visualize autumn leaf phenology trends.



Larix Decidua

1. Dormant Bud
2. Bud swelling, scales still intact
3. Leaf emergence, scales separated but still attached
4. Leaf bundle fully emerged, scales detached, leaf clusters distinguishable
5. Leaves spread radially
6. Leaves elongated (leaf length 1.5 cm minimum)

Pinus Sylvesteris

1. Dormant Bud, scales intact
2. Initial bud swelling, scales detach from bud at point of expansion
3. Linear expansion (bud length 4 cm minimum)
4. Bud greening and scale shedding, leaf sheaths visible
5. Leaf emergence from sheaths
6. Elongated leaves (leaf length 3 cm minimum)

Figure S4.4: Visual scale used to determine the progression of budburst in *Larix decidua* and *Pinus sylvestris*. Trees were visually assessed and assigned a step (phenophase) of 1-6 throughout the spring.

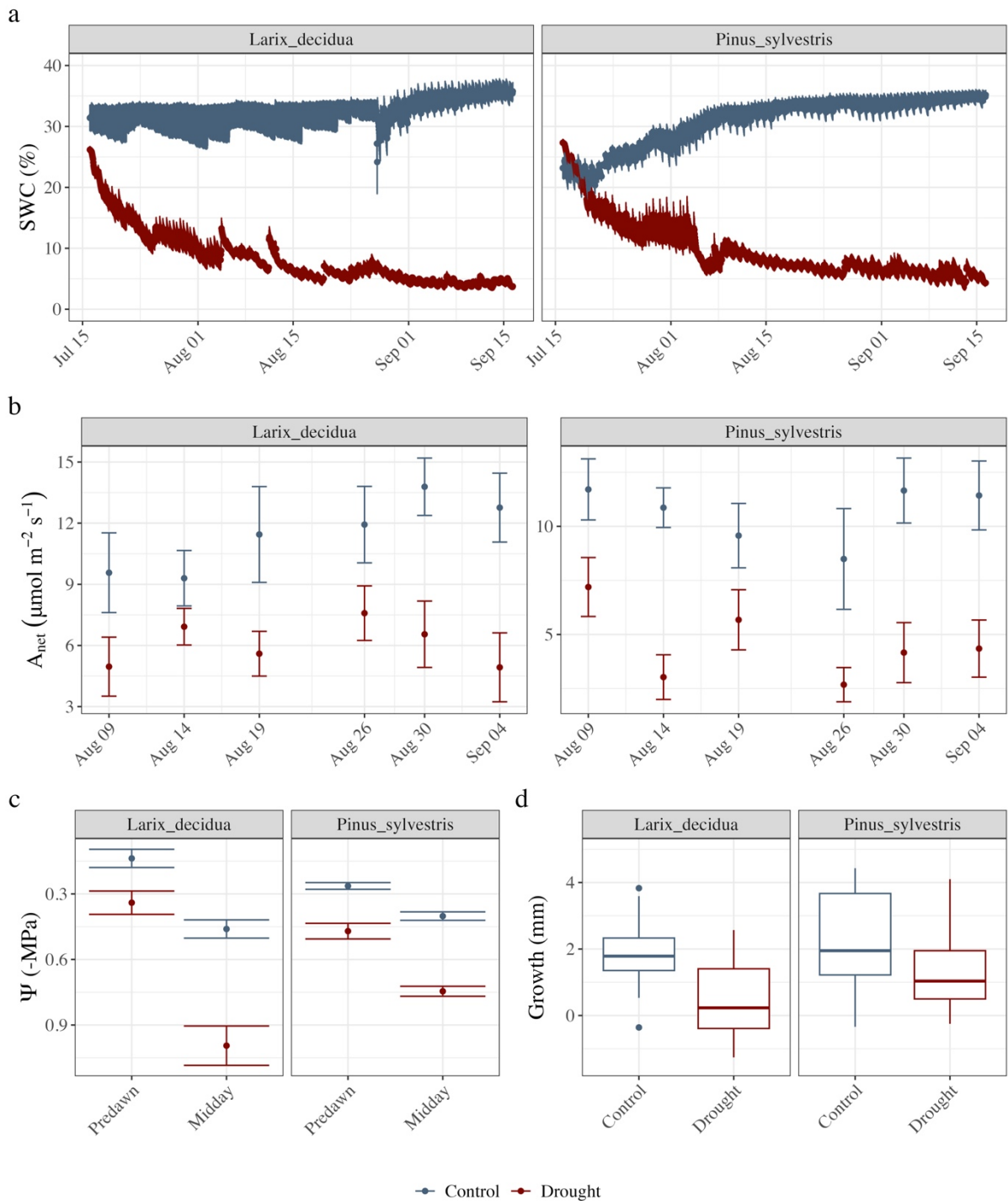


Figure S4.5: Summary of environmental and physiological stress induced during the experimental drought period. (a) Volumetric soil water content (SWC) progressively decreased during the first month of drought stress, and then maintained $\sim 5\%$ for the second month. (b) Net photosynthesis measured during peak drought stress, with error bars denoting standard error. (c) Xylem water potential (Ψ) was measured both predawn and at midday during peak drought stress (August 26th). (d) Stem growth as determined by the difference in stem diameter at the end of the drought period following rehydration and the initial diameter.

Larix decidua legacy correlations

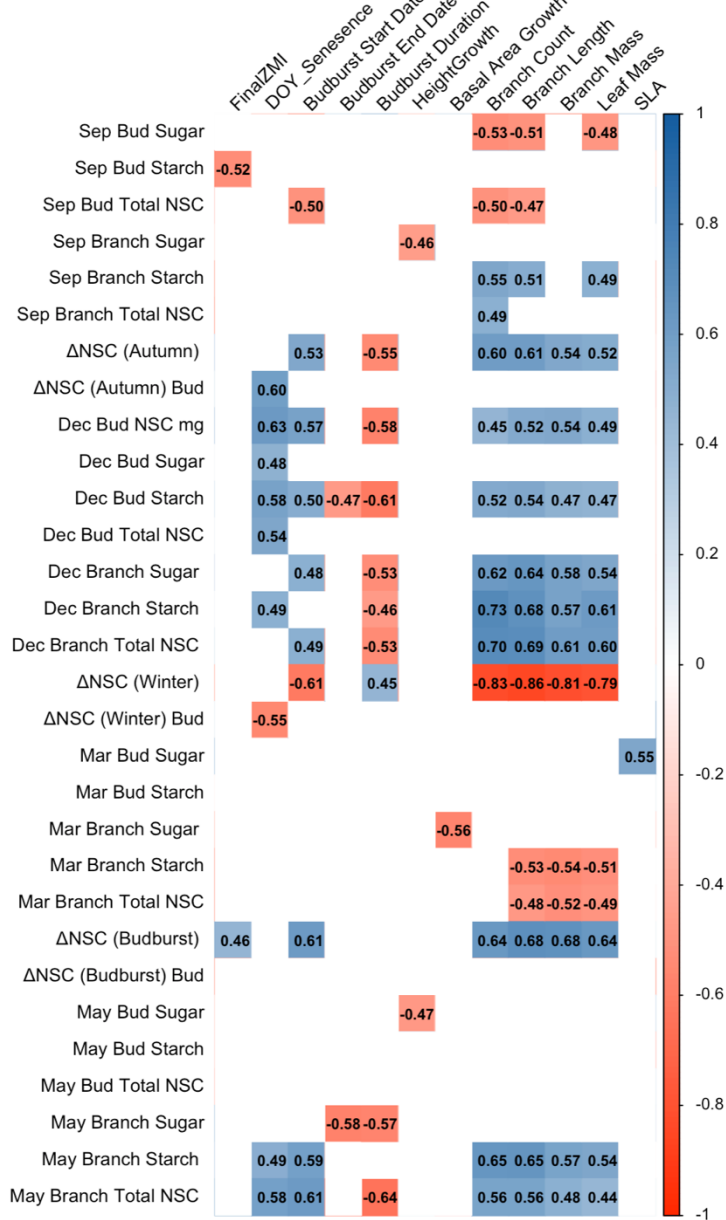


Figure S4.6: Correlation heatmap showing the relationship between all non-structural carbohydrate (NSC) parameters (bud and branch, y-axis) and measured phenological or morphological variables (x-axis) in *Larix decidua*. Monthly abbreviations denote the measurement phase (Sep = End-Drought, Dec = End-Autumn, Mar = End-Winter, May = Mid-Budburst). Pearson correlation coefficients (r) are displayed for significant correlations ($p < 0.05$). The color scale represents the strength of the correlation, ranging from -1 (strong negative, deep red) to +1 (strong positive, deep blue).

Pinus sylvestris legacy correlations

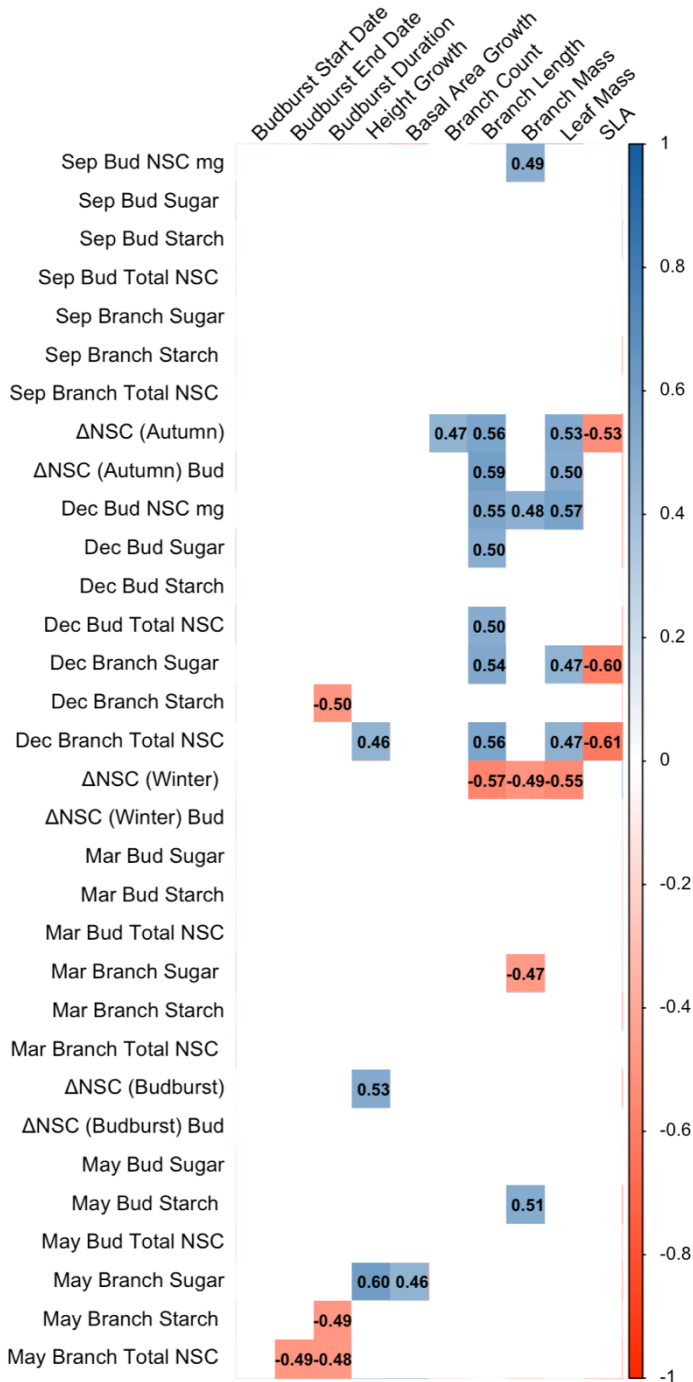


Figure S4.7: Correlation heatmap showing the relationship between all non-structural carbohydrate (NSC) parameters (bud and branch, y-axis) and measured phenological or morphological variables (x-axis) in *Pinus sylvestris*. Monthly abbreviations denote the measurement phase (Sep = End-Drought, Dec = End-Autumn, Mar = End-Winter, May = Mid-Budburst). Pearson correlation coefficients (r) are displayed for significant correlations (p < 0.05). The color scale represents the strength of the correlation, ranging from -1 (strong negative, red) to +1 (strong positive, blue).

5 Somatic Drought Stress Memory Affects Leaf Morpho-Physiological Traits of Plants via Epigenetic Mechanisms and Phytohormonal Signalling

This chapter was published as:

Alongi, F.; Petek-Petrik, A.; Mukarram, M.; Torun, H.; Schuldt, B.; and Petrik, P. 2025. “Somatic Drought Stress Memory Affects Leaf Morpho Physiological Traits of Plants via Epigenetic Mechanisms and Phytohormonal Signalling.” *Plant Gene* 42 (June):100509.

Abstract

Drought stress memory in plants is an adaptive mechanism that enhances resilience to future water stress through physiological and molecular modifications triggered by previous drought events. This review explores somatic drought stress memory within a plant's lifespan, with a specific focus on leaf and stomatal morphology, minimum leaf conductance, photosynthetic efficiency, water-use efficiency, antioxidant capacity, and leaf senescence. We examine how epigenetic mechanisms—such as DNA methylation, histone modifications, and non-coding RNAs—regulate gene expression in coordination with hormonal signalling pathways. Phytohormones, including abscisic acid, jasmonic acid, ethylene, salicylic acid, auxins and cytokinins, are central to these processes, influencing key morphological and physiological adaptations, such as stomatal regulation, cuticle thickness, water reteantion, and improved water-use efficiency. The review synthesizes current knowledge on the molecular and hormonal networks underlying these adaptations and their impact on leaf architecture and metabolism. Despite advancements, critical gaps remain in identifying the specific genes and pathways involved, understanding the longevity of epigenetic marks, and elucidating the intricate cross-talk between phytohormones during drought stress memory. This review emphasizes the need for integrated -omics approaches to map epigenetic modifications and uncover their roles in developing drought-resistant plants through targeted stress priming strategies.

5.1 Introduction

Drought stress is becoming a major driver of ecosystem disturbances worldwide (Allen et al. 2010; Seidl et al. 2017; Hammond et al. 2022). Moreover, drought stress is also threatening global food security due to negative effects on crops production (Cotrina Cabello et al. 2023; Wahab et al. 2023). The frequency and severity of the drought spells is expected to increase under current climate change scenarios (Vicente-Serrano et al. 2022). Drought stress memory in plants refers to the physiological and molecular changes that plants undergo after experiencing drought, which then influence their response to future drought events (Wojtyla et al. 2020; Jacques et al. 2021; Kambona et al. 2023). This “memory” or stress priming can lead to various adaptive changes in leaf morpho-physiological traits, enhancing the plant's ability to cope with subsequent water stress. We can distinguish between three main categories of stress memory which are somatic, inter-generational and transgenerational (Sharma et al. 2022; Lukić et al. 2023). This review focuses solely on somatic stress memory within the lifespan of the plant and is not exploring transfer of the stress priming response to subsequent generations. Drought exposure can also induce lasting negative impacts on leaf physiology, often referred to as drought legacy (Müller and Bahn 2022), but here we focus mainly on evidence of positive adaptive acclimation.

Drought stress can lead to epigenetic changes, such as DNA methylation and histone modification, which alter gene expression in response to future droughts. (Kinoshita and Seki 2014; Zhang et al. 2018). These modifications can make plants more resilient by enabling faster and more robust activation of stress-responsive genes during subsequent drought events. Moreover, histone modifications can enhance or decrease the expression of genes in phytohormonal signalling pathways, enabling plants to respond more robustly to perceived drought conditions (Chinnusamy and Zhu 2009; Banerjee and Roychoudhury 2017). Another drought memory mechanism, non-coding RNAs (ncRNAs), are largely involved in the post-transcriptional regulation of gene expression. ncRNAs can target mRNAs of phytohormone-related genes, modulating their stability and translation during and after drought stress (Contreras-Cubas et al. 2012; Gelaw and Sanan-Mishra 2021). These epigenetic modifications are often reversible but can persist across cell divisions, allowing plants to ‘remember’ previous stress conditions and respond more effectively to recurrent droughts.

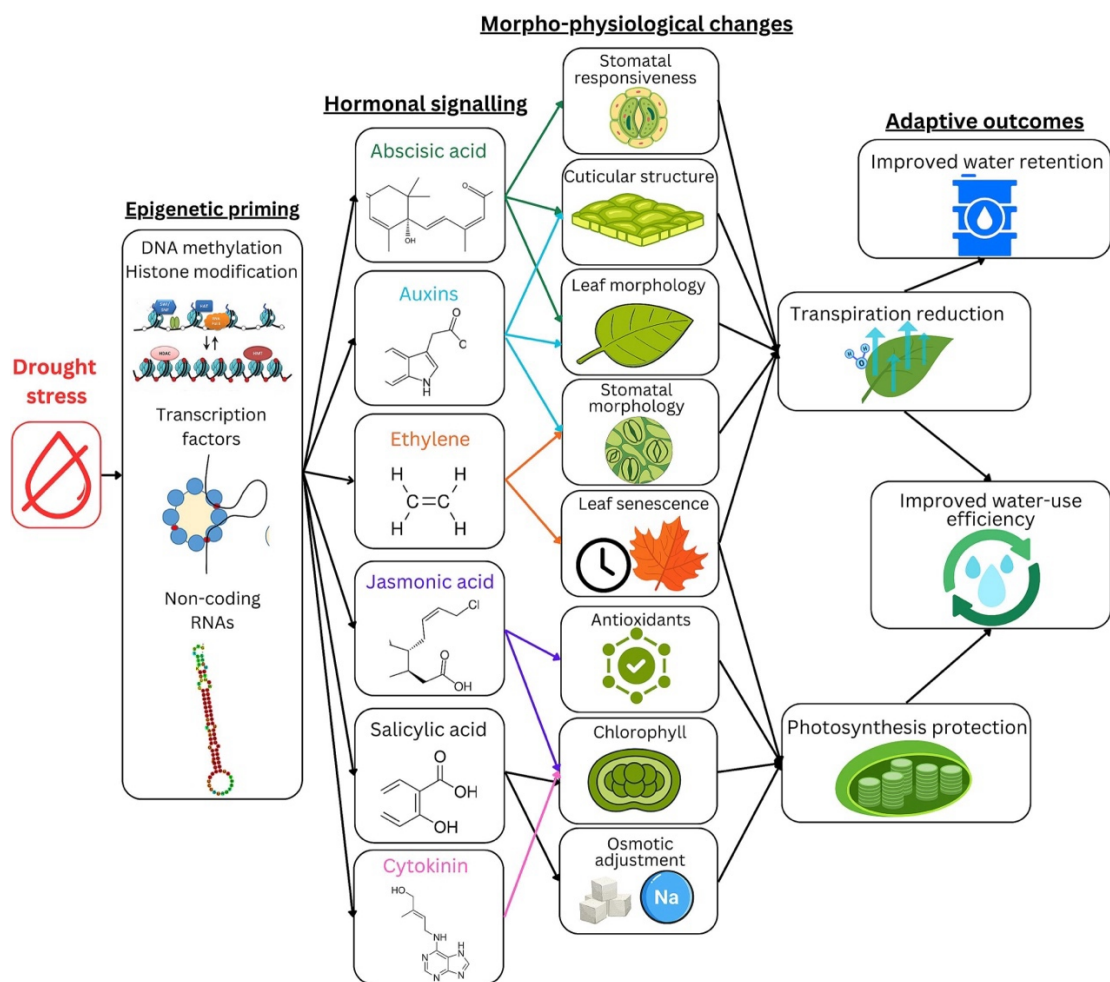


Figure 5.1: Overview of drought memory pathways from epigenetic priming to adaptive outcomes at leaf level via hormonal signalling and leaf morpho-physiological changes. The “DNA methylation and histone modification” image is adapted from previously adapted figure by Luong, P. Basic Principles of Genetics, Connexions Web site (2009). The “transcription factors” image is adapted from a figure by Adrian Baily. The “non-coding RNAs” image is authored by Paul Gardner. All three images are shared under a Creative Commons Attribution License (CC-BY 3.0). The figure was created in Canva software.

Drought memory epigenetic changes affect multiple phytohormones, among others abscisic acid (ABA), auxin, ethylene, jasmonic acid (JA), salicylic acid (SA) and cytokinin, that help improve and fine-tune future drought response by modifying leaf morphology and physiology (Fig. 1). Of these major phytohormones at play during progressive drought, ABA is the primary hormone involved in the regulation of drought responses (Sussmilch and McAdam 2017; Sircaik et al. 2021; Húdoková et al. 2022). Plants with drought stress memory often exhibit increased sensitivity to ABA, which can further regulate epigenetic mechanisms of drought tolerance (Kaya et al. 2024). This means that during subsequent drought events, these

plants more rapidly accumulate ABA, leading to faster stomatal closure and reduced water loss (Virlouvet et al. 2018; Forestan et al. 2020). ABA also influences cell division and expansion rate, with increased ABA leading to smaller and thicker leaves in plants with a history of drought stress (Sah et al. 2016; Ost et al. 2023). Similarly, drought-primed auxin signalling, largely through cross talk with ABA, can affect leaf size, stomatal patterning and cuticular structure, reducing water lost through transpiration during subsequent drought (Yuan et al. 2019; Jiang et al. 2022; Khoudi 2023). Another phytohormone that can be positively affected by drought memory and improve future drought resistance is ethylene. Drought primed plants can show more efficient nutrient reabsorption from leaves before leaf senescence via altered ethylene signalling pathways (Peerzada and Iqbal 2021). JA is also a key hormone involved in drought stress response. In plants displaying drought stress memory, JA levels may increase to enhance stress tolerance by increasing antioxidant production (Ahmad et al. 2016; Liu et al. 2016). SA contributes to drought stress resistance via systemic acquired resistance and can modulate various physiological processes under stress conditions (Miura and Tada 2014; Torun et al. 2024). Plants displaying drought stress memory may show altered SA signalling pathways, where SA help maintain higher chlorophyll and antioxidant levels during subsequent droughts, thereby improving stability of the photosynthetic apparatus (Brito et al. 2018; Kohli et al. 2022). These epigenetic and phytohormonal changes can influence leaf size, shape, cuticle formation, stomatal behaviour, phenology, photosynthesis, transpiration and water-use efficiency, which are vital for water retention and stress adaptation capability of a plant.

Information regarding past drought stress can be imprinted in the new leaf buds, which therefore affects the morpho-physiological characteristics of leaves in the subsequent vegetation season (Sadhukhan et al. 2022). In the following growing season, plants that have previously experienced drought stress may develop smaller, thicker leaves with higher leaf-mass per area (LMA, kg m^{-2}), i.e. lower specific leaf area (SLA, $\text{cm}^{-2} \text{ g}^{-1}$), in order to reduce total transpiration and improve their water-use efficiency (WUE) (Auler et al. 2021; Petrik et al. 2022). Drought stress memory can lead to long-term reductions in stomatal density (fewer stomata per unit area) or adjustments in stomatal aperture (opening size) (Mantoan et al. 2020). These changes help plants regulate gas exchange more efficiently under water-limited conditions, reducing water loss while maintaining some level of CO₂ uptake for photosynthesis. Reduction of stomatal density without an increase in stomatal size also lowers total maximal stomatal opening area and therefore limits potential transpiration

(Rathnasamy et al. 2023). This may be additionally critical during severe drought stress, as a lower minimum stomatal conductance (g_{\min}) can reduce passive water loss when stomata are completely closed. The reduction of stomatal size can have positive impact on stomatal responsiveness (Kardiman and Ræbild 2018) and water-use efficiency (Petrík et al. 2024). The cuticle, a waxy layer on the leaf surface, often becomes thicker in plants with drought stress memory (Spieß et al. 2012; Sintaha et al. 2022). This adaptation might reduce water loss by enhancing the boundary layer barrier to evaporation (Hasanuzzaman et al. 2023). Reducing transpiration improves the water retention ability of plants, leading to higher resiliency to drought conditions (Petrík et al. 2023; 2024).

While drought typically reduces photosynthesis due to stomatal closure, plants with drought stress memory may exhibit a more efficient photosynthetic response under mild stress (Gallé et al. 2007; Arend et al. 2016). This could be due to changes in the expression of genes involved in photosynthesis, allowing the plant to maintain productivity even under water-limited conditions. Drought stress memory often leads to an increase in WUE through tighter regulation of stomatal opening, allowing the plant to maximize carbon gain while minimizing water loss (Sintaha et al. 2022). Some plants may maintain higher Rubisco content in their leaves after a drought, which can help sustain photosynthetic activity during subsequent drought events (Lukić et al. 2020). Plants exhibiting drought stress memory may also accumulate higher levels of protective metabolites, sugars, and antioxidants, which help protect cellular integrity and maintain osmotic balance, reducing the damaging effects of drought on leaf tissues and decreasing hydraulic vulnerability (Wang et al. 2019; Liu et al. 2022; Vuković et al. 2022). Epigenetic modifications under water limitation can also increase proline synthesis, which assists in both stress response and recovery (Hayat et al. 2012). Recurrent drought stress can prime plants to enhance their antioxidant defences, which help mitigate oxidative radicals that can accumulate during drought (Lukić et al. 2020; Kashyap et al. 2024). This includes increased activity of enzymes like superoxide dismutase, catalase, and peroxidase in the leaves. In plants displaying drought memory, the epigenetic alterations can persist, leading to a long-term improvement in water retention, photosynthetic efficiency, and faster responses to phytohormonal signalling (Balao et al. 2018).

Taken together, drought stress memory equips plants with enhanced photosynthetic efficiency, improved water-use regulation, and bolstered protective mechanisms, allowing them to maintain productivity, limit water loss, and mitigate oxidative damage in the case of

recurrent drought events. The objective of this review was to summarise the latest research and find gaps in knowledge regarding drought stress memory mechanisms at the leaf level of plants. Understanding these mechanisms is crucial for developing effective strategies to prime crops, tree seedlings, and other plants for enhanced drought tolerance in order to provide greater resilience and productivity in the face of increasing climate challenges (Seth et al. 2024).

5.2 Epigenetic mechanisms in drought stress memory

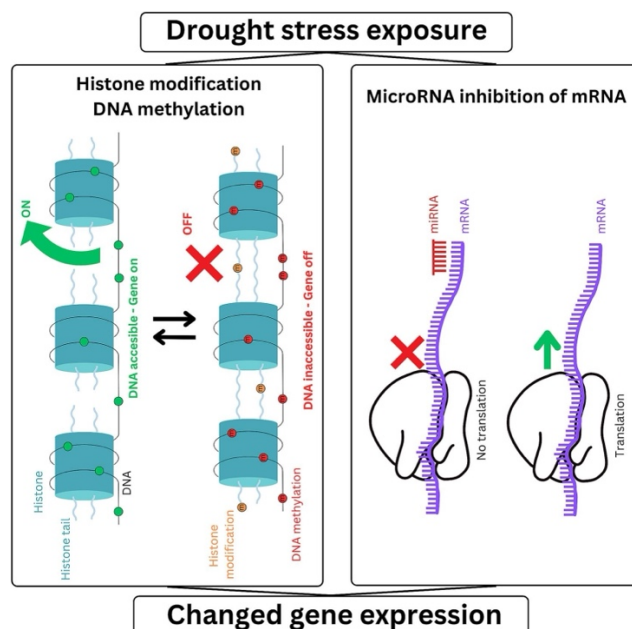


Figure 5.2: Drought stress exposure and altered gene expression mechanisms in plants. Left Panel: Histone modifications and DNA methylation regulate gene accessibility. When histone modifications promote DNA accessibility (green circles), gene expression is turned “ON.” Conversely, DNA methylation and histone modifications (red marks) make DNA inaccessible, turning gene expression “OFF.” Right Panel: miRNA binds to target mRNA, preventing translation (red cross). In the absence of miRNA inhibition, mRNA is successfully translated into protein (green arrow). (For interpretation of the references to colour in this figure legend, the reader is referred to the web version of this article.)

Epigenetic mechanisms, including DNA methylation, histone modifications, and non-coding RNAs (ncRNAs), play a pivotal role in establishing and maintaining drought stress memory in plants. These mechanisms enable plants to modulate gene expression in response to drought (Figure 5.2), leading to both immediate and long-term adjustments (drought memory) in leaf morphology and physiology.

5.2.1 DNA methylation and histone modification

DNA methylation, typically occurring at cytosine residues, can lead to the repression of gene expression by altering chromatin structure or by directly inhibiting the binding of transcription factors (Keshet et al. 1986; Mattei et al. 2022). In the context of drought stress, methylation patterns can change dynamically, allowing for the upregulation or downregulation of specific genes involved in stress responses (Luo et al. 2018; Wang et al. 2016). DNA methylation often works in conjunction with other epigenetic mechanisms, such as histone modifications and small RNAs (e.g., siRNAs and miRNAs), to regulate gene expression and maintain genome stability (J.-L. Wang et al. 2022; N. Wang et al. 2022). Major proportion (30 %) of drought-induced DNA methylation/demethylation sites (e.g. DK151, IR64) stay present even after drought release in rice (Wang et al. 2011). The differentially methylated DNA regions are one of the essential mechanisms of drought memory of plants (Kou et al. 2022). Drought stress induced methylation reduces gene accessibility (e.g. MYC2) and persists after drought release, positively affects jasmonic acid biosynthesis and antioxidant capacity of *Arabidopsis* (Liu et al. 2016). The drought induced DNA methylation/demethylation is gene specific and contributes as building block of drought memory in plants (Sun et al. 2021; Zi et al. 2024; Sadhukhan et al. 2022). Histone modifications, such as acetylation, methylation, phosphorylation, and ubiquitination, further influence chromatin accessibility and gene expression. Acetylation of histones, for instance, generally correlates with transcriptional activation by loosening chromatin structure, making DNA more accessible for transcription (S. Wang et al. 2024; F. Wang et al. 2024). Conversely, histone methylation can either activate or repress transcription, depending on the specific residues modified. During drought stress, these epigenetic marks can be selectively added or removed to fine-tune the expression of genes involved in stress response, such as via improved water retention, stomatal regulation, and modified leaf architecture (Liu et al. 2010; Luo et al. 2012). If these epigenetic modifications persist beyond the initial stress period, they can contribute to the plant's ability to "remember" drought conditions and respond more effectively to subsequent stress. Histone modifications can provide a persistent epigenetic transmission mechanism associated with drought memory in plants (Luo et al. 2012; Avramova 2015; Lämke and Bäurle 2017). Histone modifications help plants "remember"

drought by regulating stress-responsive genes, enabling quicker and more effective responses to future drought events (S. Wang et al. 2024; F. Wang et al. 2024).

5.2.2 *Role of non-coding RNAs*

Non-coding RNAs (ncRNAs) are regulatory molecules that do not encode proteins but play critical roles in gene expression regulation (Gelaw and Sanan-Mishra 2021; Abdulraheem et al. 2024). Among these, micro RNAs (miRNAs) and small interfering RNAs (siRNAs) are RNA molecules most commonly involved in post-transcriptional gene silencing, and function by guiding the degradation or inhibition of specific mRNA targets (Carthew and Sontheimer 2009). During drought, ncRNAs fine-tune gene expression, allowing plants to modulate their growth and stress response effectively. The involvement of ncRNAs in epigenetic regulation contributes to drought memory by establishing chromatin modifications, DNA methylation patterns, and histone acetylation changes that “store” stress information, enabling faster and more efficient responses to subsequent drought stress (Nguyen et al. 2022; Abdulraheem et al. 2024). Several miRNAs have been identified to play crucial roles in drought memory, impacting leaf development, morphology, and physiological processes. Specific miRNAs are upregulated or downregulated, influencing genes that affect stomatal density, leaf size, leaf xylem anatomy, cuticular structure, ABA signalling, ROS regulation and photosynthetic efficiency (Table 5.1). Apart from miRNAs, siRNAs also play a vital role in drought memory, particularly through their involvement in RNA-directed DNA methylation (RdDM) pathways (Rao et al. 2024). siRNAs can guide DNA methylation at specific genomic loci. siRNAs through modulating the activity of transposable elements (TEs) aid in the maintenance of genome stability during drought stress, protecting against deleterious effects caused by TE mobilization (Gelaw and Sanan-Mishra 2021), leading to long-lasting transcriptional silencing of genes involved in stress responses (Castel and Martienssen 2013).

Table 5.1: Overview of micro-RNAs and their regulation targets that affect leaf morphophysiological traits in relations to drought tolerance.

RNA code	Regulation target	Hormonal or morphophysiological target	References
<i>miR159</i>	<i>MYB</i> transcription factors	ABA signalling, stomatal closure	(Reyes and Chua 2007; Millar et al. 2019)
<i>miR166</i>	<i>HD-ZIP III</i> transcription factors	Leaf xylem anatomy, transpiration, WUE	(Li et al. 2017; Yadav et al. 2024)
<i>miR168</i>	<i>AGO1</i> from RNA-induced silencing complex	ABA signalling	(Li et al. 2012; Singroha et al. 2021)
<i>miR171</i>	<i>SCL6</i> transcription factors	Gibberellin, leaf morphology	(Huang et al. 2017; Pei et al. 2023)
<i>miR319</i>	<i>TCP</i> transcription factors	Leaf size and shape	(Koyama et al. 2017; Lu et al. 2023)
<i>miR393</i>	Auxin receptors of <i>TIR1</i>	Stomatal density, ABA signalling	(Yuan et al. 2019; Jiang et al. 2022)
<i>miR396</i>	<i>GRF</i>	Leaf size	(Liu et al. 2009; Liebsch and Palatnik 2020)
<i>miR398</i>	<i>APX6, CSD</i>	Leaf senescence, ROS regulation	(Chen et al. 2021; M. Chen et al. 2020; J. Li et al. 2022; Y. Li et al. 2022)
<i>miR399</i>	Phosphate homeostasis	Stomatal responsiveness	(Pant et al. 2008; Zhu et al. 2020)
<i>miR408</i>	Plastocyanin	Photosynthetic efficiency, stomatal responsiveness	(Zhang et al. 2017; Balyan et al. 2023; Yang et al. 2024)
siRNAs	<i>CER3</i> silencing	Cuticular structure and biosynthesis	(Lam et al. 2015; Sajeevan et al. 2017)

5.3 Crosstalk between epigenetic mechanisms and phytohormones

Phytohormones, such as abscisic acid (ABA), jasmonic acid (JA), ethylene, and auxins, are integral to plant stress responses, including drought. The interaction between epigenetic modifications and phytohormone signalling pathways allows plants to coordinate complex responses that modulate leaf morphology and physiology (Lu et al. 2017; Jiang et al. 2023; Kapoor et al. 2023; Rudolf et al. 2024). The interplay of phytohormones during and after drought stress involves crosstalk at molecular, genetic, and physiological levels, modulated

by epigenetic mechanisms (Shaffique et al. 2023; Kaya et al. 2024). The complex impact of DNA methylation/demethylation, histone acetylation/deacetylation and non-coding RNAs on the mentioned phytohormones is visualized in Fig. 3. A coordinated epigenetic and hormonal response is essential for establishing drought stress memory, enabling plants to adapt to recurring drought conditions by fine-tuning gene expression and physiological processes to optimize survival and resilience.

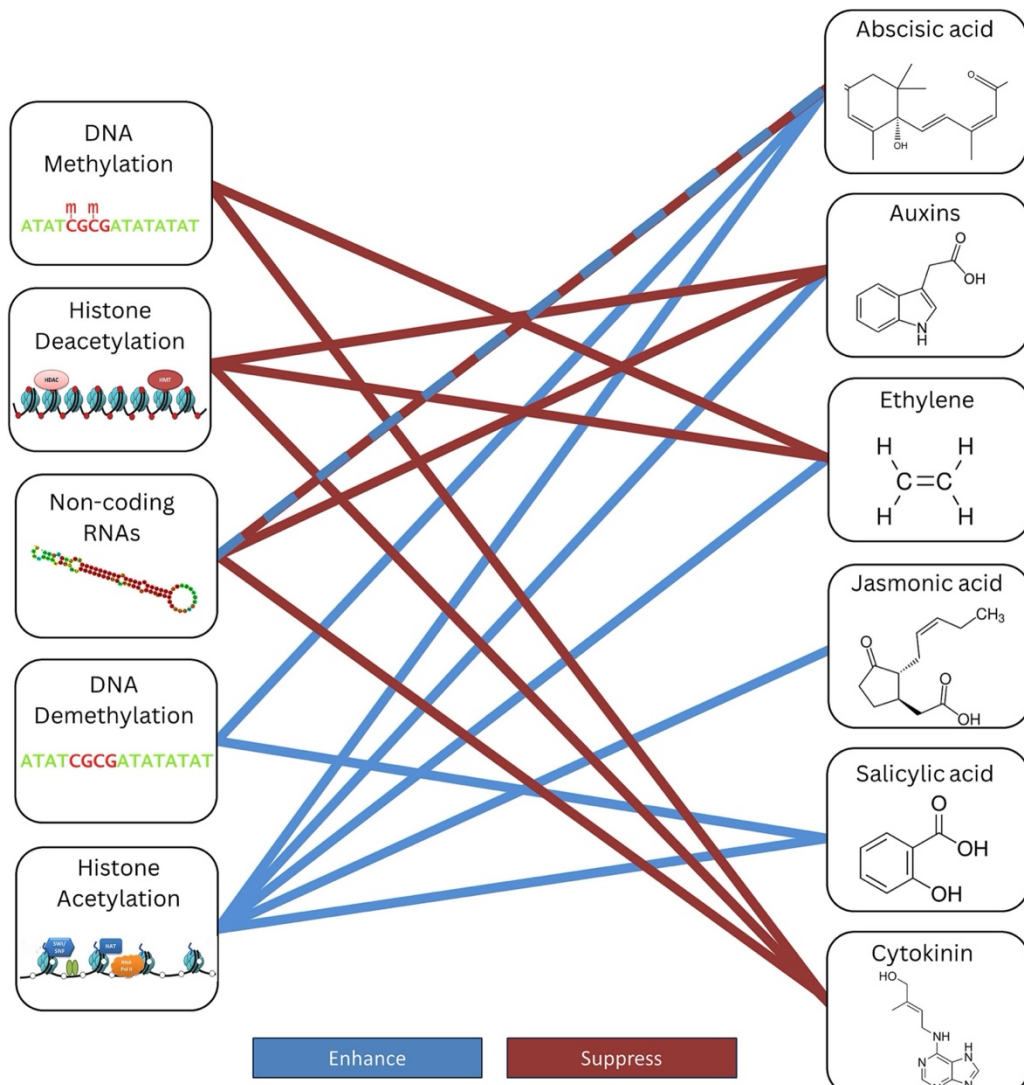


Figure 5.3: Graphical overview of epigenetic pathways of phytohormone control as drought memory components after drought stress. Epigenetic modifications can result in enhanced (blue) or suppressed (red) phytohormone levels. Note: displayed relationships are restricted to specific mechanisms discussed in the text. (For interpretation of the references to colour in this figure legend, the reader is referred to the web version of this article.)

5.3.1 *Abscisic acid*

Abscisic acid (ABA) is the central hormone regulating plant responses to drought stress. It is responsible for inducing stomatal closure, reducing water loss, cuticle biosynthesis and activating stress-responsive genes (Martin et al. 2017). The crosstalk between epigenetic modifications and ABA signalling pathways enhances the plant's ability to respond to drought stress, both immediately and during subsequent drought episodes. During drought stress, DNA demethylation of key genes involved in ABA biosynthesis, such as 9-cis-epoxycarotenoid dioxygenase 3 (NCED3) (Virlouvet and Fromm 2015), Ras-associated binding 18 (RAB18) (Ding et al. 2014) or Zeaxanthin Epoxidase 1 (ZEP1) (Forestan et al. 2020), lead to an increase in ABA production. This rapid accumulation of ABA triggers the closure of stomata, minimizing water loss. After stress release, these demethylated regions can remain active, priming the plant for quicker ABA synthesis in future droughts (Godwin and Farrona 2020), and therefore a more sensitive response of ABA-mediated drought tolerance. Additional histone acetylation at ABA-responsive genes, such as ABF2 (ABA-responsive element-binding factor 2), enhances their expression, promoting faster and more robust drought responses (Alves de Freitas Guedes et al. 2019). The memory of drought is partially encoded in these epigenetic marks, allowing the plant to respond more rapidly to future stress by activating the ABA signalling cascade (Ma et al. 2019). Epigenetic regulation of ABA receptors, such as PYR/PYL proteins, ensures that the ABA signalling pathway remains primed, with faster ABA-mediated stomatal closure even under milder future drought conditions (Lim et al. 2013; Fidler et al. 2022; Jiang et al. 2024).

5.3.2 *Jasmonic acid*

Jasmonic acid (JA) is associated with responses to biotic stress but also play roles in drought tolerance. JA levels increase during drought, modulating antioxidant defences to help plants cope with higher oxidative stress (Alam et al. 2014; Mukarram et al. 2021; Kebert et al. 2023). The crosstalk between JA and epigenetic mechanisms helps fine-tune the plant's drought response. Histone acetylation at the promoters of JA biosynthesis genes, such as LOX3 (lipoxygenase 3) and AOS (allene oxide synthase), can enhance JA production during and after drought (Avramova 2017; Su et al. 2023). This leads to an increase in antioxidant enzyme activity and ROS scavenging, which protect the plant from oxidative damage.

Epigenetic marks, such as histone methylation at specific loci in JA-responsive genes, regulate the plant's ability to modulate growth and defence mechanisms. After drought release, these marks can persist, ensuring that the plant maintains elevated antioxidant levels and is better prepared for future oxidative stress associated with drought (Ali and Baek 2020; Wang et al. 2021; Kaya et al. 2024). Conversely, cross-talk between ABA and JA pathways can lead to the repression of genes related to biotic defence during subsequent drought periods (Avramova 2019), allowing plants to prioritize their physiological and metabolic resources toward drought-specific responses, thereby enhancing water-use efficiency and stress resilience. These interactions can lead to changes in leaf morphology, such as reduced leaf size and altered leaf architecture, which help conserve water. While the longevity of these epigenetic modifications remains largely unclear, initial transcriptional changes to drought stress are known to persist throughout subsequent watering and dehydration cycles (Liu et al. 2016).

5.3.3 *Ethylene*

Ethylene interacts with epigenetic mechanisms to regulate leaf senescence under drought stress. The epigenetic repression or activation of ethylene-responsive genes can modulate this process, influencing leaf lifespan and function under drought conditions (Tan et al. 2023). Ethylene also modulates stomatal development by crosstalk with gibberellins, affecting stomatal size (Saibo et al. 2003). Epigenetic regulation of ethylene signalling pathways ensures that plants optimize resource use during and after drought (Nazir et al. 2024). DNA methylation of ethylene biosynthesis genes, such as ACS (ACC synthase), can lower ethylene production during drought. This regulation helps balance ethylene levels, preventing premature senescence and ensuring that the plant can retain functional leaves during stress (Khan et al. 2024). Histone modifications in ethylene signalling genes, such as EIN3 (ethylene-insensitive 3), regulate the timing and extent of leaf senescence. This ensures that plants only shed leaves when necessary, allowing for optimal nutrient reallocation and prolonged leaf function after drought conditions (Drenovsky et al. 2019). During drought, ethylene levels increase to facilitate senescence and nutrient reallocation from older leaves to younger tissues (Munné-Bosch and Alegre 2004). The explicit timing of leaf senescence during drought stress is critical to optimize both the continued photosynthetic function of leaves and to ensure the complete remobilization of nutrients upon leaf shedding (Tan et al.

2023). After drought release, plants with drought memory may exhibit delayed senescence, allowing them to maintain photosynthetically active leaves longer, particularly when the successful remobilization of nutrients from shed to persisting leaves occurs. Epigenetic regulation of ethylene pathways enables plants to fine-tune the timing of leaf senescence based on water availability and stress history (Li et al. 2014).

5.3.4 *Salicylic acid*

Salicylic acid (SA) is a key hormone in regulating systemic acquired resistance and defence responses, and plays a crucial role in mitigating the negative effects of stress, particularly in the context of drought (Zhang et al. 2010). SA is involved in photosynthetic stability, osmotic adjustment, and antioxidant defences, as well as helping plants maintaining chlorophyll levels and reducing oxidative damage (Khan et al. 2015; Gao et al. 2023; Torun et al. 2024). The crosstalk between SA and epigenetic mechanisms enables the integration of these defence responses, ensuring an efficient acclimation to drought stress and contributing to the plant's overall resilience during and after recovery. Histone acetylation at the promoters of SA biosynthesis genes, such as ICS1 (isochorismate synthase 1), enhances SA production during and after drought stress (Kumazaki and Suzuki 2019). This increased SA production helps plants maintain higher chlorophyll levels, reduce oxidative damage, and improve photosynthetic efficiency under stress conditions. After the release of drought stress, persistent epigenetic marks such as DNA methylation and histone modifications at SA-responsive genes allow plants to maintain elevated antioxidant levels (Ullah et al. 2024). These marks ensure that the photosynthetic apparatus remains protected, enabling plants to recover more efficiently and maintain defence readiness against future stress. SA-influenced epigenetic regulation of osmolyte-related genes enhances solute production and retention, allowing plants to adjust osmotically during and after drought (de Souza Neta et al. 2024). Epigenetic mechanisms regulate the expression of osmolyte-related genes such as P5CS (Safari et al. 2022), RD29A (Jia et al. 2012; Kinoshita and Seki 2014) and DREB (Santos et al. 2011; Shriti et al. 2024). This adjustment is critical for stabilizing cell membranes and proteins, preventing damage from dehydration, and ensuring proper cellular function.

5.3.5 *Auxins*

Auxins are primarily involved in plant growth and development but also play important roles in modulating leaf expansion, stomatal patterning, and cuticular development under drought conditions (Teale et al. 2006; Higashide et al. 2014; Verma et al. 2022). Epigenetic regulation of auxin pathways allows plants to balance growth and stress responses effectively. miRNAs, such as miR393, target auxin receptors like TIR1 (transport inhibitor response 1), modulating auxin signalling during and after drought (Jiang et al. 2022). The interaction between miRNAs and DNA methylation fine-tunes auxin responses, leading to altered leaf morphology and improved drought resilience. Histone modifications in auxin-responsive genes, such as ARFs (auxin response factors), ensure that the auxin signalling pathways remain active or suppressed as needed during stress and after stress release (Marzi et al. 2024). This epigenetic regulation affects leaf size, stomatal density, and cuticle formation (Guo et al. 2019; Yuan et al. 2019; Torii 2021). Auxin epigenetic adjustment during drought stress can also affect mesophyll cell expansion after stress release and therefore increase photosynthetic capacity due to mesophyll conductance constraints (Batista-Silva et al. 2024). After drought release, epigenetic changes in auxin signalling allow plants to modulate leaf growth and stomatal patterning, ensuring that the plant maintains conservative water-use strategies while resuming growth (J.-L. Wang et al. 2022; N. Wang et al. 2022).

5.3.6 *Cytokinins*

Cytokinins play a key role in maintaining chlorophyll content and antioxidant capacity under and after drought conditions (Gujjar et al. 2020; Mughal et al. 2024). In plants with drought memory, cytokinins help delay leaf senescence and prevent chlorophyll degradation, supporting sustained photosynthesis (Efroni et al. 2013; Vankova 2014; Prasad 2022). Drought-induced DNA methylation changes at ARR gene promoters can downregulate cytokinin responses during stress, reducing chlorophyll loss (Cortleven et al. 2016). Higher cytokinin levels during drought reduce chlorophyll loss, while cytokinin signalling recovery after stress promotes chlorophyll retention, enhancing the plant's ability to cope with future droughts (Prerostova et al. 2018). Cytokinins can also induce physiological changes at leaf level via nitric oxide (NO) signalling affecting photosynthetic performance, electron transport

rate and stomatal regulation (Shao et al. 2010; Ahmad et al. 2024). Subsequent changes in NO can persist for days following stress release, allowing for the continued enhancement of drought tolerance (Fan and Liu 2012). This dynamic regulation of cytokinin signalling, mediated by both hormonal adjustments and epigenetic modifications, helps to maintain photosynthetic efficiency and delay senescence during recurrent droughts, reinforcing the plant's ability to 'remember' previous stress events and mount a more effective response to future drought conditions.

5.4 Leaf morpho-physiological changes after drought stress release

After a period of drought stress, plants undergo significant morpho-physiological adjustments when water availability is restored. These changes are strongly influenced by the memory of previous drought episodes, which allows plants to adapt more effectively to subsequent stress events. Drought memory, established through mechanisms such as epigenetic modifications, transcriptional reprogramming, and hormonal adjustments, ensures that certain stress-responsive traits persist even after rehydration. For example, genes involved in stomatal regulation, cuticle composition, or antioxidant defence may remain primed for rapid activation during future droughts (Figure 5.4). Additionally, morphological traits such as altered leaf thickness, stomatal density, and cuticular wax are often retained to some degree, improving water retention during subsequent drought events.

Understanding how drought memory shapes leaf morpho-physiological responses highlights the balance plants maintain between recovery and resilience. These memory-driven adaptations not only contribute to efficient stress recovery but also enhance long-term plant fitness, particularly in environments where drought stress is recurrent.

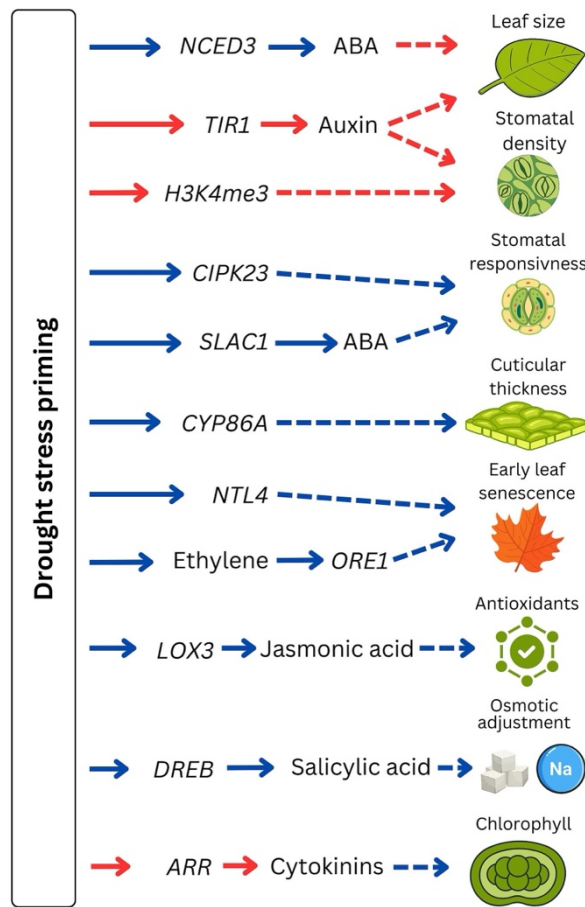


Figure 5.4: Example for specific genes and phytohormonal signals regulating drought priming responses such as stomatal density, cuticular thickness, antioxidants, osmotic adjustment, chlorophyll maintenance, and leaf senescence to enhance drought tolerance in plants.

5.4.1 Leaf morphology: size and thickness

During drought stress, leaf growth is typically suppressed as plants focus on conserving water and prioritize resources toward water-acquisition in root tissues (Kou et al. 2022). When stress is relieved, plants often resume leaf expansion, but the rate of recovery depends on the severity and duration of the prior stress (Xu et al. 2010). In plants exhibiting drought memory, this resumption may be delayed or occur at a reduced rate to prevent excessive water loss during any subsequent stress events. Persistent reductions in leaf size are commonly observed in plants following drought events (Fleta-Soriano and Munné-Bosch 2016; Metz et al. 2020). Smaller leaves reduce transpiration and water loss, serving as a protective adaptation even after water becomes available again (Smith and Geller 1980; Zhu et al. 2020). Moreover, smaller leaves are more efficient at cooling down under high

temperatures, reducing unnecessary water loss (Konrad et al. 2021). SLA, which represents the leaf area relative to its dry mass, often remains lower (or higher leaf mass per area $LMA = SLA^{-1}$) in plants that have experienced drought (Fleta-Soriano and Munné-Bosch 2016; Weithmann et al. 2022). This is indicative of thicker leaves with higher tissue density, which can aid in water retention and increase hydraulic safety margins. Reduction of leaf area post drought release, particularly when accompanied by an increased resource sink in roots, also often means increase in root:shoot ratio, which can positively affect drought resistance of plants (Fleta-Soriano and Munné-Bosch 2016). The drought memory pathways leading to reduction of leaf size after drought release are usually mediated by epigenetic crosstalk with phytohormones like ABA and Auxins (discussed in 3.1 Abscisic acid, 3.4 Salicylic acid). Especially epigenetic upregulation of NCED3 leads to ABA biosynthesis and reduced leaf growth (Lee et al. 2021). Furthermore, upregulation of DREB/CBF suppresses leaf growth during and after drought (Morran et al. 2011). This intricate balance between growth suppression and adaptive resource allocation underscores the importance of understanding the molecular and physiological mechanisms behind drought memory.

5.4.2 Stomatal morphology: size and density

Stomatal morphology, including stomatal density and stomatal size, plays a critical role in regulating gas exchange and water loss (Hetherington and Woodward 2003). Stomatal density shows higher phenotypic plasticity than stomatal size in response to precipitation conditions or drought stress (Stojnić et al. 2015; Petrik et al. 2020; Petek-Petrik et al. 2023). Therefore, any drought memory impact on stomatal morphology is often more visible in changes of stomatal density than size (Petrik et al. 2022). After drought stress release, stomatal characteristics may only partially revert to pre-stress conditions, as plants with drought memory retain modifications to minimize water loss. Drought memory induced long-term reduction of stomatal density in sorghum, which was connected with the methylated H3K4me3 epigenetic memory marker (Mantoan et al. 2020). Moreover, methylation of NCED3 (Virlouvet and Fromm 2015), RAB18 (Ding et al. 2014) or ZEP1 (Forestan et al. 2020) increases ABA synthesis and subsequently reduces stomatal density. This reduction in stomatal density helps plants regulate water loss more effectively in anticipation of future drought episodes, reducing the effective surface area through which water can be lost via transpiration (Doheny-Adams et al. 2012). Drought memory can also lead to prolonged

reduction of stomatal guard cell length, which can be also linked to increased water-use efficiency of plants (Herrera et al. 2024; Petrík et al. 2023; 2024). This retention of drought-induced stomatal modifications highlights the role of epigenetic memory in optimizing water-use efficiency, allowing plants to better prepare for and withstand future water-limiting conditions.

5.4.3 Stomatal responsiveness and transpiration

Stomatal closure is a key response to drought that limits water loss but also restricts carbon dioxide uptake and photosynthesis. Drought stressed plants often reduce their stomatal conductance and transpiration in order to prevent excessive water loss (Střelcová et al. 2013; Rui et al. 2024). Upon drought stress release, stomata typically reopen, restoring gas exchange. However, in plants exhibiting drought memory, stomatal behaviour often remains altered, with stomata showing a more conservative response to water availability (Virlouvet and Fromm 2015). Stomatal reopening is often more gradual in plants recovering from drought stress, allowing them to maintain a balance between gas exchange and water conservation (Rui et al. 2024). The delayed stomatal opening can be partially attributed to changes in the trafficking protein SYP121, which regulates ion channel activity in stomatal guard cells (Eisenach et al. 2012). This behaviour may lead to increased intrinsic water-use efficiency (iWUE) which can persist long-term, as iWUE is largely linked to the plant's methylation status (Zhong et al. 2021). Drought stress primed plants close their stomata faster under subsequent drought stress exposure due to higher accumulation of ABA and increased Ca^{2+} influx rate, which was connected to higher expression of CIPK23 and higher expression of the SLAC1 gene (Yang et al. 2023). Plants with drought memory are better capable of fine-tuning their stomatal control with ABA and therefore exhibit enhanced iWUE with sustained biomass or yield gains (Yao et al. 2021). Long-term exposure to water-deficit reduces the transpiration sensitivity to soil water content and VPD, resulting in plants maintaining low transpiration even under well-watered conditions (Grossiord et al. 2018; Zavadilová et al. 2023). This sustained reduction in transpiration enhances future drought tolerance by enabling a conservative approach to survive subsequent drought episodes and maintain physiological function.

5.4.4 Cuticular structure and residual water loss

The cuticle is a waxy layer preventing excessive water loss. The water loss after stomatal closure under drought conditions is dominated by cuticular pathway and through leaky stomata, which together comprise minimum leaf conductance (g_{\min}). Minimum leaf conductance has been characterised as one of the most critical traits affecting drought survival time of plants and biomass accumulation capacity under drought (Petek-Petrik et al. 2023; 2024; Ziegler et al. 2024). Drought memory can have significant impacts on cuticular wax composition via the aliphatic wax biosynthetic pathway, including CER1, CER2, CER3, CER4, CER10 and WSD1 (Dimopoulos et al. 2020). Nevertheless, changes of cuticular waxes are not necessarily translated into changes in minimum leaf conductance. There are few studies suggest that g_{\min} may be plastic, with plants potentially acclimating to drought stress by reducing g_{\min} (Le Provost et al. 2013; M. Chen et al. 2020; Y. Chen et al. 2020) or that changes in cuticular waxes are related more to temperature stability of the cuticular layer (VanderWeide et al. 2022). On the other hand, several studies have found very limited phenotypic plasticity of g_{\min} and no response pattern to drought stress (Schuster et al. 2017; Slot et al. 2021; Petek-Petrik et al. 2024; S. Wang et al. 2024; F. Wang et al. 2024). Therefore, the acclimation potential of g_{\min} reduction as part of drought memory mechanisms is still unknown. CYP86A family genes, which are essential for cutin and wax biosynthesis, are regulated by auxin and are important for cuticle formation (Kong et al. 2020). The CYP86A genes can be epigenetically altered following drought stress, but the precise hormonal signalling pathway is still not known (Duan and Schuler 2005). There is lack of studies directly linking drought priming or drought memory to changes in cuticular structure and residual water losses or minimum leaf conductance. As g_{\min} is a critical component of drought tolerance, it is essential that future research focuses on how drought memory influences potential g_{\min} acclimation, identifying epigenetic and physiological pathways that regulate long-term reductions in minimal stomatal conductance under recurrent drought conditions. Photosynthetic recovery and chlorophyll retention

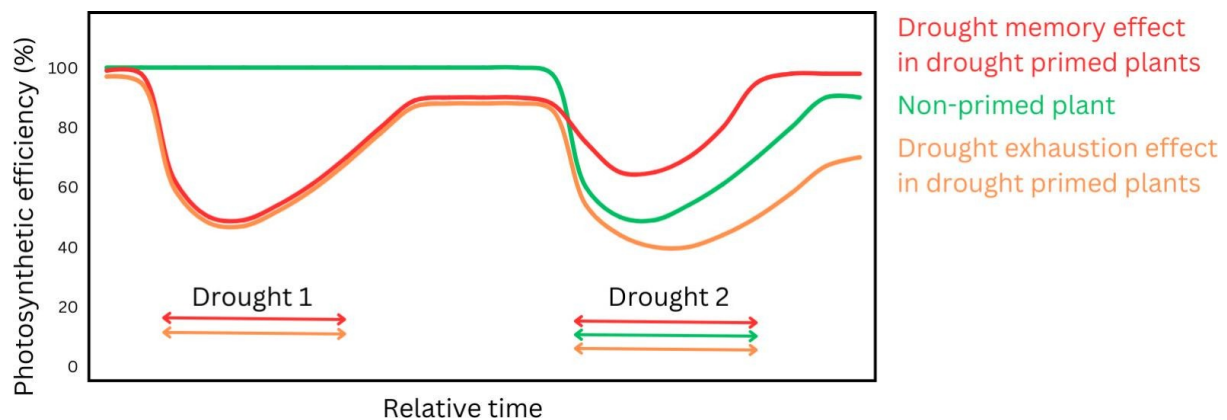


Figure 5.5: Conceptual figure showing potential pathways of photosynthetic efficiency for drought primed plants that exhibit drought memory or drought exhaustion effects, compared with non-primed plant.

Drought stress can impair photosynthesis due to reduced stomatal conductance and by damaging the photosynthetic apparatus. Upon stress release, photosynthesis usually resumes, but the recovery process is modulated by drought memory. Plants with drought memory often exhibit enhanced photosynthetic efficiency during subsequent drought compared to non-primed plants (Figure 5.5), allowing them to maintain productivity with limited water loss (Zhou et al. 2016). Specifically, plants may exhibit higher Rubisco activity and antioxidant capacity which supports photosynthetic rates (Menezes-Silva et al. 2017). Leaf level photosynthesis, electron transport rate and photosystem II performance index can be also significantly higher after drought release compared to the pre-stress state (Arend et al. 2016; Kannenberg et al. 2019; Antunović Dunić et al. 2023). Plants with drought memory have often reduced stomatal conductance, but if able to maintain their photosynthetic capacity may achieve higher water-use efficiency post drought release (Herrera et al. 2024). The faster recovery of photosynthetic rates after drought may result from altered gene expression related to photosynthetic machinery (PSBS, LHCB, PGR5), especially efficiency of photosystem II (Li et al. 2000; Damkjær et al. 2009; Arend et al. 2016; Yamamoto and Shikanai 2019). Drought stress primed plants also show increased chlorophyll and carotenoid contents under subsequent drought stress compared to non-primed plants (Ben Abdallah et al. 2017), which is intricately linked to the epigenetic silencing of genes involved in pigment decomposition and upregulation of pigment synthases (Zhang et al. 2015; Anwar et al. 2021). Drought stress priming can also lead to increase of Rubisco content, which helps maintain photosynthetic rate under subsequent drought stress (Abid et al. 2016). Drought memory can be also associated with accumulation of the D1 protein which improves the photoprotection under subsequent drought stress (Gadzinowska et al. 2021). As such, persistent epigenetic control

enables plants to maintain photosynthetic function through the maintenance of pigment and Rubisco activity, allowing for a more resilient photosynthetic apparatus during subsequent stress event.

5.4.5 Antioxidant defenses and osmolyte accumulation

Plants exposed to drought stress typically increase the production of antioxidants and osmoprotectants (e.g., proline, soluble sugars) to mitigate oxidative damage and maintain osmotic balance (Ditmarová et al. 2010; Vuksanović et al. 2023). Higher antioxidant capacity under drought helps plants to protect photosynthetic apparatus (Hasanagić et al. 2020; Alongi et al. 2024). In plants with drought memory, antioxidant enzyme classes such as superoxide dismutase, peroxidase, glutathione reductase and catalase continue to function at higher levels, helping the plant recover from stress and defend against future oxidative damage (Alves et al. 2020; Lukić et al. 2020; Carvalho et al. 2024). Drought priming can increase antioxidant capacity and is also linked to higher d13C, reflecting higher water-use efficiency of plants (Ramírez et al. 2015). Higher leaf antioxidant content after drought priming can also enable plants to accumulate more biomass in subsequent drought stress exposure by reducing ROS agents, which would otherwise weaken cellular membrane integrity (Amini et al. 2023). Increased antioxidant capacity in cotton was linked to H3K4me3 methylation (Z. Tian et al. 2024). Drought stress memory positively affects leaf soluble sugars and proline content, therefore improving osmotic balance of drought stress primed plants under subsequent drought (Ben Abdallah et al. 2017). The study also found a positive impact of drought memory on antioxidant capacity in subsequent drought. The drought memory osmotic adjustment in wheat was associated with demethylation of TaP5CS and TaBADH (Li et al. 2023). Therefore, sustained epigenetic control from drought priming can lead to both antioxidant and osmotic adjustment to improve future drought tolerance.

5.4.6 Leaf senescence: water loss avoidance, nutrient reallocation or assimilation recovery

Drought can both accelerate to prevent water losses and delay leaf senescence to conserve resources. The premature defoliation under extreme drought events is often attributed to tissue dehydration damage, rather than controlled process (Arend et al. 2022). Nevertheless, leaf senescence is largely regulated by epigenetic mechanisms, such as through the increased

methylation of senescence-specific histones (Rudy et al. 2024). Overexpression of NTL4 during and after drought stress response accelerates leaf senescence (Tan et al. 2023). Moreover, upregulation of ORE1 during drought stress can lead to faster leaf senescence (Yu et al. 2021). Nevertheless, the longevity of the epigenetic changes after stress release is still unknown. On the other hand, in plants exhibiting drought memory, leaf senescence may be delayed, allowing leaves to remain photosynthetically active for longer, which aids in the recovery of growth and productivity after stress (Arend et al. 2016). Selective leaf senescence, when plants reallocate nutrients such as nitrogen (N) from older to younger leaves, may further optimize resource allocation for new growth when conditions improve (Touche et al. 2024). Epigenetic modifications such as DNA methylation and siRNA are known to help regulate N responses, particularly under nutrient deficient conditions (Zhang et al. 2023). This is especially critical for ecosystems that experience repeated drought stress periods which can negatively affect access of plants to soil nutrients (Gessler et al. 2017; Joseph et al. 2021; Touche et al. 2022). However, impaired or incomplete nutrient reallocation during leaf senescence may occur, particularly during severe drought stress when leaf senescence is expedited due to rapidly sustained hydraulic damage (Estiarte and Peñuelas 2015). Effective epigenetic regulation of leaf senescence processes may therefore be critical to optimize the trade-off between efficient nutrient scavenging and the timely senescence of damaged or older tissues.

5.5 Conclusion and future prospects

While DNA methylation, histone modifications, and non-coding RNAs have been linked to drought stress memory, the specific genes and pathways regulated by these epigenetic marks at the leaf level are not fully mapped. Additionally, current studies have largely focused on a handful of model or crop species such as *Arabidopsis* or *Populus*, which benefit from the existence of complete and relatively simple genome maps (Ding et al. 2013; Georgii et al. 2019). Hence, species of which genomes are not completely available, particularly in perennial plants with relatively large and highly repeated genomes, remain understudied. While many epigenetic mechanisms are conserved across species, an increased focus of future research on these understudied species will likely identify orthologous genes, which enable epigenetic control. Such studies will help to elucidate the longevity of such modifications and overall duration of stress-memory. There is also a need for comprehensive profiling of both

epigenetic and metabolomic processes to understand how stress memory translates to physiological responses in leaves. The interplay between different phytohormones (e.g., ABA, auxins, cytokinins) in the context of drought memory at the leaf level is complex and not fully understood. It is unclear how epigenetic modifications influence the dynamic balance of these hormones during repeated drought events and how these interactions are integrated to produce a coordinated response toward drought memory. Although some ncRNAs are known to be involved in drought responses, their specific roles in establishing and maintaining drought stress memory at the leaf level are not well defined.

Identifying key ncRNAs within drought memory acquisition and understanding their targets and regulatory networks in leaf tissues is an ongoing challenge. The specific changes in leaf anatomy (e.g., cuticle thickness, vascular structure), ion homeostasis (Pesacreta et al. 2021; Acharya and Pesacreta 2022) that contribute to drought stress memory are not fully understood. More research is needed to link anatomical changes with physiological and molecular responses exhibited via drought memory, and to identify how long such modifications persist and therefore lead to increased stress tolerance during subsequent droughts. Integrating metabolomic and transcriptomic studies is essential for identifying how epigenetic changes translate into stress-related metabolites and gene expression patterns that sustain stress responses and result in drought memory. These -omics approaches will help clarify the connections between epigenetic modifications, metabolic pathways, and long-term stress tolerance in plants.

Understanding drought memory in plants has become increasingly critical due to the escalating impacts of climate change. With global warming driving more frequent and severe drought events, the ability of plants to “remember” previous stress episodes and adapt accordingly is vital for ensuring their survival and productivity. In agriculture, identifying and breeding crops with enhanced drought memory traits could improve food security by enabling stable yields under water-limiting conditions. Similarly, for forest ecosystems, understanding how long-lived trees retain drought memory could inform reforestation efforts and the selection of resilient species for afforestation projects in drought-prone regions.

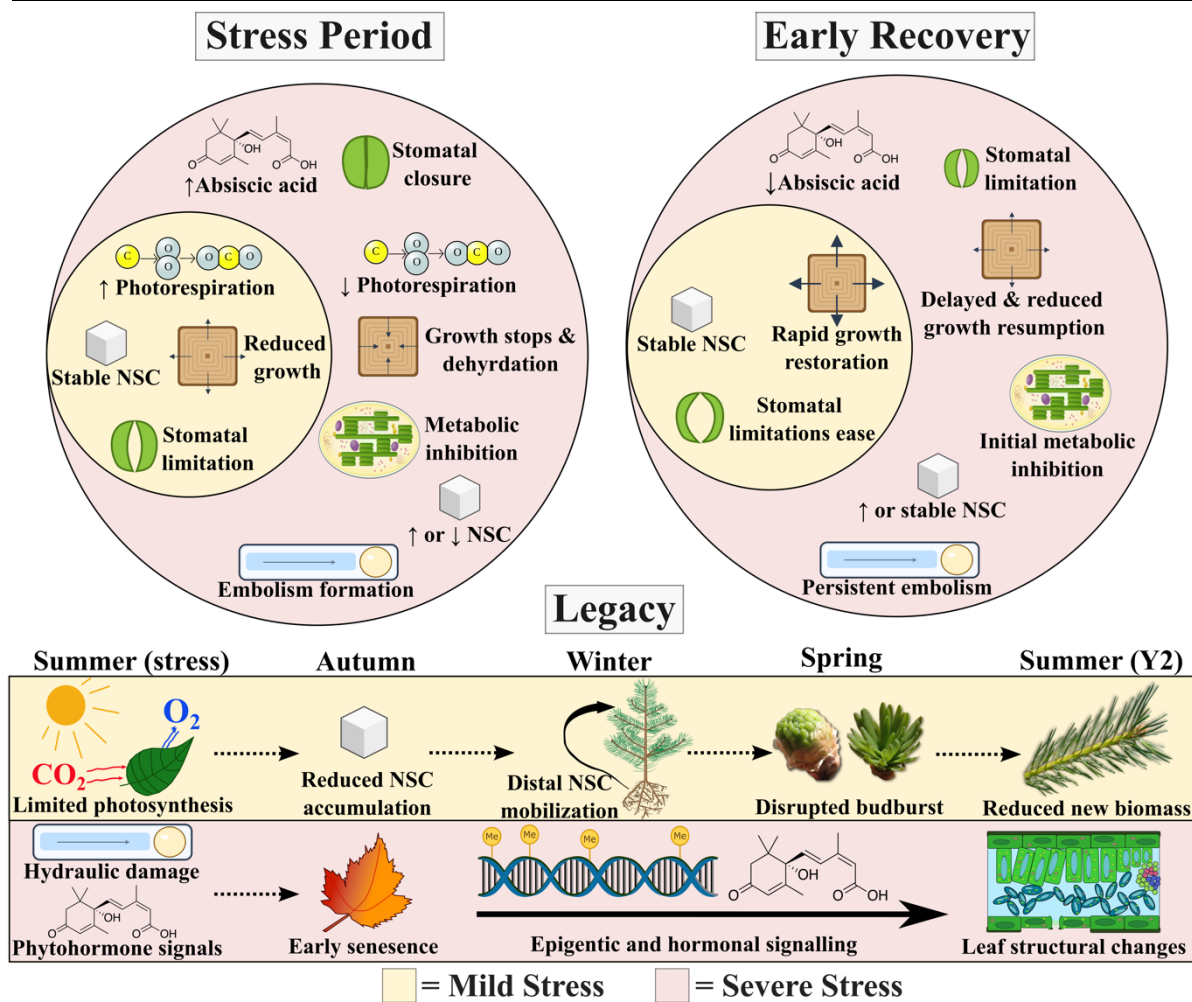


Figure 6.1: Schematic overview of the physiological processes governing the stress, recovery, and long-term legacy response. Yellow shading denotes processes occurring during or due to mild stress (defined as levels before which permanent hydraulic damage forms), while red shading denotes processes occurring during or due to severe stress (defined as levels after which permanent hydraulic damage forms).

Abiotic stress impacts tree physiology across multiple temporal scales, from short-term regulatory changes in resource acquisition and allocation, to persistent modifications which continue to alter plant function during subsequent growing seasons. Understanding forest resiliency to increasing abiotic stress requires integrating these physiological responses across time. The three experimental studies synthesized here are integrated to explore how metabolic, hydraulic, and signaling pathways interact to shape tree response during abiotic stress and recovery (Figure 6.1). Additionally, a comprehensive review of epigenetic mechanisms underlying drought stress memory (Chapter 5) provides a molecular framework for understanding how stress-induced modifications can persist beyond the immediate

recovery period, complementing the physiological processes demonstrated experimentally.

6.1 Physiological Responses to Abiotic stress

6.1.1 *Responses to mild stress*

Mild drought stress, defined as moderate soil dehydration, initiates primarily passive, stomatal-mediated adjustments that balance water conservation with continued carbon assimilation. Across all three experiments, mild drought responses reflected coordinated reductions in gas exchange without triggering significant metabolic or hormonal stress responses (Figure 6.1).

During early drought progression in silver fir (Chapter 2), soil water content declined to about 20% (half of control), corresponding to slight increases in xylem tension which remained comfortably above those associated with hydraulic damage. These slight increases in xylem tension passively decreased stomatal conductance, reducing intercellular CO₂ availability and causing a modest increase (~5%) in photorespiration as the O₂:CO₂ ratio shifted in favor of RuBP oxygenation (Ku and Edwards 1978; Wingler et al. 1999). This represented classical stomatal limitation of photosynthesis, with the photosynthetic apparatus itself remaining functional, albeit slightly less efficient. Similarly, a short-term heat exposure alone increased photorespiration by ~38% in well-watered seedlings through combined effects of reduced stomatal conductance, increased O₂ solubility relative to CO₂ at higher temperatures, and altered Rubisco substrate discrimination (Jordan and Ogren 1984; Zhang and Sharkey 2009). Although photorespiration is the main pathway for the production of the reactive oxygen species (ROS) and stress-signaling molecule H₂O₂, higher photorespiration did not induce H₂O₂ accumulation, as ROS scavenging was efficiently upregulated. This demonstrates tight enzymatic regulation that rapidly scavenges ROS even when production pathways are elevated, limiting both oxidative damage and stress signaling potential (Petrov and Van Breusegem 2012).

Similarly, Douglas fir exposed to moderate drought (Chapter 3) maintained photosynthesis and growth at reduced rates without elevating foliar ABA, indicating that passive hydraulic regulation of stomata was sufficient to conserve water without eliminating carbon uptake (McAdam and Brodribb 2014). Water potential remained near control levels, and while growth occurred at a reduced rate compared with control trees, stem expansion continued,

demonstrating that turgor conditions at this moderate drought level remained adequate for cell expansion despite reduced water availability (Körner 2015; Peters et al. 2021).

The extended mild drought in larch and pine (Chapter 4) similarly reduced photosynthesis proportionally to stomatal closure, with no evidence of non-stomatal limitations constraining gas exchange. As with silver fir in Chapter 2, hydraulic integrity was maintained at this mild drought level, as slightly increased xylem tensions remained well above cavitation thresholds throughout the 60-day drought period. Growth slowed substantially in both species, reflecting turgor limitations on cell expansion rather than complete cessation of metabolic sinks.

NSC responses under mild drought were modest and varied by tissue and species. Douglas fir under moderate stress maintained NSC concentrations similar to controls throughout the drought period (Chapter 3). In the extended mild drought (Chapter 4), bud tissues accumulated soluble sugars, likely serving osmotic adjustment and hydration maintenance functions, while branch NSC declined moderately, driven by starch depletion in larch and sugar depletion in pine. These patterns indicate that while mild drought can slightly alter NSC composition and allocation priorities, it does not trigger the dramatic accumulation or depletion characteristic of severe stress.

6.1.2 Response to severe stress

Severe stress induces a qualitative shift from passive stomatal regulation to active metabolic downregulation and hormonal signaling, accompanied by hydraulic damage and complete cessation of growth (Figure 6.1). The transition from mild to severe stress represents a physiological threshold beyond which recovery becomes substantially more complex and prolonged.

In silver fir (Chapter 2), progression to severe drought (soil water content near zero, xylem tension -1.70 MPa) fundamentally altered photosynthetic metabolism. Unlike during mild stress, severe drought *decreased* photorespiration by ~14% despite continued low stomatal conductance, as non-stomatal limitations became dominant. In support of this, electron transport rates declined substantially during severe stress, indicating impairment of the photosynthetic light reactions themselves (Flexas and Medrano 2002b; Lawlor and Tezara 2009). Thus, photosynthesis was no longer limited primarily by lower CO₂ availability from reduced stomatal conductance, but instead through an inhibited capacity to regenerate RuBP

and process absorbed radiation. Importantly, when severe drought was combined with heat stress, the heat-induced photorespiration increase observed in well-watered controls was absent, demonstrating that biochemical impairments from the severe drought override typical short-term heat responses to photosynthesis. Despite this metabolic suppression of photosynthesis from severe drought, peroxidase activity remained highly responsive to heat stress, increasing approximately 2-fold. This demonstrates that ROS scavenging capacity is maintained independently of photosynthetic function, providing resilient oxidative protection even when photosynthetic metabolism has been severely compromised.

Douglas fir under severe drought (Chapter 3) experienced xylem tensions reaching -3.8 MPa, corresponding to an estimated 70-85% loss of hydraulic conductivity (Chauvin et al. 2019). This hydraulic stress triggered a doubling of foliar ABA concentrations, which induced near-complete stomatal closure and likely contributed to active metabolic downregulation of photosynthesis (Tombesi et al. 2015). As with severe drought in Chapter 2, growth processes ceased entirely, with stems ultimately shrinking due to dehydration. During the final eight days of severe drought, trees entered net negative carbon balance as respiratory demand exceeded near-zero photosynthetic input.

The NSC dynamics under severe stress revealed critical insights about carbon economics during extreme events. Despite drastically reduced photosynthesis, stem NSC concentrations in Douglas fir *increased* rather than depleted. This accumulation likely occurred because turgor stress eliminated the primary carbon sink (cell expansion and new tissue formation) before photosynthesis stopped completely, allowing for a temporary accumulation of NSC (Hartmann and Trumbore 2016). The subsequent decline in NSC during the final week of drought, at which point study individuals were experiencing a net carbon deficit, indicates that NSC utilization occurs only when respiratory demand continues without sufficient assimilatory input. This pattern supports the interpretation that observed NSC increases during severe drought likely represents a passive consequence of sink limitation rather than an active storage strategy, and that depletion becomes a risk primarily when photosynthesis ceases for extended periods (Salmon et al. 2020; Stefaniak et al. 2024). These findings call into question the importance of carbon starvation as a primary mortality mechanism, suggesting instead that its relevance depends critically on the rate of drought progression. When soil dehydration is strong enough to halt photosynthesis but stabilizes before inducing significant xylem cavitation, similar to drought conditions achieved in Experiment 3, carbon

starvation could conceivably occur as NSC are slowly depleted by ongoing respiration. However, if soil continues to dehydrate well beyond the point of zero assimilation, which is common in rapid, severe droughts, hydraulic failure from cavitation likely represents a more immediate threat to mortality than carbon depletion (McDowell et al. 2011; Adams et al. 2017).

6.2 Drought recovery and legacy effects

Short-term recovery from drought depends critically on the severity of stress, with distinct physiological bottlenecks emerging along this gradient. While mild drought enables a relatively quick restoration of gas exchange upon rehydration, severe drought creates longer-term structural hydraulic constraints, fundamentally limiting gas exchange and growth until new sapwood formation restores hydraulic transport. Beyond these short-term recovery dynamics, moderate extended drought which limits photosynthesis while maintaining hydraulic integrity can generate carbon-mediated legacy effects, reducing subsequent-season productivity and disrupting spring phenology, with the sensitivity to these legacy effects strongly shaped by species leaf habit.

6.2.1 *Early recovery from drought*

Following mild drought in Douglas fir (Chapter 3), stomatal conductance immediately recovered to its highest seasonal levels, with intrinsic water use efficiency returning to control levels, indicating that photosynthesis and stomatal conductance increased in-step through recovery. In stark contrast, severe drought imposed stronger bottlenecks to recovery. Within two days of rewetting, both water potential and foliar ABA concentrations returned to control levels, yet stomatal conductance remained substantially depressed below pre-drought levels for approximately two weeks. This temporal decoupling demonstrates that neither water stress nor hormonal signaling limited initial gas exchange recovery as both were quickly restored, which when considering the high regulation of ROS in Chapter 2 despite severe stress combinations, demonstrates the unimpeded control of biochemical systems during and after stress.

Instead, the primary limitation of gas exchange recovery emerged from structural hydraulic constraints. Mild and severe drought progressively reduced the rate of sapwood development

during the stress period, which in the control trees was linked to the seasonal optimization in stomatal conductance. The resulting low ratio of sapwood area to leaf area (Huber value) under stress created a hydraulic supply bottleneck that persisted until new xylem formation restored transport capacity (Brodribb and Cochard 2009; Rehschuh et al. 2020). In the case of mild stress recovery, higher growth rates during and after stress facilitated a quicker recovery than under severe stress, which due to additional damage from embolism, ultimately required greater stem radial growth to achieve seasonal maxima in stomatal conductance. This strong positive relationship between Huber value and stomatal conductance throughout recovery demonstrates that new sapwood development, rather than phytohormone or NSC status, governed gas exchange restoration (Mencuccini et al. 2019; Gattmann et al. 2023).

Photosynthesis recovery, and with that the rate of carbon accumulation, was similarly coupled with increases in Huber value. As water use efficiency immediately returned to control levels following recovery from mild stress, the recovery of photosynthesis depended on new sapwood development increasing hydraulic supply to support stomatal conductance. In contrast, water use efficiency following recovery from severe stress remained below control levels during the first two weeks of recovery, indicating that non-stomatal limitations, such as those experienced under severe stress in Chapter 2 like photosystem inhibition (Lawlor and Tezara 2009), continued to limit photosynthesis. As these metabolic constraints were alleviated, the limitation to photosynthesis returned to stomatal control, which ultimately was governed by the ability to form new sapwood.

Altered diurnal growth patterns provided particularly clear evidence of persistent structural limitations. Control trees progressively developed daytime growth capacity throughout the season as sapwood area increased, with daytime radial expansion eventually accounting for ~30% of total daily growth by the end of the experimental period. The emergence of daytime growth was progressively delayed by mild and severe stress, reflecting the gradient of growth limitation which occurred during the stress period. Trees which experienced mild stress gradually increased their daytime growth capacity throughout recovery, while daytime growth remained largely absent following severe drought until the fourth week of recovery, when sapwood area eventually reached levels sufficient to buffer against daytime xylem tension increases (Zweifel et al. 2021; Ziegler et al. 2024). These results demonstrate a critical feedback loop: insufficient sapwood development during drought delays or eliminates both the seasonal maximal stomatal conductance and the ability to buffer daytime xylem

tension for turgor-dependent growth. This delayed development of stem hydraulic supply further postpones the resumption of daytime growth which would accelerate the hydraulic capacity needed for gas exchange restoration.

Importantly, carbon availability did not appear to limit recovery from severe stress. Despite reduced photosynthesis during drought, NSC concentrations remained at or above control levels throughout recovery. Growth limitations reflected hydraulic and turgor constraints rather than carbon deficits, challenging assumptions that NSC depletion constrains post-drought recovery (Palacio et al. 2014; Kannenberg and Phillips 2020).

6.2.2 *Extended recovery and drought legacy*

The extended mild drought in larch and pine (Chapter 4) isolated carbon-mediated legacy effects by substantially reducing assimilation while ensuring xylem tension remained above embolism-inducing thresholds. This study revealed how extended moderate stress generates persistent impacts on phenology and productivity through altered NSC dynamics, with the extent of legacy effects dramatically different between the deciduous and evergreen species.

Following summer drought, autumn branch NSC accumulation was reduced by >70% in *Larix decidua* despite normal autumn leaf pigment status indicating uninhibited photosynthetic capacity, suggesting increased carbon allocation to other sinks like bud development or stem radial growth. In contrast, *Pinus sylvestris* maintained normal autumn branch NSC accumulation, with enhanced leaf pigment status combined with an evergreen leaf habit facilitating sufficient photosynthesis throughout the autumn period (Moser et al. 2010). Both species, however, displayed similar drought-induced changes in winter NSC remobilization, where drought-stressed trees showed minimal over-winter branch NSC decline while controls substantially depleted reserves for respiratory demands (Hoch et al. 2003; Godfrey et al. 2020). This pattern strongly suggests that winter respiratory substrate demand in woody branch tissues was met through the import of NSC from distal storage pools, aligning with studies reporting over-winter NSC rebalancing to compensate for artificially-induced C limitation (Amico Roxas et al. 2021). By spring, *L. decidua* showed NSC deficits by mid-budburst while *P. sylvestris* largely accumulated NSC through early-season assimilation, maintaining a surplus of branch NSC content, demonstrating how leaf habit influences the delayed capacity to recover from drought-induced C-limitation.

Legacy effects manifested primarily through altered spring phenology and reduced tissue production. In *L. decidua*, budburst initiated 5 days earlier but progressed slower, and was correlated with lower branch NSC content and drought-induced winter mobilization patterns. *P. sylvestris* showed no disruption to phenology. Both species produced fewer, shorter branches with reduced foliage in the subsequent year, with more severe reductions in *L. decidua* (~50%) than *P. sylvestris* (~25-30%). These morphological reductions in biomass production were largely correlated with drought-induced changes to NSC composition and mobilization in both species, despite drought-stressed *P. sylvestris* exhibiting higher branch NSC content by mid-budburst. Critically, measures of leaf function (gas exchange, fluorescence, and pigment content) in new foliage of both species remained unaltered, suggesting that functional legacy effects are unlikely to arise through C-mediated pathways, and may instead be initiated through hydraulic or hormonal feedbacks which arise under severe drought events (McAdam and Brodribb 2014; Alongi et al. 2025).

The absence of functional trait modifications in new foliage, despite clear morphological and phenological legacy effects, supports the idea that distinct drought characteristics, such as severity and duration, activate distinct legacy mechanisms. As reviewed in Chapter 5, severe drought alters phytohormone regulation and other regulatory mechanisms like DNA methylation, histone modification, and non-coding RNAs. Epigenetic regulation of phytohormonal pathways can result in structural modifications of tissues, and could explain observations of modified tissue function in other studies (Petrik et al. 2022; Thomas et al. 2023). As the moderate extended drought imposed in Chapter 4 primarily produced carbon-mediated legacy effects, without the hormonal or epigenetic modifications that would yield tissue functional modifications.

The fitness consequences of these observed morphological shifts likely depend upon the environmental conditions in the following year. Reduced leaf area, particularly in *L. decidua*, is likely to limit the potential growing season productivity under favorable conditions, representing a fitness cost. However, in the event of recurrent drought, reductions in canopy leaf area effectively increases the sapwood: leaf area ratio (Huber value). As demonstrated in Douglas fir (Chapter 3), higher Huber values buffer xylem tension increases, maintaining greater stomatal conductance under stress, and reducing turgor-limitations to growth (Mencuccini et al. 2019; Gattmann et al. 2023), and thus could represent an increase in fitness. Similarly, increased NSC allocation observed during mid-budburst in *P. sylvestris*, if

maintained through the growing season, could represent either a greater osmotic buffering capacity in the event of drought (Mitchell et al. 2013), or conversely a loss of fitness under favorable conditions, assuming this NSC allocation increase is at the expense of new tissue development (as observed). Taken together, these observed legacy morphological adjustments trade potential growing season productivity under favorable conditions for enhanced survival in the event of recurrent stress (Zlobin et al. 2024).

These findings establish a carbon-mediated pathway for drought legacy, with deciduous species substantially more vulnerable due to a combination of limited extended-season assimilation potential and the complete reliance on stored reserves for spring development. Importantly, severe drought would likely generate different legacy mechanisms, in part because hydraulic damage requires greater new sapwood growth to restore function (Chapter 3), and also because hormonal and metabolic responses during severe dehydration may additionally induce functional tissue modifications not observed here, as discussed in Chapter 5. This interaction between drought severity, timing, and duration determines which legacy responses are likely to manifest during the subsequent growing season.

6.3 Research Advances, Limitations, and Future Directions

The studies presented in this thesis examine physiological stress responses across temporal scales, from immediate stress through recovery to subsequent-season legacy effects. However, the taxonomic scope, controlled conditions, and specific experimental designs impose constraints on the mechanistic generalizability of these results. These limitations inform directions for future work that would strengthen the mechanistic framework established here and extend it to broader ecological contexts.

6.3.1 *Key advances*

Chapter 2 demonstrated that the relative contribution of photorespiration to Rubisco activity and subsequent H₂O₂ regulation vary with drought severity, increasing under mild stress but decreasing under severe stress as metabolic limitations dominate. Despite variable production rates, tight peroxidase scavenging regulation consistently limits H₂O₂ accumulation, restricting its availability for stress signaling even under combined drought and heat stress.

Chapter 3 revealed that drought response and recovery is governed by structural hydraulic constraints rather than carbon or hormonal limitation. The ratio of sapwood area to leaf area (Huber value) emerged as the primary determinant of gas exchange and growth restoration, with drought-suppressed stem development creating a negative feedback: reduced stem sapwood development limits both maximal stomatal conductance and daytime growth capacity, delaying the hydraulic restoration needed for full recovery.

Chapter 4 established a carbon-mediated legacy pathway where moderate extended drought reduces subsequent-year tissue production without altering tissue function. Legacy magnitude differed substantially by leaf habit (~50% reduction in deciduous versus ~25% in evergreen species), providing a trait-based framework that links the dependence on stored reserves and capacity for extended-season assimilation to legacy vulnerability.

Chapter 5 provides a comprehensive review of epigenetic mechanisms underlying drought stress memory, synthesizing current knowledge of how DNA methylation, histone modifications, and non-coding RNAs interact with phytohormonal signaling to mediate persistent physiological changes. This review establishes a molecular framework for interpreting legacy effects and identifies critical knowledge gaps regarding the roles of these mechanisms in perennial woody species.

6.3.2 Limitations

Several general limitations constrain the interpretation and generalizability of these findings. All experiments utilized gymnosperm species with isohydric stomatal regulation and tracheid-based xylem anatomy, which substantially differ from angiosperm vessel-based anatomy in hydraulic vulnerability, embolism repair capacity, and parenchyma abundance (Morris et al. 2016; Choat et al. 2019). Whether the hydraulic constraints and recovery mechanisms identified here apply more broadly to anisohydric and broadleaf species remains uncertain. Additionally, pot-based experiments eliminate the possibility of root expansion to access deeper soil water, accelerating soil dehydration rates and inducing artificially rapid stress progression. This limitation particularly is relevant when interpreting results from Chapters 2 and 3, where severe drought developed over 25-28 days, whereas in field conditions similar water deficits likely develop more gradually. A more gradual drought progression would likely alter the balance between metabolic (such as hormonal regulation, growth, and NSC regulation) and hydraulic (embolism) responses.

Experiment-specific limitations further constrain mechanistic interpretation. The brief six-hour heat treatment in Chapter 2 demonstrated robust ROS scavenging enzyme upregulation but does not assess the durability of this response. Extended heat stress may eventually overwhelm scavenging enzyme production, leading to H₂O₂ accumulation not observed here (Foster et al. 2015).

In Chapter 3, the separation of destructive measurements (NSC, ABA, water potential) from continuous gas exchange monitoring limits direct temporal comparison between these processes, introducing uncertainty about the precise timing of hormonal recovery relative to physiological function. Furthermore, drought seasonality likely exerted a strong influence on our results. Specifically, the drought period in Chapter 3 occurred before the seasonal development of sufficient sapwood area necessary to support optimal gas exchange, leading to the discussed observation that drought-induced restrictions to hydraulic development determined recovery capacity. If drought were to occur following the development of sufficient sapwood area, trees would likely have a higher hydraulic capacity to buffer against reductions in gas exchange and growth, thereby enabling quicker recovery. Nonetheless, these results elevate the notion that early season droughts are particularly detrimental to tree function.

Chapter 4's focus on carbon-mediated legacies explicitly avoided the hormonal and hydraulic stresses characteristic of severe drought, precluding conclusions about how embolism-induced hydraulic damage or phytohormonal regulation might generate alternative legacy pathways. Furthermore, the comparison of only one deciduous species (*Larix decidua*) and one evergreen species (*Pinus sylvestris*) limits the generalizability of the discussed leaf habit framework. While the stark contrast in legacy response between these species suggests a strong influence of leaf habit in carbon-mediated legacy expression, establishing this mechanism robustly requires testing across multiple deciduous and evergreen species to distinguish leaf habit effects from species-specific physiological strategies.

6.3.3 Future directions

The limitations identified above inform the following areas for future research:

First, expanding the taxonomic scope to include angiosperm species with contrasting hydraulic strategies is essential for testing framework generalizability. Comparative studies

should particularly examine species with anisohydric stomatal regulation and vessel-based xylem to determine whether hydraulic supply constraints universally dominate recovery or represent a conifer-specific response, and whether carbon-mediated legacy pathways operate similarly in species which maintain photosynthetic capacity (i.e. anisohydric species) for longer during drought.

Second, field-based drought manipulations that allow natural root expansion and gradual soil dehydration would clarify whether the rapid stress progression in pot experiments alters the balance between metabolic regulation and the occurrence of hydraulic damage. Such studies could test whether slower drought development enables trees to mount compensatory responses (e.g., greater osmotic adjustment, root growth) that modify the severity thresholds identified here.

Third, multi-species comparisons within leaf habit categories (multiple deciduous and evergreen species) are needed to distinguish leaf habit-based responses from species-specific strategies. This would establish whether the leaf habit framework for legacy vulnerability presented here is robust, or instead reflects individual species differences between *Larix decidua* and *Pinus sylvestris*.

Fourth, experiments manipulating both drought severity and duration would elucidate how more severe stress responses (hormonal signaling and epigenetic modifications) versus carbon limitation from an extended moderate drought interact to mediate legacy effects in subsequent growing seasons. This approach could reveal whether functional trait modifications observed in other studies (reduced SLA, altered stomatal conductance) emerge through pathways distinct from the carbon-mediated responses documented here.

Fifth, direct investigation of epigenetic mechanisms would determine whether DNA methylation, histone modifications, or non-coding RNA expression are altered by drought and persist into subsequent growing seasons. As reviewed in Chapter 5, such mechanisms have been characterized primarily in model species and annual crops, with their relevance for long-lived woody perennials remaining uncertain. Experiments combining physiological measurements with epigenetic profiling (e.g., bisulfite sequencing, chromatin immunoprecipitation) could test whether the carbon-mediated legacy effects documented here operate independently of epigenetic regulation. Such investigation would clarify whether

different legacy effects (functional trait modifications versus phenological shifts versus productivity reductions) are mediated by distinct molecular mechanisms.

Finally, experiments spanning multiple drought cycles and growing seasons would assess the persistence of legacy effects, test whether legacy effects increase future drought resilience or represent a loss of fitness, and determine recovery timescales.

6.4 Conclusions

The findings of this thesis significantly contribute to expanding knowledge on the severity-dependent physiological mechanisms governing tree stress responses, recovery dynamics, and legacy effects. Since vegetation models continue to overestimate post-drought recovery (Anderegg et al. 2015) and lack mechanistic representation of severity-dependent physiological processes (Merganičová et al. 2019), the results presented here can improve stress and legacy modeling. The controlled greenhouse experiments enabled precise quantification of how drought severity activates distinct physiological mechanisms, from passive stomatal regulation under mild stress to active metabolic downregulation and hydraulic damage under severe stress.

The thesis demonstrated that mild drought maintains hydraulic integrity and metabolic function, enabling relatively quick recovery once water availability is restored. In contrast, severe drought induces qualitative shifts including ABA-mediated stomatal closure, non-stomatal metabolic limitations of photosynthesis, and xylem cavitation, creating structural hydraulic constraints that persist until new sapwood formation restores transport capacity. The ratio of sapwood area to leaf area (Huber value) emerged as the primary determinant of recovery potential, with drought-suppressed stem development creating negative feedbacks that delay both gas exchange restoration and the seasonal emergence of daytime growth. Carbon availability did not appear to limit short-term recovery from severe drought, challenging assumptions that NSC depletion constrains post-drought function. However, extended moderate drought that limits photosynthesis while maintaining hydraulic integrity was found to generate carbon-mediated legacy effects, reducing subsequent-season tissue production through altered NSC dynamics and seasonal remobilization patterns. Legacy magnitude differed substantially by leaf habit, with the deciduous species showing approximately twice the productivity reduction of the evergreen species, indicating that

reliance on stored reserves versus capacity for extended-season assimilation influences vulnerability to carbon legacies.

In summary, the outlined findings as well as limitations give rise to the following areas for future research to provide a more comprehensive picture of tree stress responses and recovery:

- Taxonomic expansion to angiosperm species with contrasting hydraulic strategies (anisohydric regulation, vessel-based xylem) and different carbon allocation patterns
- Field-based drought manipulations with natural root expansion and gradual soil dehydration to test whether controlled experiment constraints alter mechanism activation thresholds
- Integration of epigenetic profiling (DNA methylation, histone modifications, non-coding RNA) with physiological measurements to determine molecular mechanisms underlying legacy effects
- Multi-year experiments tracking legacy persistence, fitness consequences, and responses to recurrent drought cycles across multiple growing seasons

7 References

Abdulraheem, Mukhtar Iderawumi, Yani Xiong, Abiodun Yusuff Moshood, Gregorio Cadenas-Pliego, Hao Zhang, and Jiandong Hu. 2024. "Mechanisms of Plant Epigenetic Regulation in Response to Plant Stress: Recent Discoveries and Implications." *Plants* 13 (2): 163. <https://doi.org/10.3390/plants13020163>.

Abid, Muhammad, Zhongwei Tian, Syed Tahir Ata-Ul-Karim, et al. 2016. "Improved Tolerance to Post-Anthesis Drought Stress by Pre-Drought Priming at Vegetative Stages in Drought-Tolerant and -Sensitive Wheat Cultivars." *Plant Physiology and Biochemistry* 106 (September): 218–27. <https://doi.org/10.1016/j.plaphy.2016.05.003>.

Abogadallah, Gaber M. 2011. "Differential Regulation of Photorespiratory Gene Expression by Moderate and Severe Salt and Drought Stress in Relation to Oxidative Stress." *Plant Science* 180 (3): 540–47. <https://doi.org/10.1016/j.plantsci.2010.12.004>.

Acharya, Aniruddha, and Thomas C. Pesacreta. 2022. "Localization of Seed-Derived and Externally Supplied Nutrients in Peanut Seedling Root." *Theoretical and Experimental Plant Physiology* 34 (1): 37–51. <https://doi.org/10.1007/s40626-021-00227-9>.

Adams, Henry D., Melanie J. B. Zeppel, William R. L. Anderegg, et al. 2017. "A Multi-Species Synthesis of Physiological Mechanisms in Drought-Induced Tree Mortality." *Nature Ecology & Evolution* 1 (9): 9. <https://doi.org/10.1038/s41559-017-0248-x>.

Ahmad, Bilal, Mohammad Mukarram, Sadaf Choudhary, Peter Petrik, Tariq Ahmad Dar, and M. Masroor A. Khan. 2024. "Adaptive Responses of Nitric Oxide (NO) and Its Intricate Dialogue with Phytohormones during Salinity Stress." *Plant Physiology and Biochemistry* 208 (March): 108504. <https://doi.org/10.1016/j.plaphy.2024.108504>.

Ahmad, Parvaiz, Saiema Rasool, Alvina Gul, et al. 2016. "Jasmonates: Multifunctional Roles in Stress Tolerance." *Frontiers in Plant Science* 7 (June). <https://doi.org/10.3389/fpls.2016.00813>.

Alam, Md. Mahabub, Kamrun Nahar, Mirza Hasanuzzaman, and Masayuki Fujita. 2014. "Exogenous Jasmonic Acid Modulates the Physiology, Antioxidant Defense and Glyoxalase Systems in Imparting Drought Stress Tolerance in Different Brassica Species." *Plant Biotechnology Reports* 8 (3): 279–93. <https://doi.org/10.1007/s11816-014-0321-8>.

Ali, Md Sarafat, and Kwang-Hyun Baek. 2020. "Jasmonic Acid Signaling Pathway in Response to Abiotic Stresses in Plants." *International Journal of Molecular Sciences* 21 (2): 621. <https://doi.org/10.3390/ijms21020621>.

Allen, Craig D., Alison K. Macalady, Haroun Chenchouni, et al. 2010. "A Global Overview of Drought and Heat-Induced Tree Mortality Reveals Emerging Climate Change Risks for Forests." *Forest Ecology and Management*, Adaptation of Forests and Forest Management to Changing Climate, vol. 259 (4): 660–84. <https://doi.org/10.1016/j.foreco.2009.09.001>.

Alongi, Franklin, Anja Petek-Petrik, Mohammad Mukarram, Hülya Torun, Bernhard Schuldt, and Peter Petrik. 2025. "Somatic Drought Stress Memory Affects Leaf Morpho-Physiological Traits of Plants via Epigenetic Mechanisms and Phytohormonal Signalling." *Plant Gene* 42 (June): 100509. <https://doi.org/10.1016/j.plgene.2025.100509>.

Alongi, Franklin, Peter Petrik, and Nadine K Ruehr. 2024. "Drought and Heat Stress Interactions Modify Photorespiration and Hydrogen Peroxide Content in Silver Fir." *Tree Physiology*, September 27, tpae126. <https://doi.org/10.1093/treephys/tpae126>.

Alves de Freitas Guedes, Fernanda, Paulo Eduardo Menezes-Silva, Fábio Murilo DaMatta, and Márcio Alves-Ferreira. 2019. "Using Transcriptomics to Assess Plant Stress Memory." *Theoretical and Experimental Plant Physiology* 31 (1): 47–58. <https://doi.org/10.1007/s40626-018-0135-0>.

Alves, Rauander D. F. B., Paulo E. Menezes-Silva, Letícia F. Sousa, et al. 2020. "Evidence of Drought Memory in Dipteryx Alata Indicates Differential Acclimation of Plants to Savanna Conditions." *Scientific Reports* 10 (1): 16455. <https://doi.org/10.1038/s41598-020-73423-3>.

Amico Roxas, Adele, Jessica Orozco, Paula Guzmán-Delgado, and Maciej A Zwieniecki. 2021. "Spring Phenology Is Affected by Fall Non-Structural Carbohydrate Concentration and Winter Sugar Redistribution in Three Mediterranean Nut Tree Species." *Tree Physiology* 41 (8): 1425–38. <https://doi.org/10.1093/treephys/tpab014>.

Amini, Azadeh, Mohammad Mahdi Majidi, Niloofar Mokhtari, and Mehdi Ghanavati. 2023. "Drought Stress Memory in a Germplasm of Synthetic and Common Wheat: Antioxidant System, Physiological and Morphological Consequences." *Scientific Reports* 13 (1): 8569. <https://doi.org/10.1038/s41598-023-35642-2>.

Anderegg, W. R. L., C. Schwalm, F. Biondi, et al. 2015. "Pervasive Drought Legacies in Forest Ecosystems and Their Implications for Carbon Cycle Models." *Science* 349 (6247): 528–32. <https://doi.org/10.1126/science.aab1833>.

Antunović Dunić, Jasenka, Selma Mlinarić, Iva Pavlović, Hrvoje Lepeduš, and Branka Salopek-Sondi. 2023. "Comparative Analysis of Primary Photosynthetic Reactions Assessed by OJIP Kinetics in Three Brassica Crops after Drought and Recovery." *Applied Sciences* 13 (5): 3078. <https://doi.org/10.3390/app13053078>.

Anwar, Sidra, Eric Brenya, Yagiz Alagoz, and Christopher I. Cazzonelli. 2021. "Epigenetic Control of Carotenogenesis During Plant Development." *Critical Reviews in Plant Sciences* 40 (1): 23–48. <https://doi.org/10.1080/07352689.2020.1866829>.

Arend, Matthias, Roman Mathias Link, Cedric Zahnd, Günter Hoch, Bernhard Schuldt, and Ansgar Kahmen. 2022. "Lack of Hydraulic Recovery as a Cause of Post-Drought Foliage Reduction and Canopy Decline in European Beech." *New Phytologist* 234 (4): 1195–205. <https://doi.org/10.1111/nph.18065>.

Arend, Matthias, Krunoslav Sever, Ellen Pflug, Arthur Gessler, and Marcus Schaub. 2016. "Seasonal Photosynthetic Response of European Beech to Severe Summer Drought: Limitation, Recovery and Post-Drought Stimulation." *Agricultural and Forest Meteorology* 220 (April): 83–89. <https://doi.org/10.1016/j.agrformet.2016.01.011>.

Asargew, Mihretie Fekremariam, Yuji Masutomi, Kazuhiko Kobayashi, and Mitsuko Aono. 2024. "Water Stress Changes the Relationship between Photosynthesis and Stomatal Conductance." *Science of The Total Environment* 907 (January): 167886. <https://doi.org/10.1016/j.scitotenv.2023.167886>.

Auler, Priscila Ariane, Gustavo Maia Souza, Marcela Regina Gonçalves da Silva Engela, et al. 2021. "Stress Memory of Physiological, Biochemical and Metabolomic Responses in Two Different Rice Genotypes under Drought Stress: The Scale Matters." *Plant Science* 311 (October): 110994. <https://doi.org/10.1016/j.plantsci.2021.110994>.

Avramova, Zoya. 2015. "Transcriptional 'Memory' of a Stress: Transient Chromatin and Memory (Epigenetic) Marks at Stress-Response Genes." *The Plant Journal* 83 (1): 149–59. <https://doi.org/10.1111/tpj.12832>.

Avramova, Zoya. 2017. "The Jasmonic Acid-Signalling and Abscisic Acid-Signalling Pathways Cross Talk during One, but Not Repeated, Dehydration Stress: A Non-Specific 'Panicky' or a Meaningful Response?" *Plant, Cell & Environment* 40 (9): 1704–10. <https://doi.org/10.1111/pce.12967>.

Avramova, Zoya. 2019. "Defence-Related Priming and Responses to Recurring Drought: Two Manifestations of Plant Transcriptional Memory Mediated by the ABA and JA Signalling Pathways." *Plant, Cell & Environment* 42 (3): 983–97. <https://doi.org/10.1111/pce.13458>.

Baćurin, Marko, Ida Katičić Bogdan, Krunoslav Sever, and Saša Bogdan. 2025. "The Effects of Drought Timing on Height Growth and Leaf Phenology in Pedunculate Oak (*Quercus Robur L.*)." *Forests* 16 (3): 3. <https://doi.org/10.3390/f16030397>.

Bai, J., D. H. Xu, H. M. Kang, K. Chen, and G. Wang. 2008. "Photoprotective Function of Photorespiration in *Reaumuria Soongorica* during Different Levels of Drought Stress in Natural High Irradiance." *Photosynthetica* 46 (2): 232–37. <https://doi.org/10.1007/s11099-008-0037-5>.

Balao, F., O. Paun, and C. Alonso. 2018. "Uncovering the Contribution of Epigenetics to Plant Phenotypic Variation in Mediterranean Ecosystems." *Plant Biology* 20 (S1): 38–49. <https://doi.org/10.1111/plb.12594>.

Balyan, Sonia, Shivani Kansal, Ringyao Jajo, Pratyush Rajiv Behere, Rishika Chatterjee, and Saurabh Raghuvanshi. 2023. "Delineating the Tissue-Mediated Drought Stress Governed Tuning of Conserved miR408 and Its Targets in Rice." *Functional & Integrative Genomics* 23 (2): 187. <https://doi.org/10.1007/s10142-023-01111-2>.

Bambach, Nicolas, Kyaw Tha Paw U, and Matthew E Gilbert. 2020. "A Dynamic Model of RuBP-Regeneration Limited Photosynthesis Accounting for Photoinhibition, Heat and Water Stress." *Agricultural and Forest Meteorology* 285–286 (May): 107911. <https://doi.org/10.1016/j.agrformet.2020.107911>.

Banerjee, Aditya, and Aryadeep Roychoudhury. 2017. "Epigenetic Regulation during Salinity and Drought Stress in Plants: Histone Modifications and DNA Methylation." *Plant Gene*, Abiotic stress tolerance in plants: growth regulators and transcriptional control of multiple signaling pathways, vol. 11 (September): 199–204. <https://doi.org/10.1016/j.plgene.2017.05.011>.

Bates, Douglas, Martin Mächler, Ben Bolker, and Steve Walker. 2014. "Fitting Linear Mixed-Effects Models Using Lme4." *arXiv:1406.5823 [Stat]*, June 23. <http://arxiv.org/abs/1406.5823>.

Batista-Silva, Willian, Júlia de Paiva Gonçalves, Joao Antônio Siqueira, et al. 2024. "Auxin Metabolism and the Modulation of Plant Growth." *Environmental and Experimental Botany* 226 (October): 105917. <https://doi.org/10.1016/j.envexpbot.2024.105917>.

Bauwe, Hermann, Martin Hagemann, and Alisdair R. Fernie. 2010. "Photorespiration: Players, Partners and Origin." *Trends in Plant Science* 15 (6): 330–36. <https://doi.org/10.1016/j.tplants.2010.03.006>.

Ben Abdallah, Mariem, Kawther Methenni, Issam Nouairi, Mokhtar Zarrouk, and Nabil Ben Youssef. 2017. “Drought Priming Improves Subsequent More Severe Drought in a Drought-Sensitive Cultivar of Olive Cv. *Chétoui*.” *Scientia Horticulturae* 221 (July): 43–52. <https://doi.org/10.1016/j.scienta.2017.04.021>.

Birami, Benjamin, Thomas Nägele, Marielle Gattmann, et al. 2020. “Hot Drought Reduces the Effects of Elevated CO₂ on Tree Water-Use Efficiency and Carbon Metabolism.” *New Phytologist* 226 (6): 1607–21. <https://doi.org/10.1111/nph.16471>.

Blumstein, Meghan, Jessica Gersony, Jordi Martínez-Vilalta, and Anna Sala. 2023. “Global Variation in Nonstructural Carbohydrate Stores in Response to Climate.” *Global Change Biology* 29 (7): 1854–69. <https://doi.org/10.1111/gcb.16573>.

Blumstein, Meghan, Miranda Oseguera, Theresa Caso-McHugh, and David L. Des Marais. 2024. “Nonstructural Carbohydrate Dynamics’ Relationship to Leaf Development under Varying Environments.” *New Phytologist* 241 (1): 102–13. <https://doi.org/10.1111/nph.19333>.

Bracher, Andreas, Spencer M. Whitney, F. Ulrich Hartl, and Manajit Hayer-Hartl. 2017. “Biogenesis and Metabolic Maintenance of Rubisco.” *Annual Review of Plant Biology* 68 (April): 29–60. <https://doi.org/10.1146/annurev-applant-043015-111633>.

Bright, Jo, Radhika Desikan, John T. Hancock, Iain S. Weir, and Steven J. Neill. 2006. “ABA-Induced NO Generation and Stomatal Closure in *Arabidopsis* Are Dependent on H₂O₂ Synthesis.” *The Plant Journal* 45 (1): 113–22. <https://doi.org/10.1111/j.1365-313X.2005.02615.x>.

Brito, Cátia, Lia-Tânia Dinis, Mónica Meijón, et al. 2018. “Salicylic Acid Modulates Olive Tree Physiological and Growth Responses to Drought and Rewatering Events in a Dose Dependent Manner.” *Journal of Plant Physiology* 230 (November): 21–32. <https://doi.org/10.1016/j.jplph.2018.08.004>.

Brodrribb, Tim J., and Hervé Cochard. 2009. “Hydraulic Failure Defines the Recovery and Point of Death in Water-Stressed Conifers.” *Plant Physiology* 149 (1): 575–84. <https://doi.org/10.1104/pp.108.129783>.

Brodrribb, Timothy J., and Scott A. M. McAdam. 2013. “Abscisic Acid Mediates a Divergence in the Drought Response of Two Conifers.” *Plant Physiology* 162 (3): 1370–77. <https://doi.org/10.1104/pp.113.217877>.

Butt, Edward W., Jessica C. A. Baker, Francisco G. Silva Bezerra, Celso von Randow, Ana P. D. Aguiar, and Dominick V. Spracklen. 2023. “Amazon Deforestation Causes Strong Regional Warming.” *Proceedings of the National Academy of Sciences* 120 (45): e2309123120. <https://doi.org/10.1073/pnas.2309123120>.

Carthew, Richard W., and Erik J. Sontheimer. 2009. “Origins and Mechanisms of miRNAs and siRNAs.” *Cell* 136 (4): 642–55. <https://doi.org/10.1016/j.cell.2009.01.035>.

Carvalho, Fabricio E. L., and Joaquim A. G. Silveira. 2020. “Chapter 4 - H₂O₂-Retrograde Signaling as a Pivotal Mechanism to Understand Priming and Cross Stress Tolerance in Plants.” In *Priming-Mediated Stress and Cross-Stress Tolerance in Crop Plants*, edited by Mohammad Anwar Hossain, Fulai Liu, David J. Burritt, Masayuki Fujita, and Bingru Huang. Academic Press. <https://doi.org/10.1016/B978-0-12-817892-8.00004-0>.

Carvalho, V., M. Gaspar, and C. C. Nievola. 2024. “Drought Memory in *Acanthostachys Strobilacea*, a CAM Epiphytic Bromeliad.” *Plant Biology* 26 (2): 188–96. <https://doi.org/10.1111/plb.13605>.

Castel, Stephane E., and Robert A. Martienssen. 2013. “RNA Interference in the Nucleus: Roles for Small RNAs in Transcription, Epigenetics and Beyond.” *Nature Reviews Genetics* 14 (2): 100–112. <https://doi.org/10.1038/nrg3355>.

Čehulić, Ivica, Krunoslav Sever, Ida Katičić Bogdan, Anamarija Jazbec, Željko Škvorc, and Saša Bogdan. 2019. “Drought Impact on Leaf Phenology and Spring Frost Susceptibility in a *Quercus Robur L.* Provenance Trial.” *Forests* 10 (1): 1. <https://doi.org/10.3390/f10010050>.

Chakraborty, Sourav, Amy L. Hill, Gautam Shirsekar, et al. 2016. “Quantification of Hydrogen Peroxide in Plant Tissues Using Amplex Red.” *Methods, Current Methods to unravel Reactive Oxygen Species (ROS) Biology*, vol. 109 (October): 105–13. <https://doi.org/10.1016/j.ymeth.2016.07.016>.

Chauvin, Thibaud, Hervé Cochard, Vincent Segura, and Philippe Rozenberg. 2019. “Native-Source Climate Determines the Douglas-Fir Potential of Adaptation to Drought.” *Forest Ecology and Management* 444 (July): 9–20. <https://doi.org/10.1016/j.foreco.2019.03.054>.

Chen, Changming, Yael Galon, Maryam Rahmati Ishka, et al. 2021. “ASCORBATE PEROXIDASE6 Delays the Onset of Age-Dependent Leaf Senescence.” *Plant Physiology* 185 (2): 441–56. <https://doi.org/10.1093/plphys/kiaa031>.

Chen, Mingjie, Xiaofang Zhu, Yí Zhang, et al. 2020. “Drought Stress Modify Cuticle of Tender Tea Leaf and Mature Leaf for Transpiration Barrier Enhancement through Common and Distinct Modes.” *Scientific Reports* 10 (1): 6696. <https://doi.org/10.1038/s41598-020-63683-4>.

Chen, Ying, Jiguang Feng, Xia Yuan, and Biao Zhu. 2020. “Effects of Warming on Carbon and Nitrogen Cycling in Alpine Grassland Ecosystems on the Tibetan Plateau: A Meta-Analysis.” *Geoderma* 370 (July): 114363. <https://doi.org/10.1016/j.geoderma.2020.114363>.

Chen, Zhaoyu, Yadi Chen, Lanxi Shi, Li Wang, and Weixing Li. 2023. "Interaction of Phytohormones and External Environmental Factors in the Regulation of the Bud Dormancy in Woody Plants." *International Journal of Molecular Sciences* 24 (24): 24. <https://doi.org/10.3390/ijms242417200>.

Chinnusamy, Viswanathan, and Jian-Kang Zhu. 2009. "Epigenetic Regulation of Stress Responses in Plants." *Current Opinion in Plant Biology*, Genome Studies and Molecular Genetics, vol. 12 (2): 133–39. <https://doi.org/10.1016/j.pbi.2008.12.006>.

Choat, Brendan, Markus Nolf, Rosana Lopez, et al. 2019. "Non-Invasive Imaging Shows No Evidence of Embolism Repair after Drought in Tree Species of Two Genera." *Tree Physiology* 39 (1): 113–21. <https://doi.org/10.1093/treephys/tpy093>.

Contreras-Cubas, Cecilia, Miguel Palomar, Mario Arteaga-Vázquez, José Luis Reyes, and Alejandra A. Covarrubias. 2012. "Non-Coding RNAs in the Plant Response to Abiotic Stress." *Planta* 236 (4): 943–58. <https://doi.org/10.1007/s00425-012-1693-z>.

Cornic, Gabriel, and Jean-Marie Briantais. 1991. "Partitioning of Photosynthetic Electron Flow between CO₂ and O₂ Reduction in a C3 Leaf (*Phaseolus Vulgaris L.*) at Different CO₂ Concentrations and during Drought Stress." *Planta* 183 (2): 178–84. <https://doi.org/10.1007/BF00197786>.

Corot, Adrien, Hanaé Roman, Odile Douillet, et al. 2017. "Cytokinins and Abscisic Acid Act Antagonistically in the Regulation of the Bud Outgrowth Pattern by Light Intensity." *Frontiers in Plant Science* 8 (October). <https://doi.org/10.3389/fpls.2017.01724>.

Cortleven, Anne, Ingke Marg, Maria V Yamburenko, et al. 2016. "Cytokinin Regulates the Etioplast-Chloroplast Transition through the Two-Component Signaling System and Activation of Chloroplast-Related Genes." *Plant Physiology* 172 (1): 464–78. <https://doi.org/10.1104/pp.16.00640>.

Cotrina Cabello, Guillermo Gomer, Alfonso Ruiz Rodriguez, Aqarab Husnain Gondal, et al. 2023. "Plant Adaptability to Climate Change and Drought Stress for Crop Growth and Production." *CABI Reviews* 2023 (January). <https://doi.org/10.1079/cabireviews.2023.0004>.

Damkjær, Jakob T., Sami Kereicke, Matthew P. Johnson, et al. 2009. "The Photosystem II Light-Harvesting Protein Lhcb3 Affects the Macrostructure of Photosystem II and the Rate of State Transitions in *Arabidopsis*." *The Plant Cell* 21 (10): 3245–56. <https://doi.org/10.1105/tpc.108.064006>.

Daszkowska-Golec, Agata. 2016. "The Role of Abscisic Acid in Drought Stress: How ABA Helps Plants to Cope with Drought Stress." In *Drought Stress Tolerance in Plants, Vol 2: Molecular and Genetic Perspectives*, edited by Mohammad Anwar Hossain, Shabir Hussain Wani, Soumen Bhattacharjee, David J Burritt, and Lam-Son Phan Tran. Springer International Publishing. https://doi.org/10.1007/978-3-319-32423-4_5.

Dewar, Roderick, Teemu Hölttä, and Yann Salmon. 2022. "Exploring Optimal Stomatal Control under Alternative Hypotheses for the Regulation of Plant Sources and Sinks." *New Phytologist* 233 (2): 639–54. <https://doi.org/10.1111/nph.17795>.

Dias, M. C., and W. Brüggemann. 2010. "Limitations of Photosynthesis in *Phaseolus Vulgaris* under Drought Stress: Gas Exchange, Chlorophyll Fluorescence and Calvin Cycle Enzymes." *Photosynthetica* 48 (1): 96–102. <https://doi.org/10.1007/s11099-010-0013-8>.

Dimopoulos, Nicolas, Ricco Tindjau, Darren C J Wong, et al. 2020. "Drought Stress Modulates Cuticular Wax Composition of the Grape Berry." *Journal of Experimental Botany* 71 (10): 3126–41. <https://doi.org/10.1093/jxb/eraa046>.

Ding, Yong, Ning Liu, Laetitia Virlouvet, Jean-Jack Riethoven, Michael Fromm, and Zoya Avramova. 2013. "Four Distinct Types of Dehydration Stress Memory Genes in *Arabidopsis Thaliana*." *BMC Plant Biology* 13 (1): 229. <https://doi.org/10.1186/1471-2229-13-229>.

Ding, Yong, Laetitia Virlouvet, Ning Liu, Jean-Jack Riethoven, Michael Fromm, and Zoya Avramova. 2014. "Dehydration Stress Memory Genes of *Zea Mays*; Comparison with *Arabidopsis Thaliana*." *BMC Plant Biology* 14 (1): 141. <https://doi.org/10.1186/1471-2229-14-141>.

Ditmarová, Lubica, Daniel Kurjak, Sari Palmroth, Jaroslav Kmet', and Katarína Strelcová. 2010. "Physiological Responses of Norway Spruce (*Picea Abies*) Seedlings to Drought Stress." *Tree Physiology* 30 (2): 205–13. <https://doi.org/10.1093/treephys/tpy116>.

Dixit, Aalap, Thomas Kolb, and Owen Burney. 2020. "Provenance Geographical and Climatic Characteristics Influence Budburst Phenology of Southwestern Ponderosa Pine Seedlings." *Forests* 11 (10): 1067. <https://doi.org/10.3390/f11101067>.

Doehlert, Douglas C., and Richard B. Walker. 1981. "Photosynthesis and Photorespiration in Douglas-Fir as Influenced by Irradiance, CO₂ Concentration, and Temperature." *Forest Science* 27 (4): 641–50. <https://doi.org/10.1093/forestscience/27.4.641>.

Doheny-Adams, Timothy, Lee Hunt, Peter J. Franks, David J. Beerling, and Julie E. Gray. 2012. "Genetic Manipulation of Stomatal Density Influences Stomatal Size, Plant Growth and Tolerance to Restricted Water Supply across a Growth Carbon Dioxide Gradient." *Philosophical Transactions of the Royal Society B: Biological Sciences* 367 (1588): 547–55. <https://doi.org/10.1098/rstb.2011.0272>.

Drenovsky, Rebecca E., Nicole Pietrasik, and Thomas H. Short. 2019. "Global Temporal Patterns in Plant Nutrient Resorption Plasticity." *Global Ecology and Biogeography* 28 (6): 728–43. <https://doi.org/10.1111/geb.12885>.

Duan, Honglang, Defu Wang, Xiaohua Wei, et al. 2020. "The Decoupling between Gas Exchange and Water Potential of *Cinnamomum Camphora* Seedlings during Drought Recovery and Its Relation to ABA Accumulation in Leaves." *Journal of Plant Ecology* 13 (6): 683–92. <https://doi.org/10.1093/jpe/rtaa056>.

Duan, Hui, and Mary A. Schuler. 2005. "Differential Expression and Evolution of the *Arabidopsis* CYP86A Subfamily." *Plant Physiology* 137 (3): 1067–81. <https://doi.org/10.1104/pp.104.055715>.

Efroni, Idan, Soon-Ki Han, Hye Jin Kim, et al. 2013. "Regulation of Leaf Maturation by Chromatin-Mediated Modulation of Cytokinin Responses." *Developmental Cell* 24 (4): 438–45. <https://doi.org/10.1016/j.devcel.2013.01.019>.

Eisenach, Cornelia, Zhong-Hua Chen, Christopher Grefen, and Michael R. Blatt. 2012. "The Trafficking Protein SYP121 of *Arabidopsis* Connects Programmed Stomatal Closure and K⁺ Channel Activity with Vegetative Growth." *The Plant Journal* 69 (2): 241–51. <https://doi.org/10.1111/j.1365-313X.2011.04786.x>.

Estiarte, Marc, and Josep Peñuelas. 2015. "Alteration of the Phenology of Leaf Senescence and Fall in Winter Deciduous Species by Climate Change: Effects on Nutrient Proficiency." *Global Change Biology* 21 (3): 1005–17. <https://doi.org/10.1111/gcb.12804>.

Fan, Lei, Jean-Pierre Wigneron, Philippe Ciais, et al. 2023. "Siberian Carbon Sink Reduced by Forest Disturbances." *Nature Geoscience* 16 (1): 56–62. <https://doi.org/10.1038/s41561-022-01087-x>.

Fan, Qi-Jun, and Ji-Hong Liu. 2012. "Nitric Oxide Is Involved in Dehydration/Drought Tolerance in *Poncirus trifoliata* Seedlings through Regulation of Antioxidant Systems and Stomatal Response." *Plant Cell Reports* 31 (1): 145–54. <https://doi.org/10.1007/s00299-011-1148-1>.

Fang, Liang, Pierre Martre, Kaining Jin, et al. 2023. "Neglecting Acclimation of Photosynthesis under Drought Can Cause Significant Errors in Predicting Leaf Photosynthesis in Wheat." *Global Change Biology* 29 (2): 505–21. <https://doi.org/10.1111/gcb.16488>.

Fidler, Justyna, Jakub Graska, Marta Gietler, et al. 2022. "PYR/PYL/RCAR Receptors Play a Vital Role in the Abscisic-Acid-Dependent Responses of Plants to External or Internal Stimuli." *Cells* 11 (8): 1352. <https://doi.org/10.3390/cells11081352>.

Fleta-Soriano, Eva, and Sergi Munné-Bosch. 2016. "Stress Memory and the Inevitable Effects of Drought: A Physiological Perspective." *Frontiers in Plant Science* 7 (February). <https://doi.org/10.3389/fpls.2016.00143>.

Flexas, Jaume, and Hipólito Medrano. 2002a. "Drought-Inhibition of Photosynthesis in C3 Plants: Stomatal and Non-Stomatal Limitations Revisited." *Annals of Botany* 89 (2): 183–89. <https://doi.org/10.1093/aob/mcf027>.

Flexas, Jaume, and Hipólito Medrano. 2002b. "Energy Dissipation in C3 Plants under Drought." *Functional Plant Biology* 29 (10): 1209–15. <https://doi.org/10.1071/fp02015>.

Forestan, Cristian, Silvia Farinati, Federico Zambelli, Giulio Pavesi, Vincenzo Rossi, and Serena Varotto. 2020. "Epigenetic Signatures of Stress Adaptation and Flowering Regulation in Response to Extended Drought and Recovery in *Zea Mays*." *Plant, Cell & Environment* 43 (1): 55–75. <https://doi.org/10.1111/pce.13660>.

Foster, Nicola L, Ken Lukowiak, and Theodore B Henry. 2015. "Time-Related Expression Profiles for Heat Shock Protein Gene Transcripts (HSP40, HSP70) in the Central Nervous System of *Lymnaea Stagnalis* Exposed to Thermal Stress." *Communicative & Integrative Biology* 8 (3): e1040954. <https://doi.org/10.1080/19420889.2015.1040954>.

Frampton, C. V. 1960. "Some Aspects of the Developmental Anatomy of The 'Long' Shoot in *Larix Decidua* Mill., with Particular Reference to Seasonal Periodicity." *New Phytologist* 59 (2): 175–91. <https://doi.org/10.1111/j.1469-8137.1960.tb06215.x>.

Furze, Morgan E., Brett A. Huggett, Donald M. Aubrecht, Claire D. Stoltz, Mariah S. Carbone, and Andrew D. Richardson. 2019. "Whole-Tree Nonstructural Carbohydrate Storage and Seasonal Dynamics in Five Temperate Species." *New Phytologist* 221 (3): 1466–77. <https://doi.org/10.1111/nph.15462>.

Gadzinowska, Joanna, Katarzyna Hura, Agnieszka Ostrowska, and Tomasz Hura. 2021. "Activity of the Photosynthetic Apparatus in Dehydrated Leaves of a Perennial Shrub *Rosa Rubiginosa* L. with Different Levels of Drought Memory." *Environmental and Experimental Botany* 187 (July): 104493. <https://doi.org/10.1016/j.envexpbot.2021.104493>.

Galiano, L., J. Martínez-Vilalta, and F. Lloret. 2011. "Carbon Reserves and Canopy Defoliation Determine the Recovery of Scots Pine 4 Yr after a Drought Episode." *New Phytologist* 190 (3): 750–59. <https://doi.org/10.1111/j.1469-8137.2010.03628.x>.

Galle, Alexander, Igor Florez-Sarasa, Afwa Thameur, Rosine De Paepe, Jaume Flexas, and Miquel Ribas-Carbo. 2010. "Effects of Drought Stress and Subsequent Rewatering on Photosynthetic and Respiratory Pathways in Nicotiana Sylvestris Wild Type and the Mitochondrial Complex I-Deficient CMSII Mutant." *Journal of Experimental Botany* 61 (3): 765–75. <https://doi.org/10.1093/jxb/erp344>.

Gallé, Alexander, Pierre Haldimann, and Urs Feller. 2007. "Photosynthetic Performance and Water Relations in Young Pubescent Oak (*Quercus Pubescens*) Trees during Drought Stress and Recovery." *New Phytologist* 174 (4): 799–810. <https://doi.org/10.1111/j.1469-8137.2007.02047.x>.

Gao, Qi, Yamin Liu, Yumin Liu, et al. 2023. "Salicylic Acid Modulates the Osmotic System and Photosynthesis Rate to Enhance the Drought Tolerance of *Toona Ciliata*." *Plants* 12 (24): 4187. <https://doi.org/10.3390/plants12244187>.

Garcia-Forner, Núria, Anna Sala, Carme Biel, Robert Savé, and Jordi Martínez-Vilalta. 2016. "Individual Traits as Determinants of Time to Death under Extreme Drought in *Pinus Sylvestris L.*" *Tree Physiology* 36 (10): 1196–209. <https://doi.org/10.1093/treephys/tpw040>.

Gattmann, Marielle, Scott A M McAdam, Benjamin Birami, et al. 2023. "Anatomical Adjustments of the Tree Hydraulic Pathway Decrease Canopy Conductance under Long-Term Elevated CO₂." *Plant Physiology* 191 (1): 252–64. <https://doi.org/10.1093/plphys/kiac482>.

Gelaw, Temesgen Assefa, and Neeti Sanan-Mishra. 2021. "Non-Coding RNAs in Response to Drought Stress." *International Journal of Molecular Sciences* 22 (22): 12519. <https://doi.org/10.3390/ijms22212519>.

Georgii, Elisabeth, Karl Kugler, Matthias Pfeifer, et al. 2019. "The Systems Architecture of Molecular Memory in Poplar after Abiotic Stress." *The Plant Cell* 31 (2): 346–67. <https://doi.org/10.1105/tpc.18.00431>.

Gessler, Arthur, Marcus Schaub, and Nate G. McDowell. 2017. "The Role of Nutrients in Drought-Induced Tree Mortality and Recovery." *New Phytologist* 214 (2): 513–20. <https://doi.org/10.1111/nph.14340>.

Godfrey, Jessie, Jason Riggio, Jessica Orozco, Paula Guzmán-Delgado, Alana R. O. Chin, and Maciej A. Zwieniecki. 2020. "Ray Fractions and Carbohydrate Dynamics of Tree Species along a 2750 m Elevation Gradient Indicate Climate Response, Not Spatial Storage Limitation." *New Phytologist* 225 (6). <https://doi.org/10.1111/nph.16361>.

Godwin, James, and Sara Farrona. 2020. "Plant Epigenetic Stress Memory Induced by Drought: A Physiological and Molecular Perspective." In *Plant Epigenetics and Epigenomics : Methods and Protocols*, edited by Charles Spillane and Peter McKeown. Springer US. https://doi.org/10.1007/978-1-0716-0179-2_17.

Grossiord, Charlotte, Sanna Sevanto, Jean-Marc Limousin, et al. 2018. "Manipulative Experiments Demonstrate How Long-Term Soil Moisture Changes Alter Controls of Plant Water Use." *Environmental and Experimental Botany*, Experiments with trees: from seedlings to ecosystems, vol. 152 (August): 19–27. <https://doi.org/10.1016/j.envexpbot.2017.12.010>.

Gujjar, Ranjit Singh, Pennapa Banyen, Wannisa Chuekong, Phapawee Worakan, Sittiruk Roytrakul, and Kanyaratt Supaibulwatana. 2020. "A Synthetic Cytokinin Improves Photosynthesis in Rice under Drought Stress by Modulating the Abundance of Proteins Related to Stomatal Conductance, Chlorophyll Contents, and Rubisco Activity." *Plants* 9 (9): 1106. <https://doi.org/10.3390/plants9091106>.

Guo, Tingting, Daofeng Wang, Jingjing Fang, et al. 2019. "Mutations in the Rice OsCHR4 Gene, Encoding a CHD3 Family Chromatin Remodeler, Induce Narrow and Rolled Leaves with Increased Cuticular Wax." *International Journal of Molecular Sciences* 20 (10): 2567. <https://doi.org/10.3390/ijms20102567>.

Guo, Xinyi, Changhui Peng, Tong Li, et al. 2021. "The Effects of Drought and Re-Watering on Non-Structural Carbohydrates of *Pinus Tabulaeformis* Seedlings." *Biology* 10 (4): 4. <https://doi.org/10.3390/biology10040281>.

Hagedorn, Frank, Jobin Joseph, Martina Peter, et al. 2016. "Recovery of Trees from Drought Depends on Belowground Sink Control." *Nature Plants* 2 (8): 1–5. <https://doi.org/10.1038/nplants.2016.111>.

Hammond, William M., A. Park Williams, John T. Abatzoglou, et al. 2022. "Global Field Observations of Tree Die-off Reveal Hotter-Drought Fingerprint for Earth's Forests." *Nature Communications* 13 (1): 1761. <https://doi.org/10.1038/s41467-022-29289-2>.

Hartmann, H. 2015. "Carbon Starvation during Drought-Induced Tree Mortality – Are We Chasing a Myth?" *Journal of Plant Hydraulics* 2 (November): e005.

Hartmann, Henrik, Ana Bastos, Adrian J. Das, et al. 2022. "Climate Change Risks to Global Forest Health: Emergence of Unexpected Events of Elevated Tree Mortality Worldwide." *Annual Review of Plant Biology* 73 (Volume 73, 2022): 673–702. <https://doi.org/10.1146/annurev-arpplant-102820-012804>.

Hartmann, Henrik, Nate G. McDowell, and Susan Trumbore. 2015. "Allocation to Carbon Storage Pools in Norway Spruce Saplings under Drought and Low CO₂." *Tree Physiology* 35 (3): 243–52. <https://doi.org/10.1093/treephys/tpv019>.

Hartmann, Henrik, Catarina F. Moura, William R. L. Anderegg, et al. 2018. "Research Frontiers for Improving Our Understanding of Drought-Induced Tree and Forest Mortality." *New Phytologist* 218 (1): 15–28. <https://doi.org/10.1111/nph.15048>.

Hartmann, Henrik, and Susan Trumbore. 2016. "Understanding the Roles of Nonstructural Carbohydrates in Forest Trees – from What We Can Measure to What We Want to Know." *New Phytologist* 211 (2): 386–403. <https://doi.org/10.1111/nph.13955>.

Hasanagić, Dino, Ivana Koleška, Danijela Kojić, Sanja Vlaisavljević, Nina Janjić, and Biljana Kukavica. 2020. "Long Term Drought Effects on Tomato Leaves: Anatomical, Gas Exchange and Antioxidant Modifications." *Acta Physiologae Plantarum* 42 (7): 121. <https://doi.org/10.1007/s11738-020-03114-z>.

Hasanuzzaman, Md, Meixue Zhou, and Sergey Shabala. 2023. "How Does Stomatal Density and Residual Transpiration Contribute to Osmotic Stress Tolerance?" *Plants* 12 (3): 494. <https://doi.org/10.3390/plants12030494>.

Hayat, Shamsul, Qaiser Hayat, Mohammed Nasser Alyemeni, Arif Shafi Wani, John Pichtel, and Aqil Ahmad. 2012. "Role of Proline under Changing Environments: A Review." *Plant Signaling & Behavior* 7 (11): 1456–66. <https://doi.org/10.4161/psb.21949>.

Herrera, J. C., S. Savoi, J. Dostal, et al. 2024. "The Legacy of Past Droughts Induces Water-Sparingly Behaviour in Grüner Veltliner Grapevines." *Plant Biology* n/a (n/a). <https://doi.org/10.1111/plb.13620>.

Hetherington, Alistair M., and F. Ian Woodward. 2003. "The Role of Stomata in Sensing and Driving Environmental Change." *Nature* 424 (6951): 901–8. <https://doi.org/10.1038/nature01843>.

Higashide, Tadahisa, Megumi Narukawa, Yukihisa Shimada, and Kazuo Soeno. 2014. "Suppression of Elongation and Growth of Tomato Seedlings by Auxin Biosynthesis Inhibitors and Modeling of the Growth and Environmental Response." *Scientific Reports* 4 (1): 4556. <https://doi.org/10.1038/srep04556>.

Hoch, G., A. Richter, and Ch. Körner. 2003. "Non-Structural Carbon Compounds in Temperate Forest Trees." *Plant, Cell & Environment* 26 (7): 1067–81. <https://doi.org/10.1046/j.0016-8025.2003.01032.x>.

Hochberg, Uri, Asfaw Degu, Aaron Fait, and Shimon Rachmievitch. 2013. "Near Isohydric Grapevine Cultivar Displays Higher Photosynthetic Efficiency and Photorespiration Rates under Drought Stress as Compared with near Anisohydric Grapevine Cultivar." *Physiologia Plantarum* 147 (4): 443–52. <https://doi.org/10.1111/j.1399-3054.2012.01671.x>.

Hölttä, T., M. Mencuccini, and E. Nikinmaa. 2009. "Linking Phloem Function to Structure: Analysis with a Coupled Xylem–Phloem Transport Model." *Journal of Theoretical Biology* 259 (2): 325–37. <https://doi.org/10.1016/j.jtbi.2009.03.039>.

Huang, Wei, Shiyuan Peng, Zhiqiang Xian, et al. 2017. "Overexpression of a Tomato miR171 Target Gene SIGRAS24 Impacts Multiple Agronomical Traits via Regulating Gibberellin and Auxin Homeostasis." *Plant Biotechnology Journal* 15 (4): 472–88. <https://doi.org/10.1111/pbi.12646>.

Húdoková, Hana, Peter Petrik, Anja Petek-Petrik, et al. 2022. "Heat-Stress Response of Photosystem II in Five Ecologically Important Tree Species of European Temperate Forests." *Biologia* 77 (3): 671–80. <https://doi.org/10.1007/s11756-021-00958-9>.

Jacques, Cécile, Christophe Salon, Romain L. Barnard, Vanessa Vernoud, and Marion Prudent. 2021. "Drought Stress Memory at the Plant Cycle Level: A Review." *Plants* 10 (9): 1873. <https://doi.org/10.3390/plants10091873>.

Jan, Sumira, Nazia Abbas, Muhammad Ashraf, and Parvaiz Ahmad. 2019. "Roles of Potential Plant Hormones and Transcription Factors in Controlling Leaf Senescence and Drought Tolerance." *Protoplasma* 256 (2): 313–29. <https://doi.org/10.1007/s00709-018-1310-5>.

Jia, Haiyan, Shaojun Zhang, Meiyu Ruan, Yunlong Wang, and Chongying Wang. 2012. "Analysis and Application of RD29 Genes in Abiotic Stress Response." *Acta Physiologae Plantarum* 34 (4): 1239–50. <https://doi.org/10.1007/s11738-012-0969-z>.

Jiang, Jinjin, Haotian Zhu, Na Li, Jacqueline Batley, and Youping Wang. 2022. "The miR393-Target Module Regulates Plant Development and Responses to Biotic and Abiotic Stresses." *International Journal of Molecular Sciences* 23 (16): 9477. <https://doi.org/10.3390/ijms23169477>.

Jiang, Kai, Hongwei Guo, and Jixian Zhai. 2023. "Interplay of Phytohormones and Epigenetic Regulation: A Recipe for Plant Development and Plasticity." *Journal of Integrative Plant Biology* 65 (2): 381–98. <https://doi.org/10.1111/jipb.13384>.

Jiang, Yanke, Yingzhe Yue, Zhaoxu Wang, et al. 2024. "A Novel ABA Structural Analogue Enhanced Plant Resistance by Inducing the Plant Immunity and Inactivating ABA Signaling Pathway." *Advanced Agrochem* 3 (1): 64–73. <https://doi.org/10.1016/j.aac.2023.08.006>.

Johnson, Daniel M., Katherine A. McCulloh, and Keith Reinhardt. 2011. "The Earliest Stages of Tree Growth: Development, Physiology and Impacts of Microclimate." In *Size- and Age-Related Changes in Tree Structure and Function*, edited by Frederick C. Meinzer, Barbara Lachenbruch, and Todd E. Dawson.

Tree Physiology 4. Springer Netherlands. http://link.springer.com/chapter/10.1007/978-94-007-1242-3_3.

Jordan, Douglas B., and William L. Ogren. 1984. "The CO₂/O₂ Specificity of Ribulose 1,5-Bisphosphate Carboxylase/Oxygenase." *Planta* 161 (4): 308–13. <https://doi.org/10.1007/BF00398720>.

Joseph, Jobin, Jörg Luster, Alessandra Bottero, et al. 2021. "Effects of Drought on Nitrogen Uptake and Carbon Dynamics in Trees." *Tree Physiology* 41 (6): 927–43. <https://doi.org/10.1093/treephys/tpaa146>.

Kambona, Carolyn Mukiri, Patrice Ahossi Koua, Jens Léon, and Agim Ballvora. 2023. "Stress Memory and Its Regulation in Plants Experiencing Recurrent Drought Conditions." *Theoretical and Applied Genetics* 136 (2): 26. <https://doi.org/10.1007/s00122-023-04313-1>.

Kane, Cade, and Scott McAdam. 2023. "Abscisic Acid Driven Stomatal Closure during Drought in Anisohydric *Fagus Sylvatica*." *Journal of Plant Hydraulics* 9 (September): 002–002. <https://doi.org/10.20870/jph.2023.002>.

Kannenberg, Steven A., Antoine Cabon, Flurin Babst, et al. 2022. "Drought-Induced Decoupling between Carbon Uptake and Tree Growth Impacts Forest Carbon Turnover Time." *Agricultural and Forest Meteorology* 322 (July): 108996. <https://doi.org/10.1016/j.agrformet.2022.108996>.

Kannenberg, Steven A., Kimberly A. Novick, M. Ross Alexander, et al. 2019. "Linking Drought Legacy Effects across Scales: From Leaves to Tree Rings to Ecosystems." *Global Change Biology* 25 (9): 2978–92. <https://doi.org/10.1111/gcb.14710>.

Kannenberg, Steven A., and Richard P Phillips. 2020. "Non-Structural Carbohydrate Pools Not Linked to Hydraulic Strategies or Carbon Supply in Tree Saplings during Severe Drought and Subsequent Recovery." *Tree Physiology* 40 (2): 259–71. <https://doi.org/10.1093/treephys/tpz132>.

Kannenberg, Steven A., Christopher R. Schwalm, and William R. L. Anderegg. 2020. "Ghosts of the Past: How Drought Legacy Effects Shape Forest Functioning and Carbon Cycling." *Ecology Letters* 23 (5): 891–901. <https://doi.org/10.1111/ele.13485>.

Kapoor, Bhuvnesh, Pankaj Kumar, Rajnish Sharma, and Mohammad Irfan. 2023. "Chapter 12 - Drought-Induced Plant miRNAome and Phytohormone Signaling Cross-Talk." In *Plant Hormones in Crop Improvement*, edited by M. Iqbal R. Khan, Amarjeet Singh, and Péter Poór. Academic Press. <https://doi.org/10.1016/B978-0-323-91886-2.00006-9>.

Kardiman, Reki, and Anders Ræbild. 2018. "Relationship between Stomatal Density, Size and Speed of Opening in Sumatran Rainforest Species." *Tree Physiology* 38 (5): 696–705. <https://doi.org/10.1093/treephys/tpx149>.

Karlowsky, Stefan, Angela Augusti, Johannes Ingrisch, Mohammad Kamal Uddin Akanda, Michael Bahn, and Gerd Gleixner. 2018. "Drought-Induced Accumulation of Root Exudates Supports Post-Drought Recovery of Microbes in Mountain Grassland." *Frontiers in Plant Science* 9. <https://doi.org/10.3389/fpls.2018.01593>.

Kashyap, Sampurna, Niraj Agarwala, and Ramanjulu Sunkar. 2024. "Understanding Plant Stress Memory Traits Can Provide a Way for Sustainable Agriculture." *Plant Science* 340 (March): 111954. <https://doi.org/10.1016/j.plantsci.2023.111954>.

Kato, Masaharu C., Kouki Hikosaka, Naoki Hirotsu, Amane Makino, and Tadaki Hirose. 2003. "The Excess Light Energy That Is Neither Utilized in Photosynthesis nor Dissipated by Photoprotective Mechanisms Determines the Rate of Photoinactivation in Photosystem II." *Plant and Cell Physiology* 44 (3): 318–25. <https://doi.org/10.1093/pcp/pcg045>.

Kaya, Cengiz, Ferhat Uğurlar, and Ioannis-Dimosthenis S. Adamakis. 2024. "Epigenetic Modifications of Hormonal Signaling Pathways in Plant Drought Response and Tolerance for Sustainable Food Security." *International Journal of Molecular Sciences* 25 (15): 8229. <https://doi.org/10.3390/ijms25158229>.

Keber, Marko, Saša Kostić, Srđan Stojnić, et al. 2023. "A Fine-Tuning of the Plant Hormones, Polyamines and Osmolytes by Ectomycorrhizal Fungi Enhances Drought Tolerance in Pedunculate Oak." *International Journal of Molecular Sciences* 24 (8): 7510. <https://doi.org/10.3390/ijms24087510>.

Keshet, Ilana, Judy Lieman-Hurwitz, and Howard Cedar. 1986. "DNA Methylation Affects the Formation of Active Chromatin." *Cell* 44 (4): 535–43. [https://doi.org/10.1016/0092-8674\(86\)90263-1](https://doi.org/10.1016/0092-8674(86)90263-1).

Khan, M. Iqbal R., Mehar Fatma, Tasir S. Per, Naser A. Anjum, and Nafees A. Khan. 2015. "Salicylic Acid-Induced Abiotic Stress Tolerance and Underlying Mechanisms in Plants." *Frontiers in Plant Science* 6 (June). <https://doi.org/10.3389/fpls.2015.00462>.

Khan, Sheen, Ameena Fatima Alvi, Sadaf Saify, Noushina Iqbal, and Nafees A. Khan. 2024. "The Ethylene Biosynthetic Enzymes, 1-Aminocyclopropane-1-Carboxylate (ACC) Synthase (ACS) and ACC Oxidase (ACO): The Less Explored Players in Abiotic Stress Tolerance." *Biomolecules* 14 (1): 90. <https://doi.org/10.3390/biom14010090>.

Khorobrykh, Sergey A., Maarit Karonen, and Esa Tyystjärvi. 2015. "Experimental Evidence Suggesting That H₂O₂ Is Produced within the Thylakoid Membrane in a Reaction between Plastoquinol and Singlet Oxygen." *FEBS Letters* 589 (6): 779–86. <https://doi.org/10.1016/j.febslet.2015.02.011>.

Khoudi, Habib. 2023. "SHINE Clade of ERF Transcription Factors: A Significant Player in Abiotic and Biotic Stress Tolerance in Plants." *Plant Physiology and Biochemistry* 195 (February): 77–88. <https://doi.org/10.1016/j.plaphy.2022.12.030>.

Kinoshita, T. Kihara Institute for Biological Research, and M. Seki. 2014. "Epigenetic Memory for Stress Response and Adaptation in Plants." *Plant and Cell Physiology (Japan)* 55 (11). <https://agsr.fao.org/search/en/providers/122558/records/67655904fcfc879925c0fd8c>.

Klein, Tamir, Günter Hoch, Dan Yakir, and Christian Körner. 2014. "Drought Stress, Growth and Nonstructural Carbohydrate Dynamics of Pine Trees in a Semi-Arid Forest." *Tree Physiology* 34 (9): 981–92. <https://doi.org/10.1093/treephys/tpu071>.

Klein, Tamir, Yann Vitasse, and Günter Hoch. 2016. "Coordination between Growth, Phenology and Carbon Storage in Three Coexisting Deciduous Tree Species in a Temperate Forest." *Tree Physiology* 36 (7): 847–55. <https://doi.org/10.1093/treephys/tpw030>.

Knüver, Timo, Andreas Bär, Elias Hamann, et al. 2025. "Stress Dose Explains Drought Recovery in Norway Spruce." *Frontiers in Plant Science* 16 (March): 1542301. <https://doi.org/10.3389/fpls.2025.1542301>.

Kohli, Sukhmeen Kaur, Kanika Khanna, Renu Bhardwaj, Francisco J. Corpas, and Parvaiz Ahmad. 2022. "Nitric Oxide, Salicylic Acid and Oxidative Stress: Is It a Perfect Equilateral Triangle?" *Plant Physiology and Biochemistry* 184 (August): 56–64. <https://doi.org/10.1016/j.plaphy.2022.05.017>.

Kong, Lingyao, Yanna Liu, Pengfei Zhi, et al. 2020. "Origins and Evolution of Cuticle Biosynthetic Machinery in Land Plants." *Plant Physiology* 184 (4): 1998–2010. <https://doi.org/10.1104/pp.20.00913>.

Konrad, Wilfried, Gabriel Katul, and Anita Roth-Nebelsick. 2021. "Leaf Temperature and Its Dependence on Atmospheric CO₂ and Leaf Size." *Geological Journal* 56 (2): 866–85. <https://doi.org/10.1002/gj.3757>.

Körner, Christian. 2015. "Paradigm Shift in Plant Growth Control." *Current Opinion in Plant Biology* 25 (June): 107–14. <https://doi.org/10.1016/j.pbi.2015.05.003>.

Kou, Shuyan, Qiongyao Gu, Liu Duan, et al. 2022. "Genome-Wide Bisulphite Sequencing Uncovered the Contribution of DNA Methylation to Rice Short-Term Drought Memory Formation." *Journal of Plant Growth Regulation* 41 (7): 2903–17. <https://doi.org/10.1007/s00344-021-10483-3>.

Koyama, Tomotsugu, Fumihiko Sato, and Masaru Ohme-Takagi. 2017. "Roles of miR319 and TCP Transcription Factors in Leaf Development." *Plant Physiology* 175 (2): 874–85. <https://doi.org/10.1104/pp.17.00732>.

Ku, Sun-Ben, and Gerald E. Edwards. 1977. "Oxygen Inhibition of Photosynthesis: I. Temperature Dependence and Relation to O₂/CO₂ Solubility Ratio 1." *Plant Physiology* 59 (5): 986–90. <https://doi.org/10.1104/pp.59.5.986>.

Ku, Sun-Ben, and Gerald E. Edwards. 1978. "Oxygen Inhibition of Photosynthesis." *Planta* 140 (1): 1–6. <https://doi.org/10.1007/BF00389372>.

Kumazaki, Ayana, and Nobuhiro Suzuki. 2019. "Enhanced Tolerance to a Combination of Heat Stress and Drought in *Arabidopsis* Plants Deficient in ICS1 Is Associated with Modulation of Photosynthetic Reaction Center Proteins." *Physiologia Plantarum* 165 (2): 232–46. <https://doi.org/10.1111/ppl.12809>.

Kuster, Thomas M., Matthias Dobbertin, Madeleine S. Günthardt-Goerg, Marcus Schaub, and Matthias Arend. 2014. "A Phenological Timetable of Oak Growth under Experimental Drought and Air Warming." *PLOS ONE* 9 (2): e89724. <https://doi.org/10.1371/journal.pone.0089724>.

Lam, Patricia, Lifang Zhao, Nathan Eveleigh, Yu Yu, Xuemei Chen, and Ljerka Kunst. 2015. "The Exosome and Trans-Acting Small Interfering RNAs Regulate Cuticular Wax Biosynthesis during *Arabidopsis* Inflorescence Stem Development." *Plant Physiology* 167 (2): 323–36. <https://doi.org/10.1104/pp.114.252825>.

Lämke, Jörn, and Isabel Bärle. 2017. "Epigenetic and Chromatin-Based Mechanisms in Environmental Stress Adaptation and Stress Memory in Plants." *Genome Biology* 18 (1): 124. <https://doi.org/10.1186/s13059-017-1263-6>.

Landhäusser, Simon M., and Henry D Adams. 2024. "Getting to the Root of Carbon Reserve Dynamics in Woody Plants: Progress, Challenges and Goals." *Tree Physiology* 44 (13): 1–10. <https://doi.org/10.1093/treephys/tpae151>.

Landhäusser, Simon M., Pak S Chow, L Turin Dickman, et al. 2018. "Standardized Protocols and Procedures Can Precisely and Accurately Quantify Non-Structural Carbohydrates." *Tree Physiology* 38 (12): 1764–78. <https://doi.org/10.1093/treephys/tpy118>.

Lawlor, David W., and Wilmer Tezara. 2009. "Causes of Decreased Photosynthetic Rate and Metabolic Capacity in Water-Deficient Leaf Cells: A Critical Evaluation of Mechanisms and Integration of Processes." *Annals of Botany* 103 (4): 561–79. <https://doi.org/10.1093/aob/mcn244>.

Le Provost, Grégoire, Frédéric Domergue, Céline Lalanne, et al. 2013. "Soil Water Stress Affects Both Cuticular Wax Content and Cuticle-Related Gene Expression in Young Saplings of Maritime Pine (*Pinus pinaster* Ait)." *BMC Plant Biology* 13 (1): 95. <https://doi.org/10.1186/1471-2229-13-95>.

Lee, Sang-Uk, Bong-Gyu Mun, Eun-Kyung Bae, et al. 2021. "Drought Stress-Mediated Transcriptome Profile Reveals NCED as a Key Player Modulating Drought Tolerance in *Populus Davidiana*." *Frontiers in Plant Science* 12 (October). <https://doi.org/10.3389/fpls.2021.755539>.

Lenth, Russell V., Ben Bolker, Paul Buerkner, et al. 2024. *Emmeans: Estimated Marginal Means, Aka Least-Squares Means*. V. 1.10.0. Released January 23. <https://cran.r-project.org/web/packages/emmeans/index.html>.

Li, Chao, Jiang Xu, Jian Li, Qingyun Li, and Hongchun Yang. 2014. "Involvement of *Arabidopsis* Histone Acetyltransferase HAC Family Genes in the Ethylene Signaling Pathway." *Plant and Cell Physiology* 55 (2): 426–35. <https://doi.org/10.1093/pcp/pct180>.

Li, Jing, Qiaoqiao Song, Zhi-Fang Zuo, and Lin Liu. 2022. "MicroRNA398: A Master Regulator of Plant Development and Stress Responses." *International Journal of Molecular Sciences* 23 (18): 10803. <https://doi.org/10.3390/ijms231810803>.

Li, Qing, Xiao Wang, Zhuangzhuang Sun, et al. 2023. "DNA Methylation Levels of *TaP5CS* and *TaBADH* Are Associated with Enhanced Tolerance to PEG-Induced Drought Stress Triggered by Drought Priming in Wheat." *Plant Physiology and Biochemistry* 200 (July): 107769. <https://doi.org/10.1016/j.plaphy.2023.107769>.

Li, Wei, Xiao Cui, Zhaolu Meng, et al. 2012. "Transcriptional Regulation of *Arabidopsis* MIR168a and ARGONAUTE1 Homeostasis in Abscisic Acid and Abiotic Stress Responses." *Plant Physiology* 158 (3): 1279–92. <https://doi.org/10.1104/pp.111.188789>.

Li, Xiao-Ping, Olle Björkman, Connie Shih, et al. 2000. "A Pigment-Binding Protein Essential for Regulation of Photosynthetic Light Harvesting." *Nature* 403 (6768): 391–95. <https://doi.org/10.1038/35000131>.

Li, Xuyan, Xin Xie, Ji Li, et al. 2017. "Conservation and Diversification of the miR166 Family in Soybean and Potential Roles of Newly Identified miR166s." *BMC Plant Biology* 17 (1): 32. <https://doi.org/10.1186/s12870-017-0983-9>.

Li, Yuxia, Zongran Yang, Yuanyuan Zhang, et al. 2022. "The Roles of HD-ZIP Proteins in Plant Abiotic Stress Tolerance." *Frontiers in Plant Science* 13 (October). <https://doi.org/10.3389/fpls.2022.1027071>.

Liebsch, Daniela, and Javier F Palatnik. 2020. "MicroRNA miR396, GRF Transcription Factors and GIF Co-Regulators: A Conserved Plant Growth Regulatory Module with Potential for Breeding and Biotechnology." *Current Opinion in Plant Biology*, Growth and development, vol. 53 (February): 31–42. <https://doi.org/10.1016/j.pbi.2019.09.008>.

Lim, Chae Woo, Woonhee Baek, Sang-Wook Han, and Sung Chul Lee. 2013. "Arabidopsis PYL8 Plays an Important Role for ABA Signaling and Drought Stress Responses." *The Plant Pathology Journal* 29 (4): 471–76. <https://doi.org/10.5423/PPJ.NT.07.2013.0071>.

Liu, Chunyan, Falong Lu, Xia Cui, and Xiaofeng Cao. 2010. "Histone Methylation in Higher Plants." *Annual Review of Plant Biology* 61 (Volume 61, 2010): 395–420. <https://doi.org/10.1146/annurev.arplant.043008.091939>.

Liu, Dongmei, Yu Song, Zhixiang Chen, and Diqu Yu. 2009. "Ectopic Expression of miR396 Suppresses GRF Target Gene Expression and Alters Leaf Growth in *Arabidopsis*." *Physiologia Plantarum* 136 (2): 223–36. <https://doi.org/10.1111/j.1399-3054.2009.01229.x>.

Liu, Jun-Jun, Anna W. Schoettle, Richard A. Sniezko, et al. 2022. "Comparative Association Mapping Reveals Conservation of Major Gene Resistance to White Pine Blister Rust in Southwestern White Pine (*Pinus Strobiformis*) and Limber Pine (*P. Flexilis*)." *Phytopathology®* 112 (5): 1093–102. <https://doi.org/10.1094/PHYTO-09-21-0382-R>.

Liu, Meng, Anna T. Trugman, Josep Peñuelas, and William R. L. Anderegg. 2024. "Climate-Driven Disturbances Amplify Forest Drought Sensitivity." *Nature Climate Change* 14 (7): 746–52. <https://doi.org/10.1038/s41558-024-02022-1>.

Liu, Ning, Paul E. Staswick, and Zoya Avramova. 2016. "Memory Responses of Jasmonic Acid-Associated *Arabidopsis* Genes to a Repeated Dehydration Stress." *Plant, Cell & Environment* 39 (11): 2515–29. <https://doi.org/10.1111/pce.12806>.

Lloyd, Max K., Rebekah A. Stein, Daniel E. Ibarra, et al. 2023. "Isotopic Clumping in Wood as a Proxy for Photorespiration in Trees." *Proceedings of the National Academy of Sciences* 120 (46): e2306736120. <https://doi.org/10.1073/pnas.2306736120>.

Löiez, Sidonie, and Frida I Piper. 2022. "Phenology Explains Different Storage Remobilization in Two Congeneric Temperate Tree Species with Contrasting Leaf Habit." *Tree Physiology* 42 (3): 501–12. <https://doi.org/10.1093/treephys/tpab124>.

Long, Randall W., and Henry D. Adams. 2023. "The Osmotic Balancing Act: When Sugars Matter for More than Metabolism in Woody Plants." *Global Change Biology* 29 (7): 1684–87. <https://doi.org/10.1111/gcb.16572>.

Lu, Hongchen, Li Chen, Mengjie Du, et al. 2023. "miR319 and Its Target *TCP4* Involved in Plant Architecture Regulation in *Brassica Napus*." *Plant Science* 326 (January): 111531. <https://doi.org/10.1016/j.plantsci.2022.111531>.

Lu, Xuke, Xiaoge Wang, Xiugui Chen, et al. 2017. "Single-Base Resolution Methylomes of Upland Cotton (*Gossypium Hirsutum* L.) Reveal Epigenome Modifications in Response to Drought Stress." *BMC Genomics* 18 (1): 297. <https://doi.org/10.1186/s12864-017-3681-y>.

Lukić, Nataša, Biljana Kukavica, Biljana Davidović-Plavšić, Dino Hasanagić, and Julia Walter. 2020. "Plant Stress Memory Is Linked to High Levels of Anti-Oxidative Enzymes over Several Weeks." *Environmental and Experimental Botany* 178 (October): 104166. <https://doi.org/10.1016/j.envexpbot.2020.104166>.

Lukić, Nataša, Frank M. Schurr, Tanja Trifković, Biljana Kukavica, and Julia Walter. 2023. "Transgenerational Stress Memory in Plants Is Mediated by Upregulation of the Antioxidative System." *Environmental and Experimental Botany* 205 (January): 105129. <https://doi.org/10.1016/j.envexpbot.2022.105129>.

Luna, Celina M., Gabriela M. Pastori, Simon Driscoll, Karin Grotel, Stephanie Bernard, and Christine H. Foyer. 2005. "Drought Controls on H₂O₂ Accumulation, Catalase (CAT) Activity and CAT Gene Expression in Wheat." *Journal of Experimental Botany* 56 (411): 417–23. <https://doi.org/10.1093/jxb/eri039>.

Luo, Chongyuan, Petra Hajkova, and Joseph R. Ecker. 2018. "Dynamic DNA Methylation: In the Right Place at the Right Time." *Science* 361 (6409): 1336–40. <https://doi.org/10.1126/science.aat6806>.

Luo, Ming, Xuncheng Liu, Prashant Singh, Yuhai Cui, Laurent Zimmerli, and Keqiang Wu. 2012. "Chromatin Modifications and Remodeling in Plant Abiotic Stress Responses." *Biochimica et Biophysica Acta (BBA) - Gene Regulatory Mechanisms*, Plant gene regulation in response to abiotic stress, vol. 1819 (2): 129–36. <https://doi.org/10.1016/j.bbagr.2011.06.008>.

Lv, Pengcheng, Tim Rademacher, Xuanrui Huang, Boyi Zhang, and Xianliang Zhang. 2022. "Prolonged Drought Duration, Not Intensity, Reduces Growth Recovery and Prevents Compensatory Growth of Oak Trees." *Agricultural and Forest Meteorology* 326 (November): 109183. <https://doi.org/10.1016/j.agrformet.2022.109183>.

Ma, Siqi, Ning Tang, Xu Li, et al. 2019. "Reversible Histone H2B Monoubiquitination Fine-Tunes Abscisic Acid Signaling and Drought Response in Rice." *Molecular Plant* 12 (2): 263–77. <https://doi.org/10.1016/j.molp.2018.12.005>.

Manandhar, Anju, Ian M. Rimer, Talitha Soares Pereira, Javier Pichaco, Fulton E. Rockwell, and Scott A. M. McAdam. 2024. "Dynamic Soil Hydraulic Resistance Regulates Stomata." *New Phytologist* 244 (1): 147–58. <https://doi.org/10.1111/nph.20020>.

Mantoan, Luís Paulo Benetti, Carla Verônica Corrêa, Cláudia Aparecida Rainho, and Luiz Fernando Rolim de Almeida. 2020. "Rapid Dehydration Induces Long-Term Water Deficit Memory in Sorghum Seedlings: Advantages and Consequences." *Environmental and Experimental Botany* 180 (December): 104252. <https://doi.org/10.1016/j.envexpbot.2020.104252>.

Marchand, William, Claire Depardieu, Elizabeth M. Campbell, Jean Bousquet, and Martin P. Girardin. 2025. "Long-Term Temporal Divergence in Post-Drought Resilience Decline Between Deciduous and Evergreen Tree Species." *Global Change Biology* 31 (7): e70330. <https://doi.org/10.1111/gcb.70330>.

Marinho, H. Susana, Carla Real, Luísa Cyrne, Helena Soares, and Fernando Antunes. 2014. "Hydrogen Peroxide Sensing, Signaling and Regulation of Transcription Factors." *Redox Biology* 2 (January): 535–62. <https://doi.org/10.1016/j.redox.2014.02.006>.

Martin, Laetitia B.B., Paco Romero, Eric A. Fich, David S. Domozych, and Jocelyn K.C. Rose. 2017. "Cuticle Biosynthesis in Tomato Leaves Is Developmentally Regulated by Abscisic Acid." *Plant Physiology* 174 (3): 1384–98. <https://doi.org/10.1104/pp.17.00387>.

Martínez-Sancho, Elisabet, Kerstin Treydte, Marco M. Lehmann, Andreas Rigling, and Patrick Fonti. 2022. "Drought Impacts on Tree Carbon Sequestration and Water Use – Evidence from Intra-Annual Tree-Ring Characteristics." *New Phytologist* 236 (1): 58–70. <https://doi.org/10.1111/nph.18224>.

Martínez-Vilalta, Jordi, Anna Sala, Dolores Asensio, et al. 2016. "Dynamics of Non-Structural Carbohydrates in Terrestrial Plants: A Global Synthesis." *Ecological Monographs* 86 (4): 495–516. <https://doi.org/10.1002/ecm.1231>.

Martin-StPaul, Nicolas, Sylvain Delzon, and Hervé Cochard. 2017. "Plant Resistance to Drought Depends on Timely Stomatal Closure." *Ecology Letters* 20 (11): 1437–47. <https://doi.org/10.1111/ele.12851>.

Marzi, Davide, Patrizia Brunetti, Shashank Sagar Saini, Gitanjali Yadav, Giuseppe Diego Puglia, and Raffaele Dello Iorio. 2024. "Role of Transcriptional Regulation in Auxin-Mediated Response to Abiotic Stresses." *Frontiers in Genetics* 15 (April). <https://doi.org/10.3389/fgene.2024.1394091>.

Mattei, Alexandra L., Nina Bailly, and Alexander Meissner. 2022. "DNA Methylation: A Historical Perspective." *Trends in Genetics* 38 (7): 676–707. <https://doi.org/10.1016/j.tig.2022.03.010>.

Matthaeus, William J., Isabel P. Montañez, Jennifer C. McElwain, Jonathan P. Wilson, and Joseph D. White. 2022. "Stems Matter: Xylem Physiological Limits Are an Accessible and Critical Improvement to Models of Plant Gas Exchange in Deep Time." *Frontiers in Ecology and Evolution* 10 (September). <https://doi.org/10.3389/fevo.2022.955066>.

McAdam, Scott A.M., and Timothy J. Brodribb. 2014. "Separating Active and Passive Influences on Stomatal Control of Transpiration." *Plant Physiology* 164 (4): 1578–86. <https://doi.org/10.1104/pp.113.231944>.

McDowell, Nate G., David J. Beerling, David D. Breshears, Rosie A. Fisher, Kenneth F. Raffa, and Mark Stitt. 2011. "The Interdependence of Mechanisms Underlying Climate-Driven Vegetation Mortality." *Trends in Ecology and Evolution* 26 (10): 523–32. <https://doi.org/10.1016/j.tree.2011.06.003>.

McDowell, Nathan G. 2011. "Mechanisms Linking Drought, Hydraulics, Carbon Metabolism, and Vegetation Mortality." *Plant Physiology* 155 (3): 1051–59. <https://doi.org/10.1104/pp.110.170704>.

Mencuccini, Maurizio, Teresa Rosas, Lucy Rowland, et al. 2019. "Leaf Economics and Plant Hydraulics Drive Leaf : Wood Area Ratios." *New Phytologist* 224 (4): 1544–56. <https://doi.org/10.1111/nph.15998>.

Menezes-Silva, Paulo E, Lilian M V P Sanglard, Rodrigo T Ávila, et al. 2017. "Photosynthetic and Metabolic Acclimation to Repeated Drought Events Play Key Roles in Drought Tolerance in Coffee." *Journal of Experimental Botany* 68 (15): 4309–22. <https://doi.org/10.1093/jxb/erx211>.

Merganičová, Katarína, Ján Merganič, Aleksi Lehtonen, et al. 2019. "Forest Carbon Allocation Modelling under Climate Change." *Tree Physiology* 39 (12): 1937–60. <https://doi.org/10.1093/treephys/tpz105>.

Metz, Johannes, Christian Lampei, Laura Bäumler, et al. 2020. "Rapid Adaptive Evolution to Drought in a Subset of Plant Traits in a Large-Scale Climate Change Experiment." *Ecology Letters* 23 (11): 1643–53. <https://doi.org/10.1111/ele.13596>.

Millar, Anthony A., Allan Lohe, and Gigi Wong. 2019. "Biology and Function of miR159 in Plants." *Plants* 8 (8): 255. <https://doi.org/10.3390/plants8080255>.

Misson, Laurent, David Degueldre, Christian Collin, et al. 2011. "Phenological Responses to Extreme Droughts in a Mediterranean Forest." *Global Change Biology* 17 (2): 1036–48. <https://doi.org/10.1111/j.1365-2486.2010.02348.x>.

Mitchell, Patrick J., Anthony P. O'Grady, David T. Tissue, Donald A. White, Maria L. Ottenschlaeger, and Elizabeth A. Pinkard. 2013. "Drought Response Strategies Define the Relative Contributions of Hydraulic Dysfunction and Carbohydrate Depletion during Tree Mortality." *New Phytologist* 197 (3): 862–72. <https://doi.org/10.1111/nph.12064>.

Miura, Kenji, and Yasuomi Tada. 2014. "Regulation of Water, Salinity, and Cold Stress Responses by Salicylic Acid." *Frontiers in Plant Science* 5 (January). <https://doi.org/10.3389/fpls.2014.00004>.

Monteiro, Ana I., Helena Ferreira, Jorge V. Ferreira-Cardoso, Aureliano C. Malheiro, and Eunice A. Bacelar. 2022. "Assessment of Bud Fruitfulness of Three Grapevine Varieties Grown in Northwest Portugal." *OENO One* 56 (3): 385–95. <https://doi.org/10.20870/oenone.2022.56.3.5363>.

Morran, Sarah, Omid Eini, Tatiana Pygovarenko, et al. 2011. "Improvement of Stress Tolerance of Wheat and Barley by Modulation of Expression of DREB/CBF Factors." *Plant Biotechnology Journal* 9 (2): 230–49. <https://doi.org/10.1111/j.1467-7652.2010.00547.x>.

Morris, Hugh, Lenka Plavcová, Patrick Cvecko, et al. 2016. "A Global Analysis of Parenchyma Tissue Fractions in Secondary Xylem of Seed Plants." *New Phytologist* 209 (4): 1553–65. <https://doi.org/10.1111/nph.13737>.

Moser, Lea, Patrick Fonti, Ulf Büntgen, et al. 2010. "Timing and Duration of European Larch Growing Season along Altitudinal Gradients in the Swiss Alps." *Tree Physiology* 30 (2): 225–33. <https://doi.org/10.1093/treephys/tpp108>.

Mughal, Nishbah, Noman Shoaib, Jianhua Chen, et al. 2024. "Adaptive Roles of Cytokinins in Enhancing Plant Resilience and Yield against Environmental Stressors." *Chemosphere* 364 (September): 143189. <https://doi.org/10.1016/j.chemosphere.2024.143189>.

Mukarram, Mohammad, Sadaf Choudhary, Daniel Kurjak, Anja Petek, and M. Masroor A. Khan. 2021. "Drought: Sensing, Signalling, Effects and Tolerance in Higher Plants." *Physiologia Plantarum* 172 (2): 1291–300. <https://doi.org/10.1111/ppl.13423>.

Müller, Lena M., and Michael Bahn. 2022. "Drought Legacies and Ecosystem Responses to Subsequent Drought." *Global Change Biology* 28 (17): 5086–103. <https://doi.org/10.1111/gcb.16270>.

Munné-Bosch, Sergi, and Leonor Alegre. 2004. "Die and Let Live: Leaf Senescence Contributes to Plant Survival under Drought Stress." *Functional Plant Biology* 31 (3): 203–16. <https://doi.org/10.1071/FP03236>.

Nadal-Sala, Daniel, Rüdiger Grote, Benjamin Birami, et al. 2021. "Leaf Shedding and Non-Stomatal Limitations of Photosynthesis Mitigate Hydraulic Conductance Losses in Scots Pine Saplings During

Severe Drought Stress.” *Frontiers in Plant Science* 12. <https://www.frontiersin.org/journals/plant-science/articles/10.3389/fpls.2021.715127>.

Naumann, G., L. Alfieri, K. Wyser, et al. 2018. “Global Changes in Drought Conditions Under Different Levels of Warming.” *Geophysical Research Letters* 45 (7): 3285–96. <https://doi.org/10.1002/2017GL076521>.

Nazir, Faroza, Poor Peter, Ravi Gupta, Sarika Kumari, Kashif Nawaz, and M. Iqbal R. Khan. 2024. “Plant Hormone Ethylene: A Leading Edge in Conferring Drought Stress Tolerance.” *Physiologia Plantarum* 176 (1): e14151. <https://doi.org/10.1111/ppl.14151>.

Nguyen, Nguyen Hoai, Nam Tuan Vu, and Jong-Joo Cheong. 2022. “Transcriptional Stress Memory and Transgenerational Inheritance of Drought Tolerance in Plants.” *International Journal of Molecular Sciences* 23 (21): 12918. <https://doi.org/10.3390/ijms232112918>.

Noctor, Graham, Sonja Veljovic-Johanovic, Simon Driscoll, Larissa Novitskaya, and Christine H. Foyer. 2002. “Drought and Oxidative Load in the Leaves of C3 Plants: A Predominant Role for Photorespiration?” *Annals of Botany* 89 (7): 841–50. <https://doi.org/10.1093/aob/mcf096>.

Oksanen, Jari, Gavin L. Simpson, F. Guillaume Blanchet, et al. 2025. *Vegan: Community Ecology Package*. V. 2.7-1. Released June 5. <https://cran.r-project.org/web/packages/vegan/index.html>.

Olano, José Miguel, Juan Carlos Linares, Ana I. García-Cervigón, Alberto Arzac, Antonio Delgado, and Vicente Rozas. 2014. “Drought-Induced Increase in Water-Use Efficiency Reduces Secondary Tree Growth and Tracheid Wall Thickness in a Mediterranean Conifer.” *Oecologia* 176 (1): 273–83. <https://doi.org/10.1007/s00442-014-2989-4>.

Ost, Charlotte, Hieu Xuan Cao, Thuy Linh Nguyen, et al. 2023. “Drought-Stress-Related Reprogramming of Gene Expression in Barley Involves Differential Histone Modifications at ABA-Related Genes.” *International Journal of Molecular Sciences* 24 (15): 12065. <https://doi.org/10.3390/ijms241512065>.

Palacio, Sara, Günter Hoch, Anna Sala, Christian Körner, and Pete Millard. 2014. “Does Carbon Storage Limit Tree Growth?” *New Phytologist* 201 (4): 1096–100. <https://doi.org/10.1111/nph.12602>.

Pan, Dongjin, Qing X. Li, Zhangxing Lin, et al. 2017. “Interactions between Salicylic Acid and Antioxidant Enzymes Tilting the Balance of H₂O₂ from Photorespiration in Non-Target Crops under Halosulfuron-Methyl Stress.” *Pesticide Biochemistry and Physiology* 143 (November): 214–23. <https://doi.org/10.1016/j.pestbp.2017.09.007>.

Pan, Yude, Richard A. Birdsey, Jingyun Fang, et al. 2011. “A Large and Persistent Carbon Sink in the World’s Forests.” *Science* 333 (6045): 988–93. <https://doi.org/10.1126/science.1201609>.

Pan, Yude, Richard A. Birdsey, Oliver L. Phillips, et al. 2024. “The Enduring World Forest Carbon Sink.” *Nature* 631 (8021): 563–69. <https://doi.org/10.1038/s41586-024-07602-x>.

Pandey, Komal, Ravi Shankar Kumar, Priti Prasad, Veena Pande, Prabodh Kumar Trivedi, and Pramod Arvind Shirke. 2022. “Coordinated Regulation of Photosynthesis and Sugar Metabolism in Guar Increases Tolerance to Drought.” *Environmental and Experimental Botany* 194 (February): 104701. <https://doi.org/10.1016/j.envexpbot.2021.104701>.

Pant, Bikram Datt, Anja Buhtz, Julia Kehr, and Wolf-Rüdiger Scheible. 2008. “MicroRNA399 Is a Long-Distance Signal for the Regulation of Plant Phosphate Homeostasis.” *The Plant Journal* 53 (5): 731–38. <https://doi.org/10.1111/j.1365-313X.2007.03363.x>.

Parazoo, Nicholas C., Almut Arneth, Thomas A. M. Pugh, et al. 2018. “Spring Photosynthetic Onset and Net CO₂ Uptake in Alaska Triggered by Landscape Thawing.” *Global Change Biology* 24 (8): 3416–35. <https://doi.org/10.1111/gcb.14283>.

Parry, Martin A.J., P. John AndralojcN, Shahnaz Khan, Peter J. Lea, and ALFRED J. Keys. 2002. “Rubisco Activity: Effects of Drought Stress.” *Annals of Botany* 89 (7): 833–39. <https://doi.org/10.1093/aob/mcf103>.

Paul, Matthew J., and Christine H. Foyer. 2001. “Sink Regulation of Photosynthesis.” *Journal of Experimental Botany* 52 (360): 1383–400. <https://doi.org/10.1093/jexbot/52.360.1383>.

Peerzada, Yasir Yousuf, and Muhammad Iqbal. 2021. “Leaf Senescence and Ethylene Signaling.” In *Plant Growth Regulators: Signalling under Stress Conditions*, edited by Tariq Aftab and Khalid Rehman Hakeem. Springer International Publishing. https://doi.org/10.1007/978-3-030-61153-8_7.

Pei, Ling Ling, Ling Ling Zhang, Xin Liu, and Jing Jiang. 2023. “Role of microRNA miR171 in Plant Development.” *PeerJ* 11 (July): e15632. <https://doi.org/10.7717/peerj.15632>.

Peltier, Drew M. P., Michael Fell, and Kiona Ogle. 2016. “Legacy Effects of Drought in the Southwestern United States: A Multi-Species Synthesis.” *Ecological Monographs* 86 (3): 312–26. <https://doi.org/10.1002/ecm.1219>.

Peltier, Drew M P, Jessica Guo, Phiyen Nguyen, et al. 2022. “Temperature Memory and Non-Structural Carbohydrates Mediate Legacies of a Hot Drought in Trees across the Southwestern USA.” *Tree Physiology* 42 (1): 71–85. <https://doi.org/10.1093/treephys/tpab091>.

Peltier, Drew M. P., and Kiona Ogle. 2020. “Tree Growth Sensitivity to Climate Is Temporally Variable.” *Ecology Letters* 23 (11): 1561–72. <https://doi.org/10.1111/ele.13575>.

Peñuelas, Josep, and Joan Llusià. 2002. "Linking Photorespiration, Monoterpenes and Thermotolerance in *Quercus*." *New Phytologist* 155 (2): 227–37. <https://doi.org/10.1046/j.1469-8137.2002.00457.x>.

Perdomo, Juan A., Sebastià Capó-Bauçà, Elizabete Carmo-Silva, and Jeroni Galmés. 2017. "Rubisco and Rubisco Activase Play an Important Role in the Biochemical Limitations of Photosynthesis in Rice, Wheat, and Maize under High Temperature and Water Deficit." *Frontiers in Plant Science* 8. <https://www.frontiersin.org/articles/10.3389/fpls.2017.00490>.

Pérez-de-Lis, Gonzalo, Ignacio García-González, Vicente Rozas, and José Miguel Olano. 2016. "Feedbacks between Earlywood Anatomy and Non-Structural Carbohydrates Affect Spring Phenology and Wood Production in Ring-Porous Oaks." *Biogeosciences* 13 (19): 5499–510. <https://doi.org/10.5194/bg-13-5499-2016>.

Pesacreta, T. C., A. Acharya, and K. H. Hasenstein. 2021. "Endogenous Nutrients Are Concentrated in Specific Tissues in the *Zea Mays* Seedling." *Protoplasma* 258 (4): 863–78. <https://doi.org/10.1007/s00709-021-01606-4>.

Petek-Petrik, A., P. Petrik, M. Halmová, et al. 2024. "Contrasting Strategies in Morphological and Physiological Response to Drought Stress among Temperate Forest Understory Forbs and Graminoids." *Plant Biology* n/a. <https://doi.org/10.1111/plb.13750>.

Petek-Petrik, Anja, Peter Petrik, Laurent J Lamarque, Hervé Cochard, Régis Burlett, and Sylvain Delzon. 2023. "Drought Survival in Conifer Species Is Related to the Time Required to Cross the Stomatal Safety Margin." *Journal of Experimental Botany* 74 (21): 6847–59. <https://doi.org/10.1093/jxb/erad352>.

Peters, Richard L., Kathy Steppe, Henri E. Cuny, et al. 2021. "Turgor – a Limiting Factor for Radial Growth in Mature Conifers along an Elevational Gradient." *New Phytologist* 229 (1): 213–29. <https://doi.org/10.1111/nph.16872>.

Petrik, P., A. Petek-Petrik, D. Kurjak, et al. 2022. "Interannual Adjustments in Stomatal and Leaf Morphological Traits of European Beech (*Fagus Sylvatica* L.) Demonstrate Its Climate Change Acclimation Potential." *Plant Biology* 24 (7): 1287–96. <https://doi.org/10.1111/plb.13401>.

Petrik, Peter, Anja Petek, Alena Konôpková, et al. 2020. "Stomatal and Leaf Morphology Response of European Beech (*Fagus Sylvatica* L.) Provenances Transferred to Contrasting Climatic Conditions." *Forests* 11 (12): 1359. <https://doi.org/10.3390/f11121359>.

Petrik, Peter, Anja Petek-Petrik, Laurent J. Lamarque, et al. 2024. "Linking Stomatal Size and Density to Water Use Efficiency and Leaf Carbon Isotope Ratio in Juvenile and Mature Trees." *Physiologia Plantarum* 176 (6): e14619. <https://doi.org/10.1111/ppl.14619>.

Petrik, Peter, Anja Petek-Petrik, Mohammad Mukarram, Bernhard Schuldt, and Laurent J Lamarque. 2023. "Leaf Physiological and Morphological Constraints of Water-Use Efficiency in C3 Plants." *AoB PLANTS* 15 (4): plad047. <https://doi.org/10.1093/aobpla/plad047>.

Petrov, Veselin Dimitrov, and Frank Van Breusegem. 2012. "Hydrogen Peroxide—a Central Hub for Information Flow in Plant Cells." *AoB Plants* 2012: pls014. <https://doi.org/10.1093/aobpla/pls014>.

Pinheiro, José, Douglas Bates, and R Core Team. 2023. *Nlme: Linear and Nonlinear Mixed Effects Models*. V. 3.1-164. Released November 27. <https://cran.r-project.org/web/packages/nlme/index.html>.

Pirasteh-Anosheh, Hadi, Armin Saed-Moucheshi, Hassan Pakniyat, and Mohammad Pessarakli. 2016. "Stomatal Responses to Drought Stress." In *Water Stress and Crop Plants*. John Wiley & Sons, Ltd. <https://doi.org/10.1002/9781119054450.ch3>.

Plieth, Christoph, and Sonja Vollbehr. 2012. "Calcium Promotes Activity and Confers Heat Stability on Plant Peroxidases." *Plant Signaling & Behavior* 7 (6): 650–60. <https://doi.org/10.4161/psb.20065>.

Posit Team. 2025. *RStudio: Integrated Development Environment for R*. Posit Software, released. <http://www.posit.co/>.

Prasad, Ravindra. 2022. "Cytokinin and Its Key Role to Enrich the Plant Nutrients and Growth Under Adverse Conditions-An Update." *Frontiers in Genetics* 13 (June). <https://doi.org/10.3389/fgene.2022.883924>.

Prerostova, Sylva, Petre I. Dobrev, Alena Gaudinova, et al. 2018. "Cytokinins: Their Impact on Molecular and Growth Responses to Drought Stress and Recovery in *Arabidopsis*." *Frontiers in Plant Science* 9 (May). <https://doi.org/10.3389/fpls.2018.00655>.

R Core Team. 2022. "R: A Language and Environment for Statistical Computing. R Foundation for Statistical Computing." Vienna, Austria. <https://www.R-project.org/>.

Radermacher, Astrid Lillie, Stephanus Francois du Toit, and Jill M. Farrant. 2019. "Desiccation-Driven Senescence in the Resurrection Plant *Xerophyta Schlechteri* (Baker) N.L. Menezes: Comparison of Anatomical, Ultrastructural, and Metabolic Responses Between Senescent and Non-Senescent Tissues." *Frontiers in Plant Science* 10 (October). <https://doi.org/10.3389/fpls.2019.01396>.

Raghavendra, A. S. 2003. "PHOTOSYNTHESIS AND PARTITIONING | C3 Plants." In *Encyclopedia of Applied Plant Sciences*, edited by Brian Thomas. Elsevier. <https://doi.org/10.1016/B0-12-227050-9/00094-6>.

Ramírez, D. A., J. L. Rolando, W. Yactayo, P. Monneveux, V. Mares, and R. Quiroz. 2015. "Improving Potato Drought Tolerance through the Induction of Long-Term Water Stress Memory." *Plant Science* 238 (September): 26–32. <https://doi.org/10.1016/j.plantsci.2015.05.016>.

Rao, Xiaolan, Shengli Yang, Shiyu Lü, and Pingfang Yang. 2024. "DNA Methylation Dynamics in Response to Drought Stress in Crops." *Plants* 13 (14): 1977. <https://doi.org/10.3390/plants13141977>.

Rathnasamy, Sakthi Ambothi, Rohit Kambale, Allimuthu Elangovan, et al. 2023. "Altering Stomatal Density for Manipulating Transpiration and Photosynthetic Traits in Rice through CRISPR/Cas9 Mutagenesis." *Current Issues in Molecular Biology* 45 (5): 3801–14. <https://doi.org/10.3390/cimb45050245>.

Rehschuh, Romy, Angelica Cecilia, Marcus Zuber, et al. 2020. "Drought-Induced Xylem Embolism Limits the Recovery of Leaf Gas Exchange in Scots Pine." *Plant Physiology* 184 (2): 852–64. <https://doi.org/10.1104/pp.20.00407>.

Rehschuh, Romy, Stephanie Rehschuh, Andreas Gast, et al. 2022. "Tree Allocation Dynamics beyond Heat and Hot Drought Stress Reveal Changes in Carbon Storage, Belowground Translocation and Growth." *New Phytologist* 233 (2): 687–704. <https://doi.org/10.1111/nph.17815>.

Rehschuh, Romy, and Nadine K Ruehr. 2022. "Diverging Responses of Water and Carbon Relations during and after Heat and Hot Drought Stress in *Pinus Sylvestris*." *Tree Physiology* 42 (8): 1532–48. <https://doi.org/10.1093/treephys/tpab141>.

Reyes, José L., and Nam-Hai Chua. 2007. "ABA Induction of miR159 Controls Transcript Levels of Two MYB Factors during *Arabidopsis* Seed Germination." *The Plant Journal* 49 (4): 592–606. <https://doi.org/10.1111/j.1365-313X.2006.02980.x>.

Richards, Siân L., Katie A. Wilkins, Stéphanie M. Swarbreck, et al. 2015. "The Hydroxyl Radical in Plants: From Seed to Seed." *Journal of Experimental Botany* 66 (1): 37–46. <https://doi.org/10.1093/jxb/eru398>.

Robakowski, Piotr, Pierre Montpied, and Erwin Dreyer. 2002. "Temperature Response of Photosynthesis of Silver Fir (*Abies Alba* Mill.) Seedlings." *Annals of Forest Science* 59 (2): 163–70. <https://doi.org/10.1051/forest:2002003>.

Rödig, Edna, Andreas Huth, Friedrich Bohn, Corinna Rebmann, and Matthias Cuntz. 2017. "Estimating the Carbon Fluxes of Forests with an Individual-Based Forest Model." *Forest Ecosystems* 4 (1): 4. <https://doi.org/10.1186/s40663-017-0091-1>.

Rodríguez-Calcerrada, Jesús, Ana M. Rodrigues, Carla António, et al. 2021. "Stem Metabolism under Drought Stress – a Paradox of Increasing Respiratory Substrates and Decreasing Respiratory Rates." *Physiologia Plantarum* 172 (2): 391–404. <https://doi.org/10.1111/ppl.13145>.

Rudolf, Jiri, Lucia Tomovicova, Klara Panzarova, Jiri Fajkus, Jan Hejatko, and Jan Skalak. 2024. "Epigenetics and Plant Hormone Dynamics: A Functional and Methodological Perspective." *Journal of Experimental Botany* 75 (17): 5267–94. <https://doi.org/10.1093/jxb/erae054>.

Rudy, Elżbieta, Umesh Kumar Tanwar, Zofia Szlachtowska, Magda Grabsztunowicz, Magdalena Arasimowicz-Jelonek, and Ewa Sobieszczuk-Nowicka. 2024. "Unveiling the Role of Epigenetics in Leaf Senescence: A Comparative Study to Identify Different Epigenetic Regulations of Senescence Types in Barley Leaves." *BMC Plant Biology* 24 (1): 863. <https://doi.org/10.1186/s12870-024-05573-9>.

Ruehr, Nadine K., Andreas Gast, Christina Weber, Baerbel Daub, and Almut Arneth. 2016. "Water Availability as Dominant Control of Heat Stress Responses in Two Contrasting Tree Species." *Tree Physiology* 36 (2): 164–78. <https://doi.org/10.1093/treephys/tpv102>.

Ruehr, Nadine K., Rüdiger Grote, Stefan Mayr, and Almut Arneth. 2019. "Beyond the Extreme: Recovery of Carbon and Water Relations in Woody Plants Following Heat and Drought Stress." *Tree Physiology* 39 (8): 1285–99. <https://doi.org/10.1093/treephys/tpz032>.

Ruehr, Nadine, and Daniel Nadal-Sala. 2025. "Legacies from Early-Season Hot Drought: How Growth Cessation Alters Tree Water Dynamics and Modifies Stress Responses in Scots Pine." *Plant Biology*, ahead of print, January 15. <https://doi.org/10.1111/plb.13760>.

Rui, Mengmeng, Rongjia Chen, Yi Jing, et al. 2024. "Guard Cell and Subsidiary Cell Sizes Are Key Determinants for Stomatal Kinetics and Drought Adaptation in Cereal Crops." *New Phytologist* 242 (6): 2479–94. <https://doi.org/10.1111/nph.19757>.

Sadhukhan, Ayan, Shiva Sai Prasad, Jayeeta Mitra, et al. 2022. "How Do Plants Remember Drought?" *Planta* 256 (1): 7. <https://doi.org/10.1007/s00425-022-03924-0>.

Safari, M., S. Mousavi-Fard, A. Rezaei Nejad, K. Sorkheh, and A. Sofo. 2022. "Exogenous Salicylic Acid Positively Affects Morpho-Physiological and Molecular Responses of *Impatiens Walleriana* Plants Grown under Drought Stress." *International Journal of Environmental Science and Technology* 19 (2): 969–84. <https://doi.org/10.1007/s13762-020-03092-2>.

Sah, Saroj K., Kambham R. Reddy, and Jiaxu Li. 2016. "Abscisic Acid and Abiotic Stress Tolerance in Crop Plants." *Frontiers in Plant Science* 7 (May). <https://doi.org/10.3389/fpls.2016.00571>.

Saibo, Nelson J. M., Wim H. Vriezen, Gerrit T. S. Beemster, and Dominique Van Der Straeten. 2003. "Growth and Stomata Development of *Arabidopsis* Hypocotyls Are Controlled by Gibberellins and Modulated by Ethylene and Auxins." *The Plant Journal* 33 (6): 989–1000. <https://doi.org/10.1046/j.1365-313X.2003.01684.x>.

Sajeevan, R. S., M. S. Parvathi, and Karaba N. Nataraja. 2017. "Leaf Wax Trait in Crops for Drought and Biotic Stress Tolerance: Regulators of Epicuticular Wax Synthesis and Role of Small RNAs." *Indian Journal of Plant Physiology* 22 (4): 434–47. <https://doi.org/10.1007/s40502-017-0333-9>.

Sala, Anna, David R. Woodruff, and Frederick C. Meinzer. 2012. "Carbon Dynamics in Trees: Feast or Famine?" *Tree Physiology* 32 (6): 764–75. <https://doi.org/10.1093/treephys/tpr143>.

Salmon, Yann, Anna Lintunen, Alexia Dayet, et al. 2020. "Leaf Carbon and Water Status Control Stomatal and Nonstomatal Limitations of Photosynthesis in Trees." *New Phytologist* 226 (3): 690–703. <https://doi.org/10.1111/nph.16436>.

Salvucci, Michael E., and Steven J. Crafts-Brandner. 2004. "Inhibition of Photosynthesis by Heat Stress: The Activation State of Rubisco as a Limiting Factor in Photosynthesis." *Physiologia Plantarum* 120 (2): 179–86. <https://doi.org/10.1111/j.0031-9317.2004.0173.x>.

Santos, Ana Paula, Tânia Serra, Duarte D. Figueiredo, et al. 2011. "Transcription Regulation of Abiotic Stress Responses in Rice: A Combined Action of Transcription Factors and Epigenetic Mechanisms." *OMICS: A Journal of Integrative Biology* 15 (12): 839–57. <https://doi.org/10.1089/omi.2011.0095>.

Sanz-Pérez, Virginia, and Pilar Castro-Díez. 2010. "Summer Water Stress and Shade Alter Bud Size and Budburst Date in Three Mediterranean *Quercus* Species." *Trees* 24 (1): 89–97. <https://doi.org/10.1007/s00468-009-0381-5>.

Schönbeck, Leonie, Charlotte Grossiord, Arthur Gessler, et al. 2022. "Photosynthetic Acclimation and Sensitivity to Short- and Long-Term Environmental Changes in a Drought-Prone Forest." *Journal of Experimental Botany* 73 (8): 2576–88. <https://doi.org/10.1093/jxb/erac033>.

Schuster, Ann-Christin, Markus Burghardt, and Markus Riederer. 2017. "The Ecophysiology of Leaf Cuticular Transpiration: Are Cuticular Water Permeabilities Adapted to Ecological Conditions?" *Journal of Experimental Botany* 68 (19): 5271–79. <https://doi.org/10.1093/jxb/erx321>.

Seidl, Rupert, Dominik Thom, Markus Kautz, et al. 2017. "Forest Disturbances under Climate Change." *Nature Climate Change* 7 (6): 395–402. <https://doi.org/10.1038/nclimate3303>.

Sergent, Anne-Sophie, Philippe Rozenberg, and Nathalie Bréda. 2014. "Douglas-Fir Is Vulnerable to Exceptional and Recurrent Drought Episodes and Recovers Less Well on Less Fertile Sites." *Annals of Forest Science* 71 (6): 697–708. <https://doi.org/10.1007/s13595-012-0220-5>.

Serra-Maluquer, X., M. Mencuccini, and J. Martínez-Vilalta. 2018. "Changes in Tree Resistance, Recovery and Resilience across Three Successive Extreme Droughts in the Northeast Iberian Peninsula." *Oecologia* 187 (1): 343–54. <https://doi.org/10.1007/s00442-018-4118-2>.

Seth, Romit, Massimo Iorizzo, Tony Kipkoech Maritim, and Ram Kumar Sharma. 2024. "Editorial: Epigenetic and Gene Regulation Underlying Crosstalk in Plant Development and Stress Responses." *Frontiers in Genetics* 15 (July). <https://doi.org/10.3389/fgene.2024.1427102>.

Shaffique, Shifa, Saddam Hussain, Sang-Mo Kang, et al. 2023. "Phytohormonal Modulation of the Drought Stress in Soybean: Outlook, Research Progress, and Cross-Talk." *Frontiers in Plant Science* 14 (October). <https://doi.org/10.3389/fpls.2023.1237295>.

Shao, Ruixin, Kaibo Wang, and Zhouping Shangguan. 2010. "Cytokinin-Induced Photosynthetic Adaptability of *Zea Mays* L. to Drought Stress Associated with Nitric Oxide Signal: Probed by ESR Spectroscopy and Fast OJIP Fluorescence Rise." *Journal of Plant Physiology* 167 (6): 472–79. <https://doi.org/10.1016/j.jplph.2009.10.020>.

Sharkey, Thomas D. 1988. "Estimating the Rate of Photorespiration in Leaves." *Physiologia Plantarum* 73 (1): 147–52. <https://doi.org/10.1111/j.1399-3054.1988.tb09205.x>.

Sharma, Megha, Pankaj Kumar, Vipasha Verma, Rajnish Sharma, Bhavya Bhargava, and Mohammad Irfan. 2022. "Understanding Plant Stress Memory Response for Abiotic Stress Resilience: Molecular Insights and Prospects." *Plant Physiology and Biochemistry* 179 (May): 10–24. <https://doi.org/10.1016/j.plaphy.2022.03.004>.

Shriti, Surbhi, Anirban Bhar, and Amit Roy. 2024. "Unveiling the Role of Epigenetic Mechanisms and Redox Signaling in Alleviating Multiple Abiotic Stress in Plants." *Frontiers in Plant Science* 15 (September). <https://doi.org/10.3389/fpls.2024.1456414>.

Silva, Evandro N., Rafael V. Ribeiro, Sérgio L. Ferreira-Silva, Suyanne A. Vieira, Luiz F. A. Ponte, and Joaquim A. G. Silveira. 2012. "Coordinate Changes in Photosynthesis, Sugar Accumulation and Antioxidative Enzymes Improve the Performance of *Jatropha Curcas* Plants under Drought Stress." *Biomass and Bioenergy* 45 (October): 270–79. <https://doi.org/10.1016/j.biombioe.2012.06.009>.

Singroha, Garima, Pradeep Sharma, and Ramanjulu Sunkur. 2021. "Current Status of microRNA-Mediated Regulation of Drought Stress Responses in Cereals." *Physiologia Plantarum* 172 (3): 1808–21. <https://doi.org/10.1111/ppl.13451>.

Sintaha, Mariz, Chun-Kuen Man, Wai-Shing Yung, Shaowei Duan, Man-Wah Li, and Hon-Ming Lam. 2022. "Drought Stress Priming Improved the Drought Tolerance of Soybean." *Plants* 11 (21): 2954. <https://doi.org/10.3390/plants11212954>.

Sircaik, Shabnam, Karuna Dhiman, Geetika Gambhir, Pankaj Kumar, and Dinesh Kumar Srivastava. 2021. "Transgenic Implications for Biotic and Abiotic Stress Tolerance in Agricultural Crops." In *Agricultural Biotechnology: Latest Research and Trends*, edited by Dinesh Kumar Srivastava, Ajay Kumar Thakur, and Pankaj Kumar. Springer Nature. https://doi.org/10.1007/978-981-16-2339-4_9.

Skelton, Robert P., Timothy J. Brodribb, Scott A. M. McAdam, and Patrick J. Mitchell. 2017. "Gas Exchange Recovery Following Natural Drought Is Rapid Unless Limited by Loss of Leaf Hydraulic Conductance: Evidence from an Evergreen Woodland." *New Phytologist* 215 (4): 1399–412. <https://doi.org/10.1111/nph.14652>.

Slot, Martijn, Tantawat Nardwattanawong, Georgia G. Hernández, Amauri Bueno, Markus Riederer, and Klaus Winter. 2021. "Large Differences in Leaf Cuticle Conductance and Its Temperature Response among 24 Tropical Tree Species from across a Rainfall Gradient." *New Phytologist* 232 (4): 1618–31. <https://doi.org/10.1111/nph.17626>.

Smith, W. K., and G. N. Geller. 1980. "Leaf and Environmental Parameters Influencing Transpiration: Theory and Field Measurements." *Oecologia* 46 (3): 308–13. <https://doi.org/10.1007/BF00346257>.

Song, Wenqi, Binqing Zhao, Di Liu, et al. 2024. "Hydraulic Conductivity Regulates Tree Growth and Drought Resistance in Semi-Arid Mixed Forests of Northern China." *Ecological Indicators* 166 (September): 112471. <https://doi.org/10.1016/j.ecolind.2024.112471>.

Souza Neta, Maria Lilia de, Salvador Barros Torres, Emanoela Pereira de Paiva, et al. 2024. "Osmotic Adjustment and Antioxidant Activity of Cucumber Seeds Pre-Treated with Stress Attenuators and Subjected to Drought Stress During Germination." *Journal of Plant Growth Regulation* 43 (6): 1919–33. <https://doi.org/10.1007/s00344-023-11231-5>.

Spieß, Nadine, Mouhssin Oufir, Ildikó Matušková, et al. 2012. "Ecophysiological and Transcriptomic Responses of Oak (*Quercus Robur*) to Long-Term Drought Exposure and Rewatering." *Environmental and Experimental Botany* 77 (April): 117–26. <https://doi.org/10.1016/j.envexpbot.2011.11.010>.

Stangler, Dominik Florian, Tobias Walter Miller, Harald Honer, et al. 2022. "Multivariate Drought Stress Response of Norway Spruce, Silver Fir and Douglas Fir along Elevational Gradients in Southwestern Germany." *Frontiers in Ecology and Evolution* 10. <https://www.frontiersin.org/articles/10.3389/fevo.2022.907492>.

Stefaniak, Elisa Z, David T Tissue, Roderick C Dewar, and Belinda E Medlyn. 2024. "Optimal Carbon Storage during Drought." *Tree Physiology*, March 18, tpae032. <https://doi.org/10.1093/treephys/tpae032>.

Sterck, Frank J., Yanjun Song, and Lourens Poorter. 2024. "Drought- and Heat-Induced Mortality of Conifer Trees Is Explained by Leaf and Growth Legacies." *Science Advances* 10 (15): eadl4800. <https://doi.org/10.1126/sciadv.adl4800>.

Stojnić, Srđan, Saša Orlović, Danijela Miljković, Zoran Galić, Marko Kebert, and Georg von Wuehlisch. 2015. "Provenance Plasticity of European Beech Leaf Traits under Differing Environmental Conditions at Two Serbian Common Garden Sites." *European Journal of Forest Research* 134 (6): 1109–25. <https://doi.org/10.1007/s10342-015-0914-y>.

Strand, Deserah D., Aaron K. Livingston, Mio Satoh-Cruz, John E. Froehlich, Veronica G. Maurino, and David M. Kramer. 2015. "Activation of Cyclic Electron Flow by Hydrogen Peroxide in Vivo." *Proceedings of the National Academy of Sciences* 112 (17): 5539–44. <https://doi.org/10.1073/pnas.1418223112>.

Strelcová, Katarína, Daniel Kurjak, Adriana Leštianska, et al. 2013. "Differences in Transpiration of Norway Spruce Drought Stressed Trees and Trees Well Supplied with Water." *Biologia* 68 (6): 1118–22. <https://doi.org/10.2478/s11756-013-0257-4>.

Strømme, Christian Bianchi, Riitta Julkunen-Tiitto, Jorunn Elisabeth Olsen, Line Nybakken, and Roberto Tognetti. 2017. "High Daytime Temperature Delays Autumnal Bud Formation in *Populus tremula* under Field Conditions." *Tree Physiology* 37 (1): 71–81. <https://doi.org/10.1093/treephys/tpw089>.

Su, Shunyu, Ping Tang, Rubin Zuo, et al. 2023. "Exogenous Jasmonic Acid Alleviates Blast Resistance Reduction Caused by LOX3 Knockout in Rice." *Biomolecules* 13 (8): 1197. <https://doi.org/10.3390/biom13081197>.

Sun, Huanfa, Liming Yan, Zhao Li, et al. 2024. "Drought Shortens Subtropical Understory Growing Season by Advancing Leaf Senescence." *Global Change Biology* 30 (5): e17304. <https://doi.org/10.1111/gcb.17304>.

Sun, Run-Ze, Jie Liu, Yuan-Yuan Wang, and Xin Deng. 2021. "DNA Methylation-Mediated Modulation of Rapid Desiccation Tolerance Acquisition and Dehydration Stress Memory in the Resurrection Plant *Boea Hygrometrica*." *PLOS Genetics* 17 (4): e1009549. <https://doi.org/10.1371/journal.pgen.1009549>.

Sunil, Bobba, Deepak Saini, Ramesh B. Bapatla, Vetcha Aswani, and Agepati S. Raghavendra. 2019. "Photorespiration Is Complemented by Cyclic Electron Flow and the Alternative Oxidase Pathway to Optimize Photosynthesis and Protect against Abiotic Stress." *Photosynthesis Research* 139 (1): 67–79. <https://doi.org/10.1007/s11120-018-0577-x>.

Sussmilch, Frances C., and Scott A. M. McAdam. 2017. "Surviving a Dry Future: Abscisic Acid (ABA)-Mediated Plant Mechanisms for Conserving Water under Low Humidity." *Plants* 6 (4): 54. <https://doi.org/10.3390/plants6040054>.

Takagi, Daisuke, Masaki Hashiguchi, Takehiro Sejima, Amane Makino, and Chikahiro Miyake. 2016. "Photorespiration Provides the Chance of Cyclic Electron Flow to Operate for the Redox-Regulation of P700 in Photosynthetic Electron Transport System of Sunflower Leaves." *Photosynthesis Research* 129 (3): 279–90. <https://doi.org/10.1007/s11120-016-0267-5>.

Tan, Shuya, Yueqi Sha, Liwei Sun, and Zhonghai Li. 2023. "Abiotic Stress-Induced Leaf Senescence: Regulatory Mechanisms and Application." *International Journal of Molecular Sciences* 24 (15): 11996. <https://doi.org/10.3390/ijms241511996>.

Teale, William D., Ivan A. Paponov, and Klaus Palme. 2006. "Auxin in Action: Signalling, Transport and the Control of Plant Growth and Development." *Nature Reviews Molecular Cell Biology* 7 (11): 847–59. <https://doi.org/10.1038/nrm2020>.

Thomas, Frank M., Sebastian Preusser, Bernhard Backes, and Willy Werner. 2024. "Leaf Traits of Central-European Beech (*Fagus Sylvatica*) and Oaks (*Quercus Petraea/Robur*): Effects of Severe Drought and Long-Term Dynamics." *Forest Ecology and Management* 559 (May): 121823. <https://doi.org/10.1016/j.foreco.2024.121823>.

Thompson, M. V., and N. M. Holbrook. 2003. "Scaling Phloem Transport: Water Potential Equilibrium and Osmoregulatory Flow." *Plant, Cell & Environment* 26 (9): 1561–77. <https://doi.org/10.1046/j.1365-3040.2003.01080.x>.

Tian, Manqing, Yann Salmon, Anna Lintunen, Ram Oren, and Teemu Hölttä. 2024. "Seasonal Dynamics and Punctuated Carbon Sink Reduction Suggest Photosynthetic Capacity of Boreal Silver Birch Is Reduced by the Accumulation of Hexose." *New Phytologist* 243 (3): 894–908. <https://doi.org/10.1111/nph.19883>.

Tian, Zailong, Kun Li, Yaru Sun, et al. 2024. "Physiological and Transcriptional Analyses Reveal Formation of Memory under Recurring Drought Stresses in Seedlings of Cotton (*Gossypium Hirsutum*)." *Plant Science* 338 (January): 111920. <https://doi.org/10.1016/j.plantsci.2023.111920>.

Tixier, Aude, Gregory A. Gambetta, Jessie Godfrey, Jessica Orozco, and Maciej A. Zwieniecki. 2019. "Non-Structural Carbohydrates in Dormant Woody Perennials; The Tale of Winter Survival and Spring Arrival." *Frontiers in Forests and Global Change* 2 (May). <https://doi.org/10.3389/ffgc.2019.00018>.

Tixier, Aude, Jessica Orozco, Adele Amico Roxas, J. Mason Earles, and Maciej A. Zwieniecki. 2018. "Diurnal Variation in Nonstructural Carbohydrate Storage in Trees: Remobilization and Vertical Mixing." *Plant Physiology* 178 (4): 1602–13. <https://doi.org/10.1104/pp.18.00923>.

Tomasella, Martina, Karl-Heinz Häberle, Andrea Nardini, Benjamin Hesse, Anna Machlet, and Rainer Matyssek. 2017. "Post-Drought Hydraulic Recovery Is Accompanied by Non-Structural Carbohydrate Depletion in the Stem Wood of Norway Spruce Saplings." *Scientific Reports* 7 (1): 1. <https://doi.org/10.1038/s41598-017-14645-w>.

Tombesi, Sergio, Andrea Nardini, Tommaso Frioni, et al. 2015. "Stomatal Closure Is Induced by Hydraulic Signals and Maintained by ABA in Drought-Stressed Grapevine." *Scientific Reports* 5 (1): 12449. <https://doi.org/10.1038/srep12449>.

Torii, Keiko U. 2021. "Stomatal Development in the Context of Epidermal Tissues." *Annals of Botany* 128 (2): 137–48. <https://doi.org/10.1093/aob/mcab052>.

Torun, Hülya, Bilal Cetin, Srdjan Stojnic, and Peter Petrik. 2024. "Salicylic Acid Alleviates the Effects of Cadmium and Drought Stress by Regulating Water Status, Ions, and Antioxidant Defense in *Pterocarya Fraxinifolia*." *Frontiers in Plant Science* 14 (January). <https://doi.org/10.3389/fpls.2023.1339201>.

Touche, J., C. Calvaruso, P. De Donato, and M. -P. Turpault. 2024. "Drought Events Influence Nutrient Canopy Exchanges and Green Leaf Partitioning during Senescence in a Deciduous Forest." *Forest Ecosystems* 11 (January): 100173. <https://doi.org/10.1016/j.fecs.2024.100173>.

Touche, J., C. Calvaruso, P. De Donato, and MP. Turpault. 2022. "Five Successive Years of Rainfall Exclusion Induce Nutritional Stress in a Mature Beech Stand." *Forest Ecology and Management* 507 (March): 119987. <https://doi.org/10.1016/j.foreco.2021.119987>.

Tsonev, T., S. Wahbi, Sun PengSen, G. Sorrentino, and M. Centritto. 2014. "Gas Exchange, Water Relations and Their Relationships with Photochemical Reflectance Index in *Quercus Ilex* Plants during Water Stress and Recovery." *International Journal of Agriculture and Biology* 16 (2): 335–41.

Ullah, Abd, Akash Tariq, Fanjiang Zeng, et al. 2024. "Drought Priming Improves Tolerance of *Alhagi Sparsifolia* to Subsequent Drought: A Coordinated Interplay of Phytohormones, Osmolytes, and Antioxidant Potential." *Plant Stress* 12 (June): 100469. <https://doi.org/10.1016/j.stress.2024.100469>.

Ünlüsoy, Aybüke Güler, Seher Yolcu, Melike Bor, Filiz Özdemir, and İsmail Türkan. 2023. "Activation of Photorespiration Facilitates Drought Stress Tolerance in *Lotus Corniculatus*." *Journal of Plant Growth Regulation* 42 (3): 2088–101. <https://doi.org/10.1007/s00344-022-10683-5>.

Vander Mijnsbrugge, Kristine, Mattias Bollen, Stefaan Moreels, et al. 2025. "Timing of Drought and Severity of Induced Leaf Desiccation Affect Recovery, Growth and Autumnal Leaf Senescence in *Fagus Sylvatica* L. Saplings." *Forests* 16 (1): 1. <https://doi.org/10.3390/f16010005>.

Vander Mijnsbrugge, Kristine, Arion Turcsán, Jorne Maes, et al. 2016. "Repeated Summer Drought and Re-Watering during the First Growing Year of Oak (*Quercus Petraea*) Delay Autumn Senescence and Bud Burst in the Following Spring." *Frontiers in Plant Science* 7 (March). <https://doi.org/10.3389/fpls.2016.00419>.

VanderWeide, Joshua, Yifan Yan, Wesley F. Zandberg, and Simone D. Castellarin. 2022. "Modulation of Grape Cuticular Wax Composition Following Multiple Heatwaves Influences Grape Transpiration." *Environmental and Experimental Botany* 202 (October): 105036. <https://doi.org/10.1016/j.envexpbot.2022.105036>.

Vankova, Radomira. 2014. "Cytokinin Regulation of Plant Growth and Stress Responses." In *Phytohormones: A Window to Metabolism, Signaling and Biotechnological Applications*, edited by Lam-Son Phan Tran and Sikander Pal. Springer. https://doi.org/10.1007/978-1-4939-0491-4_3.

Verma, Swati, Neelam Prabha Negi, Shalini Pareek, Gaurav Mudgal, and Deepak Kumar. 2022. "Auxin Response Factors in Plant Adaptation to Drought and Salinity Stress." *Physiologia Plantarum* 174 (3): e13714. <https://doi.org/10.1111/ppl.13714>.

Vicente-Serrano, Sergio M., Dhais Peña-Angulo, Santiago Beguería, et al. 2022. "Global Drought Trends and Future Projections." *Philosophical Transactions of the Royal Society A: Mathematical, Physical and Engineering Sciences* 380 (2238): 20210285. <https://doi.org/10.1098/rsta.2021.0285>.

Virlouvet, Laetitia, Thomas J. Avenson, Qian Du, et al. 2018. "Dehydration Stress Memory: Gene Networks Linked to Physiological Responses During Repeated Stresses of *Zea Mays*." *Frontiers in Plant Science* 9 (July). <https://doi.org/10.3389/fpls.2018.01058>.

Virlouvet, Laetitia, and Michael Fromm. 2015. "Physiological and Transcriptional Memory in Guard Cells during Repetitive Dehydration Stress." *New Phytologist* 205 (2): 596–607. <https://doi.org/10.1111/nph.13080>.

Vitasse, Yann, Constant Signarbieux, and Yongshuo H. Fu. 2018. "Global Warming Leads to More Uniform Spring Phenology across Elevations." *Proceedings of the National Academy of Sciences* 115 (5): 1004–8. <https://doi.org/10.1073/pnas.1717342115>.

Voss, I., B. Sunil, R. Scheibe, and A. S. Raghavendra. 2013. "Emerging Concept for the Role of Photorespiration as an Important Part of Abiotic Stress Response." *Plant Biology* 15 (4): 713–22. <https://doi.org/10.1111/j.1438-8677.2012.00710.x>.

Vuković, Rosemary, Ivna Štolfa Čamagajevac, Ana Vuković, et al. 2022. "Physiological, Biochemical and Molecular Response of Different Winter Wheat Varieties under Drought Stress at Germination and Seedling Growth Stage." *Antioxidants* 11 (4): 693. <https://doi.org/10.3390/antiox11040693>.

Vuksanović, Vanja, Branislav Kovačević, Marko Keber, et al. 2023. "In Vitro Selection of Drought-Tolerant White Poplar Clones Based on Antioxidant Activities and Osmoprotectant Content." *Frontiers in Plant Science* 14 (November). <https://doi.org/10.3389/fpls.2023.1280794>.

Wahab, Abdul, Farwa Batool, Murad Muhammad, Wajid Zaman, Rafid Magid Mikhlef, and Muhammad Naeem. 2023. "Current Knowledge, Research Progress, and Future Prospects of Phyto-Synthesized Nanoparticles Interactions with Food Crops under Induced Drought Stress." *Sustainability* 15 (20): 14792. <https://doi.org/10.3390/su152014792>.

Walker, Anthony P., Martin G. De Kauwe, Ana Bastos, et al. 2021. "Integrating the Evidence for a Terrestrial Carbon Sink Caused by Increasing Atmospheric CO₂." *New Phytologist* 229 (5): 2413–45. <https://doi.org/10.1111/nph.16866>.

Wang, Fei, Chong-Hua Li, Ying Liu, et al. 2024. "Plant Responses to Abiotic Stress Regulated by Histone Acetylation." *Frontiers in Plant Science* 15 (July). <https://doi.org/10.3389/fpls.2024.1404977>.

Wang, Jun-Li, Dong-Wei Di, Pan Luo, et al. 2022. "The Roles of Epigenetic Modifications in the Regulation of Auxin Biosynthesis." *Frontiers in Plant Science* 13 (August). <https://doi.org/10.3389/fpls.2022.959053>.

Wang, Ming, Laurent Ogé, Maria-Dolores Pérez Garcia, et al. 2022. "Antagonistic Effect of Sucrose Availability and Auxin on Rosa Axillary Bud Metabolism and Signaling, Based on the Transcriptomics and

Metabolomics Analysis.” *Frontiers in Plant Science* 13 (March). <https://doi.org/10.3389/fpls.2022.830840>.

Wang, Ningning, Yanan Yu, Di Zhang, et al. 2022. “Modification of Gene Expression, DNA Methylation and Small RNAs Expression in Rice Plants under In Vitro Culture.” *Agronomy* 12 (7): 1675. <https://doi.org/10.3390/agronomy12071675>.

Wang, Songwei, Günter Hoch, Georges Grun, and Ansgar Kahmen. 2024. “Water Loss after Stomatal Closure: Quantifying Leaf Minimum Conductance and Minimal Water Use in Nine Temperate European Tree Species during a Severe Drought.” *Tree Physiology* 44 (4): tpae027. <https://doi.org/10.1093/treephys/tpae027>.

Wang, Wen-Sheng, Ya-Jiao Pan, Xiu-Qin Zhao, et al. 2011. “Drought-Induced Site-Specific DNA Methylation and Its Association with Drought Tolerance in Rice (*Oryza Sativa L.*).” *Journal of Experimental Botany* 62 (6): 1951–60. <https://doi.org/10.1093/jxb/erq391>.

Wang, Wensheng, Qiao Qin, Fan Sun, et al. 2016. “Genome-Wide Differences in DNA Methylation Changes in Two Contrasting Rice Genotypes in Response to Drought Conditions.” *Frontiers in Plant Science* 7 (November). <https://doi.org/10.3389/fpls.2016.01675>.

Wang, Xiao, Qing Li, Jingjing Xie, et al. 2021. “Abscisic Acid and Jasmonic Acid Are Involved in Drought Priming-Induced Tolerance to Drought in Wheat.” *The Crop Journal* 9 (1): 120–32. <https://doi.org/10.1016/j.cj.2020.06.002>.

Wang, Xiao, Zhiqiang Mao, Jia Zhang, et al. 2019. “Osmolyte Accumulation Plays Important Roles in the Drought Priming Induced Tolerance to Post-Anthesis Drought Stress in Winter Wheat (*Triticum Aestivum L.*).” *Environmental and Experimental Botany* 166 (October): 103804. <https://doi.org/10.1016/j.envexpbot.2019.103804>.

Weithmann, G., B. Schuldt, R. M. Link, et al. 2022. “Leaf Trait Modification in European Beech Trees in Response to Climatic and Edaphic Drought.” *Plant Biology* 24 (7): 1272–86. <https://doi.org/10.1111/plb.13366>.

Wingler, A., W. P. Quick, R. A. Bungard, K. J. Bailey, P. J. Lea, and R. C. Leegood. 1999. “The Role of Photorespiration during Drought Stress: An Analysis Utilizing Barley Mutants with Reduced Activities of Photorespiratory Enzymes.” *Plant, Cell & Environment* 22 (4): 361–73. <https://doi.org/10.1046/j.1365-3040.1999.00410.x>.

Wojtyla, Łukasz, Ewelina Paluch-Lubawa, Ewa Sobieszczuk-Nowicka, and Małgorzata Garnczarska. 2020. “Chapter 7 - Drought Stress Memory and Subsequent Drought Stress Tolerance in Plants.” In *Priming-Mediated Stress and Cross-Stress Tolerance in Crop Plants*, edited by Mohammad Anwar Hossain, Fulai Liu, David J. Burritt, Masayuki Fujita, and Bingru Huang. Academic Press. <https://doi.org/10.1016/B978-0-12-817892-8.00007-6>.

Wolf, Sebastian, and Eugénie Paul-Limoges. 2023. “Drought and Heat Reduce Forest Carbon Uptake.” *Nature Communications* 14 (1): 1. <https://doi.org/10.1038/s41467-023-41854-x>.

Wu, Chaoyang, Jie Peng, Philippe Ciais, et al. 2022. “Increased Drought Effects on the Phenology of Autumn Leaf Senescence.” *Nature Climate Change* 12 (10): 943–49. <https://doi.org/10.1038/s41558-022-01464-9>.

Xu, Zhenzhu, Guangsheng Zhou, and Hideyuki Shimizu. 2010. “Plant Responses to Drought and Rewatering.” *Plant Signaling & Behavior* 5 (6): 649–54. <https://doi.org/10.4161/psb.5.6.11398>.

Yadav, Ankita, Sanoj Kumar, Rita Verma, et al. 2024. “Overexpression of miR166 in Response to Root Rhizobacteria Enhances Drought Adaptive Efficacy by Targeting HD-ZIP III Family Genes in Chickpea.” *Journal of Soil Science and Plant Nutrition* 24 (3): 6024–39. <https://doi.org/10.1007/s42729-024-01957-w>.

Yamamoto, Hiroshi, and Toshiharu Shikanai. 2019. “PGR5-Dependent Cyclic Electron Flow Protects Photosystem I under Fluctuating Light at Donor and Acceptor Sides.” *Plant Physiology* 179 (2): 588–600. <https://doi.org/10.1104/pp.18.01343>.

Yang, Mengxiang, Jiawei He, Zhuangzhuang Sun, et al. 2023. “Drought Priming Mechanisms in Wheat Elucidated by In-Situ Determination of Dynamic Stomatal Behavior.” *Frontiers in Plant Science* 14 (February). <https://doi.org/10.3389/fpls.2023.1138494>.

Yang, Yanzhi, Lei Xu, Chen Hao, et al. 2024. “The microRNA408–Plantacyanin Module Balances Plant Growth and Drought Resistance by Regulating Reactive Oxygen Species Homeostasis in Guard Cells.” *The Plant Cell* 36 (10): 4338–55. <https://doi.org/10.1093/plcell/koae144>.

Yao, Guang-Qian, Zheng-Fei Nie, Neil C. Turner, et al. 2021. “Combined High Leaf Hydraulic Safety and Efficiency Provides Drought Tolerance in *Caragana* Species Adapted to Low Mean Annual Precipitation.” *New Phytologist* 229 (1): 230–44. <https://doi.org/10.1111/nph.16845>.

Yin, Xinyou, Peter E. L. van der Putten, Daniel Belay, and Paul C. Struik. 2020. “Using Photorespiratory Oxygen Response to Analyse Leaf Mesophyll Resistance.” *Photosynthesis Research* 144 (1): 85–99. <https://doi.org/10.1007/s11120-020-00716-z>.

Yin, Xinyou, and Paul C. Struik. 2017. "Can Increased Leaf Photosynthesis Be Converted into Higher Crop Mass Production? A Simulation Study for Rice Using the Crop Model GECROS." *Journal of Experimental Botany* 68 (9): 2345–60. <https://doi.org/10.1093/jxb/erx085>.

Young, Sophie N R, Lawren Sack, Margaret J Sporck-Koehler, and Marjorie R Lundgren. 2020. "Why Is C4 Photosynthesis so Rare in Trees?" *Journal of Experimental Botany* 71 (16): 4629–38. <https://doi.org/10.1093/jxb/eraa234>.

Yu, Yanchong, Yanan Qi, Jinpeng Xu, et al. 2021. "Arabidopsis WRKY71 Regulates Ethylene-Mediated Leaf Senescence by Directly Activating EIN2, ORE1 and ACS2 Genes." *The Plant Journal* 107 (6): 1819–36. <https://doi.org/10.1111/tpj.15433>.

Yuan, Weiyi, Jingqi Suo, Bo Shi, et al. 2019. "The Barley miR393 Has Multiple Roles in Regulation of Seedling Growth, Stomatal Density, and Drought Stress Tolerance." *Plant Physiology and Biochemistry* 142 (September): 303–11. <https://doi.org/10.1016/j.plaphy.2019.07.021>.

Zarco-Tejada, P.J., J.R. Miller, T.L. Noland, G.H. Mohammed, and P.H. Sampson. 2001. "Scaling-up and Model Inversion Methods with Narrowband Optical Indices for Chlorophyll Content Estimation in Closed Forest Canopies with Hyperspectral Data." *IEEE Transactions on Geoscience and Remote Sensing* 39 (7): 1491–507. <https://doi.org/10.1109/36.934080>.

Zavadilová, Ina, Justyna Szatniewska, Peter Petřík, Oldřich Mauer, Radek Pokorný, and Marko Stojanović. 2023. "Sap Flow and Growth Response of Norway Spruce under Long-Term Partial Rainfall Exclusion at Low Altitude." *Frontiers in Plant Science* 14 (February). <https://doi.org/10.3389/fpls.2023.1089706>.

Zhang, Chunyu, Wei Zhang, Guodong Ren, et al. 2015. "Chlorophyll Synthase under Epigenetic Surveillance Is Critical for Vitamin E Synthesis, and Altered Expression Affects Tocopherol Levels in Arabidopsis." *Plant Physiology* 168 (4): 1503–11. <https://doi.org/10.1104/pp.15.00594>.

Zhang, Hao, Xiaoyu Zhang, and Jun Xiao. 2023. "Epigenetic Regulation of Nitrogen Signaling and Adaptation in Plants." *Plants* 12 (14): 2725. <https://doi.org/10.3390/plants12142725>.

Zhang, Huiming, Zhaobo Lang, and Jian-Kang Zhu. 2018. "Dynamics and Function of DNA Methylation in Plants." *Nature Reviews Molecular Cell Biology* 19 (8): 489–506. <https://doi.org/10.1038/s41580-018-0016-z>.

Zhang, Jin-Ping, Yang Yu, Yan-Zhao Feng, et al. 2017. "MiR408 Regulates Grain Yield and Photosynthesis via a Phytocyanin Protein." *Plant Physiology* 175 (3): 1175–85. <https://doi.org/10.1104/pp.17.01169>.

Zhang, Ru, and Thomas D. Sharkey. 2009. "Photosynthetic Electron Transport and Proton Flux under Moderate Heat Stress." *Photosynthesis Research* 100 (1): 29–43. <https://doi.org/10.1007/s11120-009-9420-8>.

Zhang, Yaxi, Shaohua Xu, Pingtao Ding, et al. 2010. "Control of Salicylic Acid Synthesis and Systemic Acquired Resistance by Two Members of a Plant-Specific Family of Transcription Factors." *Proceedings of the National Academy of Sciences* 107 (42): 18220–25. <https://doi.org/10.1073/pnas.1005225107>.

Zheng, Pengfei, Dandan Wang, Guodong Jia, et al. 2022. "Variation in Water Supply Leads to Different Responses of Tree Growth to Warming." *Forest Ecosystems* 9 (January): 100003. <https://doi.org/10.1016/j.fecos.2022.100003>.

Zhong, Shanchen, Yanan Gao, Junqian Lu, Changjun Ding, Xiaohua Su, and Bingyu Zhang. 2021. "Production of an Epigenetic Mutant Population of *Populus Nigra*: DNA Methylation and Phenotype Analyses." *Journal of Plant Biochemistry and Biotechnology* 30 (2): 354–63. <https://doi.org/10.1007/s13562-020-00600-w>.

Zhou, Shuangxi, Remko A. Duursma, Belinda E. Medlyn, Jeff W. G. Kelly, and I. Colin Prentice. 2013. "How Should We Model Plant Responses to Drought? An Analysis of Stomatal and Non-Stomatal Responses to Water Stress." *Agricultural and Forest Meteorology* 182–183 (December): 204–14. <https://doi.org/10.1016/j.agrformet.2013.05.009>.

Zhou, Shuang-Xi, Belinda E. Medlyn, and Iain Colin Prentice. 2016. "Long-Term Water Stress Leads to Acclimation of Drought Sensitivity of Photosynthetic Capacity in Xeric but Not Riparian Eucalyptus Species." *Annals of Botany* 117 (1): 133–44. <https://doi.org/10.1093/aob/mcv161>.

Zhu, Jiali, Ji-Hwan Park, Seulbee Lee, et al. 2020. "Regulation of Stomatal Development by Stomatal Lineage miRNAs." *Proceedings of the National Academy of Sciences* 117 (11): 6237–45. <https://doi.org/10.1073/pnas.1919722117>.

Zi, Na, Weibo Ren, Huiqin Guo, Feng Yuan, Yaling Liu, and Ellen Fry. 2024. "DNA Methylation Participates in Drought Stress Memory and Response to Drought in *Medicago Ruthenica*." *Genes* 15 (10): 1286. <https://doi.org/10.3390/genes15101286>.

Ziegler, Yanick, Rüdiger Grote, Franklin Alongi, Timo Knüver, and Nadine K Ruehr. 2024. "Capturing Drought Stress Signals: The Potential of Dendrometers for Monitoring Tree Water Status." *Tree Physiology*, November 7, tpae140. <https://doi.org/10.1093/treephys/tpae140>.

Zlobin, Ilya E., Radomira Vankova, Petre I. Dobrev, et al. 2023. "Abscisic Acid and Cytokinins Are Not Involved in the Regulation of Stomatal Conductance of Scots Pine Saplings during Post-Drought Recovery." *Biomolecules* 13 (3): 3. <https://doi.org/10.3390/biom13030523>.

Zlobin, Ilya, Alexander Kartashov, Yury Ivanov, Alexandra I. Ivanova, and Vladimir V. Kuznetsov. 2024. *Effects of Xylem Conductivity Loss on Scots Pine and Norway Spruce Performance during Drought and Postdrought Recovery*. <https://www.authorea.com/doi/full/10.22541/au.170670012.23925012?commit=558798605cf49d0ad0970fcb6bb8735d8556a39e>.

Zweifel, Roman, Matthias Haeni, Nina Buchmann, and Werner Eugster. 2016. "Are Trees Able to Grow in Periods of Stem Shrinkage?" *New Phytologist* 211 (3): 839–49. <https://doi.org/10.1111/nph.13995>.

Zweifel, Roman, Frank Sterck, Sabine Braun, et al. 2021. "Why Trees Grow at Night." *New Phytologist* 231 (6): 2174–85. <https://doi.org/10.1111/nph.17552>.

8 Acknowledgements

There are so many people who have contributed to this thesis, that it is impossible to acknowledge them all. My time at IFU these last few years has introduced me to some truly amazing people from all over the world, and I value getting to have known them greatly.

To Nadine, thank you for sticking with me for so long before I was allowed to start. This was an opportunity of a lifetime for me, and I am so thankful I was able to be a part of the Ecophysiology team. Your persistent support has encouraged me to take scientific risks and pursue opportunities I never had thought possible. I hope that I can continue to bombard you with numerous plots and scientific comments throughout my career.

To Andi, I must say I will greatly miss your insight and constant ability for humor. I thoroughly enjoyed our time tinkering with the plant chambers, and always had something to learn from you. Your technical ability to realize whatever experimental demands I had on any given day is unmatched.

To Anna, I apologize for the likely thousands of samples I have thrown your way these past few years. So much of this thesis is due to your work not just in the lab, but also with every other aspect of the greenhouse experimental process. I wish you all the best with your paragliding career, and hope that I can join again sometime in the future for Dönerstag.

Over the past few years, I have been able to pursue my passion of learning how the natural world works in a beautiful town in the Alps, with access to state-of-the-art equipment and the best research support team. While living here I was able to be an active part of my niece and nephew's childhood, travel the continent, and make numerous memories with both my current and future families. To Lauren, thank you for taking this adventure with me. I am so grateful for my time in Garmisch.

